TRANSFORMATION OF THE KINETIC ENERGY OF RAINFALL WITH VARIABLE TREE CANOPIES

Catharine Jane Brandt

Thesis submitted to the University of London
for the degree of Doctor of Philosophy

Royal Holloway and
Bedford New College,
Egham Hill,
EGHAM,
Surrey, TW20 0EX

September 1986

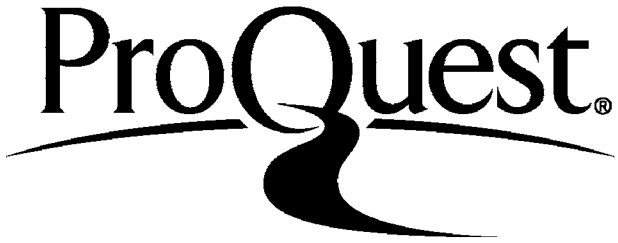

Abstract

This thesis defines a physically based model describing the kinetic energy of throughfall from any vegetation canopy. Empirical measurements of the drop-size distribution of rainfall and sub-canopy throughfall were used to develop the model which was tested in the context of splash erosion.

Comparisons are made for individual storms between rain falling in the open and through a canopy. Three canopies were used, one oak and two tropical rain forest differing in height. Through each storm raindrop sizes were frequently measured using the paper-staining technique. Kinetic energy/mm/m^2 was calculated from the drop sizes, their velocities and amount of rain or throughfall. The velocities were assumed to depend on the height of fall. In the rain forest sites splash cups surrounded by uniform areas of sand were used to measure the material splashed.

The oak canopy data was used to examine the validity of a working hypothesis relating qualitatively the size of throughfall drops to the saturation of the canopy. It was confirmed that the canopy changed the drop-size distribution of the rain and consequently changed the kinetic energy/mm/m^2. The sequences of drop-size distribution change proposed by the hypothesis were related to the cumulated canopy storage. The tropical rain forest results confirmed these findings and extended them. Although rainfall kinetic energy/mm/m^2 may be predicted from rainfall intensity, throughfall kinetic energy/mm/m^2 was independent of intensity and the frequency distribution of the energy of throughfall samples was bimodal, with a high energy group which was commonly higher than that of the rainfall. The probability of a thoroughfall sample being in either energy group depended on the cumulated canopy storage or the percentage storm duration elapsed. The relative magnitude of rainfall and throughfall total kinetic energy depended on the saturation of the canopy and on the canopy height and for some storms the throughfall energy was higher than the rainfall. Soil splash increased with increasing kinetic energy.

The model predicting throughfall energy requires inputs of canopy height, rainfall intensity and the frequency distribution of energy of discrete samples of throughfall. The model is most sensitive to canopy height.

Acknowledgements

I should like to express my gratitude to Prof. John Thornes for his supervision of the work recorded in this thesis and for his advice and encouragement throughout. For permission to use the field sites and for invaluable logistic help I should like to thank both the Botany Department at Royal Holloway College, Egham and the Instituto Nacional da Pesquisas da Amazonia, Manaus.

I should also like to thank the technical staff of the Geography Departments of both Bedford College, London and Bristol University for their assistance and interest in the research project. For their advice and supportive services, I should like to thank the staff of the Computer Centre at Bedford College and Bristol University. However, I particularly want to thank Mark Datko for all his assistance with the programming. Thanks to John Gash, Colin Lloyd and Jim Shuttleworth of the Institute of Hydrology and the staff and postgraduate students of the Geography Departments at Bedford College and Bristol University for all their constructive advice. Special thanks to Toby Stride who has helped in every project since the O'Level. For assistance in the field I want to thank Stephen Nortcliffe, John Thornes, Anne Marchington and Chris Eves.

The work was supported by a Natural Environment Research Council Studentship, grant number GT4/82/AAPS/59 which is gratefully acknowledged.

Finally it is with great pleasure that I thank my family and Gary Bolger, not only for their financial support during the last year, but also for their practical assistance and determined encouragement.

Contents

List of Figures

List of Tables

CHAPTER ONE INTRODUCTION

1) General Introduction

This thesis defines a physically based model which describes the kinetic energy of throughfall from any vegetation canopy. It tests the model in the context of splash erosion. The originality of the thesis lies in the explicit consideration of the effect of different canopy properties on changing the kinetic energy of the rainfall by changing the size distribution of the raindrops. It is important that this problem be addressed because the impact of falling raindrops on the soil is a major precursor of soil erosion.

i) Specific aims of the research

This thesis is aimed at developing a method for the inclusion of vegetation in a soil erosion model that is sufficiently flexible to include any type of canopy. The purpose is to quantify, for single storm events, the change in rainfall kinetic energy by a canopy and to explain that change in terms of the change in drop-size distribution, height of fall and depth of water. A working hypothesis was put forward which related the drop-size distribution of the throughfall to the amount of water held in storage on the canopy. Through empirical measurement of the drop-size distribution of rainfall and simultaneous throughfall the research quantified the effect of the canopy in transforming the drop-size distribution and assessed the validity of the working hypothesis. By measuring the change in drop-size distribution under a number of different canopies with different leaf sizes and orientations the research assessed the importance of different canopy parameters in transforming the energy. Similarly the importance of canopy height and interception capacity in determining the throughfall kinetic energy was examined. The empirical evidence was used to develop a model to simulate the effects of different canopies on the rainfall energy, so that the properties of rain at the

ground surface may be used as direct input to physically-based models currently being developed for splash erosion on bare soil such as that developed by Park et al. 1982.

ii) The model as an extension of previous models

The expression

$$S = k\ K.E.^{b} \qquad [1.1]$$

is used to predict the amount of splash erosion from the kinetic energy$_{(K.E.)}$ of the incident rainfall where k and b are experimentally derived values, k depending on the erodibility of the soil and b taking values from 0.8 to 1.4 (Morgan 1985). More commonly there is a substitution of rainfall intensity (I) for kinetic energy (Kirkby 1980) such that

$$S = a\ I^{b} \qquad [1.2]$$

Rainfall intensity is a more easily measured and widely available parameter than kinetic energy and has been successfully correlated with kinetic energy such that

$$K.E. = c + d \log I \qquad [1.3]$$

again values for c and d have been experimentally derived for a number of different environments (Jansson 1982). Often the intensity quoted is the maximum intensity for any 30 minute period during the storm (Wischmeier and Smith 1958) although the maximum intensity for 15 and

5 minute periods are also used (Elwell and Stocking 1975).

It is argued in this thesis that the model developed in [1.2] and [1.3] is not applicable to the prediction of splash under a vegetation canopy. Throughfall energy is independent of rainfall intensity and depends instead on the cumulated depth of storage in the canopy.

Morgan (1985) suggested that the effects of a plant cover can be accounted for by reducing the predicted detachment by a ratio, the value of which varies according to the height, canopy cover and ground cover of the plant assemblage. Hence splash detachment under a canopy may be predicted using the model

$$S = k(K.E.^{-aINCEP})^b \qquad [1.4]$$

where INCEP is the percentage of rainfall contributing to permanent interception and stemflow and therefore not contributing to splash detachment, k is an index of soil detachability, a varies from 0.03 to 0.15.

The model presented here extends Morgan's model. Instead of accounting for the presence of a vegetation canopy in terms of its interception capacity and adjusting the rainfall energy the throughfall kinetic energy is seen to be independent of rainfall energy but is determined by the structure of the canopy itself such that

$$S = k\left(\sum_{i=1}^{n} k.e._i \; d_i\right)^b \qquad [1.5]$$

where $k.e._i$ is the energy of throughfall ($J/mm/m^2$) of a particular period during the storm. The energy is a function of the percentage of storm duration elapsed and hence the probability of the throughfall

energy being of a particular level and also a function of the height of the canopy. d_i is the depth of throughfall for that period.

The kinetic energy of throughfall has been experimentally determined for several different canopy types; for red pine (Chapman 1948), beech (Mosley 1982), oak (Ovington 1954) and also for some crops; for corn (Quinn and Laflen 1981) and for Brussels sprouts (Noble and Morgan 1983). It has also been simulated by Dohrenwend (1977) who assumed from previous evidence that the effect of a canopy would be to increase the percentage of larger drops. However, none of these authors have examined the change in kinetic energy of throughfall through a storm evidence for the occurrence of which is given in this thesis. This thesis extends the existing literature by including measurements of throughfall energy under different storeys of an evergreen tropical rainforest and by including detailed measurements quantifies energy change during a number of storms.

iii) Significance of the model

Evans (1980) summarised the role of rainfall energy in promoting soil erosion. The erosive energy of rain is a function of storm depth and the change in drop size distribution through the storm. On impact, two-thirds of the raindrop energy is consumed in compressing and deforming the soil surface (Mihara 1951), the remainder of the energy is expended forming spray and splashing soil particles (Al-Durrah and Bradford 1981). The movement of soil by splash has a mechanical efficiency of about 0.2% (Morgan 1979) and consequent sediment yields directly from rainsplash are rather low even under maximal conditions (Kirkby 1980) when compared with other erosion mechanisms. Uncontained overland flow has a mechanical efficiency of 3 to 4% and the observed sediment transport rate are about 20 times higher than that of rainsplash (Morgan 1979). However the energy of impacting raindrops is important in changing the soil structure to promote sheet wash and in providing material for entrainment.

Raindrop impact and dispersed soil particles seal the soil and form a crust which is comprised of two layers, a very thin (c. 0.1 mm) non-porous layer and a zone of up to 5 mm thick of inwashed fine particles (McIntyre 1958). The crust transmits water at a rate which is betweeen 200 and 2000 times lower than that of unprotected soil, causing pools of standing water to form, coalesce and sheet flow to begin (Evans 1980). The interaction of rainsplash and sheet wash is important, each process acting separately is less efficient at moving soil particles than when the processes are acting together (Young and Wiersma 1973). This is because the soil particles are brought into suspension by raindrop splash and then transported by sheet flow. Also raindrop splash imparts turbulence to laminar flow (Evans 1980).

Park et al. (1982) have developed a physically-based model which describes the splash process in terms of the conservation of momentum. It investigates the forces of motion and friction at each stage of the process. By quantifying the erosive power of the rainfall in terms of its kinetic energy, the model in this thesis provides information which may be directly used as the input to such splash models.

Vegetation is commonly considered to be a major control of soil erosion and globally it may be suggested that areas of low sediment yield are areas with an extensive cover of vegetation. However, there are many aspects of the interaction between vegetation and the eroding processes. Langbein and Schumm (1958) considered the relationship between annual precipitation and annual sediment yield (Figure 1.1). They suggested, on the basis of empirical data collected from the United States, that as annual precipitation increased so did annual sediment yield, until the precipitation was sufficient to support an extensive vegetation cover.

The effect of vegetation of erosion and transport may be divided into three types (Jansson 1982). The effects of canopy cover, the effets of organic material on the ground and the effects of organic material in the ground. The canopy cover intercepts rain reducing a proportion of rain reaching the ground which depends on the depth of

Figure 1.1 Variation of sediment yield with precipitation and vegetation cover, determined from reservoir surveys (from Langbein and Schumm 1958)

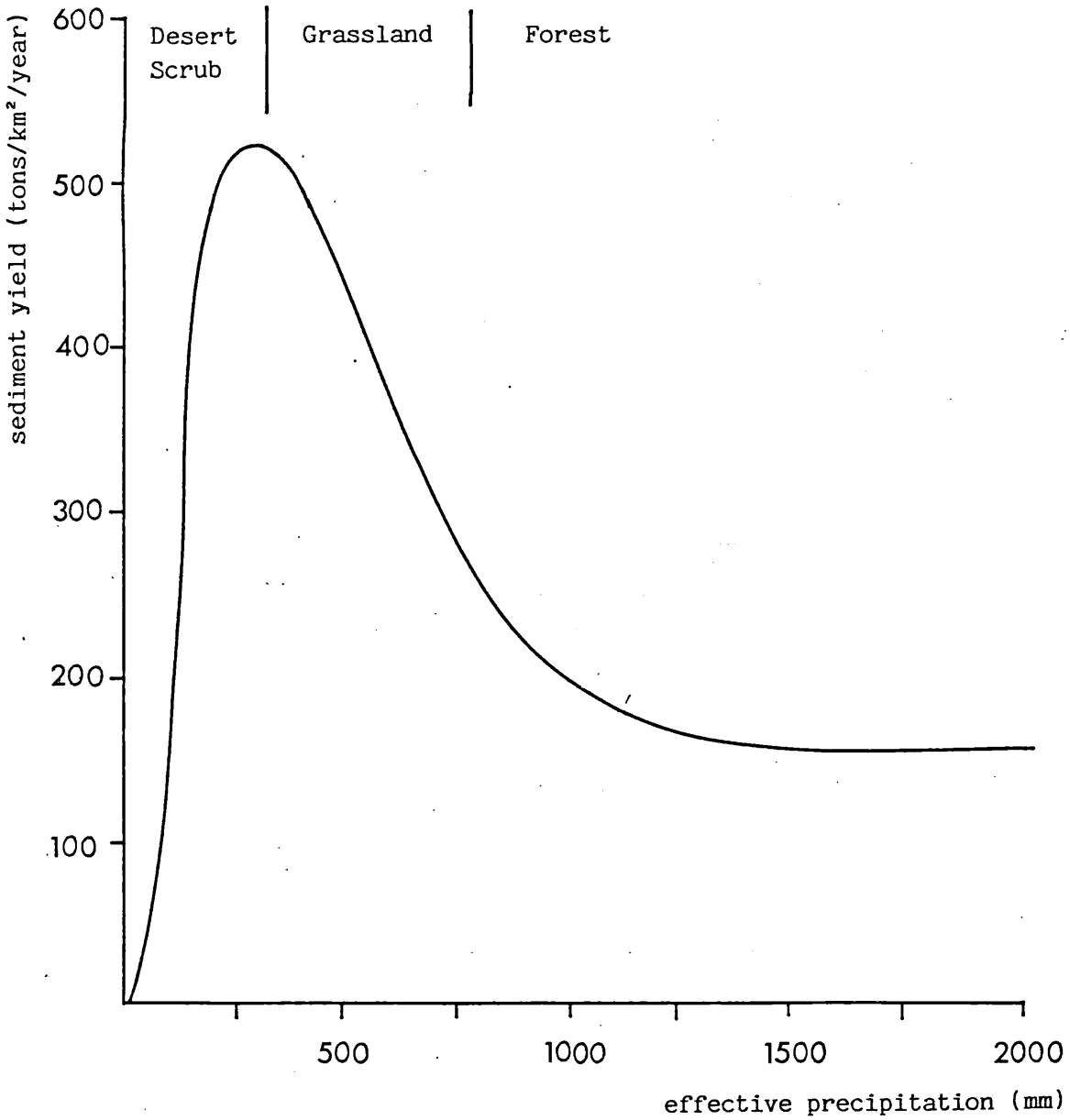

the storm. Water drops which strike the canopy may be split into smaller sizes, those which are intercepted may coalesce and form larger drops (for instance Ovington 1954) and fall with a velocity which depends on the height of the canopy above the ground. Both the change in drop size and in fall height transform the kinetic energy of the rain. Mulch, leaf litter, close growing vegetation and other organic material on the soil surface also intercept raindrops but their height above the ground effectively reduces the splash erosion (Hudson and Jackson 1959) and reduces surface sealing resulting in high infiltration rates and less surface runoff. The velocity of flow of surface water is reduced by surface friction and implies a reduction in the shear stress and in the potential of runoff to transport material (Thornes 1980). Soil texture is changed by the organic matter which becomes incorporated in the soil and increases soil aggregation (Young 1976). Associated faunal activity also tends to increase infiltration rates (Jansson 1982).

However there has been evidence published (Chapman 1948, Dohrenwend 1977, Mosley 1982, Wiersum 1985) which indicates that under some conditions the presence of a vegetation canopy may increase the kinetic energy of rainfall by transforming the drop-size distribution. Such conditions may occur in managed forests where the ground under a tree plantation is kept clear of undergrowth and ground vegetation or ploughed.

This model quantifies the effect of a canopy in terms of the change in size-distribution of the raindrops and the change in the kinetic energy as a result of the change in canopy height.

2) Structure of the thesis

The rest of the thesis is divided into seven chapters. Each develops themes suggested by the previous chapter and provides the information for the next.

Chapter Two identifies the three natural systems which interact to determine the amount of soil erosion and it defines the framework within which the working hypothesis and later the model describing throughfall kinetic energy were developed. It investigates from the available literature the characteristics of falling rain; depth, intensity change during storms and drop-size distribution. The chapter looks at the physical structure of the vegetation communities investigated by empirical measurements and finally factors affecting the erodibility of the soil surface. Building on these three sections, interactions between falling rain and vegetation in terms of interception loss and changes in drop-size distribution, and the energy of falling rain and soil movement are examined. In the last section the interactions between all three are brought together to arrive at a starting point for the main body of the work.

Chapter Three presents the working hypothesis which links the change in throughfall drop-size distribution to the canopy storage. The chapter first examines models of accumulation and drainage of water from the canopy and then gives the hypothesised changes in throughfall drop-size distribution through a storm. At the end of the chapter, seven statements are made which are designed to test the validity of the qualitative model.

In Chapter Four the parameters for measurement are outlined. The choice of parameters affected the selection of experimental sites as specific conditions were necessary to make assumptions which simplified the experimental design. The three canopy types investigated are described. Similarly the type of data required to test the working hypothesis, concerning the relationship between throughfall drop-size distribution and canopy storage, and to develop the model, predicting kinetic energy from a given canopy, determined the experimental techniques used. The development and use of the experimental techniques are discussed.

Chapter Five discusses the derivation of a continuous record of intensity and drop-size distribution change from the samples of rain

taken throughout each storm and measurements of total rain depth. The calculation of kinetic energy/mm/m^2 from a sample of rainfall or throughfall for a given period is outlined, followed by a discussion of the methods for deriving the continuous record by interpolating the depth and drop-size distribution of the unsampled rain. Finally the derivation of simultaneous records of kinetic energy for the rainfall and throughfall from the continuous record are discussed.

Chapter Six, providing the first of the results, describes temporal changes in the energy of individual storms and the corresponding changes under a canopy. The canopy used was a stand of deciduous oak in a temperate environment and the storms were largely frontal in origin. Using the statements derived in Chapter Three to structure the analysis of the results, the validity of the qualitative drop size distribution change hypothesis is examined. It is concluded that there is evidence in the data of a progressive change in the drop-size distribution of the throughfall which may be related to canopy storage regardless of the rainfall drop-size distribution.

Chapter Seven discusses the transformation of the kinetic energy of rain by a tropical rain forest on the basis of the data obtained by similarly measuring the drop-size distribution of rainfall and throughfall for individual storm events. Two canopy types were examined, one a single-layered canopy more than 8 m high and the other a canopy of unfelled forest with the understorey intact and a minimum height of 3 m. In addition splash from a controlled source was measured to indicate the sensitivity of changes in erosion to changes in the erosive potential calculated from the drops. The drop-size distribution hypothesis is re-examined in the light of data from a different environment with different patterns of rainfall and a canopy which has different water-shedding properties. The more extensive data set was used to examine more of the statements derived in Chapter Three relating to the predictability of the pattern of throughfall energy change. By contrasting the results from managed and unmanged forest sites, the impact of a particular vegetation changes are assessed.

The final chapter presents the model of rainfall energy transformation with parameters derived from the tropical rain forest data. The energy of rainfall may be simulated from a model describing the intensity for a number of increments of storm time and by use of Equation [1.3] where the parameters c and d have been experimentally determined for this environment. To simulate throughfall energy it was demonstrated to be possible to substitute cumulated storage for time elapsed. The progressive change in throughfall kinetic energy was simplified by dividing the energy of throughfall at any time into two energy groups. For each increment of storm time the probability of the energy being in the higher energy group was determined from the percentage of storm duration elapsed. The denser the canopy, the more uniform the energy of throughfall in any period. By varying the energy level in each increment, the height of fall and the depth of throughfall in each increment the effect of any canopy on transforming the kinetic energy of rainfall may be simulated.

CHAPTER TWO A REVIEW OF CURRENT LITERATURE

Introduction

This chapter reviews the current literature containing work concerned with the three broad subjects; the raindrop composition of storms, the structure of vegetation communities and the erodibility of the soil surface.

The review is divided into six sections, the first three defining and examining each of the broad systems of interest. From this foundation the other sections examine the inter-relations between the three systems. The effect of a plant canopy on rainfall and the effect of rainfall on soil splash are considered. The common theme of interest is the kinetic energy of the rain, how it is altered by the canopy and then how it determines the soil movement. Finally the three are combined to consider the effect of the canopy structure in changing the rainfall and consequently the soil splash.

Each section has its own specific introduction identifying the various themes to be examined, and each has its own conclusions.

Section 1 Characteristics of falling rain

The review of the literature on the properties of falling water is divided into three parts. The first part is concerned with early attempts to describe the distribution of raindrop sizes for rain with respect to rainfall intensity. The second part deals with mechanisms whereby the distribution is formed and the third with measurements of the velocity of raindrops as they reach the ground.

The purpose of reviewing the literature on the drop-size distribution of rain is to establish a basic pattern with which distributions of drops falling from a canopy may be compared.

Information is sought on the relationship between drop sizes falling at any instant during a storm. From this rain intensity is used as the parameter for relating changes in the distribution both to the progress of a single storm and thence to different types of storms. Finally work on the generation of raindrop spectra is considered to provide an explanation for the different drop-size distributions.

The purpose of the final part of the review is to collect and evaluate data sets concerning the velocities of falling raindrops. This information is later required for the analysis of data collected in this study.

1) The drop-size distribution of falling rain

Mason (1957) noted that in nearly all rain storms there is a considerable spread of drop sizes. From even a casual observation it is clear that the sizes of the drops change with the type of rain producing them, the largest drops being associated with thunder storms. Horton (1948) in describing the drop sizes in a thunder storm noted variation through the storm, the larger raindrops predominating in the earlier stages and the smaller drops later. Here then is the basis for starting a consideration of the sizes of raindrops. The drop-size distribution of rain varies with the type of rainfall and with the progress of any single storm.

The earliest work on the frequency distribution of raindrop sizes has been reviewed by Mason (1957). Leonard (1904) was the first to publish data on the frequency of drops of different sizes in several rains which varied widely in intensity. Both Defant (1905) and Neiderdorfer (1932) grouped their measurements according to the character of the rainfall and claimed that the most frequently occurring drops had volumes in the ratio of 1:2:4:8. However, as Mason (1957) stated, the existence of these modal classes does not appear to have been confirmed by other workers and the subsequent courses of enquiry have since followed a different route.

Drop-size distribution may be correlated with many factors such as rate of rainfall, type of rain, position relative to the centre of the rainstorm and relative humidity. However, some of these factors have been considered unsuitable for numerical treatment (Best 1950a) and many workers have concentrated on establishing a link between drop-size distribution and the rate of rainfall.

Marshall and Palmer (1948) used the data of Laws and Parsons (1943) to determine the number of drops of any given size at different intensities. They found that except for small sizes the drop-size distribution was represented by

$$N_x = N_o \, e^{-bx} \qquad [2.1]$$

where N_x = the number of drops per unit volume having a diameter between x and x + dx (cm)

$b = 41 \, I^{-0.21}$, where I is precipitation rate in mm/hr

N_o = a constant, 0.08

The relationship is illustrated in Figure 2.1 from which it can be seen that the number of drops rapidly increases as the drop size decreases, at a rate depending on the intensity of the rain. However as Mason (1957) pointed out this formula tends to over-estimate the number of smaller drops. Other workers have found that in spite of this over-estimation the Marshall-Palmer distribution formula fits their data well (Mason and Ramandham 1953).

Recently Houze et al. (1979) considered whether the Marshall-Palmer distribution holds, as it has been assumed to do, for air-borne water in frontal clouds. They measured the drop-size distribution from an aeroplane in mid-latitude frontal systems in temperatures ranging from $-40^{o}C$ to $+6^{o}C$. The observed particle sizes tended to follow a basic Marshall-Palmer distribution. Frequently a

Figure 2.1 The Marshall-Palmer distribution function (solid lines) compared with the results of Laws and Parsons (1943) (broken lines)

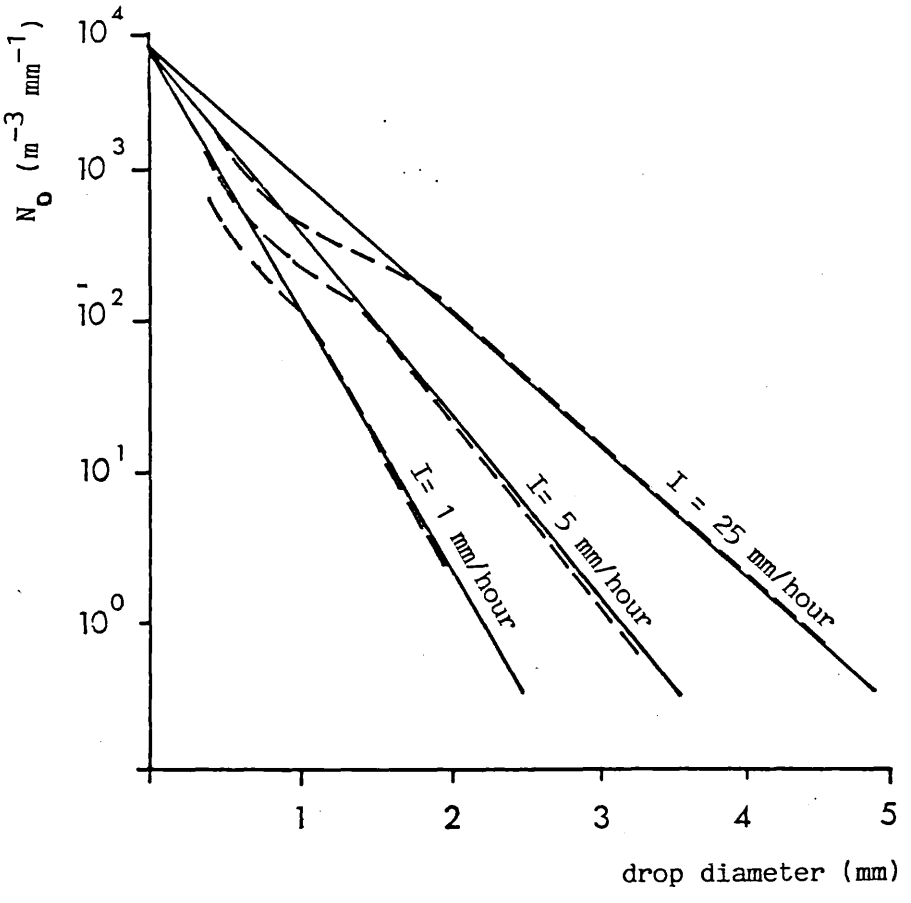

deviation from the distribution occurred at the small particle end of the spectrum but the basic form always dominated at diameters greater than 1.5 mm. This distribution also held over a wide range of temperatures.

In contrast to work relating intensity to the frequency of drop sizes, Laws and Parsons (1943) and Best (1950a) have considered the drops in terms of their volume. They related volume to intensity because for many purposes the number of drops of a particular size is considered less important than the volume of water comprising drops of that size.

Laws and Parsons (1943) compiled data from a number of samples of raindrops during several different storms. They calculated the intensity from the individual samples, grouping samples of the same intensity without reference to the original storm. Figure 2.2 predicts the drop-size distribution from different rain intensities. The diagonal "cumulative volume curves" represent the volume of water which is made up of drops smaller than the given diameters. For storms of intensity of 5 mm/hr, 50% of the volume is made up of drops below 1.68 mm. More generally the median drop diameter (D_{50} (mm)) is defined in terms of rain intensity (I (mm/hr)) such that

$$D_{50} = a\, I^{\,b} \qquad [2.2]$$

where Laws and Parsons (1943) defined a and b as 1.65 and 0.012 respectively. Figure 2.3 extracts individual curves from Figure 2.2 showing the volume contributed by drops of various sizes for three rainfall rates.

Best (1950a) formalised this approach by deriving the following equation

Figure 2.2 Relation of drop size to rainfall intensity (mm/hour) and average cumulative volume curves, defining the drop-size distribution (Laws and Parsons 1943)

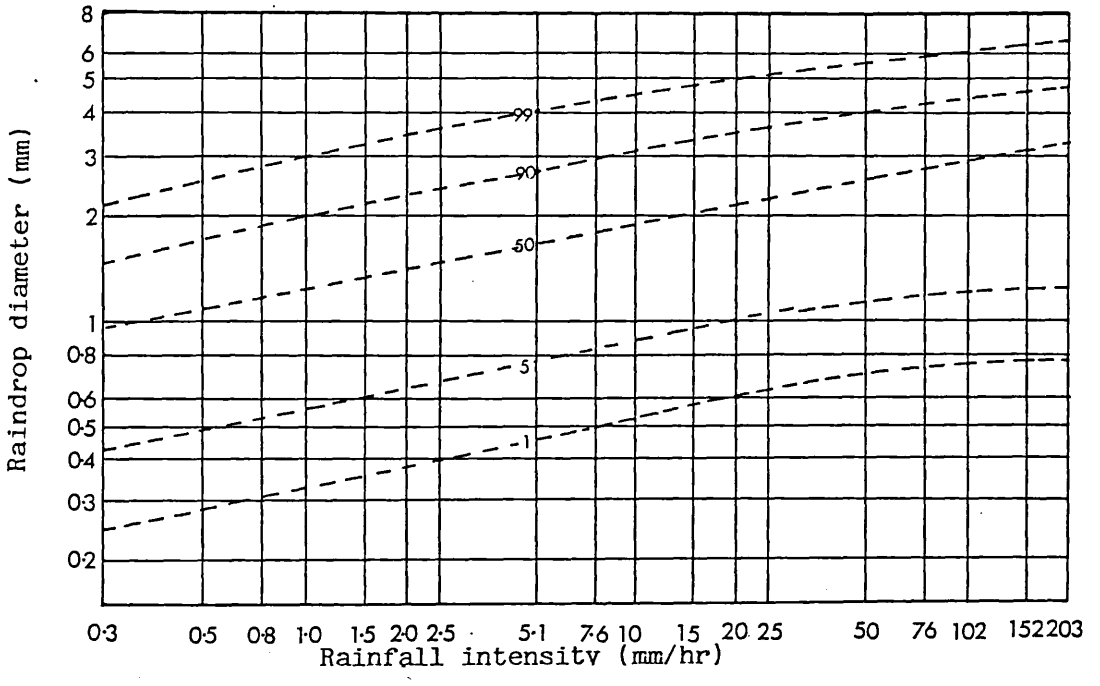

Figure 2.3 Percent of total volume contributed by drops of various sizes for three rainfall intensities (mm/hour) (Laws and Parsons 1943)

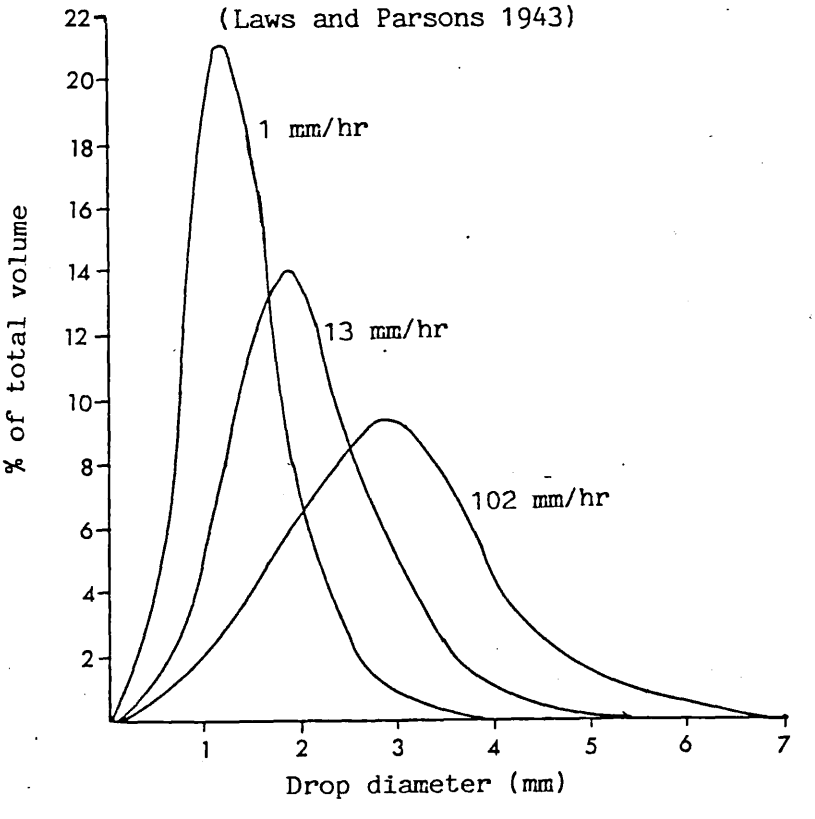

$$1 - F(x) = \exp\left[-\frac{x}{a}^{n}\right] \qquad [2.3]$$

$$a = A\, I^{p} \qquad [2.4]$$

where $F(x)$ = the fraction of liquid water in the air comprised of drops with diameter less than x (mm)

I = rate of precipitation (mm/hr)

n, A, and p are constants

Best (1950a) reviewed all the data on drop-size distribution to date and applied his formulae to it. Using the measured values for all data sets he evaluated the constants n, A, and p as 2.25, 1.30, and 0.232 respectively.

Best stated that equations [2.3] and [2.4] should give a reasonably close representation of the average distribution of liquid water in the air near the ground during precipitation if the mean values for the constants given above are inserted in the equations. This is true for about 80% of the water excluding the 20% of water comprising the smallest and largest drops. However, it is probable that the mean values of the parameters will not be appropriate either in purely orographic rain or in "rain which is essentially of the showery type".

From the literature reviewed the following conclusion regarding the drop-size distribution of rain may be drawn. The frequency of occurrence of drop sizes may be adequately described using the formula of Marshall and Palmer (1948). However it must be remembered that this formula over-estimates the number of small drops. Also the formula may not describe short term changes in some rain types nor the whole distributions of others. The median drop size of a distribution increases with the intensity of rain at a rate described by the formula $D_{50} = a\, I^{b}$. Unlike the distribution of numbers of raindrops,

the distribution of the volume of water comprising those drops is normal.

Up to this point differences in the raindrop distributions or spectra have been only examined through changes in intensity. However the type of storm also influences the drop spectrum. Mason and Andrews (1960) have compared the drop-size distributions from various types of rain. For continuous, warm frontal rain the Marshall-Palmer relationship provides a good average representation, although they comment that there may be short-term deviations. They echoed the comments of Best (1950a) in saying that thunderstorms may have a broader spectrum with considerably higher concentrations of both small and large drops than those predicted.

2) Evolution of the spectra

From a consideration of describing the spectra it is necessary to look for possible explanations for their development. This section of the review is concerned with establishing mechanisms whereby falling raindrops may change their size. Consequently also how much a distribution may change its shape between being released from the cloud and reaching the ground.

Spilhaus (1948) was one of the first to calculate the shape of a falling drop from the combined action of surface tension and aerodynamic pressures. However his over-simplified treatment did not explain the asymmetry of drops about a horizontal plane through their centre.

Blanchard (1950) suspended drops of water in a rising air flow. By taking photographs with a stroboscopic light he was able to follow the changing shapes of the drops. Blanchard observed extreme periodic deformations in drops of more than 5 mm diameter. The drops became flattened ellipsoids with the major axis horizontal. The images Blanchard observed could either have been brought about by the drop

rotating on its minor vertical axis or oscillating between major axes 90^{o} apart on the horizontal plane. The largest drop it was possible to suspend in the air stream without it breaking up was of 9 mm diameter. Pruppacher and Pitter (1971) numerically predicted the shape of falling drops of different sizes. They then verified their results in a wind tunnel. Drops with a diameter less than 0.34 mm can be considered spherical. Between 0.34 and 1.0 mm they form an oblate spheroid. From 1.0 to 4.0 mm the oblate spheroid has an increasingly pronounced base. Drops greater than 4 mm in diameter develop a concave depression in the base which is more pronounced for larger drops. Pruppacher and Pitter (1971) predicted the largest drops occurring in rain would reach a diameter of 8.6 mm.

Having considered the shapes of falling drops it is now necessary to consider their relative stability in the air. Pruppacher and Pitter (1971) proposed a mechanism for determining the maximum size that raindrops can reach before becoming unstable and breaking up. They propose that wave patterns build up on the top and bottom surfaces of the drops and that break-up is related to the conditions of instability for such waves. Klett (1971) applied a different wave pattern, circular instead of parallel, and suggested the largest stable base width should lie between 10 and 13.1 mm. Whatever the mechanism it is clear then that falling drops larger than about 10 mm are inherently unstable and will break up.

At the other end of the spectrum, as Pruppacher and Pitter (1971) noted, investigators have found that drops of diameter less than 4 mm are resistant to break-up even in very trubulent air. This diameter coincides with the critical width at which drops develop the concave base depressions. However, although it is suggested that this depression causes the break-up of the largest drops, Pruppacher and Pitter (1971) said that turbulence within a cloud is not sufficient to cause the break-up of the drops between 4.0 and 9.0 mm. The fact that the larger drops of warm clouds rarely have diameters greater than 5.6 mm suggests that another mechanism for drop break-up needs consideration.

List and Gillespie (1976) stated that break-up induced by collision with smaller drops must at present be considered as the key mechanism in the limitation of raindrop size. Blanchard (1950) noted that when one drop falls in the slip stream of another, both falling at their terminal velocity, the higher drop increases its speed, spiralling down to collide with the one below. Pruppacher and Pitter (1971) described a highly unstable oscillating system formed during the initial moments of coalescence. A dumbell system of two drops, each of diameter 5 mm passing each other on a critical collision trajectory will have a base width of 10.5 mm at the moment of collision and will disrupt into fragments. If the drops collide more directly, oscillations may lead to break-up because of the concave base depression.

From the above literature fundamental limits have been imposed on the sizes of falling drops and mechanisms have been suggested to explain the range of drop sizes actually found in rain. This next section considers the evolution of spectra through the processes of collision and coalescence.

Srivastava (1971) stated that in spite of the different physical characteristics of clouds giving rise to different rates of condensation of water vapour, average rain drop spectra for a given rainfall rate are found to be remarkably similar. Hence the success of the Marshall-Palmer size distribution formula. At low rainfall rates, large unstable drops are scarce and drop break-up may not be significant, coalescence being the major factor determining the size distribution. At large rainfall rates coalescence produces progressively larger drops which disintegrate to produce progressively smaller drops. Eventually a balance may be reached leading to a stationary distribution.

Srivastava (1971) started with an assumed drop-size distribution and solved an equation containing the concentration-density of drops at time t and the number of drops per unit volume of drops of mass x to x + dx. He represented the change in drop concentration by

coalescence and break up and determined the probability of collision occuring. After some time the distribution ceased to change any more. For a given water content the stationary distribution is independent of the assumed initial distribution. However the time taken to reach the stationary distribution depends on the initial distribution although it was usually within 15,000 s (4hrs 10 mins).

In comparing the predicted distributions with measured distributions, Srivastava found that the calculation favoured the extreme of the spectrum. The observed values were limited to a narrower range than the calculated ones.

In a later paper Srivastava (1978) linked water content in the air to the processes of coalescence or collision induced break up controlling drop sizes. In the Marshall-Palmer formulation the intercept (N_o) is assumed to be constant while the slope (b) of the distribution is a function of the rainfall intensity. An initial model linking water content to rainfall rate was proposed by Best (1950a) who defined a relationship between intensity (I (mm/hr)) and the concentration of liquid water in the air (W (mm^3/m^3)) as

$$W = C\ I^{r} \qquad [2.5]$$

where C and r are constants with values of 67.0 and 0.87 respectively, derived from data from a number of studies. Figure 2.4 shows the increasing concentrations of water with increasing intensity.

However Srivastava (1978) found that when the water content (W) exceeded 1.0 g/m^3 (1000 mm^3/m^3), collisional break up became dominant and the slope of the distribution (b) became constant and N_o increased with increasing W. Pasqualucci (1982) raised the value for W to 1.2 g/m^3 (1200 mm^3/m^3) but agreed generally with Srivastava's findings.

In conclusion, for warm rains where the water content in the air

Figure 2.4 Distribtuion of liquid water (mm^3/m^3) over drop diameters (mm) for different rain intensities (mm/hr) (Best 1950a)

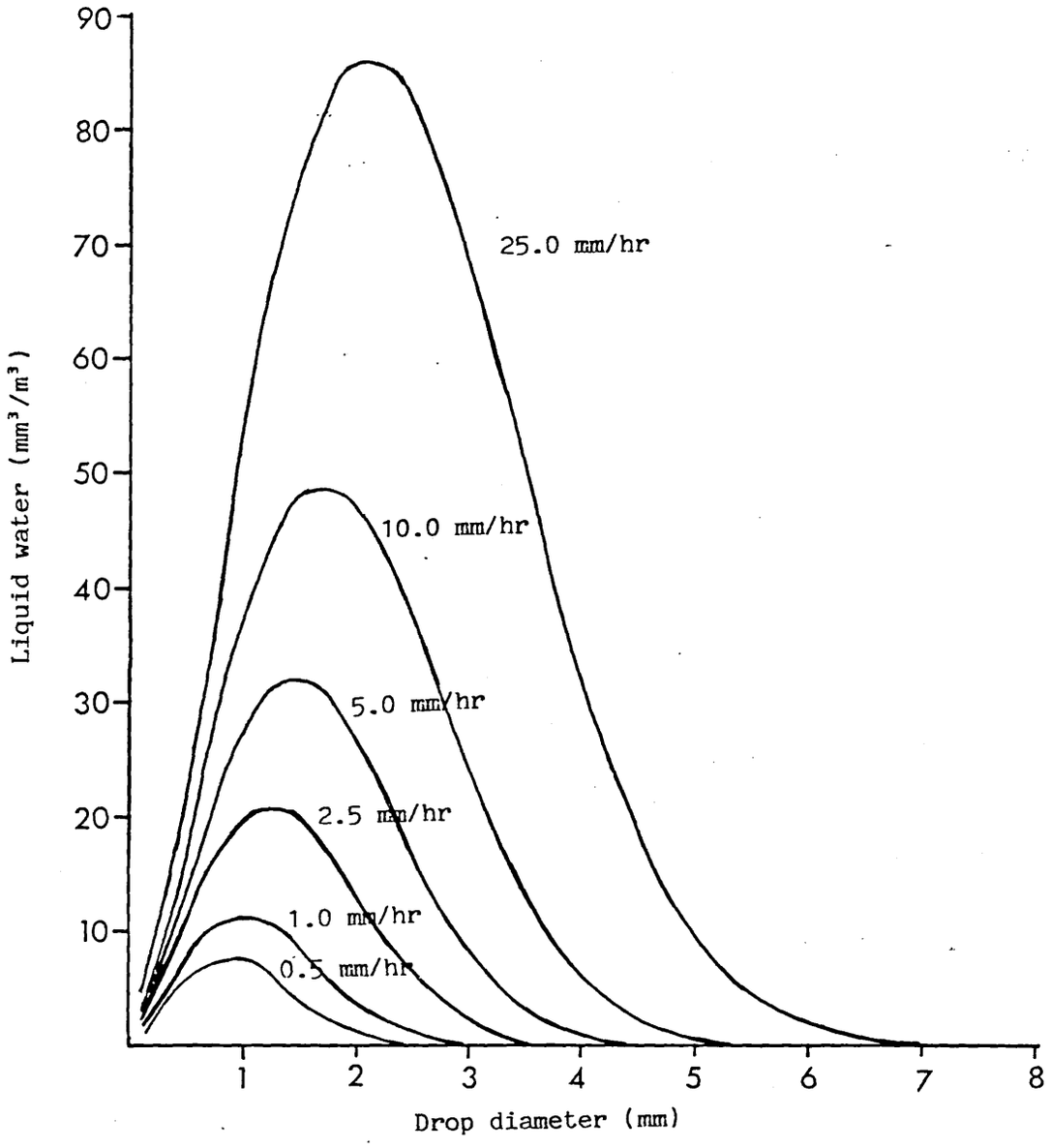

is less than 1.0 g/m^3 the distribution of drop sizes will vary with the intensity of the rain. However when the water content is greater than 1.0 g/m^3 the shape of the distribution appears constant regardless of intensity. The distinction between the two situations is related to the processes regulating drop size. It appears that once there is a certain volume of water in the air for a sufficient time, regardless of the original size distribution and for a given rainfall rate, the drop-size distributions will tend to be of the same pattern. Where the drops are originally formed from hail stones, in so-called cold storms, List and Gillespie (1976) suggested that hail stones which melt only shortly before impact with the ground will not have a chance to collide and hence the distribution of drop sizes will be broader.

3) Velocity of falling raindrops

The purpose of this last section of the review of literature on the characteristics of falling rain is to collect and evaluate data sets concerning the velocities of falling raindrops for use in later analysis. Previous work has primarily been concerned with the calculation or measurement of the velocity of fall for drops of any size in still air. Wind will normally raise actual velocities above the calculated values (Dohrenwend 1977).

An inspection of the literature shows that the work falls into two categories. The first is empirical data collected by direct measurement of falling drops. The second category is concerned with deriving formula for predicting terminal velocities.

Empirical data has commonly been used to develop the formulae for predicting drop size. Best (1950b) used unpublished data by Davies (1942) and Schottman (1978) used the data of Laws (1941). Small drops with a diameter of up to 0.05mm can be assumed to fall according to Stoke's Law (Best 1950b). However the changes in shape of falling drops above a diameter of about 1 mm make formulation more difficult;

the resultant calculation for teminal velocity depends on the shape the drops are supposed to assume. While Best (1950b) persevered with spherical drops Schottman (1978) assumed a hemispherical shape. For this project the straight empirical data was used since it has been proved accurate by other workers and contains sufficient detail for the analysis.

Early work measuring the terminal velocity of water drops was carried out by Lenard (1904), Schmidt (1909) and Flower (1928). However Hall (1970) has since shown that their values differ by as much as 15% from the later measurements of Laws (1941) and Gunn and Kinzer (1949).

Laws (1941) measured the velocities of water drops with diameters between 1.25 and 6 mm falling in still air from heights of 0.5 to 20m (Table 2.1). The drops, formed at the tip of a capillary tube were allowed to fall through an optical system, the light scattered by each drop being collected by a lense and focussed through a lense on the plate of a camera. In front of the camera a "chopper disk" rotated at a constant speed. The image of the falling drop appeared on the plate as a line broken at regular intervals through interruption by the disk. The distance fallen by the drop measured from the photograph and the time calculated from the speed of the rotating disk were used to calculate the velocity. The mass of the drops was ascertained by collecting a large number of them for weighing. By varying the height of the capillary tube above the camera it was found that drops of up to 6 mm reached 95% of their terminal velocity after falling less than 8 m.

Probably the most extensive and accurate set of measurements (Mason 1957 and Hall 1970) have been made by Gunn and Kinzer (1949) covering a range of drop diameters from 0.1 to 5.8 mm (Table 2.2). Drops were detached from a hypodermic needle by a downwardly directed flow of air. The size of the drops was controlled by varying the velocity of the air stream. The drops fell through a metal ring electrode acquiring a small electrostatic charge. The charge was

Table 2.1 The velocity of fall (m/s) of drops of different sizes after falling from a range of heights in still air (from Laws 1941)

Drop diameter (mm)	Height of fall (m)											
	0.5	0.75	1.0	1.5	2.0	2.5	3.0	4.0	5.0	6.0	8.0	20.0
1.25	2.65	3.15	3.52	3.97	4.21	4.43	4.56	4.80	4.85	4.85	4.85	4.85
1.50	2.76	3.26	3.64	4.18	4.50	4.82	4.99	5.25	5.39	5.47	5.51	5.51
1.75	2.84	3.34	3.74	4.34	4.73	5.10	5.31	5.64	5.80	5.92	6.08	6.08
2.00	2.89	3.40	3.83	4.47	4.92	5.29	5.55	5.91	6.15	6.30	6.53	6.58
2.25	2.93	3.45	3.91	4.57	5.07	5.44	5.74	6.14	6.42	6.63	6.90	7.02
2.50	2.96	3.50	3.98	4.65	5.19	5.57	5.89	6.34	6.67	6.92	7.22	7.41
2.75	2.98	3.54	4.04	4.72	5.28	5.69	6.02	6.52	6.89	7.16	7.50	7.76
3.00	3.00	3.58	4.09	4.79	5.37	5.80	6.14	6.68	7.08	7.37	7.75	8.06
3.25	3.02	3.61	4.12	4.85	5.45	5.89	6.25	6.82	7.25	7.56	7.96	8.31
3.50	3.03	3.64	4.15	4.90	5.52	5.98	6.35	6.95	7.40	7.73	8.15	8.52
3.75	3.04	3.66	4.18	4.95	5.58	6.06	6.44	7.07	7.53	7.88	8.31	8.71
4.00	3.05	3.67	4.21	4.98	5.63	6.12	6.52	7.17	7.65	8.00	8.46	8.86
4.50	3.07	3.70	4.24	5.05	5.72	6.24	6.66	7.36	7.85	8.21	8.70	9.10
5.00	3.09	3.72	4.27	5.11	5.79	6.33	6.77	7.50	8.00	8.36	8.86	9.25
5.50	3.10	3.74	4.29	5.16	5.85	6.40	6.86	7.61	8.11	8.47	8.97	9.30
6.00	3.10	3.75	4.31	5.20	5.90	6.46	6.94	7.69	8.20	8.55	9.01	9.30

Table 2.2 Terminal velocity of fall for water droplets in stagnant air (from Gunn and Kinzer 1949)

D (mm)	M (μg)	Tv (m/s)	D (mm)	M (μg)	Tv (m/s)
0.1	0.524	0.27	2.6	9,200	7.57
0.2	4.19	0.72	2.8	11,490	7.82
0.3	14.14	1.17	3.0	14,140	8.06
0.4	33.5	1.62	3.2	17,160	8.26
0.5	65.5	2.06	3.4	20,600	8.44
0.6	113.1	2.47	3.6	24,400	8.60
0.7	179.6	2.87	3.8	28,700	8.72
0.8	268	3.27	4.0	33,500	8.83
0.9	382	3.67	4.2	38,800	8.92
1.0	524	4.03	4.4	44,600	8.98
1.2	905	4.64	4.6	51,000	9.03
1.4	1,437	5.17	4.8	57,900	9.07
1.6	2,140	5.65	5.0	65,500	9.09
1.8	3,050	6.09	5.2	73,600	9.12
2.0	4,190	6.49	5.4	82,400	9.14
2.2	5,580	6.90	5.6	92,000	9.16
2.4	7,240	7.27	5.8	102,200	9.17

D = equivalent drop diameter (mm)
M = mass of drop (μg)
Tv = terminal velocity (m/s)

recorded as it passed through two induction rings about 1 m apart. The time interval between the two recordings and the distance between the induction rings gave values for the velocity. The largest drops were allowed to fall 20 m before their velocity was measured. The diameters of larger drops were determined by weighing a known number of drops. Drops less than 2 mm diameter were caught in shallow dishes of oil, their diameters being measured under a microscope. Each value represents the average of at least 50 separate determinations with an error of less than 1% being claimed for the larger drops.

In this project the data sets of both Laws (1941) and Gunn and Kinzer (1949) were used although there is a discrepancy of about 1.5% for the largest drops. Where values for terminal velocity are required the data of Gunn and Kinzer were used, this being regarded as the most accurate. However, Gunn and Kinzer do not give information on change of velocity with height of fall for single drops. Where this is needed Law's data was used. There is very little quantitative work on the velocity of drops accelerated by the wind.

Section 2 Vegetation Characteristics

The purpose of the review of literature on vegetation characteristics is to gather information about the type of canopies studied in this project. The main emphasis of the project is concerned with evergreen tropical rain forest with an initial, less detailed, study under pedunculate oak (Quercus robur). In addition to background information reviewed much of the information needed for the project was derived from field measurements. The aim of the review is to assess the potential of a canopy for intercepting rain. The probability of interception may change with height through the canopy. Characteristics of the leaves will determine how much water can be stored before dripping, and therefore will determine the size of the drops.

Initially the general structure and composition of the forest types studied are discussed with a more detailed description of biomass distribution within the tropical rain forest. Single tree parameters are examined especially the distribution of leaves within the trees. Information is then sought on leaf size, shape and inclination, together with variations in crown shape. Much of the work is based on models of light interception, however Schottman (1978) also used these models in his work on the penetration of raindrops through a canopy.

1) Forest parameters

i) Oak woodland

Typically the pedunculate oak (Q. robur) does not cast a heavy shadow, allowing shrubs like hazel and hawthorn to be scattered beneath in a discontinuous stratum. An undergrowth of bracken, soft grass, dog's mercury and wood sorrel is common. The majority of the undergrowth species flower in the spring before the tree foliage is grown. The bracken may replace the herbs during the summer to provide a patchy ground cover (Eyre 1968). The experimental work for this project was concerned only with the oak canopy although at the site there was an undergrowth layer of bluebells and bracken but no shrubs. After this background information discussion will be limited to the canopy itself.

ii) Evergreen tropical rain forest

In contrast to temperate oak woodland the enormous variety of plant species in a tropical rain forest prevents an identification by name of typical plant assemblages. However general descriptions of rain forests are abundant. Much of the work after Richards (1952) concentrated on describing the forest structure in terms of a number of strata, each containing a particular association of species. Eyre

(1968) divided rain forest trees into three distinct categories according to their height, with concentrations of individuals at around 33, 18 and 9 m. Other workers (Klinge et al. 1975) have identified different numbers of strata and include the layers of non-tree species in the heavy shadow below. However in most associations the highest A-layer is not completely continuous so that each individual tends to have more room for the development of its crown which is characteristically umbrella-shaped. The B- and C-layer trees tend to be more closely packed and to develop more conical crowns. Regardless of crown shape, however, all the trees have straight trunks almost devoid of twigs and branches beneath the level of the recognisable crown.

Below the tree layer levels of light are very low. The shrub layer which is so important in some associations of deciduous summer forests is very poorly represented. The ground strata are commonly composed of monocotyledons chiefly Palmacae with tree seedlings (Alexandre 1984). Herbaceous plants are rare. The ground is covered with a layer of dead leaves and wood and commonly a thick root mat.

Experimental work was carried out in two rain forest sites. One was simply composed of a single canopy layer of structurally similar trees between 11 and 19 m high, the other was under a complete cover of rain forest. To assess the importance of the sections of the canopy in intercepting rain water attention will be paid to the distribution of phytomass throughout the canopy. In mixed rain forest near Manaus in Amazonia Klinge et al. (1975) measured the above-ground phytomass of the vegetation on a 0.2 ha sample plot and divided it arbitrarily into six strata. They found that 58% of the total phytomass and nearly 40% of leaf phytomass was in the B-stratum (16.7 to 25.9 m) above ground level (Table 2.3). Richards (1983) quoted work in mixed forest in Thailand where the leaf area index was highest also in the B stratum. However here there was a second concentration below 5 m where there were abundant (perhaps unusually so) treelets, saplings and small palms.

Table 2.3 Vertical organisation of aerial phytomass of dicotyledonous trees and palms in tropical rain forest near Manaus (from Klinge et al. 1975)

stratum	mean height (m)	number of individuals		% of aerial phytomass
		Trees	Palms	
A	23.7 - 35.4	50	0	27.6
B	16.7 - 25.9	315	0	58.0
C_1	8.4 - 14.5	760	15	11.2
C_2	3.6 - 5.9	2,765	155	2.3
D	1.7 - 3.0	5,265	805	0.7
E	0.1 - 1.0	83,650		0.2

2) Single tree parameters

i) Tree architecture

Hallé et al. (1978) found that by using a set of simple and readily observed growth characteristics it was possible to categorise the total diversity of tree forms into 23 different architectural models. However it is not the form of the tree itself that this project is concerned with, but the distribution of leaves within the tree frame.

Lemeur and Blad (1974) reviewed models of leaf dispersion to calculate the transmission of light through a canopy. These include geometric models where the canopy is considered as a shape such as a cone. Statistical models assume leaf dispersions to be regular, clumped, random or variable. However they are not techniques which give specific information about any tree type. The change in leaf distribution through successional plants was considered by Horn (1971), who based his model on light interception. He distinguished two extreme types of distribution, monolayer and multilayer. In a monolayer leaves are spread in a single horizontal layer. Once leaves reach a certain density in this monolayer they begin to overlap and the shaded portions are a net loss to the tree. Therefore the optimal horizontal distribution of leaves in the monolayer is spaced rather than random with new leaves tending to fill the gaps between the old one. The alternative strategy is a multilayer. Here the leaves are distributed vertically so that leaves whose horizontal projections overlap are at least 70 leaf diameters away vertically. As long as the average light intensity below these leaves is greater than 20% of full sunlight, new leaves can be added and will photosynthesise at full capacity

ii) Models applicable to the forest types studied

From experimental work in an oak-hickory forest, Horn (1971)

concluded that the successional species could be categorised according to their leaf distribution. Pioneer species tend to be multilayered, climax species are almost monolayered and mid-successional species are intermediate.

Brunig (1976) drew some conclusions on the distribution of leaves in tropical forests. The short lived, pioneer species have thin leaves often arranged in a single layer. In the building phase typical species tend to have more or less horizontal branching, often with long intervals between modes and candelabra-shaped crowns on which the leaves are bunched. When young, species in the mature phase have ellipsoid shaped crowns with a multilayered leaf distribution. However on maturity these crowns often become hemispherical and monolayered. The understorey at all successional stages is multilayered.

Generally, whether the forest is temperate or tropical, the dominant species of the mature forest are monolayered, while the successional species below, in lower light conditions, tend to be multilayered

iii) General crown shape

Horn (1971) speculated on the shapes of tree crowns. He considered that although a tree will tend to fill the gap available, when growing in the open there is an inherited tendency for the tree to form a specific shape. Brunig (1976) suggested that a narrowly columnar crown of a solitary tree intercepts maximum radiation at low solar elevations. However, when grouped, the crowns tend to shade each other. A flat, disc-like crown intercepts maximum direct solar radiation at noon and least at sunrise whether solitary or not. In practice many trees tend to compromise these two shapes and grow hemispherical and broadly conical crowns.

3) Variations in leaf size, shape inclination and longevity

i) Tropical forests

Within an evergreen tropical rain forest leaf size, shape and inclination vary with plant height and amount of rain received, both between species and within plants of the same species.

Leaf sizes vary considerably with their relative height in the canopy. However in general it can be said that leaves of mature emergent and upper canopy trees tend to be smaller than those further down (Ashton 1978). Typically large leaved crown forms are found among short lived, early successional species (Brunig 1976). However although the mature leaves of an emergent Shorea spp. are small (Ashton 1978) leaves of its shade-tolerant sapling are much larger and also of a different shape.

Many leaves of many species of plants in rain forests have an elongated, pointed tip. Most hypotheses purport that leaf drip-tips facilitate drying of the leaf surface through rapid water removal after rainfall (Richards 1952). Whatever the function of these tips, a pattern has been seen in their vertical distribution. Richards observed a decline in the development of drip-tips from intermediate heights up to the canopy top. Williamson (1983) noted an increase in drip-tip occurrence from the ground to 2 m high. However, Williamson also noted that some understorey plants show increased drip-tip development on their higher leaves.

It has been repeatedly observed (for instance Medina 1983) that upper leaves on the canopy of tropical trees show a pronounced inclination and are sometimes clumped. This leaf inclination effectively reduces absorbed radiation per unit leaf area thus avoiding overheating. Brunig (1976) suggested that the erect, clumped leaves affect the flow of wind over the tree surface because erect leaves increase air turbulence over the crown. In addition light penetrates the leaf canopies when the leaves are inclined especially

at low sun angles.

ii) Temperate forests

In this present work a stand of a single oak species with no understoreys was used. Thus variation of leaves between species and with height need not be considered. However, it is necessary to make a comment on leaf inclinations and longevity.

Brunig (1976) reported that in temperate regions where the sun is at low elevations the maximum leaf surface is sunlit when the leaves are orientated horizontally. Leaf bunching may have disadvantages in a temperate climate because a given leaf surface area of clumped leaves intercepts less rain than a random or regular distributions. Most importantly, with respect to the potential for affecting falling raindrops, the canopy is deciduous and has no leaves for up to five months of the year.

Section 3 Soil Characteristics

Information is sought on the parameters which change the response of a soil to splashing from raindrops. Although the literature is very large, the subject has not been explored here in very great detail because the experiment sought to eliminate as much variability as possible in changes in splash amount due to different soil characteristics by replacing surface soil with sand.

A number of studies relating splash amount to soil movement are reviewed and the range of soil characteristics established. Finally the affect of the progression of a storm on changing the splash response is considered.

1) Characteristics affecting soil erodibility

There have been numerous attempts made to establish an erodibility index for soils based on some soil characteristics which correlate with the amount of soil moved. Bryan (1968) reviewed previous attempts at finding such an index. However there have been fewer studies made linking soil properties solely to rainsplash. Bryan's review includes amounts of soil moved by wash.

Moshovkin and Gakhov (1979) predicted mathematically that the amount of soil splashed by the impact area of a single drop is a function of several properties of the drop and soils. The soil properties are the diameter of soil particles, density of the solid soil phase and cohesion of soil particles. However they do not verify experimentally any of their predictions.

Rose (1960) found a negative correlation between the size range of soil particles and the weight moved. Yamatoto and Anderson (1973) found that the percentage of water-stable aggregates of size 0.25 to 0.5 mm produced the highest explained variation in splash. Bryan (1968) from his test of the reliability of erodibility indices concluded that the most efficient index was the percentage weight of water stable aggregates greater than 3 mm.

Bubenzer and Jones (1971) examined the soil parameters, particle size, aggregate index, organic matter, bulk density and moisture content in various combinations to relate soil type to detachment and splash. They found that by inserting a percent clay term into a multiple regression equation including terms for rain intensity and kinetic energy, they increased the correlation coefficient from 0.87 to 0.93.

Cruse and Larson (1977) investigated the effect of soil shear strength on soil detachment due to raindrop impact. Shear strength is defined as the maximum resistance a soil can offer under certain stress conditions before its particles start to slide over each other

(Baver et al. 1972). As such it can be seen as a combination of other properties. Cruse and Larson (1977) altered the soil strength by changing the contacts between solid particles and between solid particles and liquid films. They found that the amount of soil detached by a single drop correlated with the soil shearing strength.

This correlation between soil shear strength and splash has been further considered by Al-Durrah and Bradford (1981). They used a different method for determining soil shear strength but found a correlation coefficient of 0.97 between splash and the ratio of raindrop kinetic energy and soil resistance expressed as undrained shear strength. Al-Durrah and Bradford (1981) continued the earlier study but examined nine different soils. They found that for a specific soil the shear strength term does not fully account for differences in splash weights among the soils. This may be because the measured shear strength depends on the rate of loading. An impacting raindrop and the fall-cone technique they used have very different rates of impact.

Bearing in mind what was said at the beginning about the restriction here of soil material to sand, it is possible to make some observations on the factors affecting splash applicable to this study. Between the sand grains cohesion is very low so indices including clay and organic matter are not important. What is important is the size of the sand grains since the larger grains require a larger amount of kinetic energy to be applied to move them.

2) Change in splash amount through a storm

For many soils it is the properties of the surface horizon and not the complete soil profile which influence the amount of splash detachment (Bryan 1977). These properties may change through a storm as the raindrops impact on the soil surface reducing infiltration and hence enhancing detachment by surface water, or by changing the composition of the surface.

McIntyre (1958) carried out detailed photomicrography of soil surfaces and found that the surface seal was a two layer structure including a washed-in zone of 1.5 mm thickness overlain by a clay seal of 0.1 mm thickness. The clay seal was ten times as effective in reducing infiltration as the washed-in zone. Bryan (1977) stated that the forming of a clay seal is most likely to occur after the storm when the clay platelets settle out of the water made turbulent by the raindrops. If this is so, reduced infiltration capacity and increased splash through the accumulation of a layer of water (Mihara 1951) are not related to clay sealing during a storm.

Yamatoto and Anderson (1973) made an important addition to the information available. They considered the change in the amount of splash through a storm due to the formation of the soil surface into a crust. They found that splash from their samples was maximum during the first three minutes of exposure to the rain. It then declined steadily to the end of the test. A hard crust-like layer formed on the surface of most of the soils. This layer resisted detachment and reduced infiltration rate. This research has specifically avoided these effects by providing a quasi-infinite supply of sand, so that storm-storage effects are not compounded with the effects of depletion of materials and surface armouring.

Section Four Effects of vegetation on falling rain

The purpose of this section of the literature review is to locate, within the suite of interception process areas in which changes to the original rain occurs under a forest canopy. Work has been done under lower plants, such as vegetable and cereal crops, but the effects are strikingly different. Reduction in rainfall volume by a canopy is considered first, this includes measurement of the loss of volume through interception and the effects of changing canopy and rainfall parameters on the amount of loss. Secondly the change in water

reaching the ground as throughfall is considered including the change in drop-size distribution and the change in the spatial distribution of the raindrops.

1) Definition of the interception processes

It is necessary to review, briefly, the terms used in the context of the interception processes. This description largely follows that of Jackson (1975). Unless the canopy cover is 100%, a portion of the rain, the free throughfall coefficient, reaches the ground directly as clear throughfall. The remaining portion strikes the canopy surface at some level. It may strike the surface with such impact that it is not retained, passing to a lower layer and reaching the ground, or it may be retained on the canopy surface. The amount of water held in the canopy will gradually increase until drainage begins. The depth required to wet all the leaf surfaces is termed the canopy capacity. Drainage may simply impinge on lower layers or may reach the ground as re-precipitated throughfall. Part of the drainage may be diverted as stem flow. After cessation of rain, drainage will proceed for a time depending on the environmental conditions. Throughout the storm, and once dripping has ceased, water will be evaporated from the canopy surfaces. Water may also be absorbed into the plant through the leaves (Zinke, 1967).

Rutter et al. (1971) summarised the components of the water balance. Let R, T and E be rates of rainfall, throughfall and evaporation respectively and $\sum R$, $\sum T$ and $\sum E$ be totals of these components in a given time. Let the amount of rain diverted to stemflow be p_t. The interception loss in a storm (I), which is the water intercepted and evaporated between the time when rain begins to fall on a dry canopy and the time when the canopy is finally dry again, may be written as

$$I = \sum E = \sum R - \sum T - p_t \qquad [2.5]$$

Let the proportion of rain which falls through the canopy without striking a surface be p. Then the water balance of the canopy for any period within a storm may be written

$$(1 - p) \sum R = \sum D + \sum E + p_t \pm \Delta C \qquad [2.6]$$

where $\sum D$ is the rate of water draining or dripping from the canopy and ΔC is the change in the amount of water, C, stored in the canopy. Rutter et al. (1971) assumed that there was a minimum quantity of water, S, required to wet all the canopy surfaces. This corresponded to the storage capacity of Zinke (1967) or the canopy saturation of Leyton et al. (1967). At any time C may have values greater or less than S. All the above quantities are expressed as mm depth of water.

2) Measured differences between rainfall and throughfall

i) Total interception loss

Almost without exception the proportion of total rain reaching the ground through a canopy is decreased (Leonard 1967). This is a topic which has been under investigation for a long time by workers concerned with the water balance for forested areas. The usual technique employed is a comparison between precipitation measurements under a vegetation canopy and measurements taken in the open. The average difference between the two is the interception loss (Leonard 1967). Values for interception loss are commonly obtained from a plot of gross rainfall versus throughfall for a number of storms and a given canopy. This is the method used by Gash and Morton (1978) and illustrated in Figure 2.5. A straight line is drawn to envelope all the points; it is assumed to go through only those points representing conditions with minimal evaporation. Storms less than 1.5 mm not considered large enough to fill the canopy capacity are excluded from such calculations. The average interception loss is read from the

Figure 2.5 The relationship between throughfall and rainfall for storms of different size to determine the amount of interception (Gash & Morton 1978)

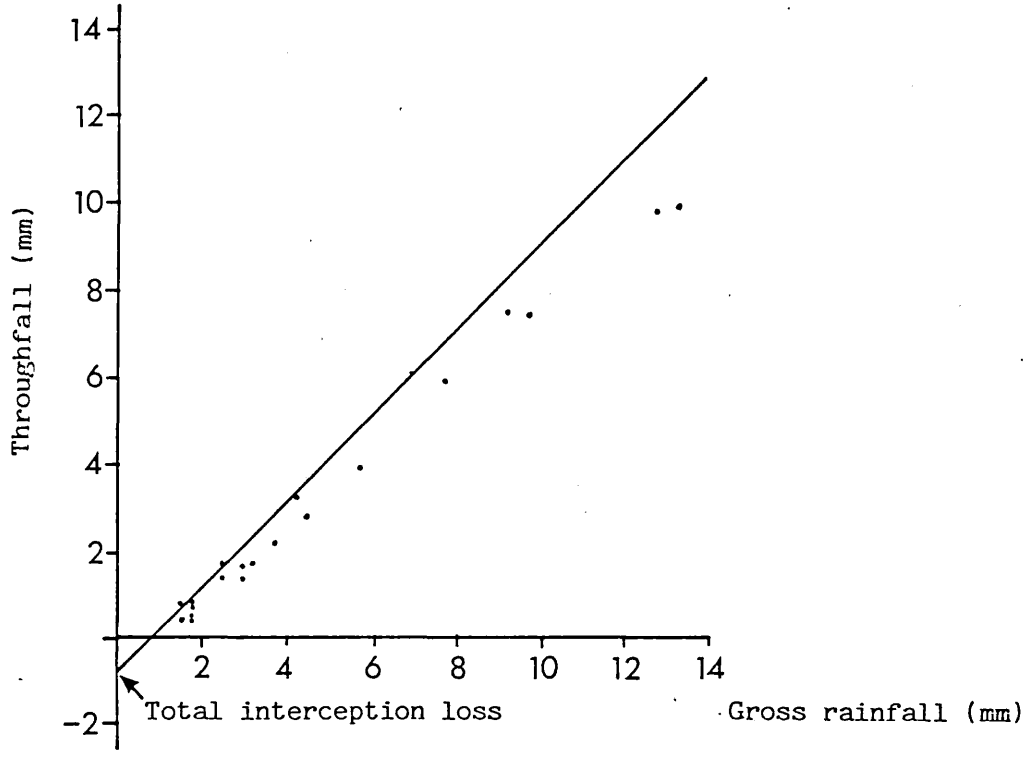

Figure 2.6 The relationship between throughfall and rainfall for storms of different size, including some where there was insufficient rain to saturate the canopy (Rutter et al. 1971)

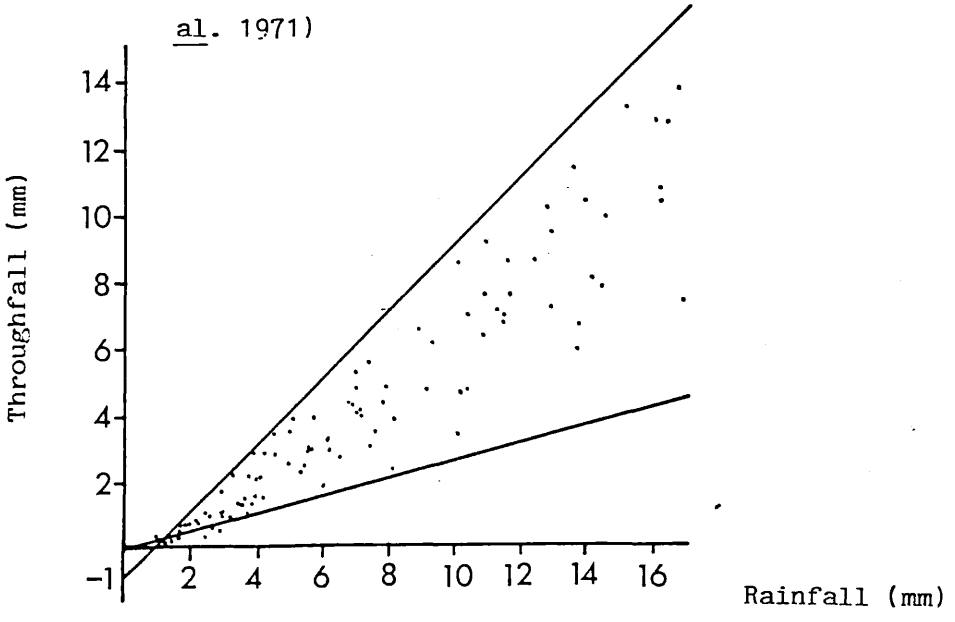

intersect on the throughfall axis.

Zinke (1967) reviewed to date, the American literature on interception loss and quoted a range of depths from 0.25 mm to 9.14 mm for different vegetation types. However he said that "one would not be greatly in error to estimate about 1.3 mm interception loss for most grasses, trees and shrubs". Thompson (1972) measured interception loss specifically under an oak (Quercus robur) canopy. From storms greater than 2.5 mm he calculated total losses of 1.0 and 0.4 mm in summer and winter respectively. Under the tropical rain forest at Reserva Ducke, Manaus, Franken and Leopoldo (1983) estimated an average interception loss of 0.8 mm while, for a nearby site, Gash (unpublished data) estimated a loss of 0.72 mm.

The values for interception loss are surprisingly constant for a wide range of species and plant communities. Tropical rain forest has the highest biomass of any plant community. The relatively low average interception losses here must be due to the specific adaptations of rain forest plants to the rapid shedding of water.

ii) Interception losses to an unsaturated canopy

Interception loss to a given canopy varies according to the rainfall intensity, duration and the interval between storms and will not always be equal to the maximum amounts quoted above.

Rutter et al. (1971) collected data from rainfall and throughfall under a stand of Corsican pine for a series of 24 hour periods including some where there was insufficient rain to saturate the canopy. The throughfall is plotted against rainfall in Figure 2.6. From the origin throughfall increases at first in a fairly constant ratio. Between rainfalls of 1 and 1.5 mm the upper envelope of observations steepened and the values of throughfall for a given value of rainfall showed considerable scatter. It is assumed that the inflection of the upper envelope represented the attainment of canopy

saturation and that to the left of this point the data may be represented by $\sum T = p \sum R$. The canopy parameters influence the point of this inflection for any given rainfall.

iii) Measurement of interception loss to stemflow

Interception measurements often include separate measurement of stemflow to be added to throughfall. Speculation on the relative importance of stemflow has varied greatly and differs according to the plant type. Ovington (1954) gave a value of 0.32% for rainfall diverted as stemflow through Quercus rubra. Other workers confirm this low percentage for other species. Gash and Morton (1978) quoted 2% for Scots Pine and Pearce and Rowe (1981) 1.5% for multi-storied evergreen mixed forest. However some species of plant may concentrate a lot more water into stemflow. Particularly well adapted to this purpose are some rain forest palms (C. Lloyd pers. comm.).

3) Evaporation of intercepted water during and after a storm

A major term in the water balance equation [2.6] is the evaporation of intercepted water. The depth of water retained on the canopy at the end of the storm will ultimately be evaporated and evaporation may also take place from the leaves during a storm.

i) Methods of estimation

Two approaches to estimating the evaporation of intercepted water from the canopy will be reviewed here. The first is a rigorous physically based but data demanding model, the second an analytical model which is a simplification of the first, requiring much less data.

Rutter et al. (1971) constructed a model which calculated an

hourly water balance for a canopy using data which described the atmospheric conditions. They assumed that there is a potential evaporation rate E_p which obtains when all canopy surfaces are wet, that is when C is greater than S. E_p could be calculated from

$$E_p = \frac{(s\ R_n + c_p\ d\ \frac{D}{r_a})}{(l\ (s + g))} \qquad [2.7]$$

where c_p = specific heat of air at constant pressure (J/kg/K)
R_n = net radiational energy (W/m^2)
r_a = aerodynamic resistance (s/m)
d = vapour pressure deficit (m bar)
g = psychrometric constant (m bar/K)
s = slope of saturated vapour pressure curve (m bar/K)
l = latent heat of vaporization of water (J/kg)
d = density of air (kg/m^3)

When C is less than S Rutter et al. (1971) assumed that

$$E = E_p \times \frac{C}{S} \qquad [2.8]$$

This somewhat arbitrary assumption has been shown by Shuttleworth (1978) to lead to a theoretically reasonable description of evaporation from a partially wet canopy. Hence a running water balance of a forest canopy of known structure may be calculated, thereby producing an estimate of water loss.

Gash (1979) assumed that evaporation from the wet canopy occurred at a fixed rate equal to the average rate of evaporation from the wet canopy ($\bar{E}$). The average evaporation rate $\bar{E}$ is obtained from a regression of interception loss on gross rainfall for a period outside the time span for which loss estimates were made. Gash showed that $\bar{E}$

is equal to the slope of such a regression multiplied by the average rainfall rate during the events used in calculating the regression. He assumed that the logarithmic dependence of the drip rate on the degree of canopy saturation observed by Rutter et al. (1971) means that there is virtually no drainage from the canopy before it is saturated and that the amount of water on the canopy at the end of the storm is quickly reduced to S, the minimum value necessary for saturation.

Hence for storms sufficiently large enough to saturate the canopy

$$I = a P_g + b \qquad [2.9]$$

then

$$\bar{E} = a \bar{R} \qquad [2.10]$$

where P_g is the gross rainfall, $\bar{R}$ is the hourly mean rainfall rate sufficient to saturate the canopy and a and b are coefficients of regression.

Evaporation from a partially wet canopy was assumed to be similar to that predicted by Rutter et al. (1971) [2.8] where

$$\bar{E} = \frac{C}{S} E_p \qquad [2.11]$$

ii) Estimates of evaporation

Gash et al. (1980) calculated the rate of evaporation of intercepted water for three sites in Britain with spruce and pine canopies. They suggested that there was a small range of variation between the optimised values of $\bar{E}$ despite a large range of altitude and latitude. It was suggested that the major cause of variation in the absolute magnitude of interception loss across Britain was not a

result of variation in the rates of evaporation, but rather of the size of the canopy capacity and the length of time over which evaporation occurred during saturated conditions. Gash et al. (1980) suggested a mean optimised value of $\bar{E}$ = 0.22 mm/hour for the climate of Great Britain.

Shuttleworth et al. (1984) suggested that although in temperate forests the interception component can make an important and possibly dominant contribution to total evaporation, interception is of less relative importance in the humid tropics. They carried out detailed measurements of evaporation of both transpired and intercepted water at Reserva Ducke, Manaus. Preliminary estimates suggested a total daily evaporation of 3.73 mm for the period of study with about 0.25 mm of that coming from the evaporation of intercepted water (J. Gash pers. comm.). Gash suggested that this amount is more constant in the tropical rain forest than in temperate forests. The temperature regime, size, duration and frequency of storms in the rain forest tend to be more predictable.

4) Effects of canopy parameters on throughfall

i) Canopy density

The denser a canopy the greater the probability of any drop being intercepted. Rothacher (1963) measured average crown density with a spherical densitometer (Lemon 1956) and related it to the average throughfall using a linear regression. For six plots Rothacher reported an apparently linear relationship with a correlation coefficient of 0.87.

Gash and Morton (1978) measured the percentage canopy cover, recording the presence or absence of leaves and branches above 496 points within their sampling area. From this they concluded that the free throughfall coefficient was 26% of the rainfall. However a

regression of throughfall on rainfall for all those storms insufficient to saturate the canopy capacity implied a value for the free throughfall coefficient of 32%. Gash and Morton concluded that often an estimate of percentage cover is not sufficient to estimate the amount of throughfall when the storms are too small to saturate the canopy. They suggest that changes in the canopy depth and angle of falling rain account for the differences in the estimates.

Schottman (1978) reviewed work using models predicting the penetration of light through a canopy and stated that the techniques were directly applicable to predicting the percentage of raindrops which will avoid striking a leaf. However, most of the models have assumed a uniform leaf distribution, with each leaf having an equal probability of being located anywhere within the canopy. In fact the key to the prediction of interception lies in the orientation of the leaves and the orientation of the drops. Steeply inclined leaves afford less protection than horizontal ones. Nearly half the vertically falling raindrops would be predicted to penetrate a canopy having a leaf area index of 3.0 and average leaf inclination of 75%.

ii) Canopy storage capacity

Canopy storage capacity has been defined by Horton (1919) as the depth of water on the projected area covered by the plant which can be stored or detained on the plant surface in still air. Rutter et al (1971) defined it as the amount of water required to wet all the canopy surfaces. Grah and Wilson (1944) distinguished three states of canopy storage "transitory storage" from which water will drain away under still air conditions; "conditional storage" from which water can be removed by wind or shaking; and "residual storage" from which water can only be removed by evaporation. It is clear that the canopy capacity has an important effect on interception loss, particularly in small storms. Indeed Gash (1979) stated that earlier writers have often equated interception loss with canopy capacity. The review by Zinke (1967) contains many such examples.

iii) Changes in canopy storage by accumulation and drainage

The amount of water stored in the canopy (C) may at any time be greater or less than the storage capacity (S) (Rutter et al. 1971). Gash (1979) defined the rate of accumulation of water in the canopy, assuming there is no drainage until the canopy is saturated, thus

$$\frac{dC}{dt} = (1 - p - p_t)\,\bar{R} - \left(\frac{\bar{E}}{S}\right) C \qquad [2.12]$$

The assumption that there was no drainage until the canopy was full does not agree with the findings of many other workers. Herwitz (1985) subjected the leaves of a number of saplings taken from a tropical rain forest in Queensland, to artificial rain of intensity 85 mm/hour and drop size diameter of 2.7 mm. He recorded the accumulation of water on the leaves. In all cases drainage started within the first 30 s of the experiment. After 30 s less than 35% of simulated rain was detained. Most of the saplings had more than 50% of their storage capacities filled after 7 mm and 80% after 20 mm. He also concluded that the canopies did not become saturated as early in the storm as had been previously proposed. All the saplings continued to accumulate water after at least 40 mm of simulated rain.

Both drainage and accumulation may be taking place at different parts of the canopy at any given time and generally the rate of accumulation has been described with some form of inverse exponential function. Merriam (1973) used such a function, describing the accumulation thus

$$C = S\,(1 - e^{Pg/S}) \qquad [2.13]$$

Massman (1980) modelled the accumulation of water in the canopy in terms of a dimensionless constant (a) which depended on the tree

species and the meteorological conditions (Figure 2.7). The general relationship, assuming the rate of drainage is proportional to the rate of interception, is expressed thus

$$D(t) = I(t) \frac{(e^{a(C/S)} - 1)}{(e^{a} - 1)} \qquad [2.14]$$

where $D(t)$ = drip rate
$I(t)$ = interception intensity
C = amount of stored water
S = maximum storage

During an initial phase, immediately after rain begins all curves are nearly linear. As time progresses all solutions tend to unity but (a) strongly influences how the curves approach this limit. The extreme "cup" solution (as (a) tends to infinity) represents a situation where there is no drainage from the canopy until it is full and then it overflows. All other "leaking cup" solutions represent situations where water is draining out as the canopy is filling.

The drainage rate has been considered both through measurement and theoretical modelling. The rate is changed by the rate of addition of water to the foliage and the way in which the foliage reacts to that input.

Dripping rate was been considered in a general mathematical model by Massman (1980) similar to the model for accumulation. He made a common basic assumption that drip rate is proportional to the amount of water stored in the tree. When the tree is initially dry, the drip rate is zero. When the maximum storage is reached the drip rate is equal to the interception intensity.

Rutter et al. (1971) stated that the drainage rate (D) is linearly related to the amount of water on the canopy (C) by a drainage

Figure 2.7 Accumulation of water on the canopy as modelled by Massman (1980)

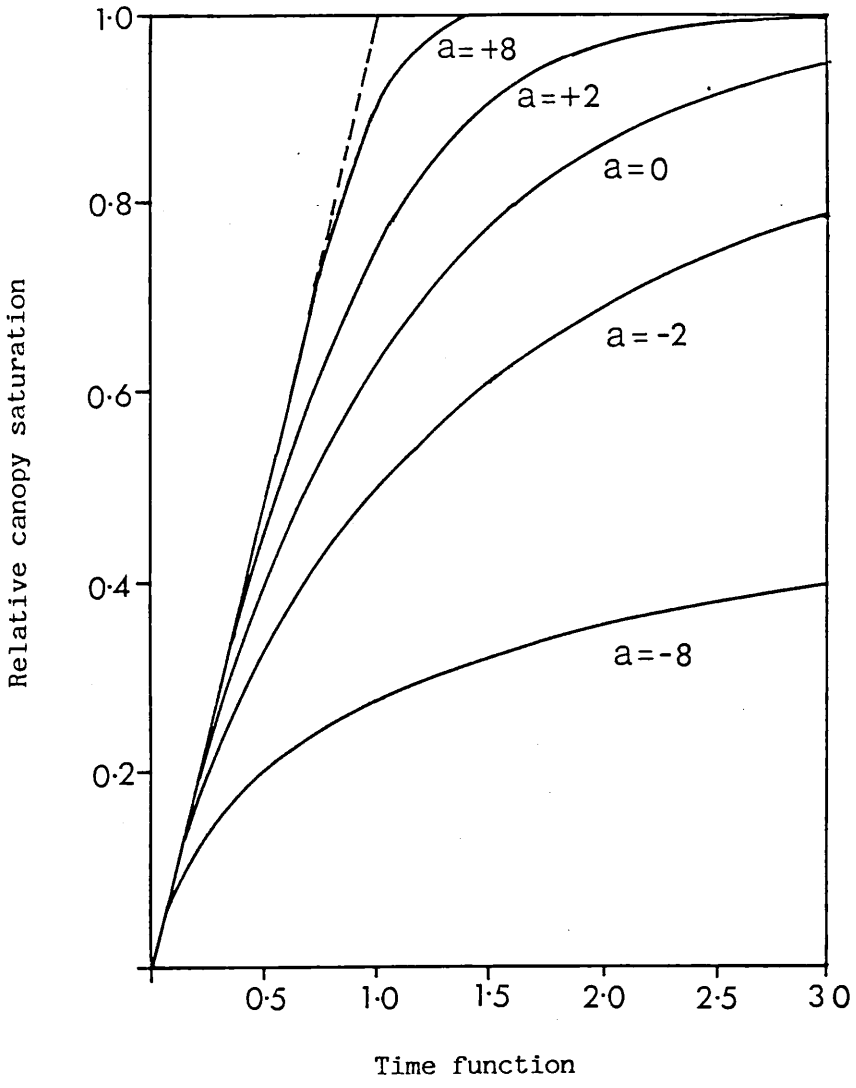

drainage coefficient b such that

$$D = \exp (a + b\ C) \qquad [2.15]$$

From experimental results illustrated in Figure 2.8, Rutter et al. (1971) have suggested the following draining reaction from a given canopy of capacity 1.5 mm under storms of varying intensity. Throughfall is less than rainfall while the water accumulates on the canopy. Thereafter rainfall and throughfall are approximately equal. The water content of the canopy depends on the rainfall intensity. The graph shows that under rainfall intensities of 12 mm/hour and 1.2 mm/hour, the canopy may reach a steady water content of 2.3 mm and 1.6 mm respectively. This corresponds to the transitory storage phase of Grah and Wilson (1944). However when rain ceases, water in excess of 1.5 mm drains off very rapidly so that after 20 to 30 minutes drainage the water on the canopy is almost independent of the value from which the decline began.

Interestingly, Herwitz (1985) noted that post rain drainage from the saplings subjected to simulated rain was negligible although vigorous shaking consistently removed more than 50% of the volume detained in still air.

iv) Sensitivity of interception loss to variation in canopy parameters

Gash and Morton (1978) assessed the sensitivity of the Rutter interception model to the canopy structure parameters storage capacity (S) and the free throughfall coefficient (p) holding the meteorological and rainfall data constant. The aim was to provide an insight into the likely variation of interception loss which might be expected between different species of trees growing in the same geographical location. It was shown that the interception loss is

Figure 2.8 Accumulation and drainage from a canopy under different rainfall intensities (Rutter et al. 1971)

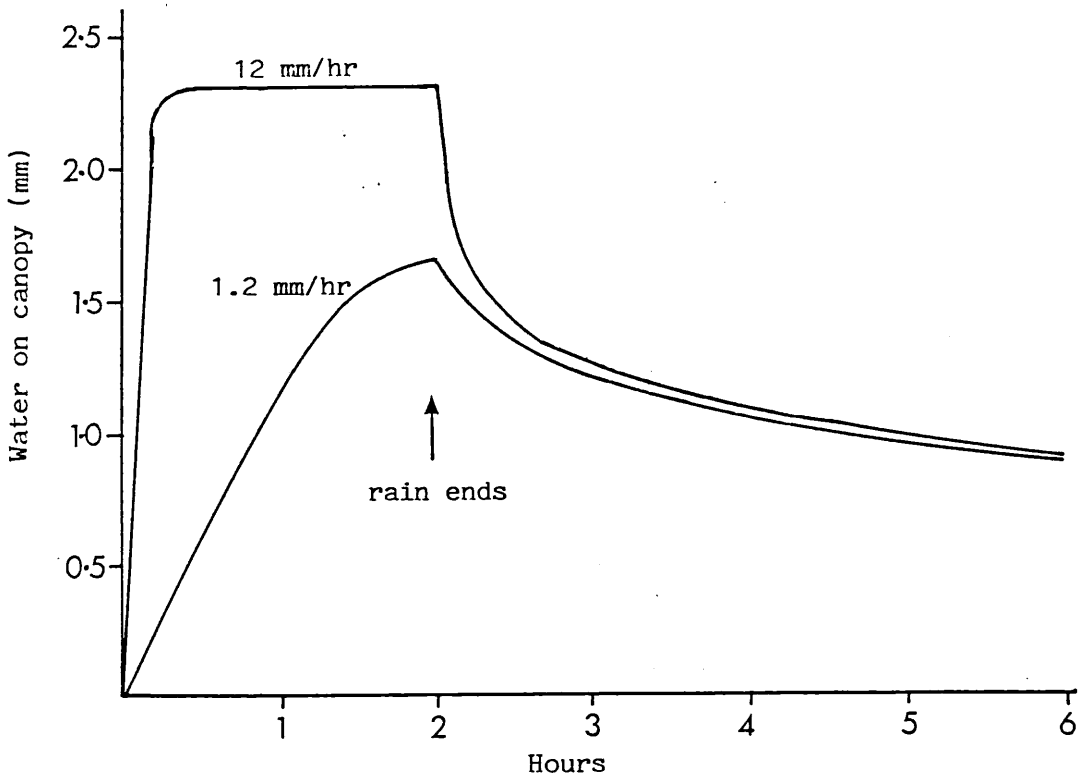

relatively insensitive to both S and p. For example a change of 50% in S at p = 0.3 produced a variation in the interception loss of 15%. A change of 50% in p produced a variation in the interception loss of 7%.

Gash and Morton (1978) explained the low sensitivity of the model to changes in canopy structure in terms of the relative sizes of rainfall and evaporation. Except under conditions of very light rain, the rainfall rate will always exceed the evaporation rate and the canopy will remain wet during rainfall. The evaporation rate will then depend on the meteorological variables. The influence of canopy structure on long term interception loss should be restricted to periods of rain falling in small showers or at low rates and the small amount of water left on the canopy after rainfall has ceased.

v) Effects of rainfall parameters on throughfall

Interception loss has been successfully correlated with rainfall intensity and amount. Research has suggested that after it has been saturated, the canopy intercepts a decreasing proportion of the gross rainfall.

Ovington (1954) measured throughfall under thirteen different canopies including two of oak, making comparisons with open rain. He concluded that for a given canopy the intensity of the rainfall is the most significant factor controlling the retention of water by the tree canopy. Figure 2.9, plotting the percentage of gross open rainfall to be intercepted by the two oak canopies for storms of varying intensity, shows that a greater percentage of the gross rainfall is retained by the canopy in a light shower than a heavy one.

Rothacher (1963) correlated storm depth with throughfall under a Douglas Fir canopy. He found that storm depth accounted for 96% of the variation in throughfall in the summer. Figure 2.10 shows the relationship between throughfall as a percentage of rainfall and gross

Figure 2.9 Percentage of gross rainfall to be retained on an oak canopy after rains of varying intensity (Ovington 1954)

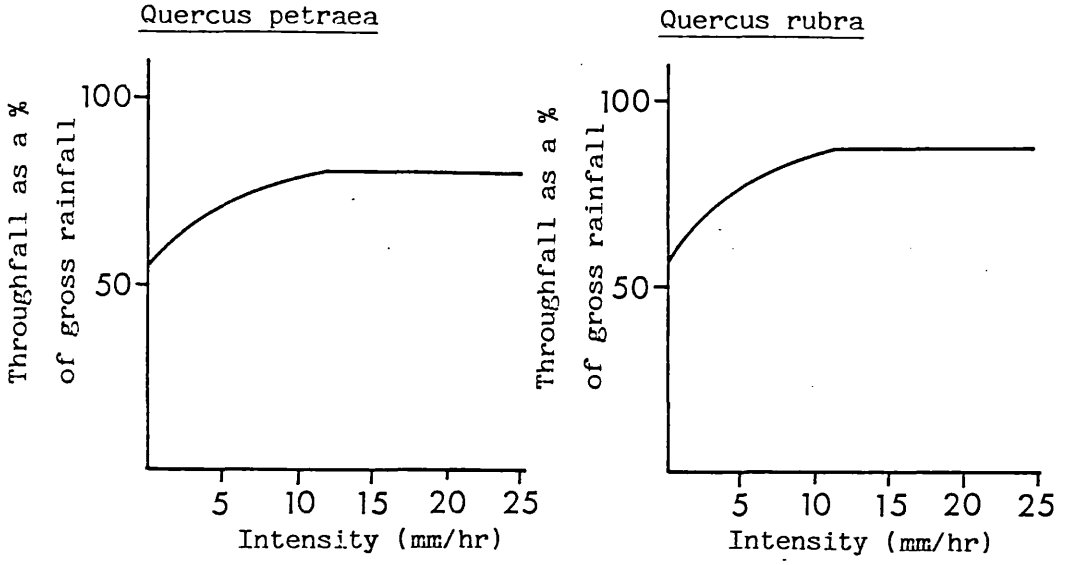

Figure 2.10 The increase in throughfall as a percentage of gross rainfall under a Douglas Fir canopy (Rothacher 1963)

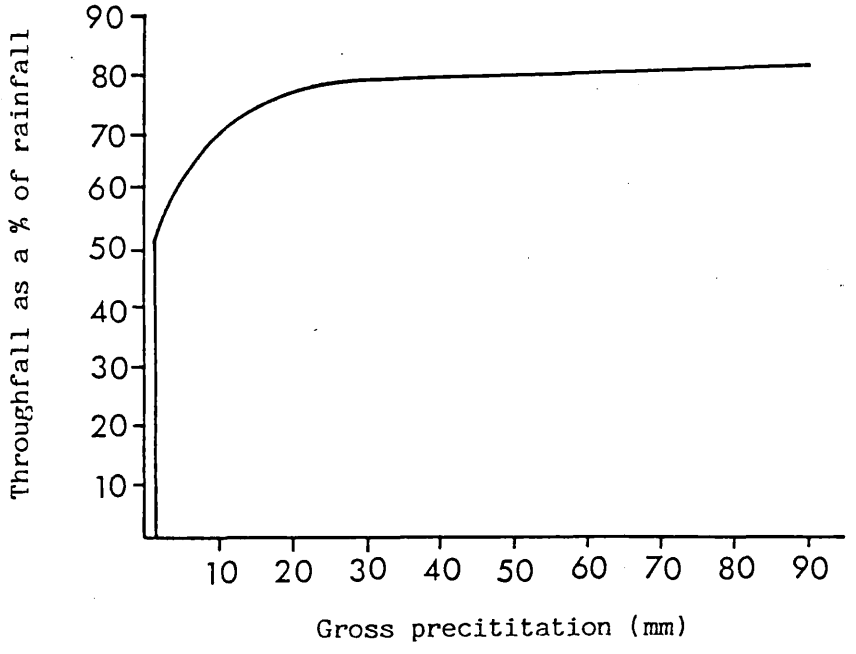

rainfall.

Leonard (1967) stated that canopy storage will be a function of, among other things, storm intensity and size to the point of maximum storage. He quoted previous work also suggesting that interception of precipitation takes the form of an exponential curve in the same manner as here suggested by Ovington and Rothacher.

An explanation for these observations is more recently given by Rutter et al. (1971). From the start of rain until the canopy capacity is filled, throughfall will be less than rainfall, depending on the canopy cover. Thereafter rainfall and throughfall are approximately equal. The longer the storm continues with rainfall equal to throughfall, the smaller will be the proportion of rain lost to interception.

5) Change to the drop-size and spatial distributions of the throughfall

A canopy may change the total drop-size distribution of rain in three ways. It can alter the proportion of rain falling straight through the canopy and hence remaining unchanged. It can shatter raindrops into drops of smaller size. It can combine raindrops into larger units.

i) General observations

Before Chapman (1948) it appears that there was no quantitative information published on the size of raindrops under forest canopies. Numerous writers have observed and recorded the fact that raindrops under forest stands are frequently much larger than the largest raindrops falling in the open. Using the flour pellet technique described below, Chapman measured the drop-size distribution of rain both in the open and under a canopy of red pine. Following the theme

suggested in Laws and Parsons (1943), relating median drop size to rain intensity, Chapman recorded the drop-size distribution under a variety of rain intensities. His results are presented in the Figure 2.11.

Chapman concluded that the most noticable feature of the curves of throughfall drop sizes is their flatness indicating a tendency for more or less equal distribution by volume of rain among drops of all sizes. Thus under a pine canopy a much greater percentage of the total volume of water falls in the form of large drops. Furthermore the distribution curves indicate that the intensity of rain, within the range measured, has little effect on the size characteristics of raindrops under the canopy.

Ovington (1954) measured the drop-size distribution under saturated canopies of thirteen tree types, together with rain in the open, within as short a time as possible. To measure the drops he used the paper staining method described in the techniques section below. The results are illustrated in Table 2.4. In the forest plots the majority of the falling water drops were within the range of drops falling in the open, but there were also an additional number of larger drops. He suggested that these large drops were formed by smaller drops uniting on the canopy. Although their numbers were few, they usually constituted the greatest weight of water falling in the forest plots.

An indirect confirmation of this increase in drop size under a forest canopy comes from the distribution of plants such as Tirella which have a spring-board mechanism for seed dispersal which requires being dropped on by large raindrops (Saville and Hayhoe 1978). Generally such species are limited to forest environments "because of the enormously greater effectiveness of drops falling even from a low canopy than that of raindrops".

Figure 2.11 The percentage of total volume of rainfall contributed by drops of various sizes in the open and under a Red Pine canopy for storms of different intensity (Chapman 1948)

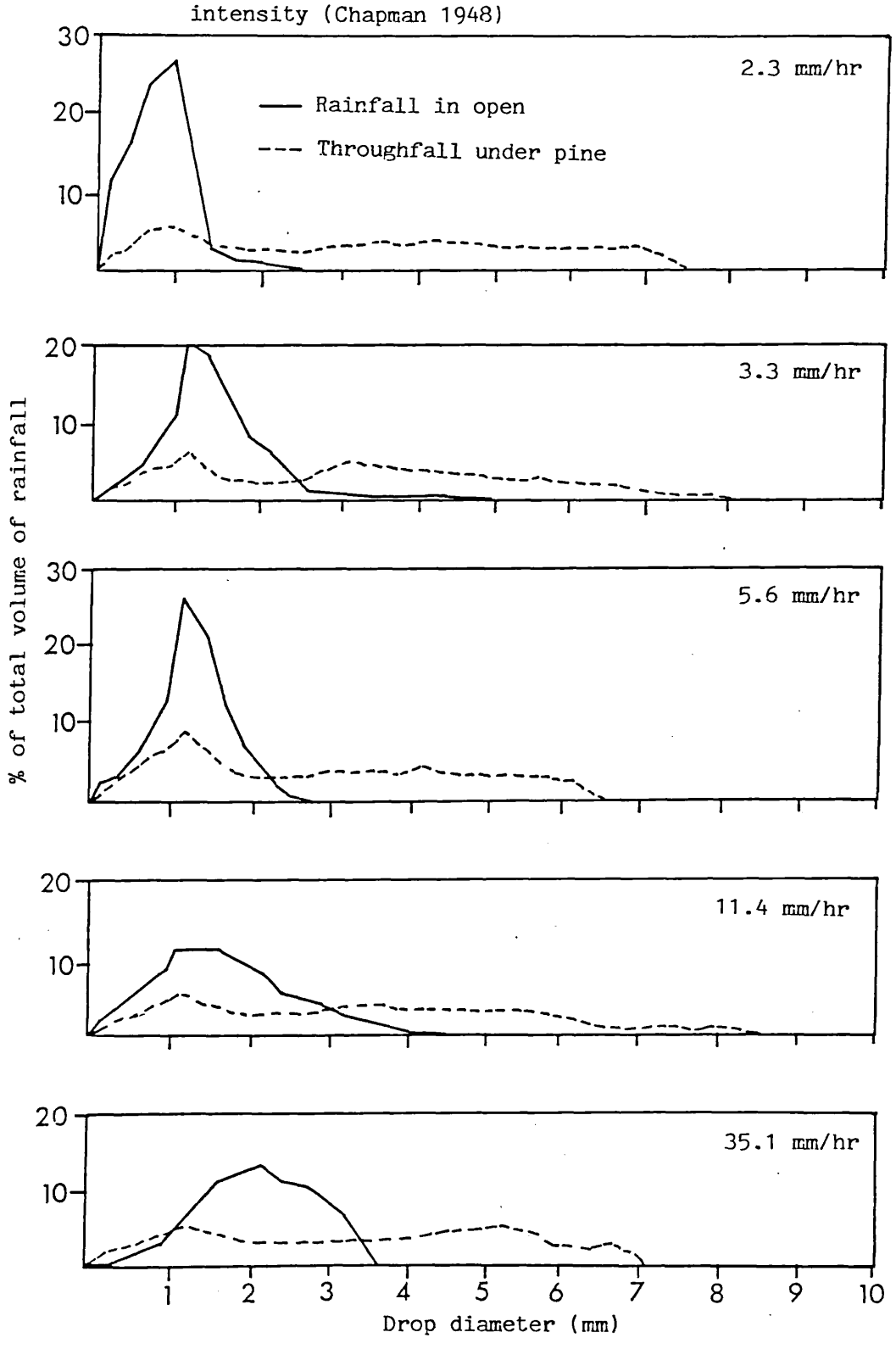

Table 2.4 Numbers of drops of different sizes falling in the open and under two oak canopies (Ovington 1954)

Site	Diameters of raindrops on filter papers (mm)										
	1-5	10	15	20	25	30	35	40	45	50	%
open rain	1920	78	3								
Q. petraea	1900	66	13	2	5	3	3	5	1	2	67
Q. rubra	178	136	31	20	11	6	9	3	2	1	68

% = % weight of drops greater than those falling in the open

ii) Effects of leaf characteristics in changes in drop-size distribution

Schottman (1978) stated that most leaf surfaces are sufficiently rough for a splash crown to be formed from an impacting drop. The size of ejected droplets depends on the development of the crown. In contrast small drops of low velocity such as may fall from a leaf above will tend to spread out on impact and will not break into smaller droplets.

From observations of water splashing on inclined leaf surfaces Schottman concluded that the point of impact on unsupported leaves was critical. If the drops fell at any point away from the main vein then the leaf deflected enough to allow the water to flow off with negligible velocity changes, the drop fragmenting. However, when struck near its middle the leaf flexed, absorbed the momentum and acted as an effective trap for drop fragments.

Examining the build up of water in storage from fog on artificial leaves Merriam (1973) stated that the differences in the shape of leaves with the same surface area had a pronounced effect on the water storage capacity. Leaf shapes imitating clusters of needles showed a tendency to store more water which bridged the gaps between needles. The moment of drainage from a leaf will depend upon a balance between forces adhering the drops to the leaf such as surface tension, and forces tending to shed the water, such as angle of inclination of the leaf and weight of the water droplet.

Work by Williamson (1981 and 1983) using leaves with drip tips showed that the width of the leaf, measured 3 mm from its tip, is highly correlated with the drop size (Figure 2.12). Williamson also studied the effect of removing a leaf drip tip on the length of time it took for the first drop to fall. He found the initial drop fell more quickly when the tip was excised and attributed this to a decreased distance of travel. However the fact that smaller drops fell from leaves with drip tips indicates that generally the rate of

Figure 2.12 Drop size as a function of (log_{10}) leaf width, measured 3.0 mm from the end of the leaf (Williamson 1981)

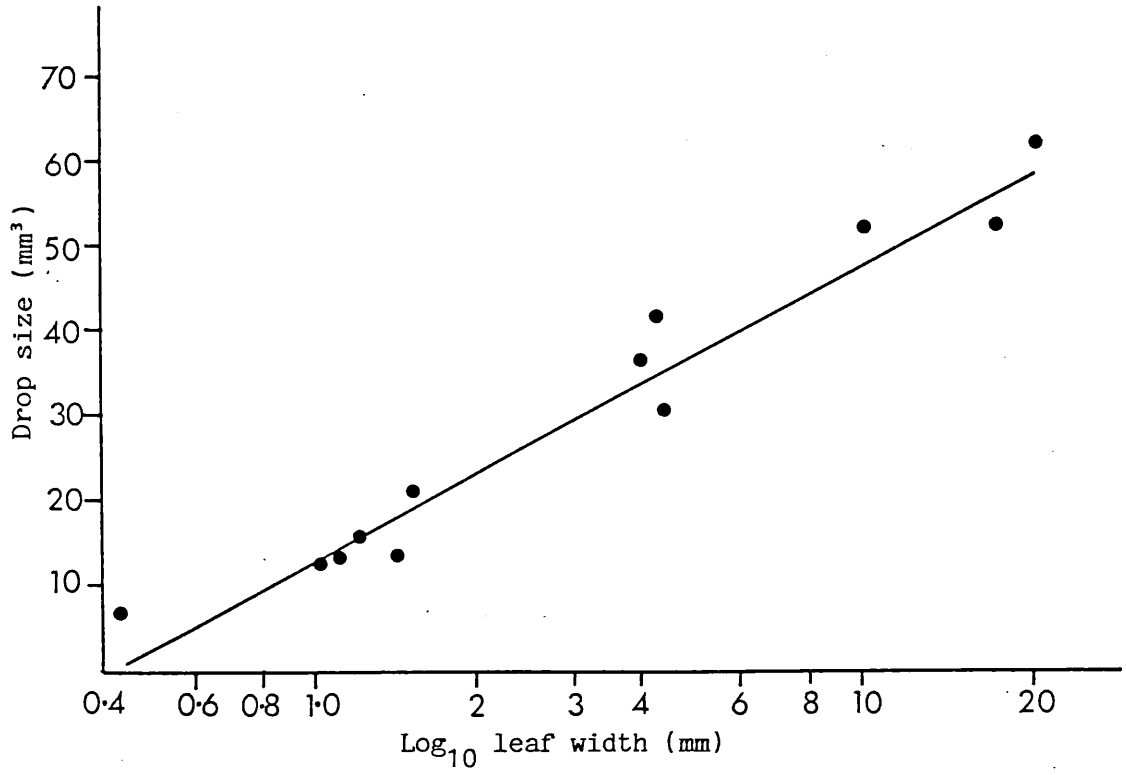

drop fall will be more rapid for smaller drops.

iii) Change in the spatial distribution of water

A vegetation canopy also has the effect of redistributing the rain water, concentrating it in some patches and diverting it from others.

Ovington (1954) considered the change in spatial variability under the canopy and in the open. Figure 2.13 shows the spatial variability of the rain gauge depths, expressed as the standard deviation of the values, against the intensity of the rain. All the graphs show a linear increase in spatial variation of water depth with an increase in intensity. However the rate of the increase is greater under the vegetation. The unevenness of the water distribution in the forest results primarily from the concentrated dripping of water from the canopy and will be especially marked where there is little wind to move the canopy.

Reynolds and Leyton (1961) and Voigt (1960) have looked at the relationship between throughfall and distance from the trunk of a single tree. Figure 2.14 shows that there was a drip zone located near the edge of the crown where higher rainfall was found than in the gaps. However the most marked discontinuity in the pattern occurred near the stem where water, trickling down from the stem concentrated over a small but ill-defined area round the base.

Voigt (1960) found the same pattern measuring the soil moisture under tree crowns. The high concentration of water near the base, lower soil moisture under the crown and increasing towards the crown edge. The clearest illustration of canopy effect was from a single storm of more than 51 mm under a canopy of 90% cover.

Figure 2.13 Spatial variability of rainfall and throughfall depth under an oak canopy for rain storms of increasing intensity (Ovington 1954)

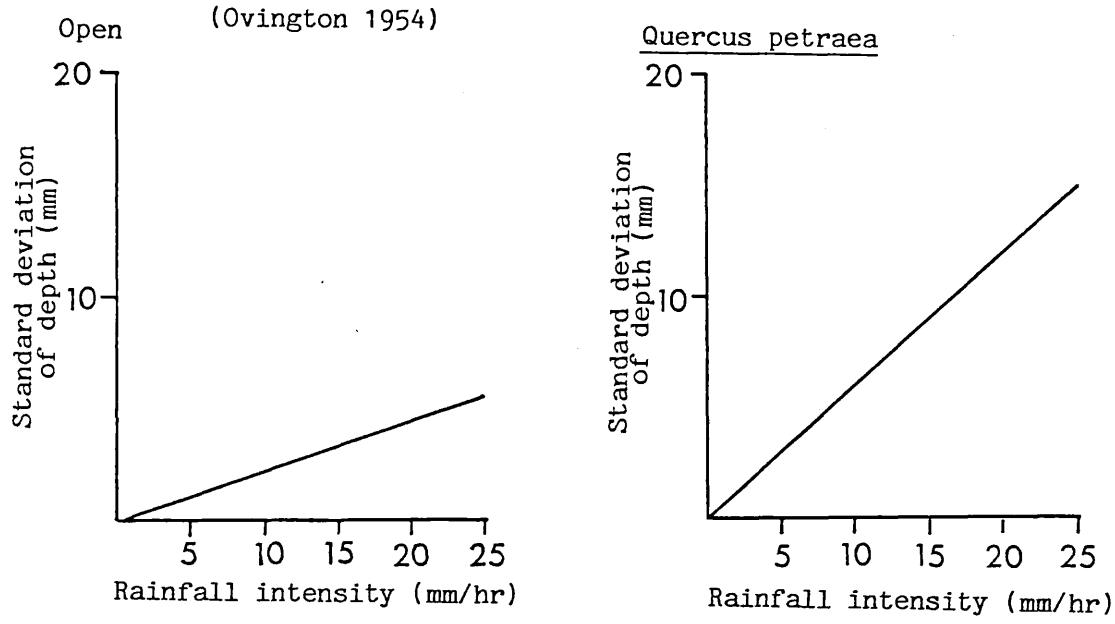

Figure 2.14 Depth of throughfall related to distance of gauge from the stem of a tree (Reynolds & Leyton 1961)

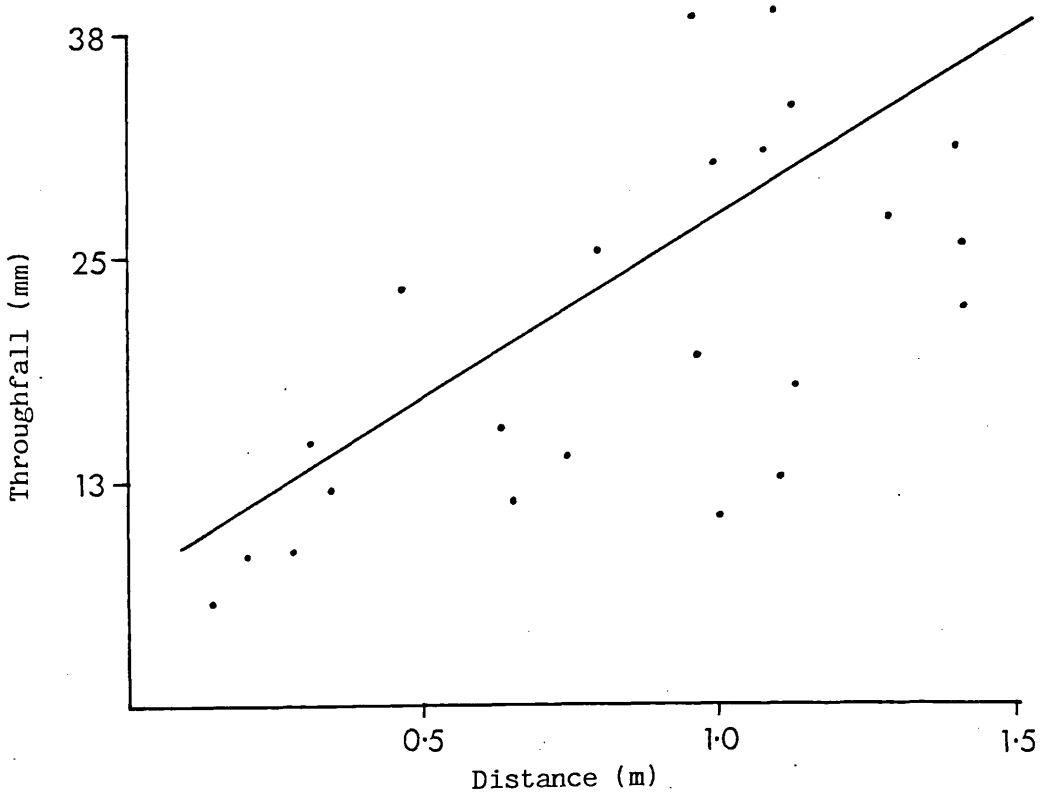

Section Five Effects of the impact of water on soil movement

The aim of this section of the literature review is to consider the effect of changing raindrop size and velocity on the amount of soil material splashed. First an understanding is sought of the mechanics of rain splash in literature describing a water drop splash. The forces operating in the splash are located and estimated and finally the process of entrainment of soil by splash are reviewed. Having considered the mechanisms of the splash process it is then possible to review the more extensive literature which relates the erosivity of rain, however it is defined, to rain splashed soil movement.

1) The splash of a liquid drop

i) A description of water drop splash

The appearance of a water drop splash has been described in two ways. Firstly from observations of high speed photographs and secondly by numerical simulation. Harlow and Shannon (1967) used the numerical "marker and cell" technique. The moving drop is divided into a number of cells. For each cell the velocity and pressure are calculated for some small time t, and then recalculated for t + 1. Repeated calculations reveal changes in the shape of the drop. Mutchler (1967) used a high speed photographic technique. Both techniques reveal similar patterns of movement.

Following the impact of the drop with a hard surface, horizontal flow away from the point of impact is resisted by the surface which causes the splash sheet to rise and form a corona. As the sheet flows and becomes thinner, fluid threads are formed which in turn break into droplets. Once the water drop's energy is expended, sheet flow ceases and the splash shape collapses. When the drop falls into deep water Park et al. (1982) reported a return flow on the collapse of the

corona to the point of impact. Such a return flow is called a Raleigh Jet. However it is uncertain whether the Raleigh Jet exists on relatively dry soil surfaces.

ii) Estimating the forces involved

The same two methods, numerical and photographic have been used to estimate the location and size of the forces involved during a splash. Ghadiri and Payne (1979), using the high speed photographic technique to calculate the velocity of the water, measured the impact of water drops on several different surface textures. On all surfaces and within 0.1 m secs of impact, a sheet of water moved outwards at 45^{o} with a velocity of three times that of the impact velocity. The impact stress, force per unit perimeter and kinetic energies calculated are presented in Table 2.5. It was originally assumed that the impact stress was uniformly distributed over the surface of the impact. However the increase in impact stress with a decrease in drop size suggested that the impact stress was higher round the periphery of the drops.

Huang et al. (1982) used the "marker and cell" technique in calculating the change in velocity and pressure in different components of the drop on impact. Like Ghadiri and Payne they found that as the impact progressed, velocities of components at the contacts were laterally dominant, but with values ranging from near zero at the contact centre to 1.9 times the initial impact velocity at the contact circumference. After 18 micro-seconds a jet stream started to develop with a velocity 2 times the impact velocity. Within 1 micro-second, extremely high pressures were calculated at the impact surface. This high pressure diminished within 4.8 micro-seconds. The stress distribution was not uniform on the impact surface, the maximum stress being calculated at the contact circumference. Huang et al. believed that the large shearing stress of the lateral jet moving across the irregular soil surface is the most important process in soil detachment by raindrops.

Table 2.5 Impact stress, force per unit of perimeter and kinetic energy of falling drops of different size (Ghadiri and Payne 1979)

Drop diameter (mm)	Stress (kN/m^2)	Force/perimeter (N/m)	Kinetic energy (mJ)
6.1	15	23	1.3
5.4	25	33	1.5
5.3	26	39	1.5
4.6	27	31	1.1
4.5	25	28	0.9
3.3	31	25	0.4

In conclusion, upon impact there is the development of very high pressure at the impact surface. This rapidly diminishes and there is the development of a high velocity lateral jet with high shearing stress. Micro-irregularities in the soil surface may deflect the jet upwards to form a corona from which droplets may become detached.

2) The process and magnitude of soil detachment

i) The formation of a splash crater

Mihara (1951) using high speed photography noted that at early stages of impact a drop simultaneously penetrates the sand surface and spreads out. The depth of penetration depends on the sand surface conditions, especially the water content. The bottom surface of the crater was found to be convex rather than flat. The crater depth decreased with increasing sand compaction and decreasing velocity of the impacting drop. The cavity diameter was slightly larger than the diameter of the drop and increased as the velocity of the drop increased.

From the results of high speed photography of splash on soils of different shear strength and from soil mechanics principles, Al-Durrah and Bradford (1981) proposed a mechanism of splash due to raindrops impacting onto saturated soil surfaces. A schematic diagram of the splash mechanism is given in Figure 2.15.

At the instant of impact the pressure and shear stress distribution are symmetrical about the centre of impact. As already shown above, the peak pressure occurs at the circumference of the contact surface and diminishes in about 6 to 10 micro seconds. For such high rates of load application on saturated soils there will not be enough time for drainage to take place since the external loads change at a rate much faster than the rate at which the pore pressure can dissipate. Under this condition the impact area will be strained vertically and the change in shape will be compensated for by the

Figure 2.15 Schematic diagram of rain splash (Al-Durrah & Bradford 1982)

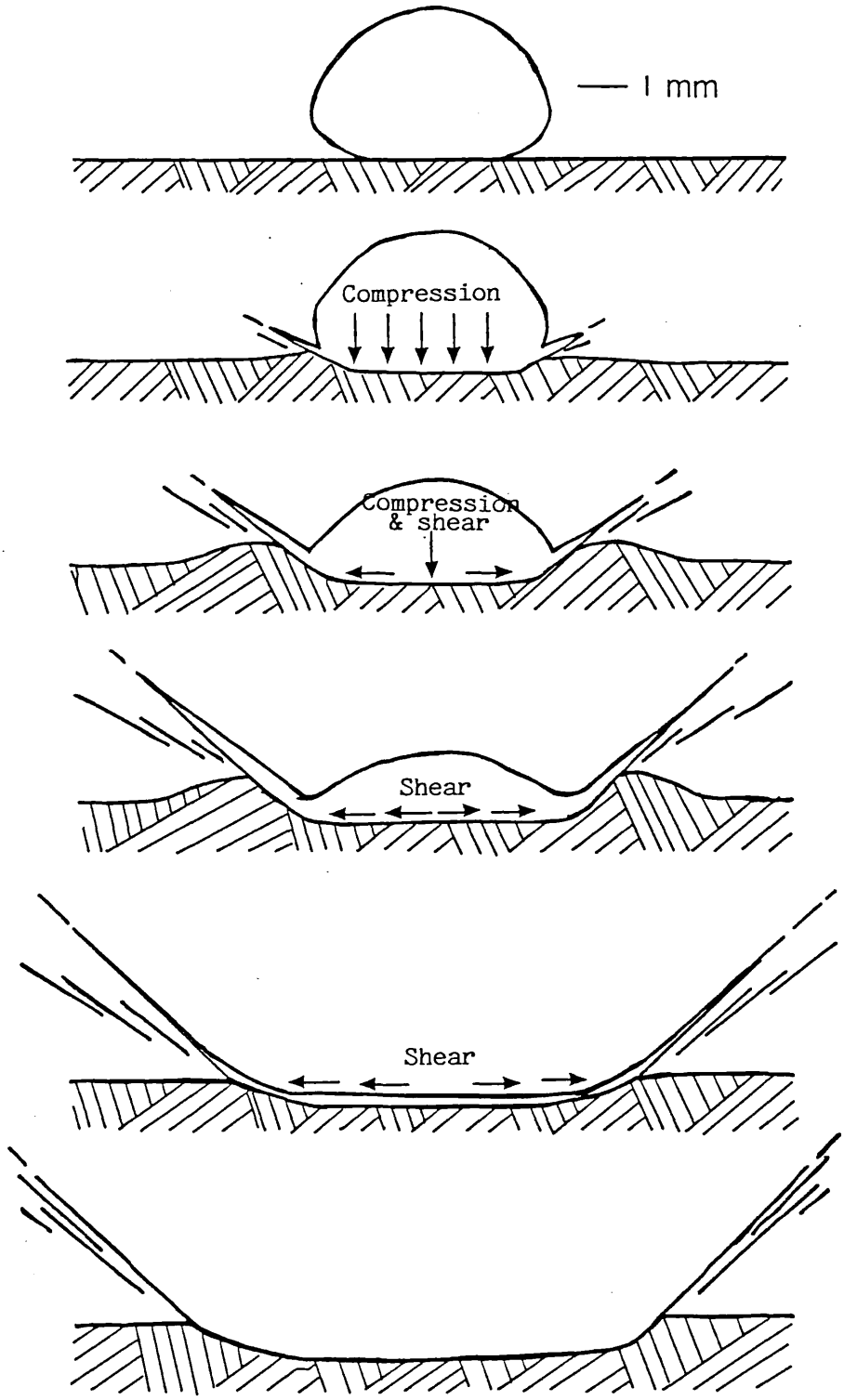

development of a bulge around the perimeter of the depression. The magnitude of the vertical strain and area of application are determined by the raindrop size and velocity at the instant of impact.

The compressive stresses are transformed into shear stresses due to the lateral jetting water with a greater velocity than the impact velocity. The shear stresses act on the bottom and sides of the cavity and on the circular bulge. The amount of detachment is determined by the magnitude of soil deformation that took place earlier and by the cohesive forces resisting shear stress. The greater the depth of cavity and size of bulge, the larger is the splash angle as a result of the greater interception of lateral flows.

Ellison (1947) examined photographs of splashing soil and found that most of the soil splash trajectories are parabolic, their length being four times the height. Since then the angle of splash has been examined in much greater detail.

Al-Durrah and Bradford (1981) found that soil strength influenced the angle of the splashed drops. The greater the depth of water drop penetration into the soil surface, the larger the volume of soil pushed to the bulge around the perimeter and hence the greater the splash angle. The size of the splash angle was shown to be related to the weight of material splashed with higher angles associated with more soil splash. Splash weight is also related to the process of detachment due to lateral flow across the crater boundary. It may be concluded from their work that the lower the shear strength of the soil, the higher the splash angle and the greater the amount of splash.

ii) Splash corona development and soil detachment

Apart from the influence of crater size on splash angle and hence splash weight, there is also a relationship between factors affecting

the growth of the corona and splash weight. Ghadiri and Payne (1979) reported that the time during which splash droplet formation continues is important in determining the size of droplets released. If splash ceases before droplets are formed, which are equal in size to the surface solid particles, then no movement of the solid occurs. On fine sand (200 micrometers) at 10 cm water tension, splash ceased 3 milliseconds after the impact. The largest drops formed were 0.2 mm diameter. On the same surface covered with 2 mm of water, splash continued for 80 milliseconds and droplets of 2 mm diameter were formed. The largest amounts of solid particles were lifted when the surface was just saturated but not submerged; conditions which combine moderate duration of splash with no cushioning effect of surface water (Park et al. 1982).

These results support the work of many earlier workers (for instance Palmer 1965) who have reported increases in amounts of splash with slight increases of water level. Park et al. (1982) ascribe this change in ability to move material to a change in the method of movement or erosion domaine. From the drop-solid interaction where momentum is conserved like colliding billiard balls, to the drop-liquid-solid interaction where the hydrodynamic effects of the lateral jets are included.

iii) Soil detachment and raindrop size and velocity

As mentioned above, the magnitude of the vertical strain from a raindrop and the area of impact are determined by the raindrop size and velocity (Al-Durrah and Bradford, 1981). This relationship is of great importance in assessing the erosive potential of the rain as will be seen in the next section and will be considered in a little more detail here.

Ellison (1944) developed an empirical expression for splash erosion as a function of fall velocity, drop diameter and rainfall intensity. In analysing Ellison's data, Park et al. (1982) found that

the ratio of mass of splashed soil (W_s) to mass of raindrops (W_d) increased non-linearly with impact velocity. Figure 2.16 also suggests that there is a threshold impact velocity below which rainfall drops are too small, or their impact velocity is too low to overcome the inertia of the soil particles.

3) The erosive power of rain

A mechanism has been reviewed whereby the forces operating within a raindrop on impact with the soil are transformed into soil movement. The next stage if the review deals with the success of workers to relate these factors to the amount of splash movement. The literature on the erosive power of rain is extensive. However, it is possible to make some general observations on the direction of the work and draw some general conclusions from the results which are relevant to this particular investigation.

Generally the aim of the research has been to select an easily measured and widely available rainfall parameter and to ascribe to it an erosive power. The choice of a suitable parameter has depended on the level of correlation between it and measured soil movement. It is intended to divide the literature into that concerning different parameters. However utimately they are all linked to the most widely used parameter, kinetic energy.

i) Erosive power of rain related to volume, drop-size distribution, velocity and intensity

The relationship between the erosive power of rain and its total volume was considered by Free (1960). He reported a correlation coefficient of 0.72 for sand and 0.42 for soil relating rain volume and splash loss. In the experimental work of Ekern (1953) the soil loss was directly proportional to the amount of water applied.

Figure 2.16 Variation of erosion rate, per unit drop weight with drop impact velocity (Park et al. 1982)

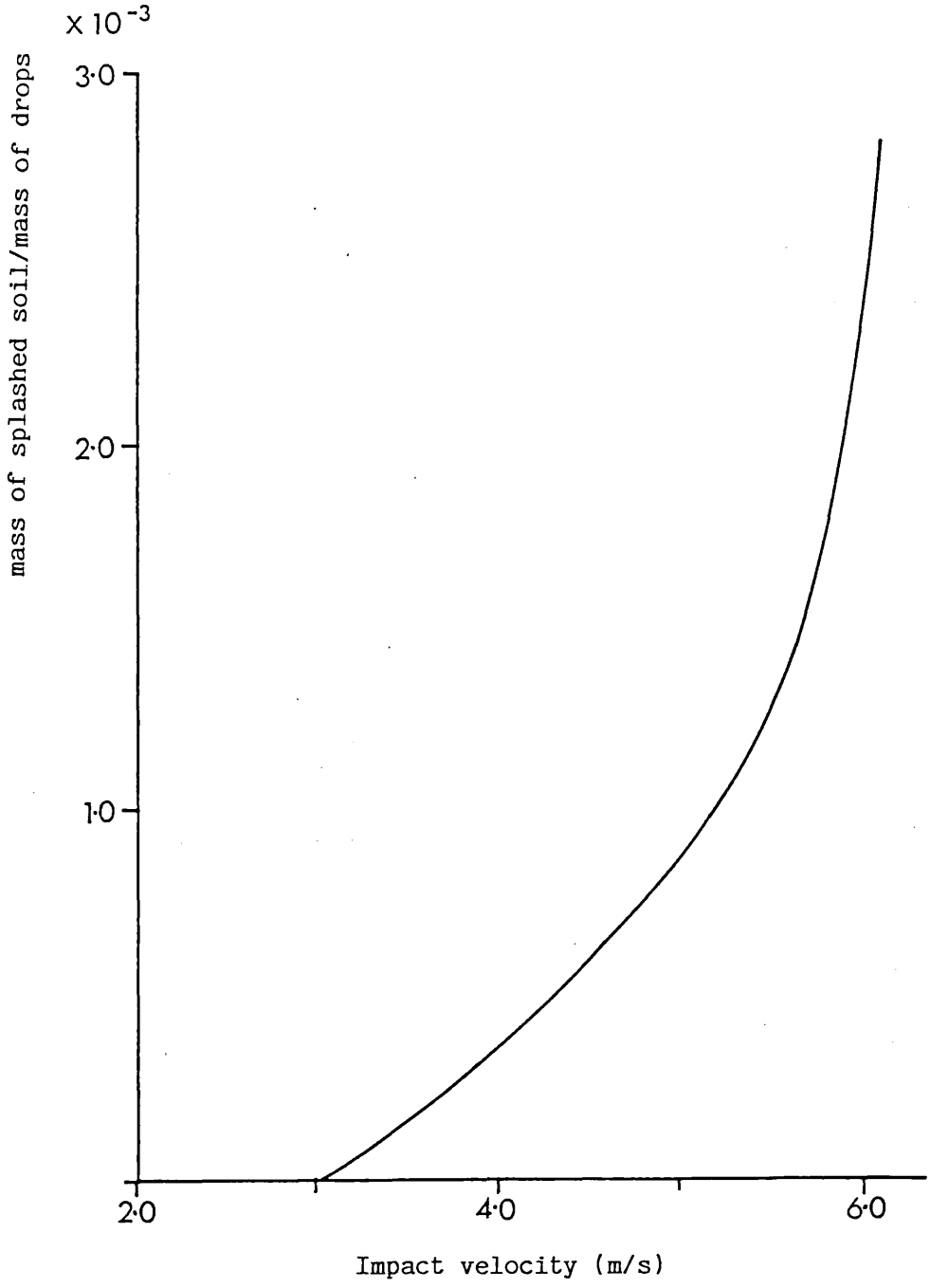

Bisal (1960) noted that by increasing drop size the splash amount increased. Ekern (1953) also considered the effect of drop size on the amount of splash. He found that the oscillations of a given drop size falling from a given height caused variation in the splash amount. Maximum transport coincided with drops which impacted with a minimum area, while drops at their maximum horizontal area caused less splash.

Riezebos and Epema (1985) also included the shape of the raindrop on impact as an erosivity parameter. The results are shown in Table 2.6 from which it appears that the introduction of actual drop diameter in calculating an index of erosivity does not produce a significant improvement in the relationship between erosivity over other estimates and detachment or transport. However, Riezebos and Epema (1985) showed that if an individual drop should strike the ground with a prolate shape, with the veritical axis longer than the horizontal, as opposed to an oblate shape the amount of soil detached was 2 to 3 times higher.

Ellison (1944) found that the resulting splash was proportional to the drop velocity to the power 4.33. Bisal (1960) suggested a power of 1.4 and Ekern suggested movement directly proportional to the velocity squared.

The relationship between splash and rain intensity has been considered individually by Ellison (1944), Ekern (1950, 1953) and Kneale (1982). Ekern said splash is proportional to the intensity and Ellison suggested intensity to the 0.65 power. Kneale gave a correlation coefficient of 0.71 between intensity and splash movement.

ii) Kinetic energy related to splash detachment

Kinetic energy and momentum both assess the erosivity of raindrops from their fall velocity and mass and the choice of the parameter used depends on the degree of correlation between it and the amount of

Table 2.6 The correlation between erosivity parameters and splash detachment and transport (Riezebos and Epema 1985)

Erosivity parameters	Detachment				Transport			
function:	linear	log	exp.	power	linear	log	exp.	power
Mv	0.87	0.69	0.84	0.93	0.79	0.62	0.79	0.87
$\frac{1}{2}Mv^2$	0.96	0.75	0.81	0.98	0.91	0.70	0.79	0.95
Mv^2/d_{eq}	0.83	0.71	0.86	0.94	0.78	0.66	0.85	0.93
Mv^2/d^2_m	0.90	0.74	0.84	0.93	0.89	0.73	0.85	0.95
Mv^2/d^2_{eq}	0.95	0.74	0.84	0.98	0.90	0.69	0.82	0.96
Mv^2/d_m	0.95	0.76	0.84	0.99	0.92	0.71	0.82	0.97

d_{eq} is the equivalent drop diameter
d_m is the real drop diameter measured at impact

splash. Table 2.6 shows that Riezebos and Epema found that kinetic energy had the higher correlation. The majority of the work reviewed for this topic concerns the relationship between kinetic energy and soil movement. There is agreement on the fact that splash increases with increasing kinetic energy although methods for obtaining a value for kinetic energy differ. Kinetic energy may be calculated from the detailed measurement of drop size data or by establishing a relationship between the more easily measured rainfall intensity and kinetic energy. Although the first method is more desirable in terms of an accurate calculation of the value for kinetic energy, the latter has more potential for use in cases where the detailed data is not available.

Direct measurement of kinetic energy

Using the terminal velocity data of Laws (1941) and knowing the drop sizes, Bubenzer and Jones (1971) calculated the kinetic energy applied by simulated rainfall to a soil surface. They grouped together drops of different size and velocity at constant energy levels and correlated energy with soil moved. The coefficient of correlation was 0.84. Young and Wiersma (1973) calculated the terminal velocity and size of raindrops from high speed photographs. They decreased rainfall energy by 89% by placing a mesh over the ground surface and found a corresponding decrease of more than 90% in soil movement. Ekern (1950) reported the following relationship between calculated kinetic energy and measured soil movement.

$$G = 25.4I \left(\frac{T}{60}\right) \left(-0.515 + 0.1 \frac{J}{A}\right) \qquad [2.16]$$

where G = rate of movement of fine sand (g/hour)
I = intensity (mm/hour)
T = time (hours)
$\frac{J}{A}$ = average energy per unit area

Kneale (1982), also from direct measurements of kinetic energy and soil movement reported a correlation coefficient of 0.72 between the two.

Kinetic energy implied from rain intensity

Wischmeier and Smith (1958) showed how energy may be correlated with soil movement using an indirect method of calculating the energy. They used the drop size data of Laws and Parsons (1941) and the terminal velocities of Gunn and Kinzer (1949) to produce a table of kinetic energies for a large number of storm intensities based on an assumed medium drop size. A multiple regression was carried out relating variables concerning rain fall and soil characteristics. It was found that the kinetic energy variable gave the highest correlation. Free (1960) found a correlation coefficient of 0.82 between sand and energy and 0.58 between soil and energy defining the energy in terms of the rainfall intensity. Both groups of authors found that kinetic energy and rainfall intensity may be related using the following general equation

$$K.E. = c + d \log I \qquad [2.17]$$

where kinetic energy (K.E.) is expressed in $J/mm/m^2$ and intensity (I) in mm/hour. The parameters c and d vary according to the drop-size distribution of different types of rainfall. The fact that both Wischmeir and Smith and Free combine a measure of energy with maximum 30 minute intensity is not really of concern here, since the basic relationship between soil movement and kinetic energy has been established. Jansson (1982) reviewed a number of different studies relating kinetic energy to intensity and the results are presented in Figure 2.17. All cases show that the kinetic energy/mm/m^2 increases with rainfall intensity, but at different rates.

Figure 2.17 The relationship between kinetic energy of rainfall (J/mm/m²) and rainfall intensity (mm/hour) as observed in different countries (from Jansson 1982)

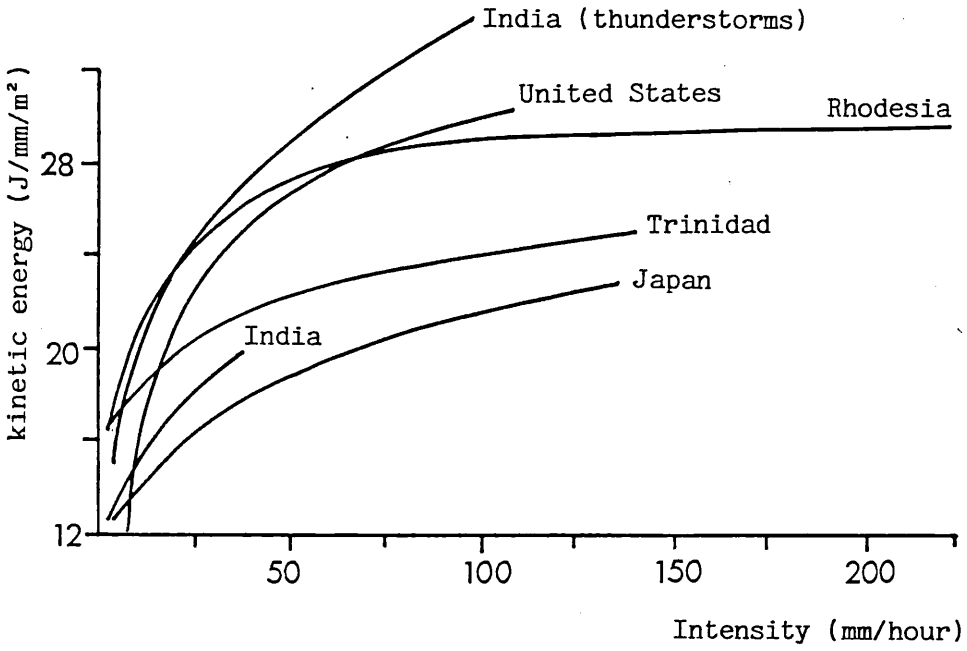

A justification for the use of the relationship between measured intensity and assumed kinetic energy has more recently been sought. It is important that this be established if the methods of Wischmeir and Smith and Free are to be extended for accurate use in a variety of environments. Kinnel (1973) used drop size data from five rain types to provide a more general relationship. He reported correlation coefficients of 0.9961, 0.9961, and 0.9689 between intensity and momentum, kinetic energy and kinetic energy per unit horizontal area of drop. Hence the parameters show essentially the same type of relationship with rainfall intensity. Provided that the variation in drop size distribution is maintained within fixed limits, the rate of detachment by raindrops will be related to rain intensity.

In conclusion a number of parameters have been shown experimentally to relate to soil movement. Soil movement increases with: increasing drop size, decreasing impact area for a drop of constant volume, increasing drop velocity, increasing intensity and increasing kinetic energy. The exact nature of the relationship varies with the location of the experiment. An attempt to estimate the erosive power of rain from commonly available rainfall intensity data through kinetic energy has been made. The success of this depends on the accuracy of the formula used to predict kinetic energy over a wide range of intensities.

Section Six Effects of vegetation on falling rain and consequent soil movement

The final part of this review concerns literature closest in subject to this project. A combination of the effects of vegetation on falling rain and on the soil movement. It has been shown above in the section on water induced soil movement that splash amount is closely correlated with the kinetic energy of the rain. It also has been shown that a canopy may have the effect of changing the drop-size

distribution of the rain. In this section it will be illlustrated that the change in drop-size distribution results in a change in the kinetic energy. Likewise, changing the spatial distribution of the drops results in a change in the distribution of the kinetic energy.

Having established the link, in the form of kinetic energy, studies considering the effect of vegetation presence on soil movement will be reviewed. Firstly the effect of the tree canopy. There has been work on the assessment of kinetic energy from drop-size distribution, with speculation as to the effect on soil movement under single and multi-layered canopies. This is complemented by work on the actual measurement of soil movement.

Without wishing to steal any of the thunder from these works which are, after all, directly comparable with the present thesis, it is necessary, for the sake of a complete argument, to consider also work concerning lower vegetation layers, either low plants or a litter layer. It will be shown that although the canopy has a potential for greatly increasing the erosivity of the rain, a low plant or litter layer has an even greater protective value.

1) Potential for change in the kinetic energy of rain by a canopy

i) Definition of the kinetic energy

The kinetic energy of falling raindrops in still air may be expressed by the equation:

$$\text{Kinetic energy} = \tfrac{1}{2} \text{ mass } (\text{velocity})^2 \qquad [2.18]$$

Since mass of a raindrop (assumed spherical) is proportional to the cube of its diameter, $m = 1/6.\text{density}.\pi.\text{diameter}^3$, and since

terminal velocity is a function of drop diameter, kinetic energy increases rapidly with increasing drop size (Dohrenwend, 1977). The rate of increase is shown in Figure 2.18, the upper line of the set of curves was calculated for drops falling at terminal velocity.

ii) Change in kinetic energy with height of fall

The kinetic energy depends on the height from which the drop has fallen. As Schottman pointed out, to exceed the kinetic energy of uninterrupted, uncoalesced rain the canopy has to be of a sufficient height. Indeed it is the difference in height more than anything else which governs the effect of vegetation on changing the erosivity of the rain beneath it. Using the data of Laws (1941) the kinetic energy of drops of different size falling from different heights has been calculated, the results are presented in Figure 2.18.

However for drops falling from vegetation the relationship between kinetic energy and splash may not be simple. Riezebos and Epema (1985) have studied the shapes of falling drops and as discussed above have demonstrated that the weight of splash detached by prolate drops may be 2 to 3 times as great as that detached by oblate drops of the same volume. They suggest that in rainfall, with the drops at terminal velocity, the majority of drops with a sufficiently large diameter to deviate from a sphere have an oblate shape with the horizontal axis longer than the vertical. An estimated 10% have a prolate shape. It is suggested that the situation may be different under a canopy. The short distances do not allow the drops to assume the equilibrium oblate shape and the majority of the drops are prolate when they reach the ground hence causing greater potential for erosion.

iii) Change in kinetic energy with a change in wind speed

Quantitative work on the effects of wind speed in changing the

Figure 2.18 The kinetic energy (J) of water drops of different diameter (mm) after falling from various heights (m) (after Laws 1941)

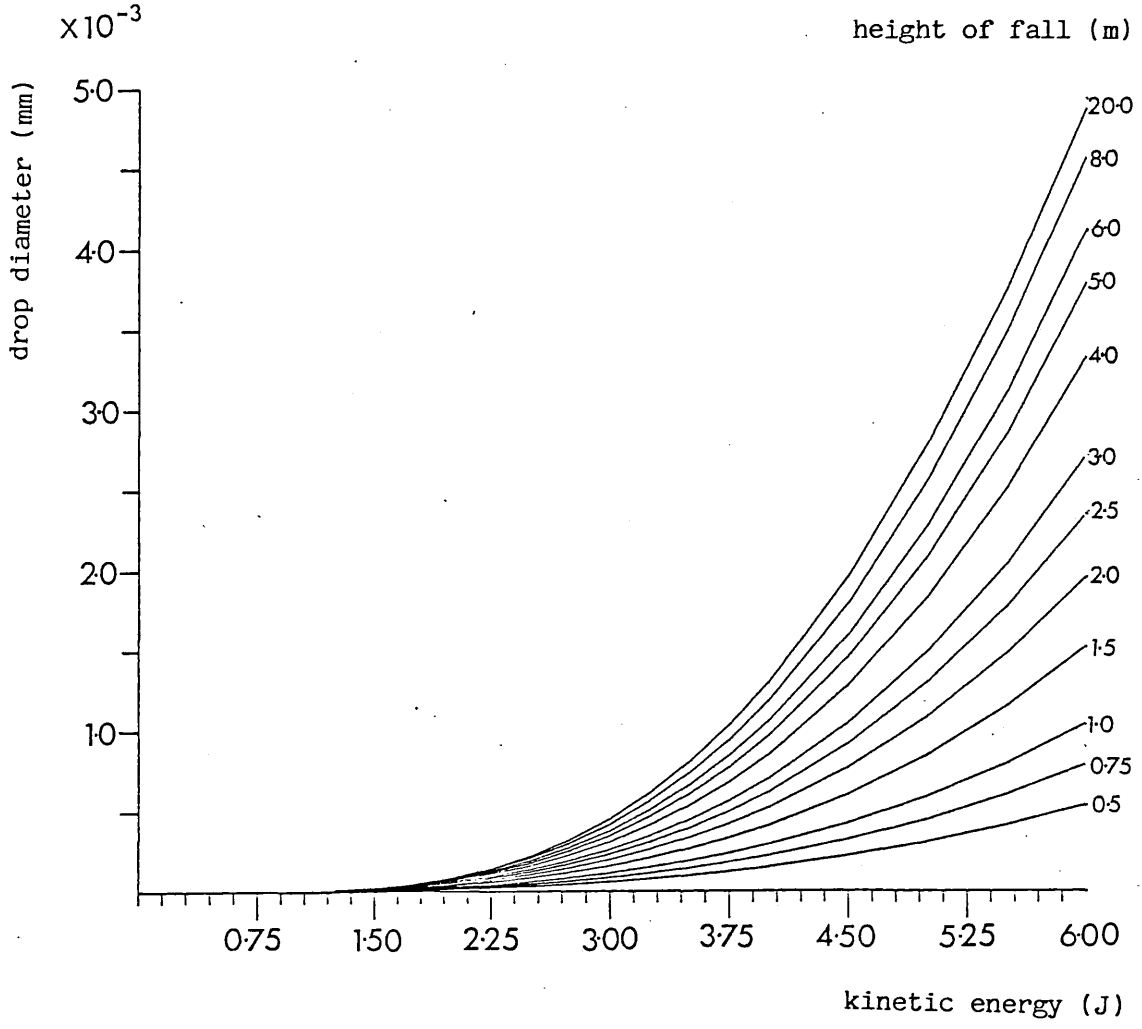

kinetic energy of throughfall under a canopy is scarce. Dohrenwend (1977) remarked that low wind speeds are characteristic of the sub canopy environment and assumed that the effect of the canopy was to remove and wind acceleration that might be present in the open, so that under the canopy all drops fell in still air.

iv) Change in kinetic energy resulting from change in drop size distribution

Schottman (1978) commented on the effect of drop coalescence on erosive potential. At terminal velocity a single, large drop will always have more kinetic energy than the sum of energies possessed by a number of smaller drops with the same total volume. Hence a single large drop of diameter 1.87 mm (20.4 mm^3) falling at terminal velocity will possess 1.04×10^{-3} J kinetic energy. Nine drops of diameter 0.90 mm (3.04 mm^3) whose total volume is the same as that of the large drop will possess 5.56×10^{-5} J kinetic energy each, resulting in a sum of energy of 5.0×10^{-4} J, approximately half of that of the large drop. Hence a change in the drop-size distribution of rain alone by the canopy will result in a change in the kinetic energy.

2) Measurements of kinetic energy changes by a canopy

i) Assessment of kinetic energy from the drop-size distribution

Chapman (1948) measured the change in drop-size distribution due to the presence of a red pine canopy. Combining the drop diameters with Laws's (1941) data, for the velocity of fall of drops from different heights, he calculated the kinetic energy for each intensity of rain falling at up to 150 mm/hour (Figure 2.19). Throughout the range sampled the striking force of the rain under this canopy was considerably greater than it was in the open.

Figure 2.19 Measured kinetic energy per mm of rain per unit area of soil surface under a canopy and in the open for varying rainfall intensities (Chapman 1948)

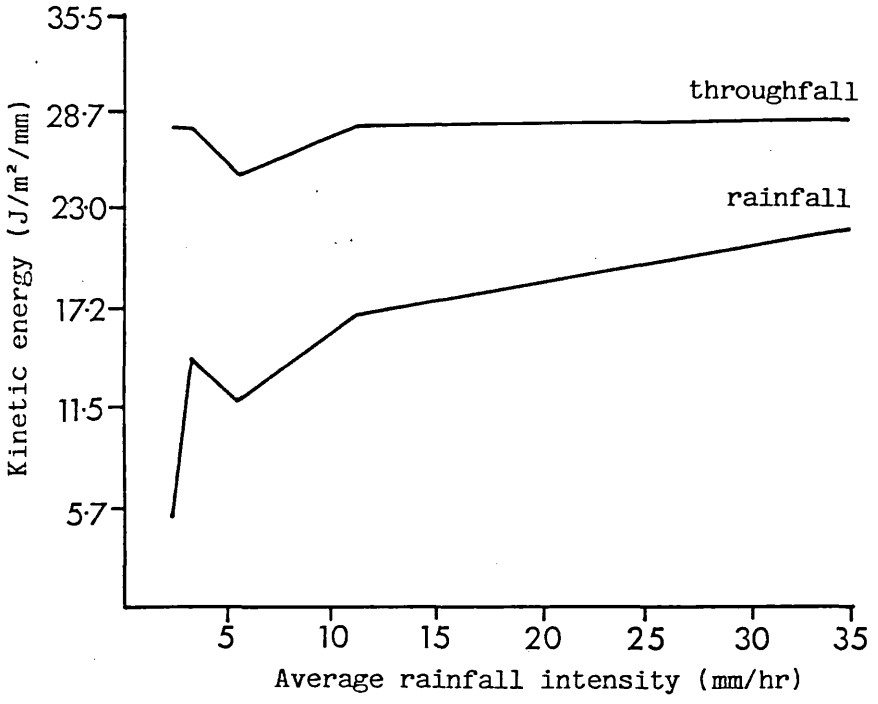

Figure 2.20 Extrapolated average kinetic energy per mm of rain per unit area of soil surface under a canopy and in the open for varying intensities (Chapman 1948)

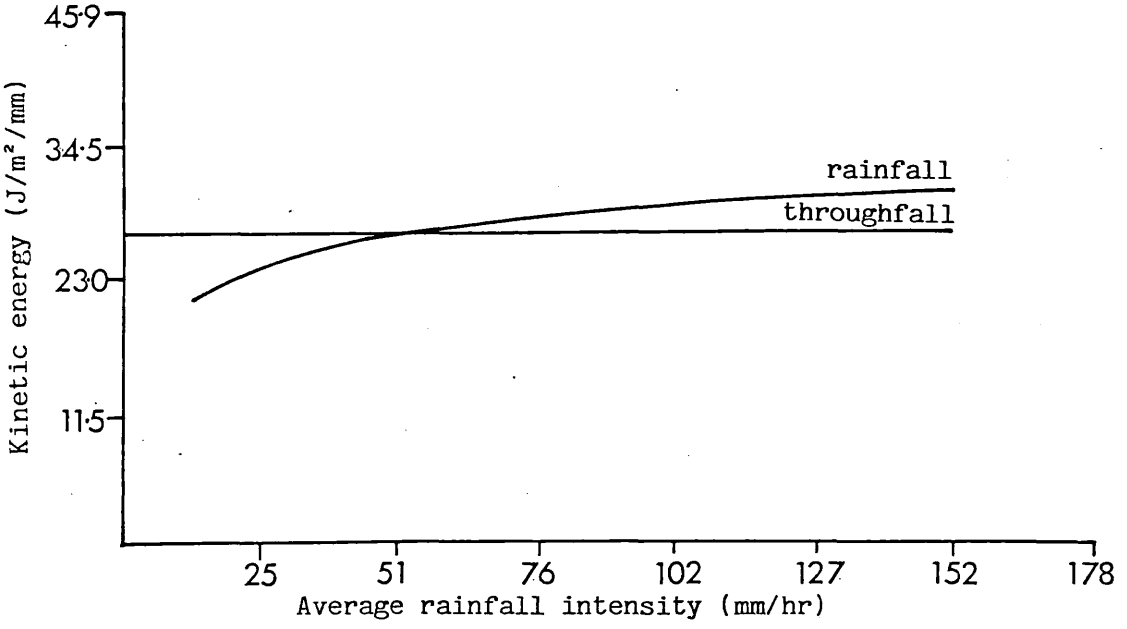

Chapman (1948) also stated that the energy of throughfall under the pines tended to be constant per mm of rainfall regardless of rainfall intensity. In the open, because of the greater proportion of water falling in the form of large sized drops during heavy rainfalls, the kinetic energy of each mm of rain per unit area of soil surface increased as the intensity increased. Chapman estimated that at rainfall intensities of 50 mm/hour the average kinetic energy per mm of rain would exceed that under the canopy (Figure 2.20). Hence for intensities of rain less than 50 mm/hour the canopy will increase the kinetic energy of rain but for intensities more than 50 mm/hour the kinetic energy will be decreased.

Tsukamoto (1966) (quoted in Dohrenwend, 1977) studied raindrop behaviour and splash erosion in a variety of forest types and found that canopies normally caused an increase in the kinetic energy of falling rain. He also observed that under the same forest canopy, variations in the frequency and range of drop sizes of throughfall from a variety of rainfall intensities are vanishingly small, confirming Chapman's observations. Tsukamoto stated that while in the open kinetic energy of rainfall is constant for a given intensity, in the forest the kinetic energy increases with the height of falling raindrops. Therefore raindrops will have more kinetic energy in well-developed mature forests and plantations.

Dohrenwend (1977) simulated the effects of both a single and a multiple canopy on changing the kinetic energy of the rain. For a single-layered canopy he estimated that the kinetic energy of throughfall below the canopy would be 150% of the above canopy rain. In the case of the multi-layered canopy, the under storey canopy was assumed to be uniformly 150 cm above the forest floor. The calculation for kinetic energy of throughfall in this case showed that below the understorey the kinetic energy was 85% of the main canopy throughfall but still 129% of the above canopy rainfall.

ii) Assessment of kinetic energy of throughfall from a measurement of soil splash

Wiersum (1985) measured the erosive power of falling water drops using Ellison-type splash cups filled with sand, under an Acacia plantation in Java. Although rainfall in the forest was only 79% of incident rainfall there was an increase of 24% in erosive power of the throughfall. This implied an increase of 57% in erosive power per unit precipitation falling on the splash cups. Although no measurements of drop-size distribution of the rainfall and throughfall were made, Wiersum noted a distinct increase in the size of raindrop imprints on the sand under the canopy. Mosley (1982) carried out an integrated project, measuring both drop-size distribution, using the paper-staining technique, and surface splash from sand filled splash cups. He found that the kinetic energy of the throughfall was consistently 1.5 times higher than that of rainfall in the open and, as suggested by Chapman, was independent of intensity (Figure 2.21). Extrapolation of the regression lines suggested that the kinetic energy of rainfall and throughfall would become equal at a rainfall intensity of about 40 mm/hour.

Mosely measured more sand material, and in some cases much more, lost from the sand cups exposed beneath the canopy. Mean values of splash loss are for open and canopy respectively, 3.9 and 11.9 g. These values were 3.1 times greater under the canopy than in the open.

3) Effect of lower vegetation layers on kinetic energy

i) Low plants

By contrast, and because of the effect of the height of the canopy mentioned above, a low vegetation cover tends to reduce the kinetic energy of the rain and thereby protects the soil from splash. This topic has received much attention particularly because of the

Figure 2.21 Kinetic energy per unit mass of rainfall and throughfall as a function of instantaneous rainfall intensity (Mosely 1980)

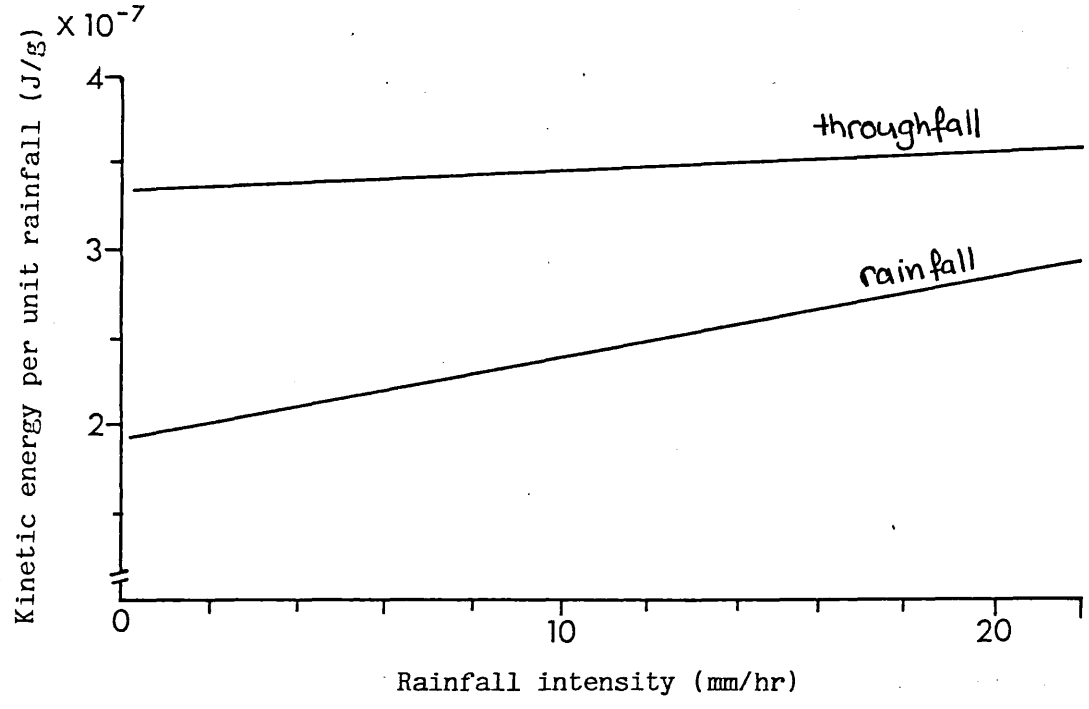

agricultural value of protecting soil and a few examples will be quoted here.

Hudson (1971) reported on work contrasting erosion on a bare soil surface with a surface protected by a fine-mesh wire gauze representing a vegetation cover of 100%. The soil loss from the bare plots was more than 100 times that from the protected plot. Reductions in splash detachment under low growing crops compared with bare ground have been measured by Sreenivas et al. (1947), Bollinne (1978) and Morgan (1982). Complementing these works Quinn and Laflen (1981) reported that maize with a canopy cover of 36% to 78% reduced the kinetic energy of the rain by 38% to 66%. McGregor and Mutchler (1978) found reductions of 75% to 90%.

Combining the two approaches, Noble and Morgan (1983) measured both kinetic energy and soil splash under Brussels sprouts. The plants were found to reduce the storm energy of rainfall at the ground surface to 10% to 81% with a mean of 34%. Detachment of soil under the plant ranged from 0.91 to 1.54 kg/m^2 compared with a value of 1.21 kg/m^2 when no plant was present. The reduction in kinetic energy did not in this case result in a reduction in the mean amount of splash. They ascribed this to the effects of the drips swamping the splash cups, causing soil to be washed instead of splashed out.

ii) Litter layer

Despite all that has been said above about trees and low plants altering the potential of rain for splashing soil, it would seem that the presence and degree of cover of a litter layer, being the last barrier before the soil, must ultimately govern the amount of kinetic energy the rain possesses when it reaches the soil.

At present much of the work has been speculative. Chapman (1948) stated "the protection afforded the mineral soil under forest stands ... arises not from the overhead canopy breaking the impact of the

raindrops, but rather from the presence of a layer or layers of unincorporated organic matter on the mineral soil surface". Tsukamoto (1966) concluded his work stating that the controlling role of the forest vegetation on erosion rates is due "mainly to the litter layer on the surface of the forest soil". Dohrenwend (1977) concluded that the extremely resilient litter layer absorbs virtually all the kinetic energy of the impacting raindrops.

Wiersum (1985) determined experimentally loss of soil from forest plots both with litter and with the litter removed. The Acacia stand decreased the amount of water reaching the soil by 11.8% but increased the erosive power by 24.2%. The litter layer caused erosion to decrease by as much as 93.5% in comparison with erosion on a bare soil plot. The presence of undergrowth decreased erosion by a further 3.7%. Figure 2.22 shows the rates of increase in erosion with increase in rainfall for different vegetation covers. Wiersum concluded that the direct soil cover was the single most important vegetation factor in protecting the soil.

In conclusion the canopy may increase the kinetic energy of the rain by up to 150%. This increase in kinetic energy corresponds with an increase in soil splashed in forests with no undergrowth or litter layer. Where there is undergrowth, or a low plant later, kinetic energy is reduced because of the height of the barrier above the ground. The amount of soil splashed also tends to be reduced. However, as Wiersum (1985) has shown in Figure 2.22 above, soil lost under a litter and undergrowth layer is independent of the presence of a tree canopy above. Thus a very low layer of vegetation seems to ultimately control the amount of erosion no matter how the potential is increased by the canopy above.

Figure 2.22 Rates of increase in soil erosion (kg/m²) with increase in rainfall (mm) for soil with a variety of overlying vegetation layers (Wiersum 1983)

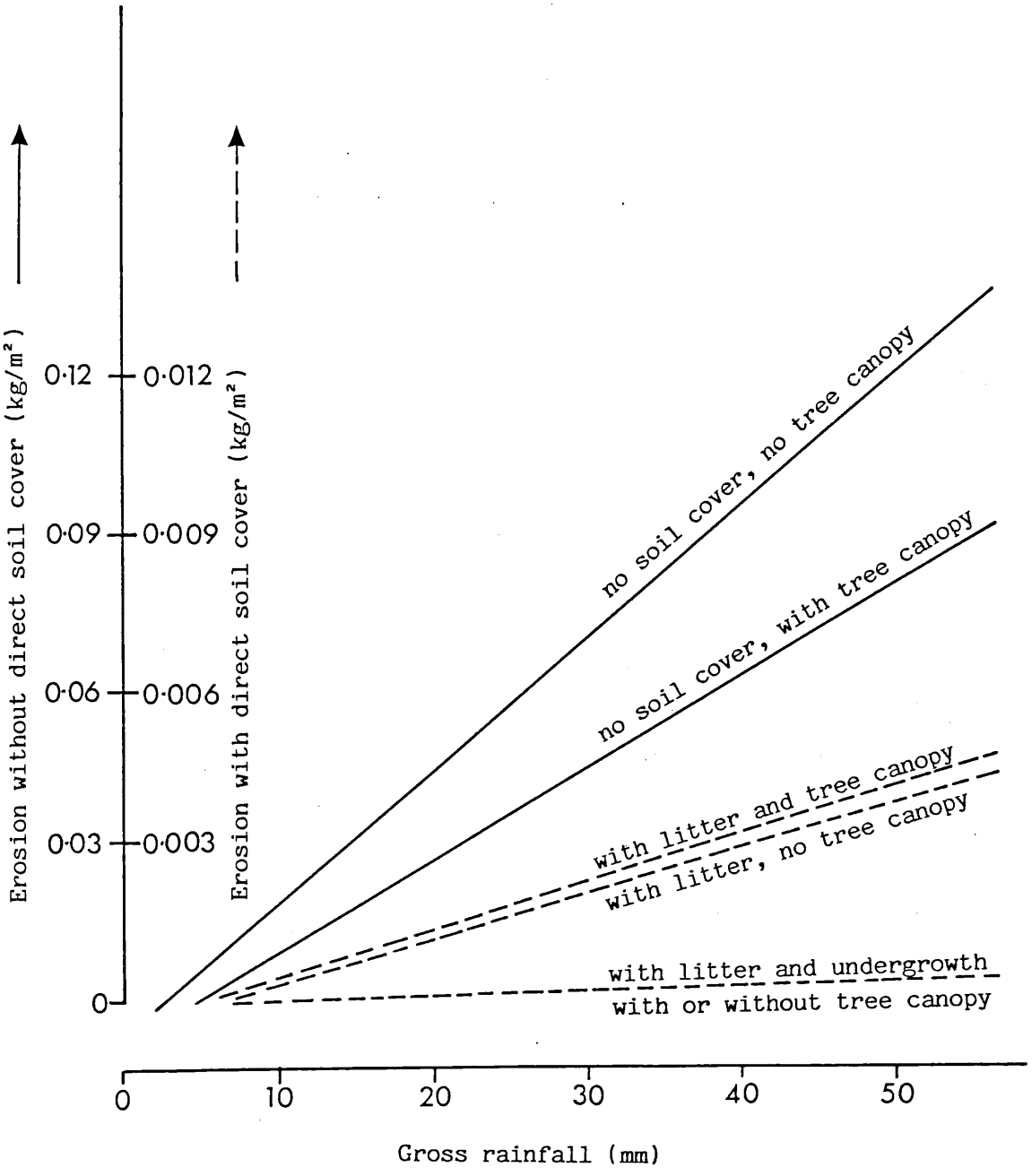

CHAPTER THREE THE WORKING HYPOTHESIS

Introduction

A canopy may change the kinetic energy of falling rain by altering the mass and number of the drops and by changing their height of fall. The changes in energy are to be described in this thesis in terms of a working hypothesis whereby changes in the the drop-size distribution are considered to reflect the amount of water storage in the canopy.

The model of accumulation and drainage of water stored in the canopy is presented first. Then follows a discussion of a qualitative model of drop-size distribution changes. The two sets of changes are assumed to be linked and the purpose of the experimental part of this thesis is to establish the relationship between the two models.

1) Canopy storage models

In Chapter Two works were presented which considered the accumulation and drainage of water stored on a canopy during and soon after a storm (Massman 1980 and Rutter et al. 1971). From these two models a composite graph of the canopy storage may be drawn (Figure 3.1).

The shape of the rising limb is given by Massman's dimensionless constant, (a), which depends on the tree species and meteorological conditions. The extreme "cup" solution is one where water does not drain from the canopy until it is saturated and overflows. All other solutions are as for leaking cups, allowing water to flow out while the storage level is still rising. During an initial phase, immediately after rain begins, all curves are nearly linear. As time progresses all solutions tend to the value for canopy saturation, but (a) strongly influences how the curves approach this limit.

Figure 3.1 A composite graph from the models of Massman (1980) and Rutter et al. (1971) showing variation in the rates of accumulation and drainage of stored water, depending on tree species and meteorological conditions

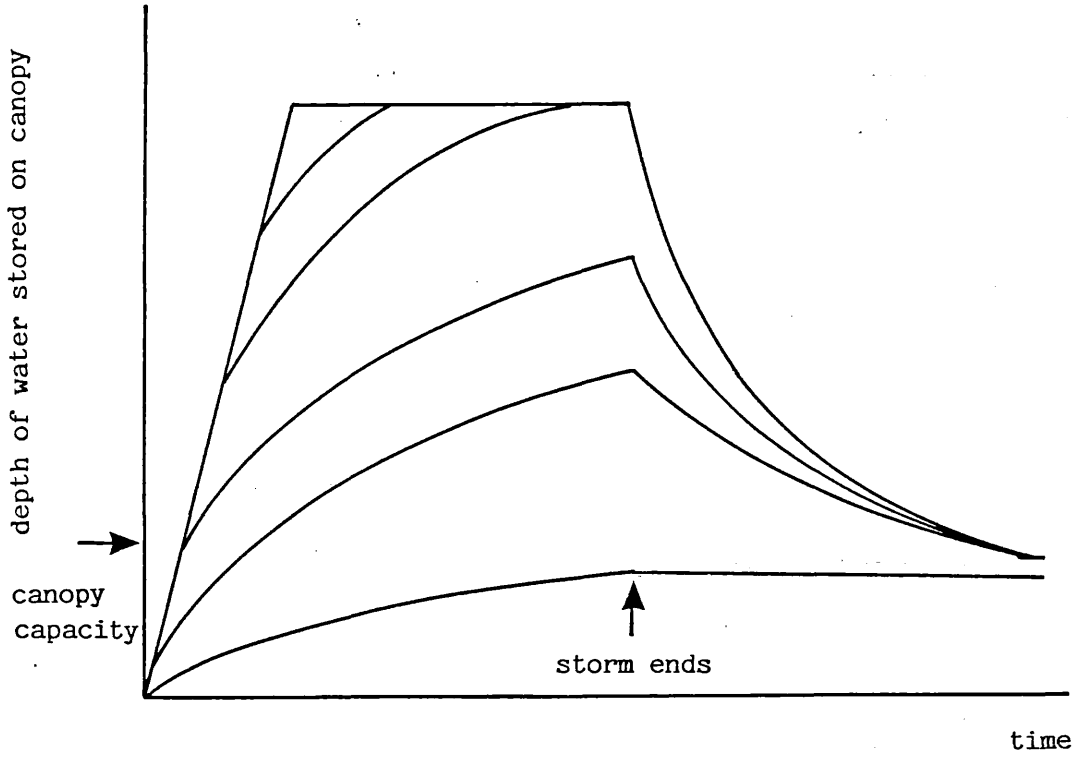

Regardless of how close the canopy comes to saturation, Rutter et al. considered that after the cease of rain there is a rapid loss of water. The intensity of drainage decreases exponentially with time as the head of intercepted water decreases. After 20 to 30 minutes drainage the storage is almost independent of the value from which the decline began and tends to a value for the storage capacity.

This then is the model of canopy storage, a variety of rising limbs which depend on the tree species and meteorological conditions and a falling limb which drains off water in excess of the canopy capacity rapidly. It is suggested that the drop-size distribution of water falling from the canopy is intimately linked with the level of saturation of the canopy; that the drop-size distribution is a measurable expression of Massman's term (a). It is suggested that each section of the graph has a gradient which can be matched with specific changes in the drop-size distribution of the throughfall.

2) A qualitative description of changes in the drop-size distribution

The canopy is considered in terms of the frequently used analogy, the leaking bucket and is illustrated in Figure 3.2. All rain must pass through the bucket. Through the centre and out through the bottom, a cylinder has been inserted to represent the portion of rain falling straight through the canopy. Holes in the sides of the bucket at different heights allow for the storage of water in different parts of the canopy.

For a given storm, a proportion of the rainfall input (I) will pass straight through as clear throughfall (T). The rest will enter the storage section. Assuming that I exceeds losses from evaporation (E), the canopy will fill in a time which depends on the rate of I, the rate of E, the storage capacity and the rate of loss of water from all point stores (P).

Figure 3.2 A schematic illustration of the canopy in terms of a leaking bucket

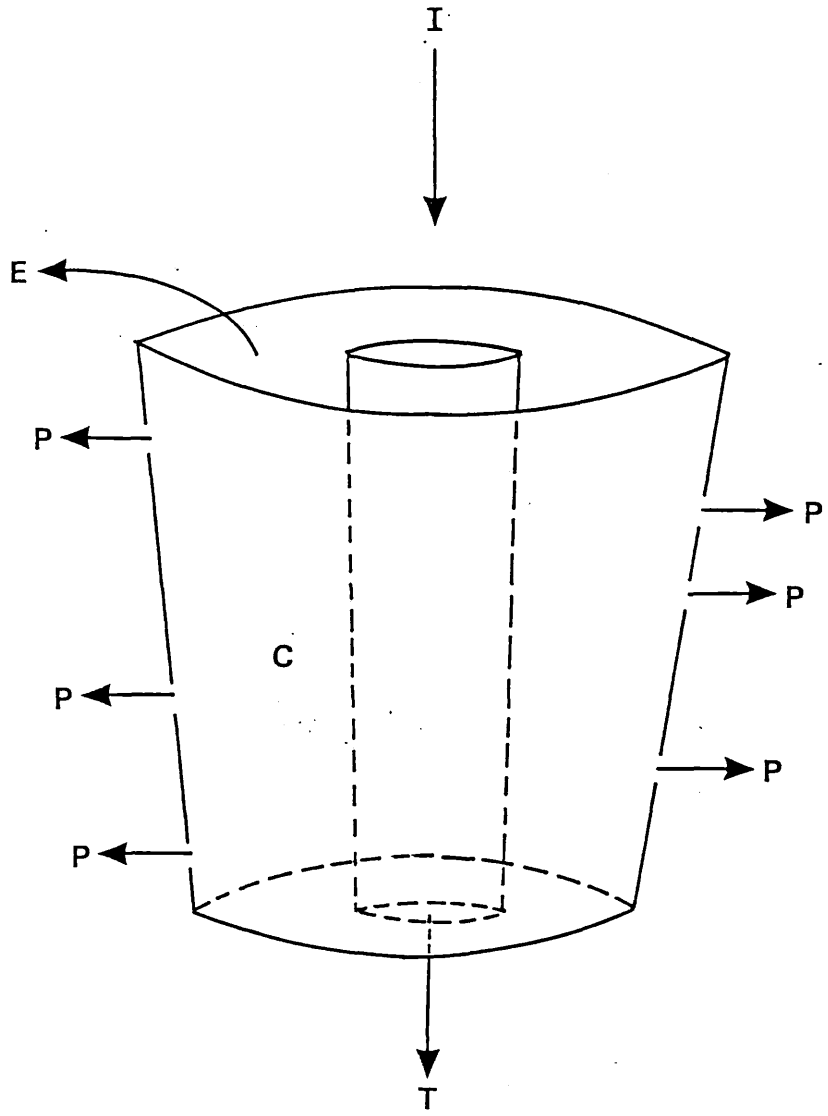

I = rainfall
T = throughfall
P = drainage from point stores
C = canopy capacity
E = evaporation

i) Consider water losses from the point stores

The rate at which the point stores are filled depends on the factors outlined in the section of Chapter Two concerning the effects of vegetation on falling rain. Whether or not a drop initially adheres to a leaf depends on the point of impact with the leaf (Schottman, 1978). Subsequent build up depends on a balance between the opposing adhering and shedding forces which are influenced by the leaf surface, size, shape and inclination (Merriam, 1973 and Williamson, 1983).

Water droplets which contact the leaf, but do not adhere, may be fragmented by the formation of a splash corona (Schottman, 1978). Those which do adhere form drops larger than those in the original storm as is shown by the experimental evidence of Chapman (1948) and Ovington (1954).

If the input is such that the water level stored in the canopy rises, first that point store which is most easily filled will be emptied, then others will follow. Following Massman (1980), the dripping rate (or rate of drainage of intercepted water from the canopy) is assumed to be proportional to the amount of water stored in the canopy. As the storage level rises, so the dripping rate increases until the throughfall intensity may be the same as the interception intensity (Rutter et al. 1971) and hence the rate at which water falls from the canopy is the same as the rate at which water lands on it. A change in storage level may also mean a change in the size of the drops. Saturated leaves may have a different surface resistance and inclination enabling intercepted water to drain more rapidly and in smaller drops.

ii) Considering the change in drop-size distribution likely to occur under the canopy using this model

Let the drop-size distribution of rain input, I, falling on the

canopy remain constant throughout the storm. Let the canopy cover be such that about 50% of the input falls straight through, the rest is either shattered or goes into a store. During a heavy storm the leaves may be beaten down presenting a smaller covered area. Hence the proportion of straight throughfall may be increased. It is suggested that there are a number of states which may be observed during the course of the storm. These are illustrated in Figure 3.3 together with the curve of cumulated canopy storage. A storm may not progress beyond [a], or it may successively add the other stages up to [d]. If the original rain filled at least one of the stores, it will end with [e].

[a] Input rate is greater than evaporation rate but the storm is small and the smallest P is not filled. Throughfall below the canopy is comprised of the 50% which is falling straight through, the drop-size distribution being the same as rain in the open. There are also those drops which have struck the canopy, been shattered but not slowed in their progress through it resulting in a decreased number of larger drops, but an increased number of smaller drops. These give a skew towards smaller values in the throughfall drop-size distribution and the standard deviation about the mean throughfall drop size may be less than that for open rain.

[b] Input rate is greater than evaporation rate, the cumulative depth causes the lowest P to be filled before the end of the storm. The intensity of throughfall is not sufficient to beat down the leaves. Rain below the canopy is comprised of 50% of the input as straight throughfall, shattered drops and a drop from the first point store adding the beginnings of the second peak in the drop-size distribution.

[c] Input rate is greater than evaporation rate, the cumulated depth causes more of the point stores to be filled and the rise in dripping intensity causes some of the leaves to be beaten down. Rain below the canopy is comprised of a

Figure 3.3 A schematic illustration of the change in drop-size distribution by a canopy with changing canopy storage through a storm of constant rainfall intensity and drop-size distribution

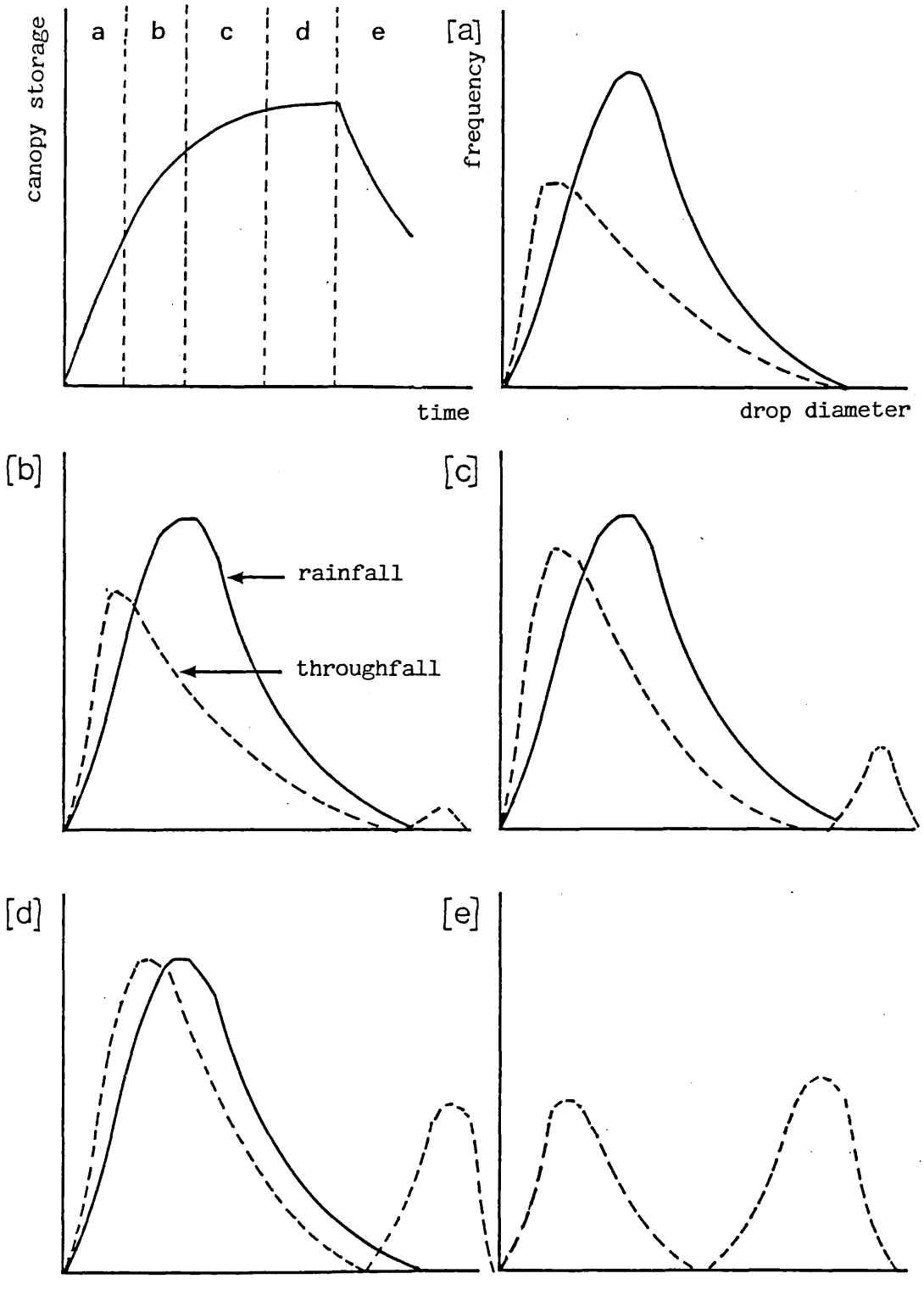

slightly increased proportion of the rain falling straight through, smaller drops from some of the point sources because of increases in leaf inclination, an increase in drops available for shattering both from unaltered rain and from reprecipitated drops higher up the canopy. The smaller canopy area could also decrease the number of drops affected by the canopy. The standard deviation of the throughfall drop sizes about the mean may now be larger than that of the incident rainfall.

[d] Input rate is greater than evaporation rate and the cumulated depth is sufficient to fill the canopy storage so that gross throughfall occurs at the same rate as the input. The leaves are bent down and the time available for droplet formation on the leaves decreases. Rain below the canopy comprises an increase in original rain falling straight through, drips from all point sources with a general reduction in drip size because of the increase in leaf inclination and the increased rate of dripping. The standard deviation of the throughfall drop-size distribution about the mean may be higher than in the previous stage.

[e] Input ceases. There is now no direct throughfall. Depending on the cumulated depth and hence the rate of drainage from the canopy, the drips will either be made smaller from accelerated progression, or will be at their maximum size. Some of the reprecipitated drops will be shattered.

iii) Kinetic energy changes with stage

The difference between gross kinetic energy possessed by the rainfall input and the gross throughfall output is the prime concern of this thesis. In each stage the balance is different and so the succession of stages encompassed by each storm will change the

resultant total difference in kinetic energy.

The kinetic energy of both rainfall and throughfall in any section of the storm is a function of the drop-size distribution (and hence the kinetic energy/mm/m^2) and the depth of rain or throughfall fallen. As illustrated above in the section of Chapter Two discussing the change in kinetic energy resulting from a change in drop-size distribution, a large drop can have almost twice the kinetic energy possessed by the same volume of water divided into smaller droplets. This is because the loss due to friction with the air is relatively less with larger drops.

Consider the extreme stages, [a] and [e]. In stage [a] the rainfall kinetic energy must be greater than the throughfall energy for the simple reason that less water is let through the canopy, and some of that is being shattered into smaller droplets. In stage [e] there is no rainfall kinetic energy but there is throughfall. At some intervening stage it might be expected that there is a transition between the phases when the energy of the rainfall is dominant and when the energy of the throughfall is dominant. The amount of water falling in each phase will determine whether the canopy increases or decreases the total kinetic energy of a storm.

3) Testable statements drawn from the model

The model in this chapter suggests a sequence of interactions between rainfall and a tree canopy resulting in a sequence of changes in the drop-size distributions of the rainfall here described qualitatively. As a logical extension to the arguement, and with the support of previous workers, it has been suggested that the changes in drop-size distribution may be related to the amount of water stored in the canopy.

From the model, the following testable statements may be made. Statements (i) to (v) examine the structural base of the model, and

statements (vi) and (vii) examine how far the model may be applied to cases where there is only limited information available.

(i) The canopy changes the drop-size distribution of the rain.

(ii) The kinetic energy of the rain changes as a result of the change in the drop-size distribution. It also changes as a result of the change in height of fall of the drops.

(iii) There is a sequence of changes in the drop-size distribution through a storm and hence the storm may be divided into a series of stages, each with a particular change in the drop-size distribution.

(iv) Each stage in the sequence has a different balance between the kinetic energy of the rainfall input and the kinetic energy of the throughfall output.

(v) The sequence of changes in drop-size distribution is predictable.

(vi) The predictable changes can be related to constants in
a) the rainfall
b) the canopy storage.

(vii) The ultimate difference between the kinetic energy of the input and output depends on the amount of water falling during the different stages.

It is the object of this research is to derive data from experimental techniques in different environments to test each of these statements. This will allow the working hypothesis to evolve and changes in the kinetic energy of rainfall by different canopies for any given storm to be predicted. To assess the accuracy of the measurements and predictions, the kinetic energy of each storm will be independently assessed using measurements of splash erosion.

CHAPTER FOUR EXPERIMENTAL DESIGN, TECHNIQUES AND SITES

This chapter is divided into two sections the first considers the choice of parameters, experimental design and techniques and the second considers the effect of experimental techniques on the choice of field site and provides a description of all the sites.

Section One Choice of parameters, experimental design and techniques

1) Identification of parameters for measurement and experimental design

The aim of this thesis as defined in Chapter One is to consider the change in the erosive power of rain by canopies of different structures and heights above the ground. The model put forward in the previous chapter suggested that for a given canopy the differences between the erosive power of rainfall and throughfall may be predicted from the depth of the storm and drop-size distribution. The hypothesis described the change in erosive power, in terms of the increasing occurrence of large drops in the throughfall canopy, as the amount of water stored in the canopy accumulated.

The basic experimental strategy adopted was to make comparisons between the erosive power of the rain and the erosive power of throughfall from a variety of canopies of known characteristics throughout individual storms. The differences between the measurements in the open and under the canopy were assumed to be due to the presence of the canopy.

The information required to satisfy the objectives was sought from four specific areas; the energy change by the canopy, the accumulation of water on the canopy, details of the structure of each canopy

investigated, and an independent measure of erosive power. Some of the parameters identified give information in several of the specific areas.

i) Energy change by the canopy

Following other workers (Bubenzer and Jones (1971), Young and Wiersma (1973), Ekern (1950), Kneale (1982), Wieschmeir and Smith (1958), Free (1960), Kinnel (1981)) the kinetic energy/mm/m^2 of the rainfall was taken to be the index of erosive power. For any number of drops, whether from a sample of the rain taken part way through a storm or all the drops falling in a storm, the total kinetic energy may be assumed to be the sum of the energy possessed by each drop. The kinetic energy of a falling drop is calculated from its size and velocity of fall.

It has been shown in Chapter Two that the sizes of raindrops vary with the type of storm and throughout single storms. The hypothesis put forward here suggests that the sizes of throughfall drops also vary through storms. To provide information to test the hypothesis, it was necessary to compensate for drop size changes in the rainfall. Samples of the drop sizes of both rain and throughfall had to be taken at frequent intervals through each storm. To calculate the total amount of energy from both rain and throughfall either the energy of every drop had to be calculated or the amount and drop-size distribution of water in the unsampled gaps had to be inferred from the samples.

The velocity of an impacting drop varies with its height of fall and was needed also to calculate the kinetic energy. Drops falling from an open sky may be assumed to have reached their terminal velocity but since there is insufficient evidence to quantify any wind acceleration it may be suggested that the values calculated are a minimum value. Likewise drops falling from tree canopies of more than 8 m may be assumed to have reached terminal velocity and there is some

justification for assuming that the velocities of fall are as for still air. Where parts of the canopy are lower the problem is complex since it is impossible to tell from which part of the canopy individual drops fell. Calculating the kinetic energy as if all drops fell from the height of the lowest point of the canopy gave a minimum possible value for total kinetic energy. It was assumed that the actual value lies between this and the value calculated assuming terminal velocity.

The change in the rainfall energy by the canopy at any time, may vary spatially with the structure of the canopy (as shown by Ovington 1954), so that the sampling point may not be representative of energy change generally. Therefore some account was taken of spatial differences changes in the drop-size distribution for given instances of time.

ii) The accumulation of water on the canopy

The sequence of samples of the sizes of drops of rain and throughfall through each storm was also used to calculate the cumulative depth. Since the samples of rain were not continuous the depth of water fallen unsampled was inferred from the samples. Details of the interpolation methods are given later. However in order to minimise the errors accumulated in adding the depth of each drop, the total amounts of rainfall and throughfall were measured independently.

It was assumed that at any time since the start of the storm the difference between the cumulated rainfall and throughfall represented the amount of water stored on the canopy less that lost to evaporation and stemflow. The initial hypothesis suggested that the change in throughfall drop sizes was due to the level of canopy storage.

iii) Canopy structure

It was assumed by the initial hypothesis that the canopy structure controls the erosive potential of the rain and that changes to the canopy structure will result in changes to the erosive potential. The canopy cover, the canopy density and height and the shape, size, orientation and texture of the leaves are elements of the canopy structure which have been identified in the literature as important in the interception, storage and drainage of rain. Particularly in the rain forest such information about specific plants is difficult to obtain since many plants are barely visible from the ground. Where possible the literature review considered, for similar environments, the distribution of phytomass within the forest canopy together with the orientation and size and shape of the leaves. However the probability of a raindrop being intercepted is determined by the percentage cover of the canopy. Seasonal variations in the canopy cover are especially important in deciduous forest sites. The cover of the canopy will vary spatially both under the same tree and trees of different species, causing variation in the energy of the throughfall. The spatial variability in throughfall kinetic energy under a canopy was assessed by taking a number of samples at different points at the same time.

iv) Independent measure of erosive power

Although the erosive power of rain and throughfall may be calculated from the drop sizes an independent measure of erosion was required to test the calculations which are subject to systematic errors. Wiersum (1985) and Mosley (1982) both measured the erosive power in terms of the amount of soil splash although splash has been shown to vary greatly with the soil properties. To provide a standard response to given rainfall energy the splash medium was limited to uniform grain size and structural strength. It has been shown that the lower the cohesion between particles the greater the splash and hence the more sensitive to changes in erosive power. Again to

compensate for spatial variability in the canopy, measurements were taken over an area which maximises the variation within a single species or stand. Measurements of the amount of splash per storm could only be used to compare the total kinetic energy of rainfall or throughfall for any storm. It was not possible to measure the amount of splash for different stages of the storm.

v) Summary of parameters

The parameters selected for measurement were:

a) The drop-size distribution of both rain and throughfall sampled thoughout storms in one location but with an estimate of variability over the whole plot.

b) The depth of rain and throughfall for each storm, the latter especially at a number of points under the canopy to quantify the spatial variability.

c) The canopy height and percentage cover above all measuring points to determine the minimum fall height and spatial variability.

d) The amount of sand splashed erosion by rainfall or throughfall for all storms.

The rest of this section describes the techniques used to measure these parameters. Although the descriptions of the field sites is deferred until the next section, reference to them is made here. The deciduous oak forest was located at Egham, Surrey and there were two sites in the tropical rain forest at Manaus, Brazil.

2) Measurement of rainfall and throughfall depths

i) The main source of information

Both the total volume of rain falling in a storm and the spatial

variability of throughfall under the canopy were measured using a set of funnel and beaker rain gauges. The gauges were made in Egham from 90 mm diameter funnels inserted into polythene bottles and half buried in the ground to keep them stable. In Manaus the same principle was involved, the funnels being 86 mm in diameter. Under the canopy the gauges were arranged at 2 m intervals, 25 of them being placed on a grid 10 m by 10 m. The arrangements at the two rain forest sites are illustrated in Figures 4.5 and 4.6 and will be discussed in greater detail in the next section.

The problem of measuring rainfall incident on the canopy is beset with many complications. Usually it has been measured in adjacent ground but Reynolds and Leyton (1961) said that if this is so evidence must be presented to show that the measurement is not subject to errors due to difference in location. In both the oak forest and single canopy rain forest sites of this project, the incident rainfall was measured not more than 10 m from the canopy plots. As far as could be seen the open gauges were not being shielded by the trees. In the multiple canopy rain forest site the open site measurements were taken about 150 m away. In measuring rainfall in the open Jackson (1971) used 4 gauges, all of which had very similar readings. The same number was used in this project.

As far as was possible at the Egham site, and always at the Manaus sites, the gauges were emptied after each storm. Jackson (1971) suggests a delay of two hours after rain has stopped to allow the canopy to drain before taking the readings. While this delay was not always possible, because of encroaching darkness, the gauges were always checked again before the next storm to see if further drainage had taken place.

ii) Alternative sources of rain depth data

At the Egham site daily rainfall totals for the Meteorological Office weather station at Virginia Water, the nearest station to the

site, were obtained. The research design for this project is based on storm events and it is not known how many storms there were per day. However this data serves as an independent source with which to compare the data from the site.

Under the oak forest the rainfall amount was automatically recorded on a "Solatron" data logger at five points under the canopy and in the open using tipping bucket rain gauges. Readings were taken every four minutes and it was hoped that this would also provide information on the intensity changes during a storm. Unfortunately the size of the bucket in the gauge, with one tip every 0.84 mm was too coarse for the storms during the experimental period which were of low intensity. Trouble with a constant power supply meant that the data recovery rate was low.

At Reserva Ducke, in the rain forest, a meteorological station, 500 m from the sites provided a continuous rainfall chart enabling the timing of the storms, duration and intensity changes to be much more successfully monitored.

3) The technique for measuring the drop-size distributions

The choice of techniques, from those available, was governed by the requirements of the experiment. Firstly the technique had to be able to record the size of every drop sampled to give a sufficiently detailed description of the drop-size distribution. Because of the relatively short time available for experimentation the technique needed a quick and easy calibration relating the original drop size to the recorded diameter. The need to use the technique in difficult field conditions without great technical back up, especially in the humid tropics, necessitated a simple approach. It is for these reasons that the first group of techniques suggested were rejected at the start of the project.

i) Description of methods available for measuring drop-size distributions.

Within the literature there are descriptions of a wide range of methods for determining the sizes of raindrops. These include scanning clouds with radar (Mason and Andrews 1960); measuring the impact of a drop on a pressure sensitive membrane (Schindelhaur 1925 (reported in Mason 1957), Palmer 1963); the use of a photo-electric spectrometer (Mason and Ramandham 1953). These are the techniques which were rejected at the start of the project. The two techniques which were considered in more detail were those which have been used for projects similar to this one.

The early development of techniques for measuring the drop-size distribution of rainfall have been described by Laws and Parsons (1943). They themselves favoured the use of the flour pellet method, a technique more recently used by Best (1950a) and Kneale (1982). Flour is sieved into a pan and then exposed to the rain for a known time. The raindrops form pellets in the flour. The pellets are allowed to harden in an oven and are then separated from the flour by sieving. It has been found to be possible to relate pellet size to original drop size by measuring the size of pellets formed by drops of known diameter.

The choice of the paper staining technique rather than the flour pellet one was made because of the necessity of keeping fieldwork at its simplest level. Paper is less bulky to transport than flour and once exposed paper can be stored immediately and does not require further attention. This technique was first used by Wiesner (1895) and its use until 1943 has been described by Laws and Parsons (1943). More recent users include Mosley (1982), Hall (1970) and Noble and Morgan (1983). The technique involves colouring absorbant paper with a dye which reacts with the raindrops to leave a circular stain. As in the flour pellet method the size of this stain may be related to the original drop size by considering the sizes of stains produced by drops of known diameter.

ii) Development of the technique

Hall (1970) reviewed the choices of absorbant paper previously used. Whatman No. 1 filter paper had most frequently been chosen, because of the need for standard thickness and uniform texture. The same paper was used for this project.

The choice of dye was more complex and trial experiments were made before the final selection. Initially the papers were dyed with a pH indicator, methyl red, dissolved in alcohol following Mosley's (1982) use of ethyl blue reagent. However, although easily visible stains were made using large drops of tap water, raindrops made little or no impression. Obviously the pH of the rain is a critical point in the selection of a suitable indicator. This method had the added disadvantage of stains fading with time.

Attention was then turned on water-soluble dyes in a powdered form brushed onto the paper. Such dyes were recommended by Laws and Parsons (1943) and again by Hall (1970), although this dye was also pH sensitive. The dye Janus Green, described in the BDH catalogue as "highly soluble in water" was chosen at random and has proved to be highly successful. It gives stains of a distinct dark blue and records drops of as small as 0.14 mm diameter.

Both Hall (1970) and Laws and Parsons (1943) recommended that humidity is controlled in the paper storage. A brief experiment comparing the stain produced on air-dried paper with that on paper which had been recently steamed confirmed this. The steamed paper gave a much larger stain. Hall (1970) suggested storing the paper over self-indicating silica gel before and after exposure. This has been incorporated in the present design.

Neither Laws and Parsons (1943) nor Mosley (1982) say what they used to contain the paper. Hall (1970) suggested a box with an aperture in a sliding lid. For this project each paper was placed over the lower portion of a petri dish containing silica gel. The top

was then be taped on with masking tape all round. The top could be removed by slitting the tape with a knife, leaving the paper attached to the bottom and protected from wet fingers by the tape. The dishes and silica gel were reusable. On each lid was stuck a blank label. The boxes were placed in evacuated plastic bags. In practice it was observed that unused boxes stored like this, remained desiccated for over a month even in the field.

iii) Method of use of the paper staining technique

The papers were exposed to rain at intervals during the storms with a maximum interval of five minutes between sampling. The distinctive pattern of storms in the rain forest allowed a standard sampling procedure to be adopted. During the first ten minutes of heavy rain, samples were taken every two minutes. After that they were taken every five minutes until rain stopped in the open or dripping stopped under the trees. The papers were left exposed for a time which depended on the intensity of the rain, sufficiently long enough for there to be a uniform covering of stains, but not so long that the stains overlapped. The length of exposure was noted on the label on the lid correct to the nearest second. After exposure the lid was replaced and the papers thus protected. Once dry, the papers were removed and stored in envelopes awaiting analysis.

The stains were sampled by placing a ruler on a random diameter of the paper and drawing transects 1 cm wide and 1 cm apart across the sheet. Sampling started in the central transect and continued in transects on alternate sides until 200 stains were measured. The mean diameter of each stain was measured using a grid photocopied onto a transparent sheet. Measurements were made to the nearest 0.5 mm with the smallest diameter being 0.25 mm.

To count the total number of stains on the sheet, another transparent overlay was made, dividing the circle into 16 segments. Most commonly the number of stains was counted for one quarter of the

whole and then multiplied up. However where the stains were particularly numerous or small, smaller segments of the circle were used.

iv) The calibration of stain diameter to drop diameter

In order to relate the diameters of the stains recorded to the original drop diameters, it was necessary to calibrate the stain sizes.

Drops of known diameter were produced on the tip of a hypodermic needle. The needle was attached to a burette which was fed water at constant pressure from a reservoir through a constant head device. The rate of flow of water from the reservoir to the constant head device was controlled with a screw clip. The height of the burette was adjusted so that the water level was constantly at the top. The arrangement of equipment which was positioned over a stairwell is shown in Figure 4.1.

Experimentation showed that the size of the drop produced depended on the size of needle used and the rate of dripping. The dripping rate for each needle was adjusted to between 60 and 120 drips per minute. It was thereafter held constant during that drop size measurement.

To measure the diameter of the drops, 100 drops were counted into a small flask of known weight, held just under the needle. They were then weighed. Another 100 drops were added and again the flask was weighed. This was continued until there were 500 drops in the flask. The mean weight of each of the 100 drop lots was taken and from that the weight of a single drop. Between the collection of each 100 drops the dripping rate was checked. Table 4.1 gives the results for each drop size.

Each set of 100 drops was measured to the nearest 0.0001 g. For

Figure 4.1 Diagram of equipment used for the calibration of drop diameter from stain diameter

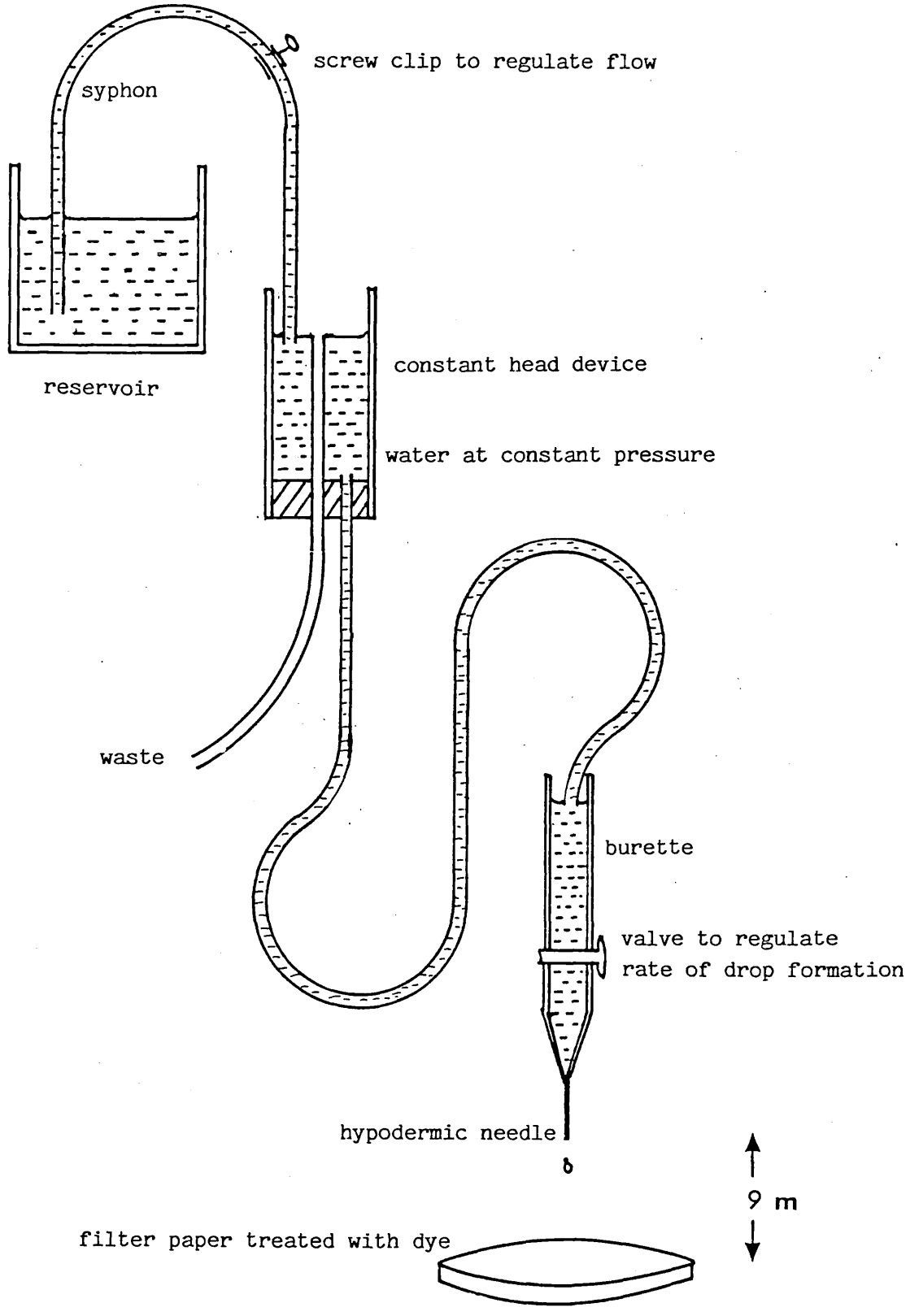

Table 4.1 The weight (g) of 100 drop lots for each dripping rate and needle to determine the weight (g) and diameter of a single drop (mm).

needle no.	weight of 100 drop lots (g)					mean	max. % diff.	drop diam(mm)
1	0.5224	0.5155	0.5140	0.5121	0.5108	0.5150	1.44%	2.14
2	0.6216	0.6488	0.6556	0.6566	0.6583	0.6482	4.10%	2.31
3	0.8190	0.8133	0.8142	0.8132	0.8126	0.8141	0.60%	2.49
4	1.3118	1.3060	1.3061	1.3049	1.3037	1.3065	0.41%	2.92
5	1.3819	1.3813	1.3769	1.3770	1.3774	1.3789	0.22%	2.98
6	1.5804	1.5883	1.5927	1.5843	1.5845	1.5860	0.42%	3.12
7	1.6501	1.6457	1.6456	1.6502	1.6708	1.6566	0.86%	3.16
8	2.1317	2.1080	2.1266	2.1069	2.1059	2.1158	0.75%	3.43
9	2.1367	2.1300	2.1491	2.1248	2.1460	2.1373	0.58%	3.44
10	2.4451	2.4397	2.4415	2.4161	2.4381	2.4361	0.82%	3.60
11	3.4660	3.4178	3.4347	3.4227	3.6670	3.4816	5.33%	4.05
12	3.8102	3.8074	3.8155	3.8539	3.8601	3.8294	0.80%	4.18

Where:

mean = the mean of the 100 drop lots

max. % diff. = the maximum difference between all readings and the mean, expressed as a percentage

drop diam. = the diameter of a drop of that weight, assumed to be spherical

each drop size the weight per 100 drops varied on average $\pm$ 1.36% from the mean. The variation was larger for some drop sizes, up to $\pm$ 5.33% for drops of diameter 4 mm.

The diameter of a single drop, d (m) assumed to be spherical, was calculated from the drop weight, w (g), using the following equation.

$$d\ (m) = 2\ (\ \frac{3}{4pi}\ x\ w\ (g)\ x\ 10^{-6})^{1/3} \qquad [4.1]$$

The question of evaporation during measurement was not considered quantitatively. The drops were collected directly under the needle to avoid water loss through splash.

Immediately after weighing all the drops, the dripping rate again being checked, the filter papers were exposed to the drops at the foot of the stairwell 9 m below. Hall (1970) stated that "stain size is also a function of velocity of fall for drops over 1.1 mm in diameter and therefore they must be allowed to fall at terminal velocity for the calibration". It was assumed that the 9 m drop was sufficient for all drops generated to attain terminal velocity.

By combining needles of different bore with different dripping rates, drops of 12 different diameters were produced. For each drop size the corresponding stain diameter was calculated from the mean diameter of 25 stains. Table 4.2 shows the results for each drop size and the percentage error of two standard deviations from the mean. The average percentage deviation from the mean was 2.6%, ranging from values of 1.7% to 4.5%.

Stain diameters were plotted against their corresponding drop mass to produce a calibration curve shown in Figure 4.2. Drop mass, m (g), was regressed against stain diameter, d (mm), such that

Table 4.2 The mean stain sizes (mm) and standard deviations produced by drops of known diameter for the calibration.

needle no.	mean (mm)	± 2 s.d.	2 s.d. as a % of mean
1	18.35	0.62	1.7
2	16.98	0.74	2.2
3	12.04	0.76	3.2
4	20.23	0.74	1.8
5	10.74	0.50	2.3
6	26.22	1.20	2.3
7	16.34	0.74	4.5
8	13.27	0.48	3.6
9	20.00	1.16	2.9
10	17.62	0.84	2.4
11	27.06	1.44	2.7
12	20.04	0.68	1.7

Figure 4.2 The calibration curve relating drop mass (g) to mean stain diameter (mm)

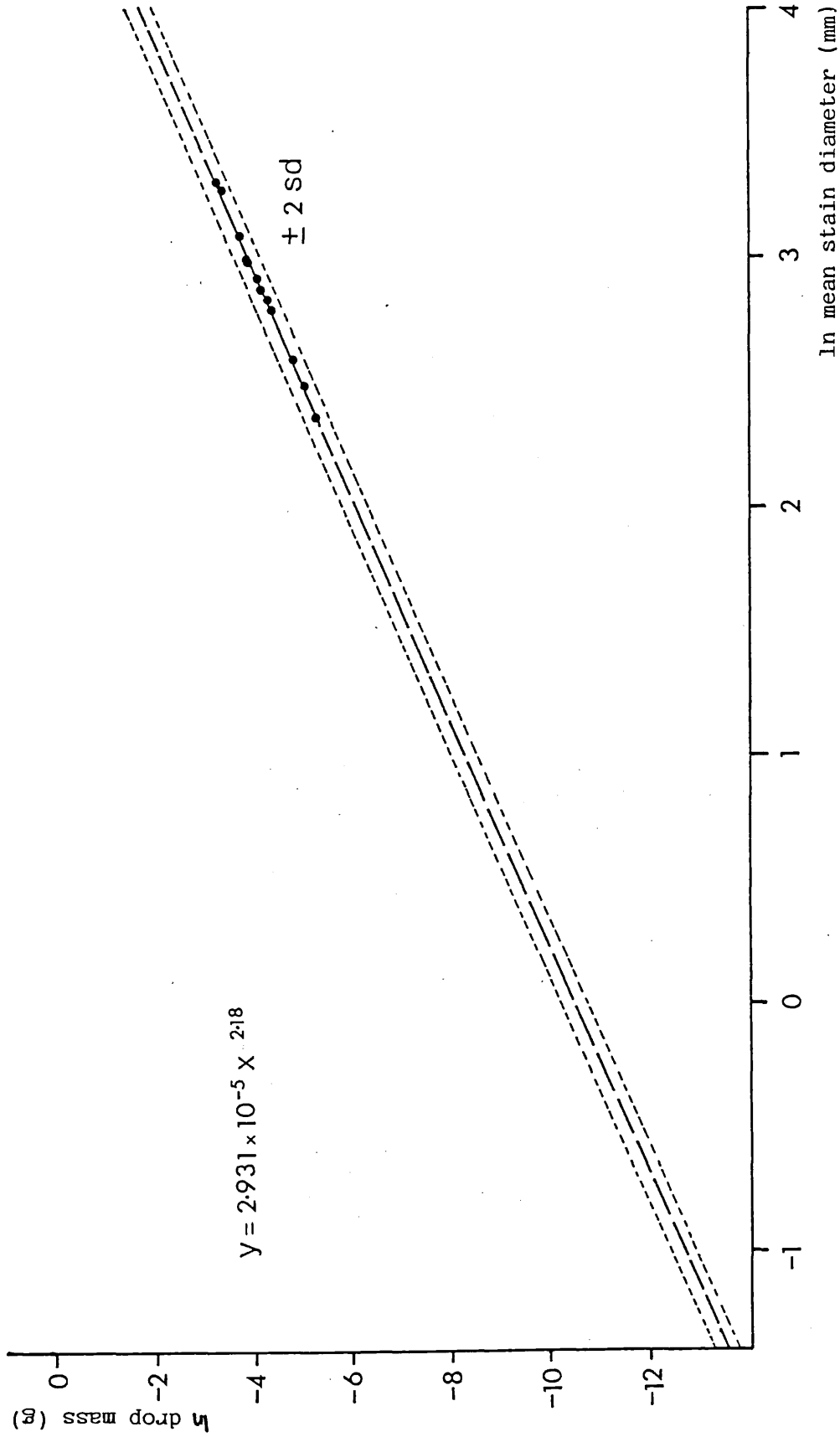

$$m\ (g) = 2.931 \times 10^{-5}\ d\ (mm)^{2.18} \qquad [4.2]$$

The standard deviation of the data about the intercept was 2.76×10^{-6}. Therefore the drop mass calculated from the stain diameter are accurate to $\pm$ 5.51×10^{-6} g (two standard deviations).

This calibration has several problems. The relation of stain diameter to drop diameter at the lower end of the scale has to be an extrapolation of the line because of the practical difficulties in producing drops of small enough size. Extrapolating to the smallest stain diameters of 0.25 mm the smallest drop diameter to be recorded was 0.14 mm. Hall (1970) quoted Lane (1947) who formed the drops in a stream of air, thus causing them to break earlier. A range of drop sizes could be produced by varying the velocity of the air stream.

From this calibration it is possible to calculate the original drop diameter for each stain measured. The drop-size distribution for each sample sheet may be calculated from the frequency of occurrence of drops in each stain size class in the sample and the total number of drops on the sheet. It is assumed that the sample of drops measured is representative of all the drops on the sheet. Details of the analytical procedure are given later.

v) The number of drop-size distribution sampling sites

Ovington (1954) related the spatial variability of rainfall and throughfall depth to rainfall intensity. The standard deviation of depth increased with increasing intensity, but the increase was greater under a canopy because of the concentration by the canopy of throughfall in certain points (Figure 2.13). Consequently it may be expected that the drop-size distribution of throughfall will vary spatially and account should be taken of it when considering the number of the sampling points.

To examine the extent of the spatial variability in throughfall drop-size distribution, a number of samples of throughfall were taken simultaneously under a sycamore in full leaf and again when some of the leaves had fallen, although the canopy cover was not considered quantitatively. The kinetic energy/mm/m^2 of each throughfall sample is presented in Table 4.3. In storm A the values range from 8.1 to 38.3 J/mm/m^2 and in storm B from 10.0 to 29.6 J/mm/m^2 with means of 25.1 (s.d. 11.3) and 18.0 (s.d. 7.4) respectively. The wide variability in the data and high standard deviations indicate that the drop-size distributions were significantly different at different locations and spatial variability should be taken into account when measuring the kinetic energy of throughfall.

However, apart from storm d178, the drop-size distribution was sampled at one point only under the oak and rain forest canopies. Insufficient manpower during the experimental work and the length of the data processing time effectively precluded sampling in more than one location. However the question of drop size sampling sites will be discussed again with reference to the experimental data in Chapters Six and Seven. In Chapter Six it will be shown that simultaneous samples in different places under the oak canopy in storm d178 recorded an increase in drainage rate at the same time and in Chapter Seven it will be shown that the apparent variability in the data for storms A and B may be explained in a manner which lessens the importance of multiple sampling sites.

4) Techniques for measuring soil splash

It has been shown in Chapter Two that the energy possessed by the rain is transmitted to the soil surface when the rain hits the ground. This transmission of energy to the soil surface results in movement of the surface particles. It is expected that a measurement of the quantity of rain-splashed surface particles will correlate with the calculation of the amount of kinetic energy available for such splash.

Table 4.3 Kinetic energy (J/mm/m²) of throughfall samples taken simultaneously under a sycamore canopy for two storms

sample	kinetic energy (J/mm/m²)	
	storm A	storm B
1	24.83	9.98
2	8.10	29.61
3	34.24	26.81
4	33.73	11.84
5	12.56	14.58
6	32.06	17.14
7	16.78	16.01
8	38.27	
mean	25.07	18.00
(s.d.)	11.31	7.43

This part of the experiment was carried out at the Reserva Ducke site after initial trials at Egham to determine the best equipment and methods.

i) Description of the techniques available

There are several methods described in the literature for measuring the amount of material moved by splash. Several workers have used techniques which defined the source material. Morgan (1978) designed a "splash cup" which consisted of a round tin with a hole of 10 cm diameter in the middle. Material from this central source was splashed onto the surrounding tin bottom. Ellison (1947) described a technique where the source area was also identified for work using a rainfall simulator. Rain was directed through a slit in the roof of the simulator, to fall on a band of bare earth. On either side of this exposed ground strips of absorbant material were placed to register how far the splash was carried.

The majority of the methods do not attempt to define the source of the material, or to estimate amounts of material transported to the unit area. Such techniques are reviewed by Froelich (1980). Ellison (1947) used a vertical splash board with catching troughs attached at the ground surface. Gerlach (1976) and Chmielowiec (1977) used vertical boards with catching troughs attached at 10 cm intervals up the board. Grzés (1971) used a sheet of flannel, stretched on a wooden frame although Chmielowiec (1977) found blotting paper attached to the board provided the best adhesive surface. However a funnel with an absorbant lining was used in the present study.

Bollinne (1978) and Froelich (1980) made splash traps from funnels inserted into the ground. The rims were at 5 mm from the soil surface to prevent inundation by surface wash. The funnels contained a "rot proof" filter which collected particles projected by the splash. Bollinne weighed the funnel and the filter before installing the trap. After each period of rain he washed the outside, dried and weighed it,

the difference being the weight of the soil retained. Froelich reports weighing the filter only, which he weighed to an accuracy of 0.0001 g. Froelich also inserted the funnel into a pipe so that it could drain freely.

ii) Control of source material

It was realised that local variation in soil conditions might produce a variation in the response to raindrop impacts. In an attempt to standardise soil conditions it was decided that a uniform material should be placed around each splash trap. A circle of radius 0.5 m was cleared of surface litter around each trap. A layer of well-sorted river sand about 5 cm thick, of known grain size distribution, was laid on the circle. This effectively limited and splash material caught to coming from this area.

iii) Development of the technique

A funnel of 90 mm diameter was chosen to form the main part of the trap. This shape effectively reflected all material caught into the bottom of the trap. It was assumed that escape was minimal. The spouts of the funnels were cut off and the funnels were placed in 4 inch plastic flower pots in which they fitted neatly and through which they could drain. The flower pots were permanently placed in a hole in the ground, the funnels easily being lifted out for collecting.

The process by which a suitable funnel lining is chosen will be described. Previous workers do not discuss in sufficient detail the type of lining used nor the reasons for a specific choice. It will be shown that the accuracy of the results depends very much on the lining used. The lining of the funnel should provide an absorbent surface on which the soil may collect and through which water may drain. However it must also be possible to remove the soil from the absorbant surface for weighing.

Initially Whatman No. 1 filter paper was considered because it was already being used for measuring the raindrop sizes. However, since the surface of this paper is relatively rough, after the soil had been removed by brushing it was clear upon inspection that some soil particles were being retained on the surface. With this problem in mind, Whatman No. 540 (hardened, ashless) paper was considered, the aim being to separate the soil and paper by igniting the paper. However after four days in the furnace there were still signs of paper ash in the sample. The small sample size made this paper ash unacceptable. The lining eventually chosen was Whatman No. 50 (hardened) paper. This paper has a relatively glossy surface and on inspection less soil particles were retained when the paper had been brushed. It had a disadvantage in that it drained slowly and heavy storms tended to fill it up with water.

During the development of the technique, a number of methods for weighing the amount of soil collected in the splash traps were explored. Following Bollinne (1978) the filter papers were dried to a constant weight and weighed before and after exposure, the weight difference being the accumulated soil. However, a major difficulty was encountered in involving the paper in the process. As soon as the dried papers were exposed to the air, and despite being handled with tweezers and plastic gloves, they absorbed atmospheric moisture and visibly increased in weight on the scales.

Experiments were made allowing the filter papers to come to equilibrium with the atmospheric humidity on removal from the desiccator before weighing. This took around two hours on the laboratory bench. However unknown variability in the humidity itself caused this whole track to be abandoned.

The next method considered weighing only the soil and the shiny Whatman No. 50 paper was used. Soil was removed from the surface of the paper using a stiff brush. It was collected on glossy paper and weighed. Plastic weighing boats became too highly charged with static, causing the sample to fly out. Unlike paper the soil showed

no visible sign of gaining weight on contact with the air. The disadvantage was that even using No. 50 paper some of the particles were retained on the filter.

iv) Method of use as adopted at Reserva Ducke

Before a storm each filter paper was numbered, folded and placed in its funnel in the ground. It was found that by dampening the paper with distilled water, it moulded itself to the funnel. The loss of several filters during high winds necessitated placing a small, washed pebble in the bottom of each paper to hold it down. The circle of sand was prepared before each storm. It was dug with a trowel and smoothed to prevent compaction and armouring by larger grains. When necessary the funnel was re-set, its rim always being flushed with the sand surface.

After exposure the pebbles were washed and removed. The outside of the paper was washed down and the inside swilled to concentrate the sand in the tip of the cone. The top of the cone was then folded over and sealed with staples. The papers were allowed to dry in the air before being stored for later measurement.

Once in the lab the papers could be dried overnight at 110 ^{o}C and placed in a desiccator to cool. The final weighing procedure has been described above, the sand being brushed off the filter onto a separate glossy sheet for weighing to an accuracy of 0.0001 g. The sheet of glossy paper was reweighed after every sample.

5) Techniques for measuring the canopy parameters

The methods for determining the canopy cover were developed under the oak forest. However more detailed measurements of the canopy characteristics were made only for the rain forest sites.

i) Percentage canopy cover

Among the parameters selected for measurement is included the percentage canopy cover above each of the 50 rain gauges and splash traps and also the drop size sampling point for each plot.

Many estimates of canopy cover have been made for tracts of woodland, taking the average of a number of points. Lemon (1956) suggested using a curved mirror fixed above a point with a grid engraved on it to measure the probabiltiy of a drop penetrating the canopy cover directly. The ratio of light to dark points gives the canopy cover. Clark (1961) employed the same principle but permanently recorded the image above a point through a pinhole camera on photographic paper. It is this idea which has been extended in this study to give a record of canopy cover above each point and a percentage canopy cover for any site by averaging the point values (Gash and Morton 1978).

A single lens reflex camera on a tripod was positioned, lens upwards, directly above each trap and gauge. Looking back through the 50 mm lens the outline of the funnels could be placed in the centre of the image. A photograph was taken with the maximum depth of field on automatic exposure. Care had to be taken to take photographs when the sun was low so that it did not distort the picture. The film used was a fine-grained black and white film, Pan F, ASA 125.

The resulting photograph was an image of an area of canopy which depended on the canopy height. In the photographs each white patch represented a path through which a raindrop could fall freely. Away from the centre of the picture this path is inclined to the vertical.

The photographs were printed on 5 by 7 inch glossy paper. An estimate of percentage canopy cover was made using a transparent acetate sheet through which pin holes had been punched at random co-ordinates. A count of over 200 such points was made for each photograph.

ii) Height of canopy above the ground

Above each splash trap the height of the lowest leaf was measured using a tape and Abney level. In the multiple canopy rain forest site the low height of the canopy enabled direct measurement with a pole. Above each drop size sampling point the height of each successive layer was measured. Measurement of the higher canopy layers was particularly difficult in the multiple canopy site because of the density of the vegetation.

iii) Leaf sizes

Leaf sizes were noted above each measuring point using a rough micro-, meso-, macro-scale. Leaflets on a single stem were termed "micro". Palm leaves and large understorey saplings "macro", and the majority in between, "meso".

6) The design of the experimental plots

The basic design of the sampling plot for the measurement of throughfall, splash and drop-size distribution developed at Egham was used in both rain forest canopy sites and will be described here. An area of ground and canopy 10 m by 10 m was chosen. The size of the plot was chosen to allow variations in the canopy to come into play without including large identifiable gaps, limiting tree species and avoiding low branches.

Within the plots there was a grid of 25 raingauges, 2 m apart. Under the rain forest plots there was a grid of splash traps offset from the first by 1 m. Samples of throughfall drop-size distribution were taken in the same place each storm. Jackson (1971) used 20 gauges of 12.7 cm diameter in a plot of side 24.4 m plot to measure the throughfall. Reynolds and Leyton (1961) used 20, 12.7 cm gauges in a grid of 42.7 m side. Both sets of authors assess the spatial

variability of the throughfall in terms of the percent standard error of the means, such that

$$\% \text{ s.e.} = 100 \ (\text{s.d.} / \bar{T}) \qquad [4.3]$$

where, $\bar{T}$ = mean throughfall

s.e. = standard error of the mean = $\text{s.d.}/\sqrt{n}$

s.d. = standard deviation

n = number of throughfall values

Conversely Jackson (1971) suggested that the percent standard error be reduced to some pre-defined limit, such as 5%, by controlling the number of gauges used. Hence

$$n = (\text{s.d.})^2 / (\text{s.e.})^2 \qquad [4.4]$$

If this formula is applied to the throughfall data from storm j10b, for example, in the rain forest sites the number of gauges needed to gain data at the 5% error level is 13. Under the multiple canopy site however, to get a similar error the number required is 345. The depth of rain recorded in each of the throughfall gauges is given in Appendix 2.

Reynolds and Leyton (1961), among others, have suggested that when measuring throughfall the gauges should be randomly located within the plot and moved regularly to increase the variety in the canopy cover. In this experiment the positions of the gauges was not changed between storms. Information about the percentage cover of the canopy above each gauge was collected so that the variety of conditions could be assessed. If the gauges had been moved, control over the response of particular canopy conditions to change in the storms would have been lost. Additionally the space within each plot taken up by the splash

traps limited the room available for moving the rain gauges.

Section Two The choice and description of experimental sites

1) The choice of experimental sites

The area of concern for this thesis has been clearly identified and with it the parameters to be investigated. Just as the parameters influenced the choice of experimental technique so they and the need to examine a simplified system influenced the choice of experimental sites.

The initial hypothesis development phase was concerned with investigating the nature of the changes to the drop sizes of rainfall by a canopy and consequent energy change. It was necessary that rainfall in the open and throughfall under a canopy were sampled in sites close to each other and for the same storms. The first chapter has revealed that the change to drop-size distributions depends on the density and capacity of the canopy and the size, shape and orientation of the leaves. The change to the energy depends on the height of the canopy above the ground surface. The largest drops occurring naturally in rain reach their terminal velocities after a fall of 8 m. In a desire to limit these variables as far as possible a site was sought under a mono-specific stand of trees more than 8 m in height under which there was no undergrowth or saplings.

The second stage of the project aimed to examine a more extensively monitored system in a tropical rain forest environment in terms of the hypothesis developed. Here the storms tend to be larger and more intense and consequently the effects of the rain, especially in terms of the amounts of splash caused, tend to be more exaggerated and hence more easily measurable. Meteorological factors such as ambient temperature and humidity are more predictable as are the

patterns of intensity change within storms limiting the background noise from rates of evaporation and changes in raindrop sizes.

Additional to the aim of examining the proposed model in a new environment was the aim of selecting forest sites which were analogous to forests in an unmanaged state and those subjected to some potentially damaging management practice. Consequently the site representing an unmanaged forest, with its different life forms and the addition of undergrowth, showed considerably more variability in the parameters identified as influencing the extent of change in the drop-size distribution and energy of the rain. The managed site was selected to show an extreme in energy change. Hence the height of the canopy was maximised but with trees of similar type forming the upper canopy, other sources of variation in the canopy itself were limited.

2) Site descriptions

i) Deciduous oak canopy site

The field experiments for the first stage of the thesis were carried out from September 1983 to May 1984 under an area of deciduous oak forest in the grounds of the Botany Department of Royal Holloway College, Egham ($0^{o}34'W$ $51^{o}25'N$). The purpose of the research was to measure the depth and drop-size distribution for individual storms underneath the canopy and in the open and to assess the effect of seasonal change on the canopy cover.

An area was selected over which the height of the canopy was measured to be constantly more than 8 m and in which there were no tree boles. Although composed solely of oak, the canopy above the plot was made up from several individual trees. Underneath the tree canopy there was no sub-canopy of shrubs or saplings but the ground surface was normally covered with seasonal growths of bluebells and bracken. For the purposes of this project the ground surface was cleared so that low plants did not obstruct the gauges.

Mean monthly rainfall totals for Egham are shown in Figure 4.3. There is an average annual rainfall of 648 mm. Seasonal trends are slight with, on average 60 mm, falling in months between July and December and about 45 mm between January and June. Table 4.4 shows the actual monthly rainfall during the experimental period and the mean amount of rain per rain day. In general the rain for the period September 1983 to May 1984 was less than the average with a mean amount of rain per pain day of 3.7 mm

Seasonal changes in canopy cover are listed in Table 4.5 and range from an average 74% at the beginning of November and before leaf fall, to 19% in March when there were no leaves.

ii) Tropical rain forest plots

Experimental work in the tropical rain forest was carried out in the Reserva Ducke Experimental Station 35 km N. E. of Manaus, Brazil ($2^{o}27'S$ $59^{o}57'W$) during August and September 1984. The reserve is mostly primary rain forest with some experimental forest and an area which has been clear cut. The mean annual precipitation is about 2500 mm (Franken and Leopoldo 1983). The average monthly rainfalls are shown in Figure 4.4 and range from 300 mm per month in the wet season to 40 mm per month in the middle of the dry season when the research was done.

Table 4.6 breaks down 437 storm events between September 1976 and 1977 at the Reserva Ducke site into events of different size. While the majority of the storms are in the range 0.0 mm to 4.9 mm the largest volume of water falls in the fewer storms between 10.0 and 19.9 mm. Rainfall events of more than 3 mm are needed to generate overland flow (Franken and Leopoldo 1983).

Table 4.7 divides 416 storms according to their intensity for the same period as above. Small rains, less than 4.9 mm/hr yield only 27% of the rainfall while 52% of the rainfall falls in heavier storms

Figure 4.3 Mean monthly rainfall (mm) at Egham, Surrey, for the study period 1983 to 1984 (Meteorological Office data)

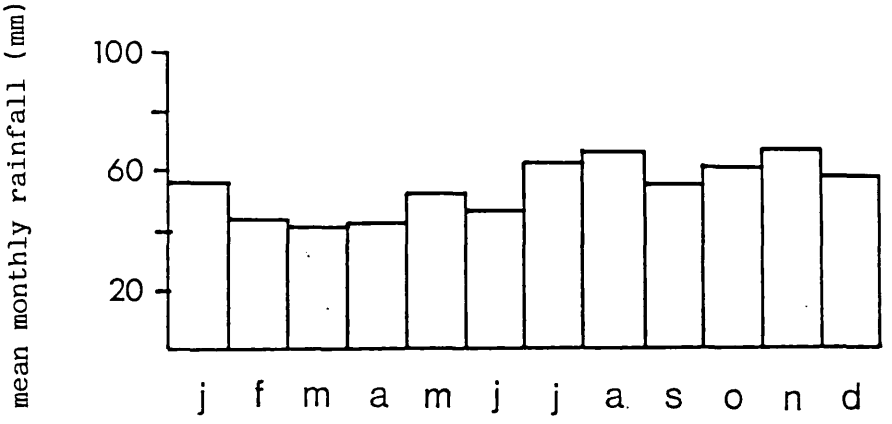

Figure 4.4 Mean monthly rainfall (mm) for Manaus, Brazil, compiled over the period 1931 to 1960 (Ministerio da Agricultura)

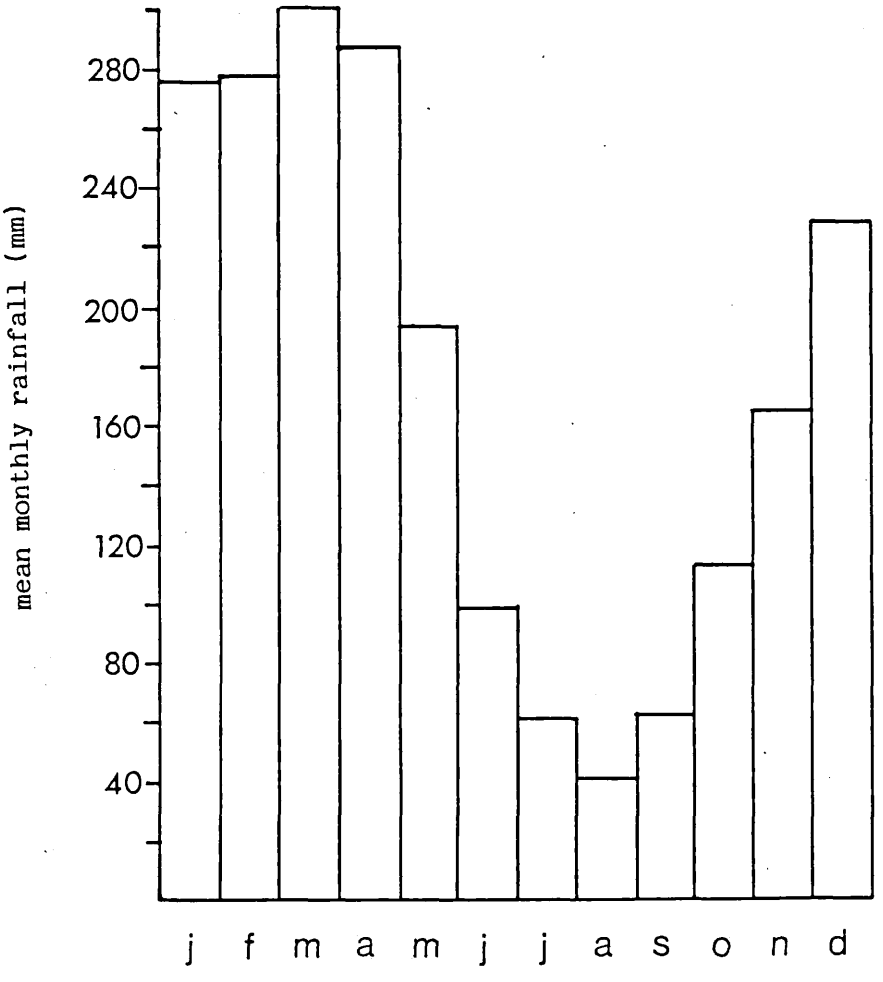

Table 4.4 Monthly rainfall (mm), and the number of rain days recorded at Virginia Water (Meteorological Office data) for the period September 1983 to August 1984

	Sept	Oct	Nov	Dec	Jan	Feb
Total rainfall (mm)	48.3	45.1	55.1	62.8	87.0	48.8
No. of rain days	15	17	9	19	28	18
Rain/rain day (mm)	3.2	2.7	6.1	3.3	3.1	2.7

	Mar	Apr	May	Jun	Jul	Aug
Total rainfall (mm)	80.7	5.3	105.2	26.9	18.4	26.5
No. of rain days	17	7	15	7	10	11
Rain/rain day (mm)	4.7	0.8	7.0	3.8	1.8	2.4

Table 4.5 Seasonal changes in the percentage cover of the oak canopy

date	mean % canopy cover	(s.d.)
07-11-83	74.4	9.1
21-11-83	59.6	11.5
24-01-84	21.5	7.5
14-03-84	19.4	11.0
01-05-86	36.9	6.7

these results are taken from 25 readings over an area 100 m^2

Table 4.6 The size distribution of 437 rain events from September 1976 to September 1977 at Reserva Ducke, Manaus (Franken and Leopoldo 1983)

Range (mm)	n events	% n	Total Depth (mm)	% Total depth
0.0 - 4.9	328	75.1	392.4	19.0
5.0 - 9.9	49	11.2	352.2	17.0
10.0 - 19.9	40	9.2	577.7	27.9
20.0 - 29.9	10	2.3	240.6	11.6
30.0 - 39.9	2	0.4	68.0	3.3
40.0 - 49.9	3	0.7	130.7	6.3
>50.0	5	1.1	308.5	14.9
Total	437		2070.1	

Table 4.7 The intensity distribution of 416 rain events from September 1976 to September 1977 at Reserva Ducke, Manaus (Franken and Leopoldo 1983)

Range (mm/hr)	n events	% n	Total depth (mm)	% Total depth
0.0 - 4.9	241	57.9	543.8	27.0
5.0 - 9.9	91	21.9	550.6	27.4
10.0 - 14.9	40	9.6	493.8	24.5
15.0 - 19.9	22	5.3	140.1	7.0
> 20.0	22	5.3	253.3	14.1
Total	416		1981.6	

between 5.0 and 14.9 mm/hr. For 75% of all rain events the rainfall lasts for less than 1 hr (Franken and Leopoldo 1983).

Evaporation rates have already been discussed in Chapter Two and have generally been put at 4 mm per day, 0.25 mm of which is the evaporation of intercepted water, suggesting that over the course of a 1 hour storm the loss due to evaporation is negligible.

The rain forest at Manaus has a layer of mature trees with their crowns between about 11 to 15 m above the ground. Above that at about 19 m there are occasional emergents. The percentage cover of this layer is around 89% and below it there is a layer of tree palms and saplings at about 6 to 8 m increasing the percentage cover to 93%. The ground surface is commonly covered by a continuous layer of dead leaves and herbaceous plants are rare. Running through the litter layer and protecting the soil surface to a depth of about 5 cm is a dense root mat. The soil appears sandy with the organic content concentrated at the level of the root mat.

Three sites were chosen to represent conditions of no forest, primary rain forest and some form of managed forest. The first was an open clearing of some several hundred meters square in which the depth and change in drop-size distribution through a storm of the rain were measured. These were assumed to be the same as those incident on the top of the canopy. Changes to the kinetic energy of rainfall by the canopy were measured at two other sites, 10 m and 200m away from the open site.

Both the canopy plots were laid out in the manner described above. Diagrams of the location of sampling points and plants within and overshadowing both canopy plots are given in Figures 4.5 and 4.6. While large tree boles were excluded from the plots as under the oak canopy, in some cases saplings or dead vegetation prevented the placing of gauges of traps in position in the grid. All plants occurring in the plots have been grouped according to their life form and identified by their local names and where possible by their

Figure 4.5 Plan of the rain forest single canopy site

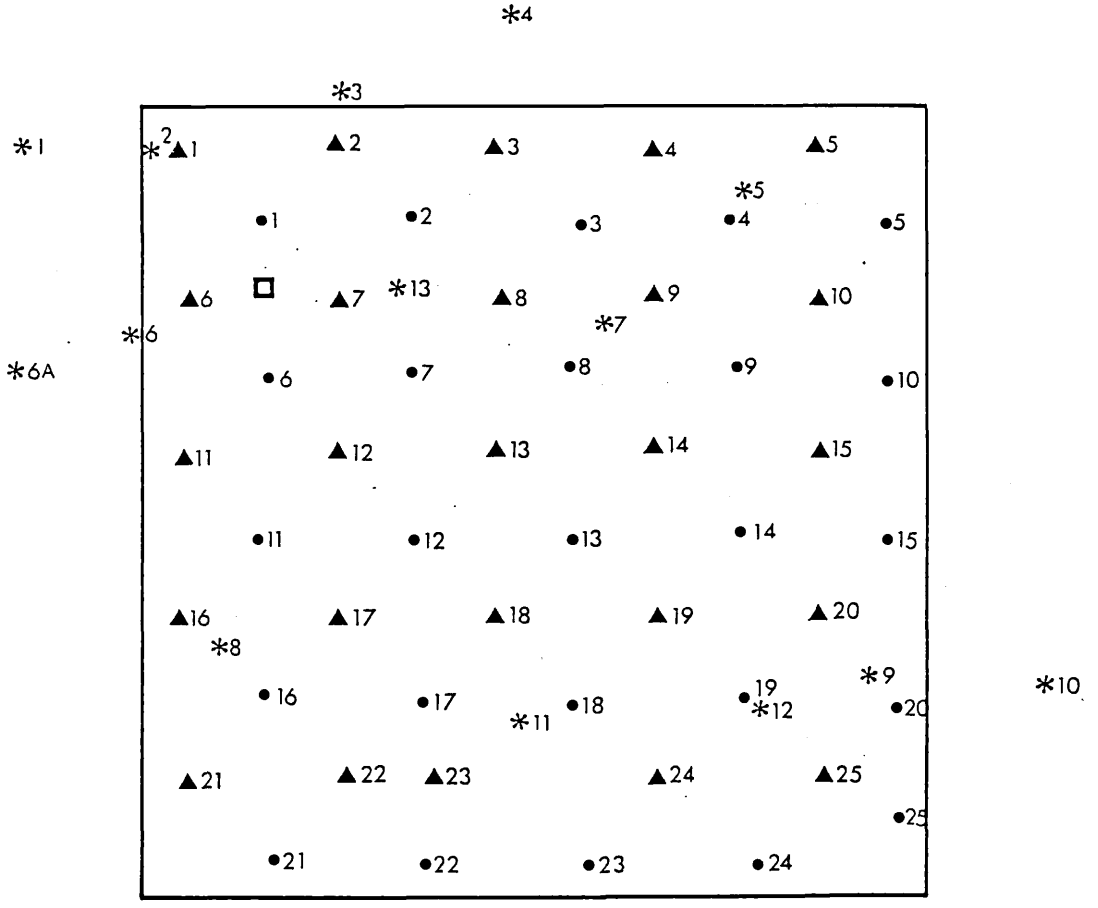

Legend

- ● raingauge
- ▲ splashtrap
- * centre of boles of trees
- □ throughfall drop size sampling point

Sampling Area = 100 m²

Figure 4.6 Plan of the rain forest multiple canopy site

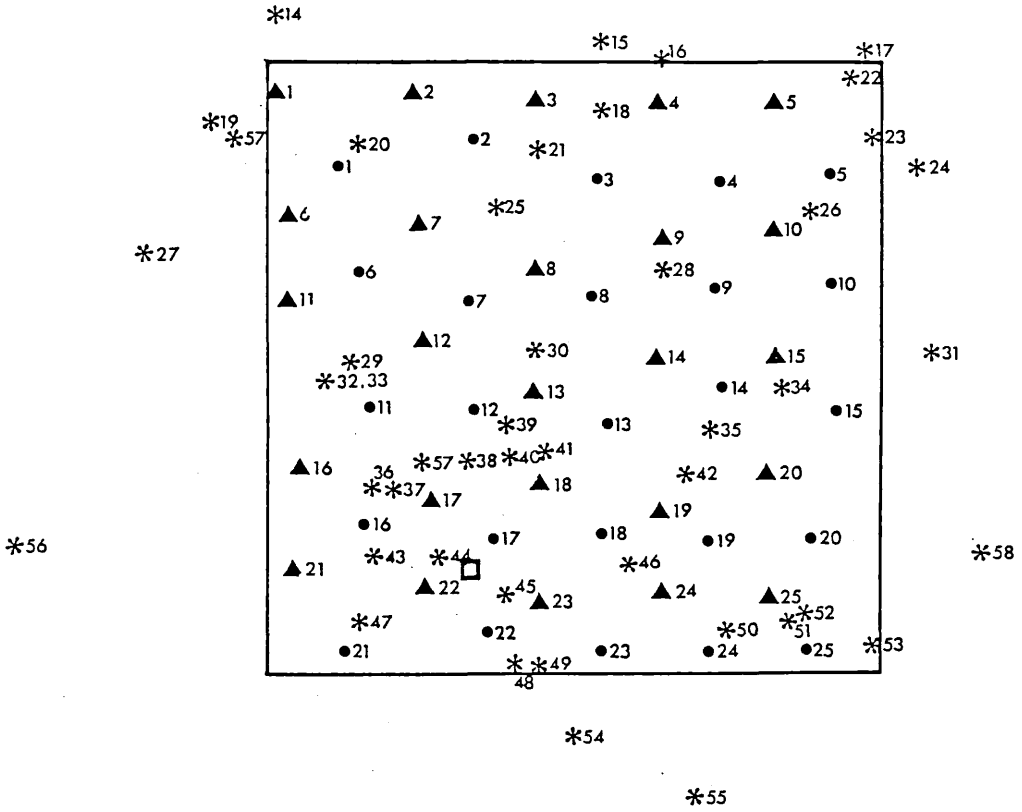

Legend

• raingauge

▲ splash trap

* centre of boles of trees, saplings and palms

□ throughfall drop size sampling point

Sampling Area = 100 m²

scientific names (Tables 4.8 and 4.9).

In the first plot, representing a managed forest, all vegetation below the single upper canopy layer at 11 m had been removed. There were 10 different species of tree identified in the canopy, but they were all of similar structural form and leaf size and shape. The heights of the lowest part of the canopy above each splash trap is given together with the approximate leaf size and percentage cover in Table 4.10. The average height of the lowest part of the canopy above ground was 11.3 m.

The second, multiple, canopy site was probably an area of complete secondary regeneration with the layers of palms and saplings intact below the upper canopy. There were 23 different identifiable species with more variable life forms and leaf sizes and orientations than at the single canopy site. Table 4.11 shows that the majority of the plants over the sampling points are substorey species, palms and saplings. In contrast to the single canopy site most of the leaves are large. Over the whole plot the the mean lowest height of the canopy was 2.9 m above the ground surface.

Table 4.8 Identification of trees, palms and saplings on single canopy site

Plant number	Life form	Identification	
		Local name	Latin name
1	tree	goaba de anta	---
2	tree	(dead)	---
3	tree	enuira preta	---
4	tree	lacre vermelho	---
5	tree	enuira preta	---
6	tree	enuira preta	---
6a	tree	angelim rafado	
7	tree	piriquiteira	---
8	tree	lacre vermelho	---
9	tree	murici da mata	---
10	tree	bren bronco	---
11	tree	dima	---
12	tree	casca periciosa	---

Table 4.9 Identification of trees, palms and saplings on multiple canopy site

plant number	life form	identification	
		local name	scientific name
14	tree	mura piranga	---
15	sapling	---	---
16	sapling	---	---
17	tree	ucuuba branca	Virola surinamensis
18	tree	bren vermelho	---
19	tree	ucuuba branca	Virola surinamensis
20	palm	palha vermelha	---
21	palm	marafa	---
22	sapling	---	---
23	sapling	---	---
24	palm	---	---
25	tree palm	pantua	---
26	sapling	---	---
27	tree	---	---
28	palm	palha vermelha	---
29	palm	mumura	---
30	tree	mura piranga	---
31	tree	mura piranga	---
32	sapling	---	---
34	tree	iga vermelha	---
35	palm	mumura	---
36	palm	pantua	---
37	sapling	---	---
38	tree palm	pupriarana	---
39	palm	palha vermelha	---
40	tree	inga vermelha	---
41	sapling	---	---
42	sapling	---	---
43	sapling	---	---
44	sapling	muragiboa preta	---
45	sapling	ucuquirana	Ecclinusa balata
46	sapling	muiratinga	Olmediophaena maxima
47	sapling	inbanba branca	---
48	sapling	ucuuba branca	Virola surinamensis
49	sapling	louro do bracho	---
50	sapling	ucrubo puno	---
51	tree	cordeino	---
52	sapling	---	---
53	sapling	---	---
54	tree	igai	---
55	palm	palha vermelha	---
56	tree	---	---
57	tree palm	pantua	---
58	palm	---	---

Table 4.10 The lowest height and percentage cover of the canopy above each splash trap in the single canopy site

Splash trap number	Plant above trap	Approx. leaf size	Height (m)	Percentage cover
1	tree (3)	meso	10.5	88.6
2	tree (3)	meso	4.9	94.1
3	tree (3)	meso	7.2	91.9
4	tree (5)	meso	9.8	92.9
5	tree (5)	meso	11.0	88.7
6	tree (13)	meso	17.0	91.1
7	tree (13)	meso	16.2	88.1
8	tree (13)	meso	11.3	84.9
9	tree (5)	meso	8.9	95.6
10	tree (5)	meso	9.8	87.3
11	tree (6a)	micro	4.1	89.8
12	tree (13)	meso	11.5	86.9
13	tree (13)	meso	10.2	88.3
14	tree (13)	meso	11.0	85.3
15	tree (9)	meso	19.3	87.6
16	tree (8)	meso	11.9	72.7
17	tree (13)	meso	14.6	89.1
18	tree (13)	meso	9.1	89.5
19	tree (13)	meso	15.6	85.5
20	tree (12)	meso	5.7	90.8
21	tree (8)	meso	15.4	missing
22	tree (8)	meso	17.7	89.3
23	tree (11)	meso	15.2	91.3
24	tree (12)	meso	4.7	89.7
25	tree (12)	meso	7.9	90.1
Drop size sampling point	tree (13)	meso	13.3	87.9
mean			11.3	88.7
(s.d.)				4.30

Table 4.11 The lowest height and percentage cover of the canopy above each splash trap in the multiple canopy site

Splash trap no.	Plant above trap	Approx. leaf size	Height (m)	Percentage cover
1	tree (14)	meso	4.4	92.9
2	tree palm (21)	macro	4.7	89.4
2	tree palm (21)	macro	2.7	95.5
4	palm (28)	macro	3.0	93.8
5	palm (28)	macro	2.3	92.4
6	sapling (19)	meso	6.7	95.9
7	sapling (19)	meso	4.6	94.1
8	palm (35)	macro	3.1	91.1
9	palm (28)	macro	2.3	92.1
10	palm (35)	macro	1.8	94.2
11	sapling (27)	micro	1.9	96.0
12	palm (35)	macro	2.5	94.2
13	palm (35)	macro	2.5	93.4
14	palm (35)	macro	2.5	98.4
15	palm (35)	macro	3.1	92.5
16	palm (36)	macro	2.2	94.9
17	palm (39)	macro	1.9	97.5
18	palm (39)	macro	1.5	93.6
19	palm (35)	macro	2.2	95.9
20	palm (35)	macro	2.8	98.8
21	sapling (47)	meso	3.5	95.0
22	sapling (44)	meso	2.4	94.6
23	sapling (45)	macro	3.1	92.8
24	palm (35)	macro	2.2	96.6
25	palm	macro	3.1	99.2
Drop size sampling point	sapling (44)	meso	2.7	97.0
mean			2.9	94.7
(s.d.)				2.35

CHAPTER FIVE DERIVATION OF A CONTINUOUS RECORD OF KINETIC ENERGY CHANGE

Introduction

The parameters which define the energy of the rain have been identified in the previous section and methods for their measurement outlined. This chapter discusses the derivation of a continuous record of intensity change and drop-size distribution change from the samples of rain taken throughout each storm and measurements of total rain depth. Four sections are presented. The first outlines the calculation of the depth and kinetic energy for a given period from a sample of the drop-size distribution. The second section discusses the methods for deriving a continuous record by interpolating the depth and drop-size distribution of unsampled rain from the discrete samples. The third section presents the results of a number of different interpolations and assesses their accuracy in terms of the intensity profile produced and the difference between the interpolated total depth and the measured depth. The fourth section discussed the derivation of simultaneous records of kinetic energy for the rainfall input and the throughfall output from the continuous record.

The information derived by the methods outlined in this chapter is then used to examine the different testable statements identified in Chapter Three concerning the change of energy by a canopy. Throughout the chapter errors arising from the original sampling methods and from the interpolation process are discussed.

Section One Calculation of sample volume and kinetic energy

Samples of raindrops were taken on sheets of dyed filter paper throughout a number of storms to determine the drop-size distribution and the intensity of rain for the sample period. Appendices 1 (a) and (b) record the number of drops in each size class for each sample

of rainfall and throughfall in each site and the duration of each sample and gap.

From each sample sheet a subsample of stains was measured. The total number of stains on each sheet was counted.

1) To calculate the drop-size distribution for a sheet from the drop-size distribution of the subsample

Let the stains range over a number of size classes (i), let f_s be the number of drops in the subsample, let f_i be the number of drops in each size class, therefore

$$f_s = \sum_{i=1}^{n} f_i \qquad [5.1]$$

if $$F_i = \frac{F}{f_s} . f_i$$

and, $$F = \sum_{i=1}^{n} F_i \qquad [5.2]$$

where F is the counted total number of stains in the sample and F_i is the number of stains of size i in the sample.

2) To calculate the volume of the sample (V) and hence the depth of the sample (d)

To calculate the volume of a single drop of a given stain size class (v_i), the the calibration of drop mass, m (g), and stain diameter, i (mm) may be taken from equation [4.2], thus,

$$m_i = 2.931 \times 10^{-5} \; i^{2.18}$$

hence to calculate the drop volume v_i (m^3)

$$v_i = m_i \times 10^{-6} \qquad [5.3]$$

Let the volume of the sample on the sheet be V (m^3) where

$$V = \sum_{i=1}^{n} F_i \, v_i \qquad [5.4]$$

3) To calculate the kinetic energy of the sample J (J)

The kinetic energy (j_i) of a single drop in stain class (i) falling at a given velocity (s_i) may be calculated from

$$j_i = \tfrac{1}{2} m_i \times (s_i)^2 \qquad [5.5]$$

Hence the energy for a whole sheet (J) may be calculated from

$$J = \sum_{i=1}^{n} j_i \cdot F_i \qquad [5.6]$$

The velocity of a drop depends on its height of fall. Data published by Gunn and Kinzer (1949) gives terminal velocities for drops of different sizes. Laws (1941) published data giving the velocity of fall of drops of different sizes from different heights. Both data sets are shown in Figure 5.1 which plots the fall velocity of drops of different diameters from different heights.

In the sites where drops fell from an open sky or from a canopy

Figure 5.1 The velocity of fall (m/s) of drops of different diameter (mm) in still air, after falling from various heights (m) (from Laws 1941 solid line, Gunn and Kinzer 1948 broken line)

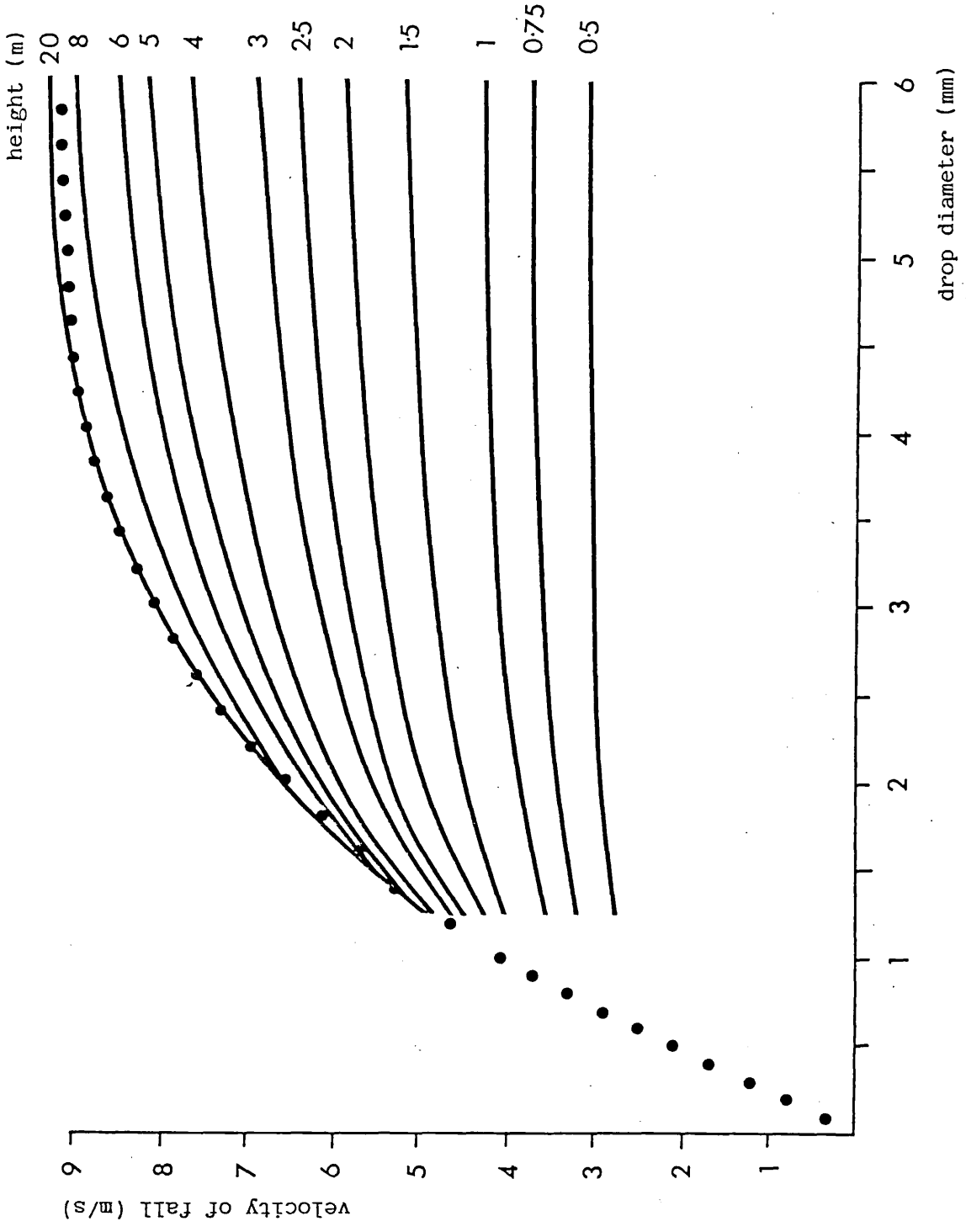

over 8 m in height it was assumed that all the drops were falling at terminal velocity. Although Dohrenwend (1977) stated that wind may accelerate raindrops to speeds greater than their terminal velocity, no measurement of wind speed was made in this project. Consequently it was not possible to quantify the effect of wind and the velocities of fall for raindrops should be regarded as minimum values. It was assumed that throughfall drops fell in still air beneath the canopy. In the cases of the multiple-layered rain forest canopy, branches and leaves descended to less than 8 m above the ground. In consequence, to calculate the kinetic energy of the drops, an estimation of their fall velocities had to be made.

Table 5.1 records the life form, approximate leaf size and height above ground of all plants directly above the multiple canopy sampling point which are illustrated in Figure 5.2. From the photograph and the table it can be seen that the drops recorded in the sample could have fallen from a number of heights. The lowest height of the canopy above the sampling point is 3.14 m. From Table 4.10 it can be seen that the lowest height above the plot varied spatially with a mean height of 2.88 m. Since Laws's data is restricted to integer heights a height of 3 m was chosen as the minimum height of fall for all drops. The maximum velocity of fall for any drop was terminal velocity and the true velocities are assumed to lie betwen these extreme values.

Section Two The derivation of a continuous drop size record from a discrete data set: methods

The samples of rain and throughfall throughout each storm gave discrete measurements of the change in drop-size distribution. However to calculate the cumulated kinetic energy or the cumulated depth of rainfall or throughfall for any given time a continuous record was derived from the discrete data set.

Table 5.1 The life forms, leaf size and heights of all plants directly over the multiple canopy sampling point

Plant	Approx leaf size	Height above sampling point (m)
sapling 44	meso	3.14
tree palm 57	macro	4.70
tree palm 38	macro (fine-leaved palm)	6.80
tree 54	meso	more than 8

Figure 5.2 The multiple canopy vertically above the drop size sampling point

1) General methods of interpolation

Frequently samples of a continuous process are recorded for discrete time intervals. In order to reconstruct the underlying process some form of interpolation between the sampling points is needed. The interpolation can be carried out in a number of ways which depend on the number of samples and the interval between them. The approaches can be divided up into three sections. Firstly there are those methods which do not involve explicit computation of the interpolating function but derive intermediate values from preceding and succeeding samples. Secondly there are those which select a specific mathematical function thought to be similar to that of the underlying process. The specific function may be adjusted to minimise the differences between the actual interpolated values. Similarly there are those methods which compare the series to be interpolated with another series but in this case the reference series is empirically derived from other measurements of the same process.

For the purposes of this discussion it is assumed that the independent variable x_i range within x_1, x_2, .. x_i, .. x_n and the corresponding dependent variable $y(x_i)$ range within $y(x_1)$, $y(x_2)$, .. $y(x_i)$, .. $y(x_n)$ (Figure 5.3).

i) Methods of interpolation not involving the explicit computation of the interpolation function

Simple linear interpolation

The simplest method of interpolating to determine y for a given x is to take the mean of the values at adjacent points such that:

$$y(x_i) = y(x_1) + \left(\frac{x_i - x_1}{x_2 - x_1}\right) (y(x_2) - y(x_1)) \qquad [5.7]$$

Figure 5.3 The interpolation of intermediate points (x_i, y_{xi}) from a range of dependent and independent variables

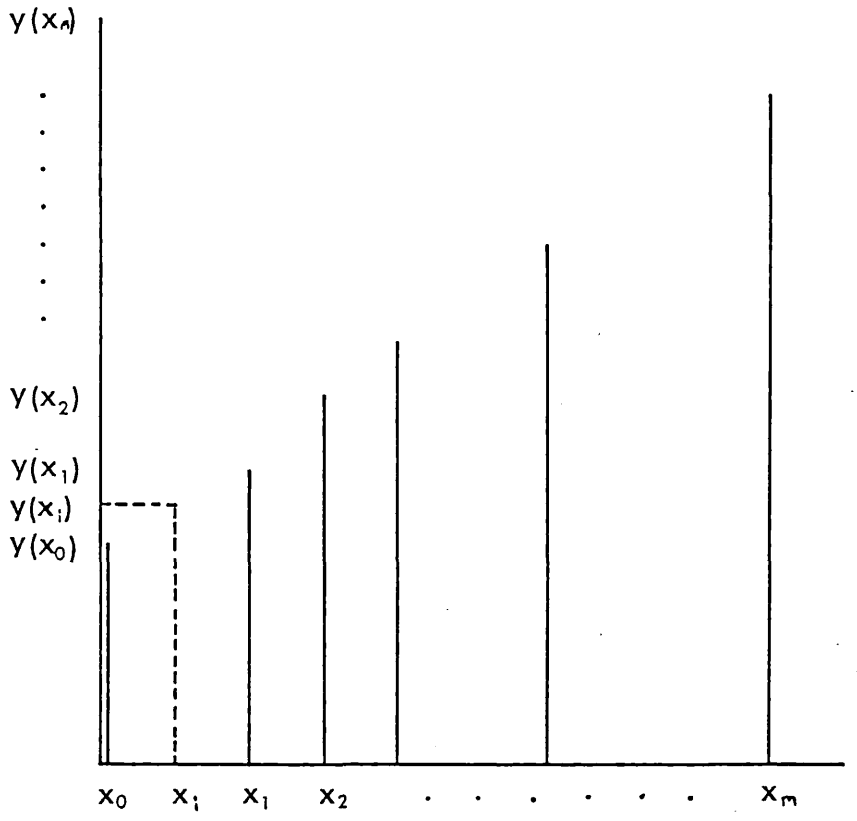

This method can be used when there is a minimum of additional data. It assumes that there is a linear relationship between adjacent points and obviously is most accurate with small gaps between the known values. The straight line interpolation is commonly used as a first interpolation on which to base more advanced methods (e.g. Friedman 1962). Other interpolations should only be used when they reduce the errors between interpolated and known values.

Smoothing

An alternative method of interpolation to the mean between adjacent points is to identify a curve which follows general trends in the data. With small scale, perhaps random, variations smoothed out the interpolation depends on the values of an increasing number of preceeding and succeeding points. Such a smoothing of the data inevitably looses information and the heights of the peaks tend to be reduced. T. Culling (pers. comm.) advocates the drawing of such a curve using the "bold freehand sweep" as being the swiftest method. Indeed when there is a large number of points and replicability is not necessary there is much to recommend this method.

However where trends are not clear to the eye and replicability is important, purely mathematical methods are better although the results they achieve may be similar. By taking a moving average the curve connecting a series of known points is smoothed by averaging several preceding and succeeding values, the number of points (n) used determines the extent of smoothing. For series when the data is equally spaced, the moving average is calculated thus,

$$y(x_i) = \frac{1}{(2n + 1)} (y(x - n) + \ldots y(x) + \ldots y(x + n)) \quad [5.8]$$

It is more common however, to weight the values for $y(x_i)$

according to the position, relative to the value to be interpolated, according to the weight of a given distribution. If the general trend was considered to reflect a Gaussian distribution the weights for $y(x_i)$ would be approximated with a binomial distribution. To smooth the data by averaging over adjacent known values with a binomial distribution spanning three values the following formula is suggested by (Bevington 1969)

$$y(x_i) = 0.25\ y(x_i - 1) + 0.5\ y(x_i) + 0.25\ y(x_i + 1) \qquad [5.9]$$

Such an averaging tends to make the data more similar to the suggested distribution but is only applicable where the number of known values (n) is large; when the Gaussian and binomial distributions are similar. Alternatively Yevjevich (1972) extended the interpolation to including higher value polynomials whose least squares fit gives the weights of the smooth moving average scheme.

Increasingly complex methods of moving average, for example those involving a component relating the autocorrelation of adjacent points, need increasingly large amounts of data. McCleary and Hay (1980) recommended such methods should not be used on series of less than 50 readings, nor on series where the time between readings is not constant.

ii) Methods using explicit mathematical functions

If there is sufficient information available to suggest that the underlying process may be of a specific mathematical function it is possible to use that function as a base for interpolation. Most commonly the general function is "fitted" to the data using the method of least squares to enhance the goodness of fit, often after the data has been generally smoothed. Bevington (1969) explained in detail the processes involved. The success of such an interpolation depends on

the choice of mathematical function as an approximation to the true function and it should be realised that the method will always enhance the resemblance.

There is a wide range of functions from which to select the most similar function and Bevington (1969) suggested that others should be compared with the selected function to assess the importance on the choice on determining the interpolated values.

Polynomials are frequently used as the interpolating function although they can exhibit unwanted fluctuations between data points especially at the end of a data set where the points are widely spaced. Thus higher order polynomials can be fitted than are exhibited in the original data (Numerical Algorithms Group 1984). Similarly logarithmic functions could be fitted to sections of the curve provided there was sufficient justification through knowledge of the underlying system.

iii) Methods using a related series

Friedman (1962) gave an account of how a series may be interpolated taking information from a related series. The related series may derived from the same process but using a different measuring method or from a process which is assumed to cause or affect the series of interest. Although intuitively it might be expected that interpolation using the related series will be better than that using the linear mean between adjacent points, Friedman stressed that the correlation between the trends in the two series at any point should be greater than 0.5. If this is not so the result of using the related series can be worse than the linear mean interpolation.

2) The choice of interpolation method

It has been stated above that the choice of interpolation method

is governed by the extent of the information available, the more complex methods having stricter data requirements. In addition it has been suggested that any interpolation should be compared with the linear mean interpolation to ensure that there is a gain in accuracy through using another method.

i) Information available

From the rain drop samples between 3 and 27 measurements of rainfall intensity, averaged over periods of between 1 second and several minutes, were made during a number of storms. The gaps between sampling varied between about 2 and 5 minutes. The interpolation curve was required to estimate the intensity of rain in the unsampled gaps. The area under the interpolation curve was required to equal the total depth of rain measured for each storm. For storms at the Reserva Ducke site a continuously recording raingauge gave the intensity of rain averaged over 10 minute intervals.

Given the small number of known points in the data series and the unequal duration of both samples and unsampled gaps use of the complex moving average techniques was not possible. Simpler moving average interpolations were hindered by the pronounced positive skewness of high intensity readings in some storms. Although a related series was obtained for some of the storms, the coarseness of the intervals prohibited the interpolation using related series suggested by Friedman (1962). However it was possible to identify general trends in the data from this related series to guide the choice of method.

ii) General principles of the interpolations

The following general principles were applied in selecting the appropiate interpolation given the limitations of the data. Each known sample was represented as a bar, the width and height of which

were determined by the duration and intensity of the sample. The area of each bar represented the depth of rain. Two different basic interpolations were compared both incorporating a simple moving average which attempted to compensate for the skewness of the data by interpolation from one preceding and then successive inclusion of succeeding known values only. The first simply calculated a linear mean between the intensity of adjacent bars. The second aimed to weight both bars and unsampled gaps according to their duration. The area under each interpolated curve was calculated by summing the areas of each bar. Total interpolated depths thus derived were compared with the total measured depth. Selection of the best interpolation depended on the size of the error between interpolated and measured depths and on the qualitative similarity between the shape of the interpolated curve and the shape of the curve derived from continuous measurement.

3) Detailed description of the interpolation methods

i) Notation

Discrete samples of rain, of duration t (s), were taken throughout the storms leaving unsampled gaps in between (Figure 5.4). Let the time range from t0 to T so that t1 - t0 is the duration of sample 1 and d_{t0t1} is the depth of water in sample 1. Hence the intensity of of rain in sample 1 may be written

$$I_{t0t1} = \frac{d_{t0t1}}{(t1 - t0)} \qquad [5.10]$$

ii) To find the depth of rain in the unsampled gap (t1t2) using the intensity interpolation

This is a linear interpolation using a progressive number of succeeding samples, but weighting all samples equally.

Figure 5.4 The interpolation of rainfall depth during unsampled gaps in a storm

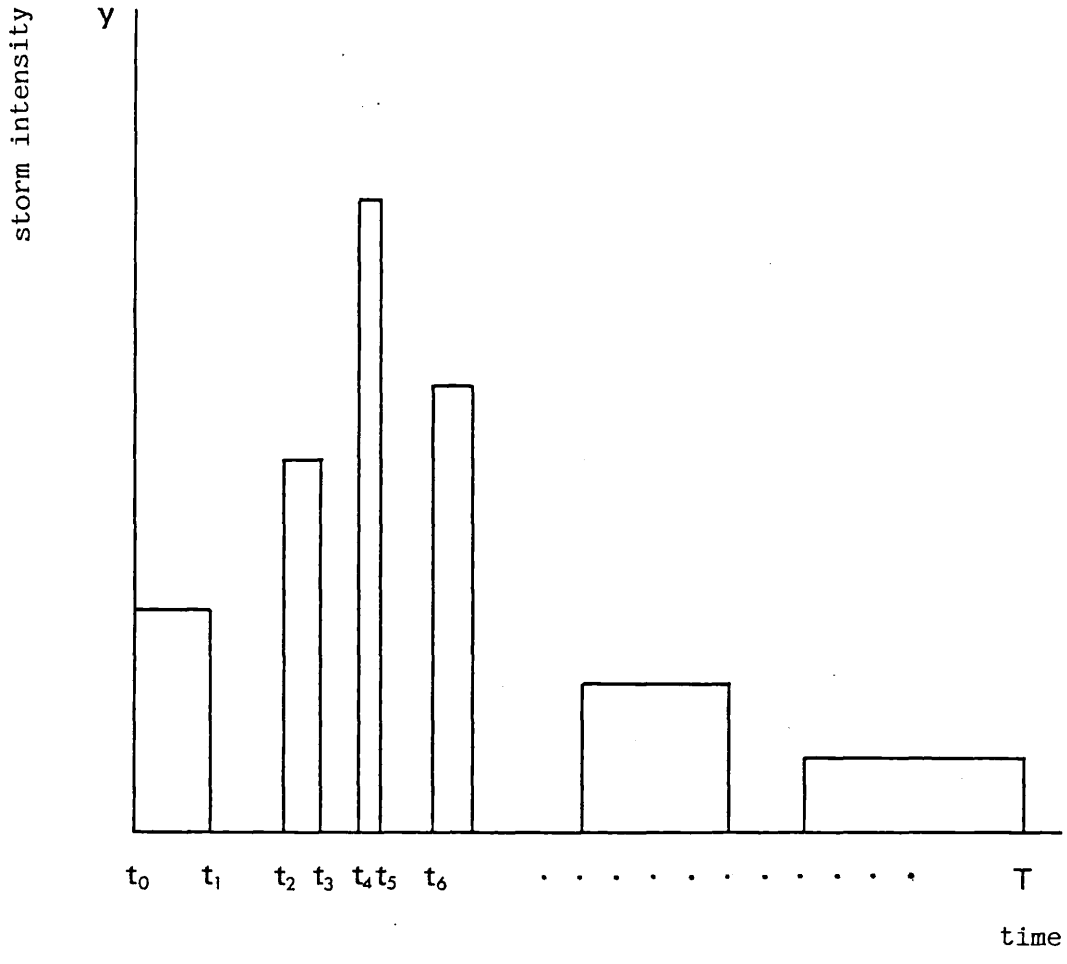

Weight 2, a simple linear interpolation between the intensity of adjacent points such that I^{y}_{t1t2} may be calculated from

$$I^{y1}_{t1t2} = \frac{1}{2} (I_{t0t1} + I_{t2t3}) + e^{y1}$$

hence from [5.10],

$$I^{y1}_{t1t2} = \frac{1}{2} \left(\frac{d_{t0t1}}{(t1 - t0)} + \frac{d_{t2t3}}{(t3 - t2)} \right) + e^{y1} \quad [5.11]$$

where e^{y} is the error in the calculation of intensity using this method

Weight 3, a linear mean moving average including the preceeding and two succeeding points such that I^{y}_{t1t2} is calculated from

$$I^{y2}_{t1t2} = \frac{1}{3} (I_{t0t1} + I_{t2t3} + I_{t4t5}) \, e^{y2}$$

hence from [5.10],

$$I^{y2}_{t1t2} = \frac{1}{3} \left(\frac{d_{t0t1}}{(t1 - t0)} + \frac{d_{t2t3}}{(t3 - t2)} + \frac{d_{t4t5}}{(t5 - t4)} \right) + e^{y2} \quad [5.12]$$

etc.

The interpolated depth of rain (dg) for the gap t1t2 may be calculated from

$$dg_{t1t2} = (t2 - t1) \, (I^{y}_{t1t2} + e^{y}) \quad [5.13]$$

iii) To find the depth of rain in the unsampled gap (t1t2) using the depth interpolation I^{z}

The depths and times of preceeding and succeeding samples are

combined to weight those samples which were of longer duration.

Thus for weight 2, the interpolation is between adjacent points such that

$$I^{z1}_{t1t2} = \frac{(d_{t0t1} + d_{t2t3})}{(t1 - t0) + (t3 - t2)} + e^{z1} \qquad [5.14]$$

where e^2 is the error in the calculation of intensity using this method.

Weight 3, interpolation between preceeding and two succeeding points

$$I^{z1}_{t1t2} = \frac{(d_{t0t1} + d_{t2t3} + d_{t4t5})}{(t1 - t0) + (t3 - t2) + (t5 - t4)} + e^{z1} \qquad [5.15]$$

Similarly the interpolated depth of rain in the gap may be calculated from [5.13] from the interpolated intensity.

iv) To find the total interpolated depth (Dc)

$$D^{xw}_c = \underset{t=0}{\overset{T}{\sum}} d_{t,t+1} + \underset{t=1}{\overset{T}{\sum}} dg^{xw}_{t,t+1} \qquad [5.16]$$

(even nos) (odd nos)

where x = interpolation y or z
w = weight 2, 3, 4, or 5

v) To select the interpolation method

The selection of the interpolation method was based on a

comparison between the curve of intensity change produced by the interpolation and that from the continuously recording gauge. In addition, Dc (interpolated storm depth) was compared with Dm (measured storm depth) to select the interpolation which minimised the e^{xw} (the error due to the choice of a particular interpolation and weight)

$$Dm = Dc + e^{xw} \qquad [5.17]$$

vi) "Fitting" each interpolated depth (dg) and measured depth (d) so that Dc = Dm

The error term e^{xw} was divided in proportion to the depth of all measured depths from the samples (d) and the interpolated depths (dg). If

$$d' = d \cdot \frac{Dm}{Dc} \qquad [5.18]$$

$$\text{then } Dm = \underset{t=0}{\overset{T}{\sum}} \frac{Dm}{Dc} \cdot d_{t,t+1} + \underset{t=1}{\overset{T}{\sum}} \frac{Dm}{Dc} \cdot dg_{t,t+1}$$

(even nos) (odd nos)

$$\text{hence } Dm = \underset{t=0}{\overset{T}{\sum}} d'_{t,t+1} + \underset{t=1}{\overset{T}{\sum}} dg'_{t,t+1} \qquad [5.19]$$

(even nos) (odd nos)

where d' = adjusted sample depth
d'g = adjusted gap depth

vii) Recalculating the drop-size distributions in the samples using adjusted depths

To find the adjusted volume of sample (V')

$$V'_{t0t1} = d'_{t0t1} \times pi \times k^2 \qquad [5.20]$$

where k = radius of sampling area (70 mm)

To find the adjusted volume for each size class ($\bar{v}'_i$)

$$\bar{v}'_{i(t0t1)} = \frac{V_{t0t1}}{V'_{t0t1}} \times \bar{v}_{i(t0t1)} \qquad [5.21]$$

To find the adjusted number (F'_i) of stains in class i and hence the adjusted number of all drops on the sheet (F')

$$F'_i = \frac{\bar{v}'_i}{v_i} \qquad [5.22]$$

where v_i = volume of a single drop is size class i

hence, $$F' = \sum_{i=1}^{n} F'_i \qquad [5.23]$$

To find the number of drops in the gaps in size class i (Fg_i) and the total number of drops falling in the gap (Fg), it is assumed that the size distribution of drops in each gap is the same as the combination of drop sizes from adjacent samples. Hence

$$Fg_{i(t1t2)} = F_{i(t0t1)} + F_{i(t2t3)} \qquad [5.24]$$

therefore the estimated volume of the drops in the gap (Vg) is

$$Vg = \sum_{i=1}^{n} Fg_i \, v_i$$

or $$Vg = \sum_{i=1}^{n} \bar{v}g_i \qquad [5.25]$$

where v_i = the volume of a single drop in size class i.

To correct the estimate gap volume (Vg) to the corrected gap volume (Vg') obtained from the interpolation

$$\bar{v}g' = \frac{Vg}{V'g} \bar{v}g_i \qquad [5.26]$$

hence $$Vg' = \sum_{i=1}^{n} \bar{v}g'_i \qquad [5.27]$$

Finally the number of drops in the gaps, calculated from the number of drops in adjacent samples and the volume interpolated for the gap (Fg) is

$$Fg'_i = \frac{\bar{v}g'_i}{v_i}$$

and therefore $$Fg' = \sum_{i=1}^{n} Fg'_i \qquad [5.28]$$

viii) To calculate the kinetic energy ($J_{t,t+1}$) of each sample, and gap using the adjusted numbers of drops and hence to obtain the total kinetic energy of the storm

For both samples and gaps, the energy may be calculated from

$$J_{t,t+1} = \sum_{i=1}^{n} j_i \cdot F'_{i(t,t+1)} \qquad [5.29]$$

where j_i is defined in equation [5.5]

Hence the kinetic energy for the storm (J) is

$$J = \sum_{t=0}^{T} J_{(t,t+1)} \qquad [5.30]$$

Section Three Derivation of a continuous record from a discrete data set: results

This section will discuss the results of the interpolation of a continuous record from the discrete samples of drops. The accuracy of the interpolation will be increased if there are measurements of total depth of the rainfall and throughfall and an independent continuous record of rain intensity with which to compare the interpolated depth and intensity profile. However, only the tropical rain forest sites have accurate measurements of storm depth and an independent continuous record of intensity. Therefore it is proposed that the selection of a suitable interpolation will be made with the tropical rain forest data and the results applied to the oak forest data.

1) Summary of the tropical rain forest data available

i) Rainfall depth

Measurements of storm depth from the independent, continuously recording gauge, the on-site gauges and measurements of throughfall estimated using both averaging techniques are shown in Table 5.2. The value for the on-site gauges is the mean of the 4 readings which are presented in Appendix 2. A two-sample t-test, to test the significance of the difference between the means of both data sets, was conducted for the records of storm depth from the continuous and on-site gauges. The test shows that there was a 0.78 probability of the means being the same. The variations between measurements may be accounted for by the difference

Table 5.2 Storm depth (R) (mm) recorded by the continuously recording raingauge, on-site raingauges, different estimates of mean throughfall ($\bar{T}$) (mm) under both canopies

Storm	Open R (mm)		Single Canopy $\bar{T}$ (mm)		Multiple Canopy $\bar{T}$ (mm)	
	met. sta.	on-site	mean	regression	mean	regression
j7	1.2	1.2	0.88	0.87	---	---
j10b	3.85	3.7	3.11	3.14	1.67	1.39
j10c	---	1.2	0.87	0.87	0.45	0.36
j11	12.3	12.7	11.53	11.29	4.63	5.08
j12	1.5	1.41	0.97	1.06	0.17	0.45
j13	0.2	0.11	0.01	---	0.00	---
j14b	1.9	1.80	1.56	1.42	0.50	0.61
j15	2.55	2.83	2.22	2.35	0.99	1.03
j16a	4.4	8.86	7.63	7.81	4.17	3.50
j16b	0.45	0.36	0.12	0.11	0.03	0.02
j20	2.6	2.93	2.39	2.44	0.84	1.07
j22	9.9	13.46	11.93	11.98	---	---
mean	3.71	4.21	3.60	3.61	1.35	1.35

single canopy regression $\bar{T} = 0.41R - 0.13$

multiple canopy regression $\bar{T} = 0.91R - 0.21$

in locations between the two sites.

ii) Throughfall depth

The depth of rain recorded for each storm in each of the 50 gauges under the canopies are recorded in Appendix 2. The estimation of average throughfall ($\bar{T}$) over a given area, from point measurements of rain by gauges located within the area under a canopy which may vary in density and capacity, is a common problem. The most obvious solution, employed by among others Jackson (1975) and Reynolds and Leyton (1961), is a straight averaging of the throughfall depths from each gauge for each storm (Tg), such that

$$\bar{T} = \frac{Tg}{n} + e_1 \qquad [5.31]$$

where Tg = throughfall in any gauge
n = number of gauges
e_1 = error which reflects the differences in canopy characteristics above each gauge

The second solution is to consider the throughfall for each gauge for all storms, regressing throughfall for each gauge (Tg) against rainfall (R) thereby obtaining 25 individual estimates of throughfall for a storm of any size (Gash and Lloyd pers. comm.). Hence

$$T_g = a_g R - b_g + e_2 \qquad [5.32]$$

where T_g = throughfall for each gauge
b_g = capacity of the canopy above each gauge
a_g = rate of increase in throughfall with rainfall

R = rainfall depth

e_2 = error which depends on errors in throughfall measurement due to alterations in the canopy configuration between storms

The mean throughfall $\bar{T}$ for any storm is calculated from an average regression of throughfall on rainfall from each of the individual estimates. The average regression is obtained from the mean of the intercepts and the mean of the slopes. The deviation of the intercepts about the mean for each regression reflects the variation in canopy configuration above given points between storms and the deviation for the average regresion curve reflects spatial variation in the canopy.

The results of both estimates of throughfall under each canopy for each site are presented in Table 5.2. The two estimates of mean throughfall were compared using a two-sample t-test. For the single canopy site and the multiple canopy site the values for the probability, p, of the estimate using both methods were 1.0 and 0.99 respectively. Hence with the results statistically indistinct either method was justified for use.

iii) Intensity change during a storm

Figure 5.5 shows the intensity profiles for the 13 storms recorded during the study period. For most of the storms the initial high intensity burst is easily seen with the following rapid decay. These storms are charactistically small for the middle of the dry season.

2) Summary of the oak forest data available

It has already been stated in this chapter that neither accurate measurements of the depth of rainfall nor the depth of throughfall are

Figure 5.5 The intensity profiles for the 13 storms sampled during the study period by the continously recording meteorological station

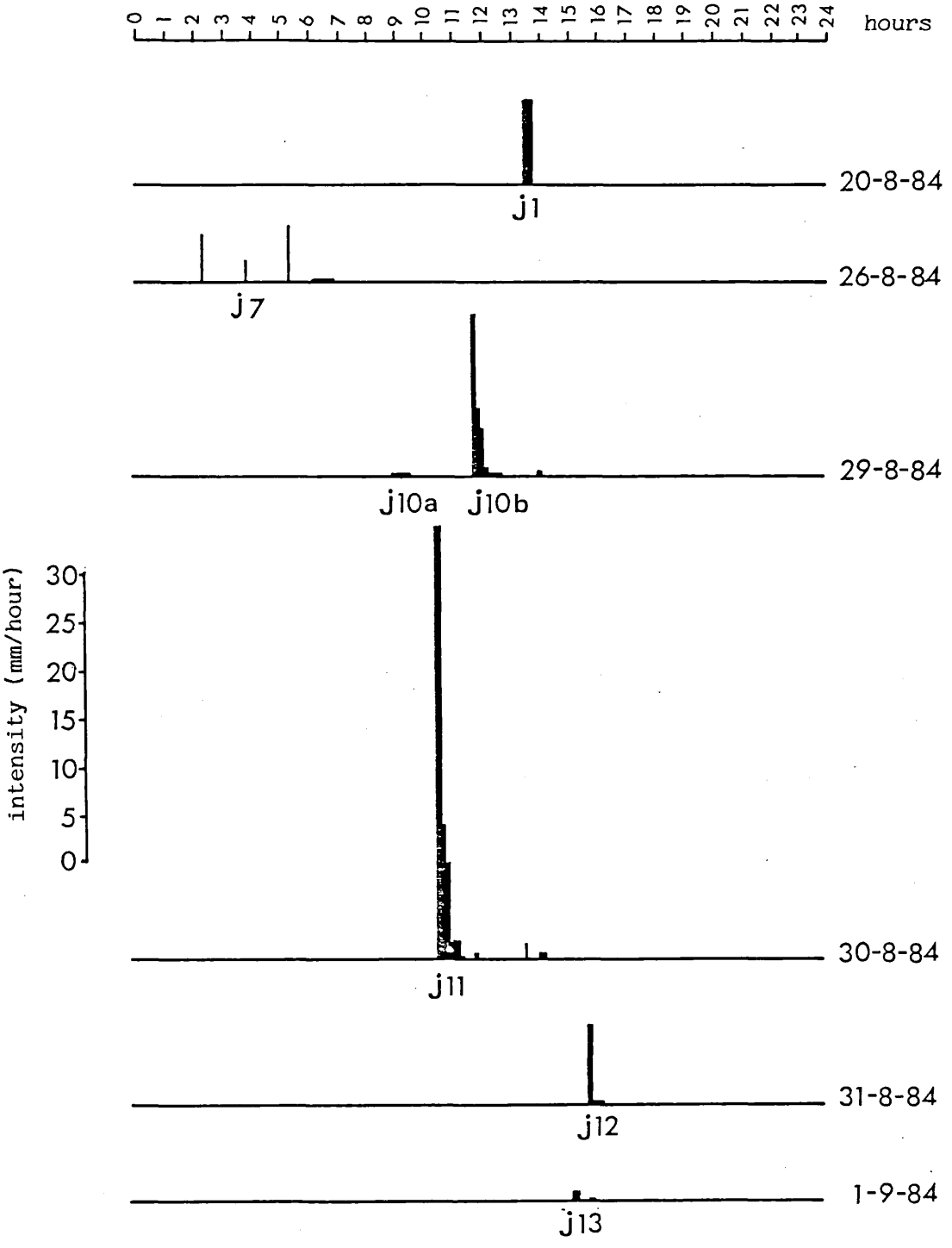

(Figure continued overleaf)

Figure 5.5 (continued)

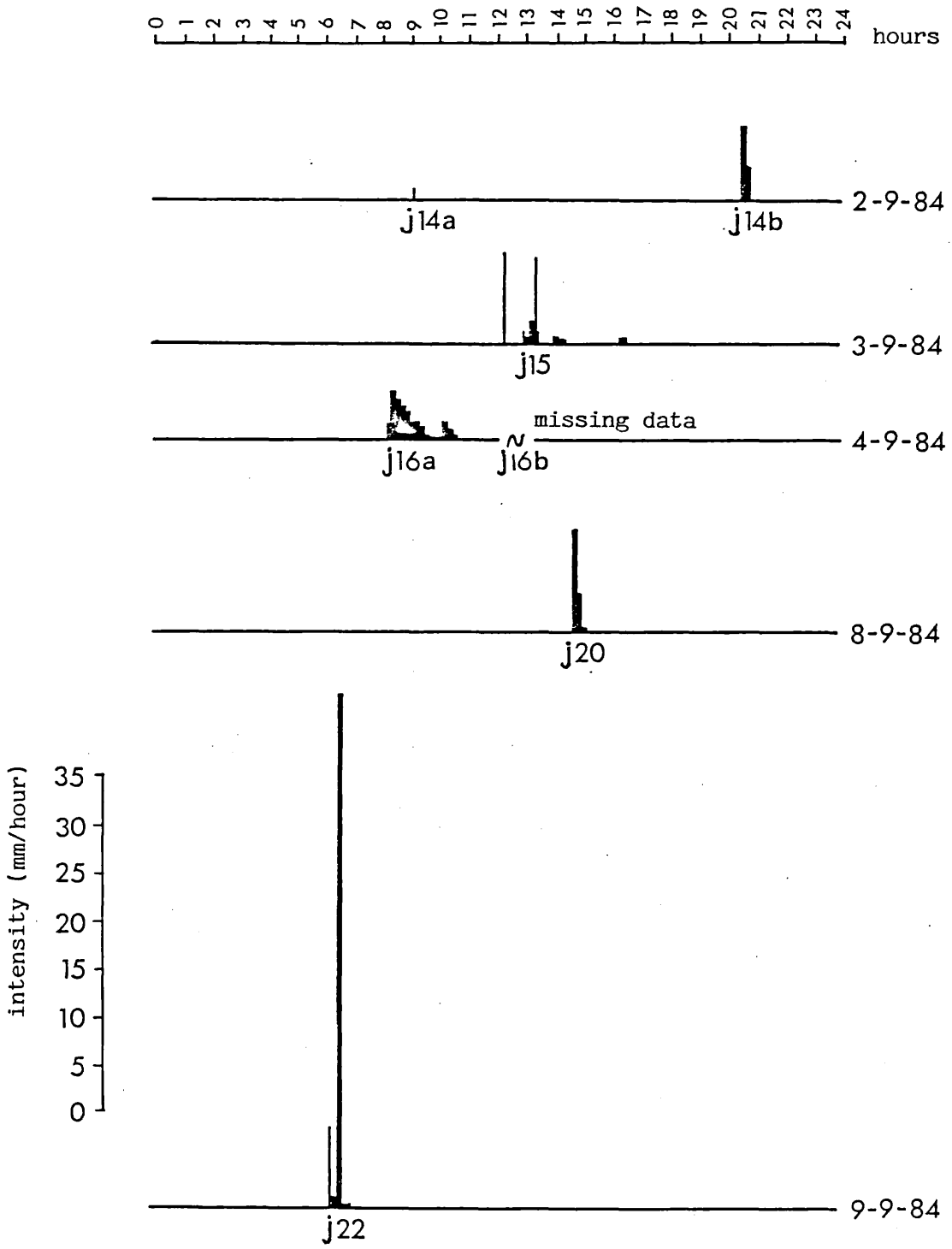

available and arbitrary depths have had to be chosen.

i) The selection of rainfall depths

Each drop-size distribution is a function of the size of and intensity of the storm from which it comes. Hence rather than selecting arbitrary depths for each storm, the information available on daily rainfall totals, records of hourly rainfall from Silwood Park (5 miles away) and intermittent tipping bucket measurements were used to obtain approximate storm depths. Table 5.3 sumarises the information available and presents the selected total depths.

On each storm day it was noted whether the storm sampled was the only storm, if there were other storms or whether the rain sampled was part of a longer period of rain. From these notes it is possible to identify storms where the daily rainfall total was the same as the storm depth. If the storm was part of a longer period of rain an estimate of depth was made from the length of the sampling time. These were usually small storms, less than the canopy saturation value.

ii) The selection of throughfall depths

It was assumed that the throughfall for storms which were larger than the canopy capacity was equal to the rain depth less the canopy capacity. Patric (1966) defined the capacity of an oak canopy as 1.17 mm in the summer and 0.21 mm in the winter. Thompson (1972) gave values of 1.0 mm and 0.4 mm for summer and winter canopies respectively. Table 5.4 shows that in storms d125 and d178, rainfall depths of 3.0 mm and 2.2 mm were assumed to have exceeded the canopy capacity and hence throughfall depths were assumed to be equal to the rainfall depth less 0.4 mm.

Storms d3, d52, d211 and d237 were all assumed to be too small to

Table 5.3 Summary of data available to determine the storm depths (mm) at the oak canopy site.

Storm	Time of rain	Met. Office daily total (mm)	Silwood Park hourly total (mm)		Assumed depth (mm)
d3	10.12 - 12.26	0.4	12.00	0.5	0.4
d52	13.11 - 15.02	5.7	---		0.5
d125	10.40 - 12.00	3.0	---		3.0
d178	14.10 - 16.38	2.2	---		2.2
d211	16.32 - 16.52	15.6	18.00	7.5	0.4
			19.00	4.0	
d237	12.36 - 16.13	1.0		0.0	0.3

Table 5.4 The estimation of mean throughfall depth $\bar{T}$ (mm) under the oak canopy from the storm depth and percentage canopy cover.

storm	date	canopy condition	% cover	rainfall depth (mm)	throughfall depth (mm)
3	07-10-83	capacity not exceeded	74%	0.4 mm	0.1 mm
52	25-11-83	capacity not exceeded	65%	0.5 mm	0.2 mm
125	06-02-84	capacity exceeded	20%	3.0 mm	2.6 mm
178	06-04-84	capacity exceeded	17%	2.2 mm	1.8 mm
211	16-05-84	capacity not exceeded	30%	0.4 mm	0.3 mm
237	11-06-84	capacity not exceeded	35%	0.3 mm	0.2 mm

Canopy capacities assumed: summer 1.0 mm, winter 0.4 mm.

have saturated the canopy capacities and that the throughfall was directly proportional to the percentage canopy cover, such that with a 74% cover, 26% of the rain will fall as throughfall. Merriam (1973) and Massman (1980) showed that this assumption of a linear relationship between rainfall and throughfall will be true for the early part of the storm. However with an assumed canopy capacity of 1.0 mm for the summer storms and a depth of 0.5 mm for the largest of these small storms it was assumed that the linear relationship held. Table 5.4 summarises the assumed throughfall depths for these storms.

The values for rain and throughfall for each storm are consistent only with each other. As far as possible, given the depth of rain and canopy cover, a throughfall value has been selected to match. However because these values were not measured it is not possible to relate the level of canopy storage to the onset of dripping or to construct sequences of changes with a common time or storage level scale.

3) Calculation of the interpolations

For each storm the depth of rainfall in the unsampled gaps was interpolated using the two methods described in Section Two, each with four different weights. The shapes of the intensity profiles were compared with those from the continuously recording gauge and the total depth of water calculated (Dc) was compared with the measured depth (Dm). The choice of interpolation method to be used was made with the more extensive tropical rain forest data and depended on the similarity between the measured and calculated intensity profiles and the size of the error between Dc and Dm. For each storm the same interpolation method selected for the rainfall data was used for the throughfall data.

i) Comparisons between intensity profiles

Storm j10b has been selected to illustrate the effect of different

interpolations on the intensity profile. This storm was of sufficient duration (1 hr 15 mins) for a detailed profile to be registered on the continous rain gauge which had a maximum resolution of about 5 mins (Figure 5.5). The continuous gauge revealed an initial peak with an intensity of 17 mm/hr which rapidly decayed. The intensity calculated from the samples of drop sizes show a peak in intensity of about 26.5 mm/hr, 7 minutes from the start of the storm. Figures 5.6 and 5.7 show the profiles calculated from the different interpolations and weights. The total depths of each have not been corrected to equal the measured depth.

Generally it can be seen that the set of "depth" interpolations reduced the tail of the intensity profiles more rapidly than the set of "intensity" interpolations. This is because the "depth" interpolation had the effect of giving an increased weighting to the samples with a longer duration and these tend to occur towards the end of the storm. If the intensity profiles are compared with that drawn from the automatic gauge, the set of "depth" interpolations tended on inspection to reproduce more successfully the rapid decay in intensity after the initial peak.

However not all the storms had intensity profiles shaped like j10b. From the intensities calculated from the drop samples it can be seen that some of the rain forest storms and all of the oak forest storms had no well defined profiles with initial high intensity burst and rapid decay. Many had highly irregular profiles with periods of high and low intensity alternating throughout the storm.

ii) Comparison between Dc and Dm

Table 5.5 shows that the values for total interpolated depths (Dc) for each sample and gap for each interpolation and weight for each storm, compared with the measured depth, Dm. In most cases (except j14a and j15) the initial estimate, with a weight of 2, give values for Dc greater than Dm. However in all cases the addition of

Figure 5.6 The intensity profiles for storm j10b derived from different weights of the "intensity" interpolation

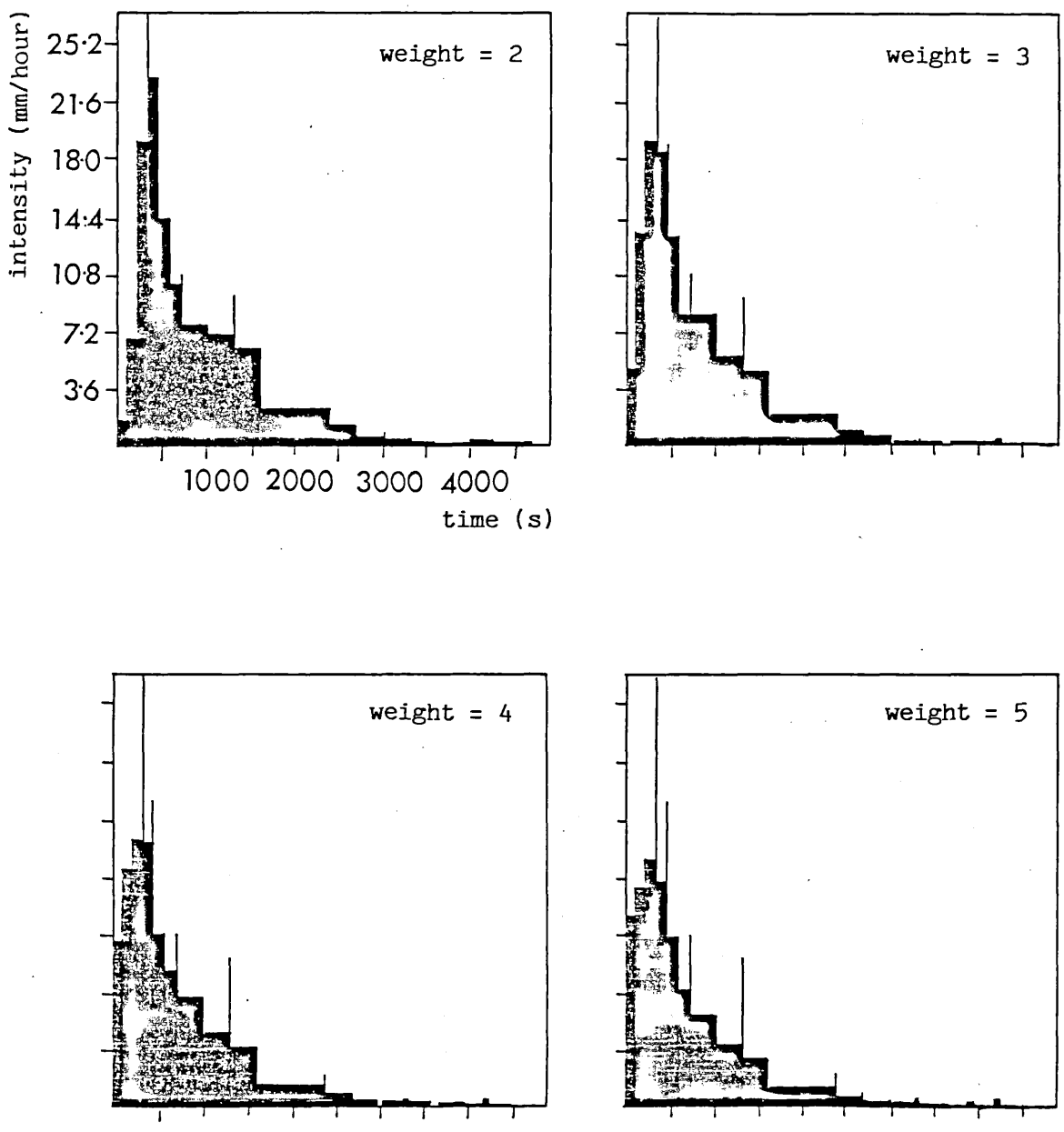

Figure 5.7 The intensity profiles for storm j10b derived from different weights of the "depth" interpolation

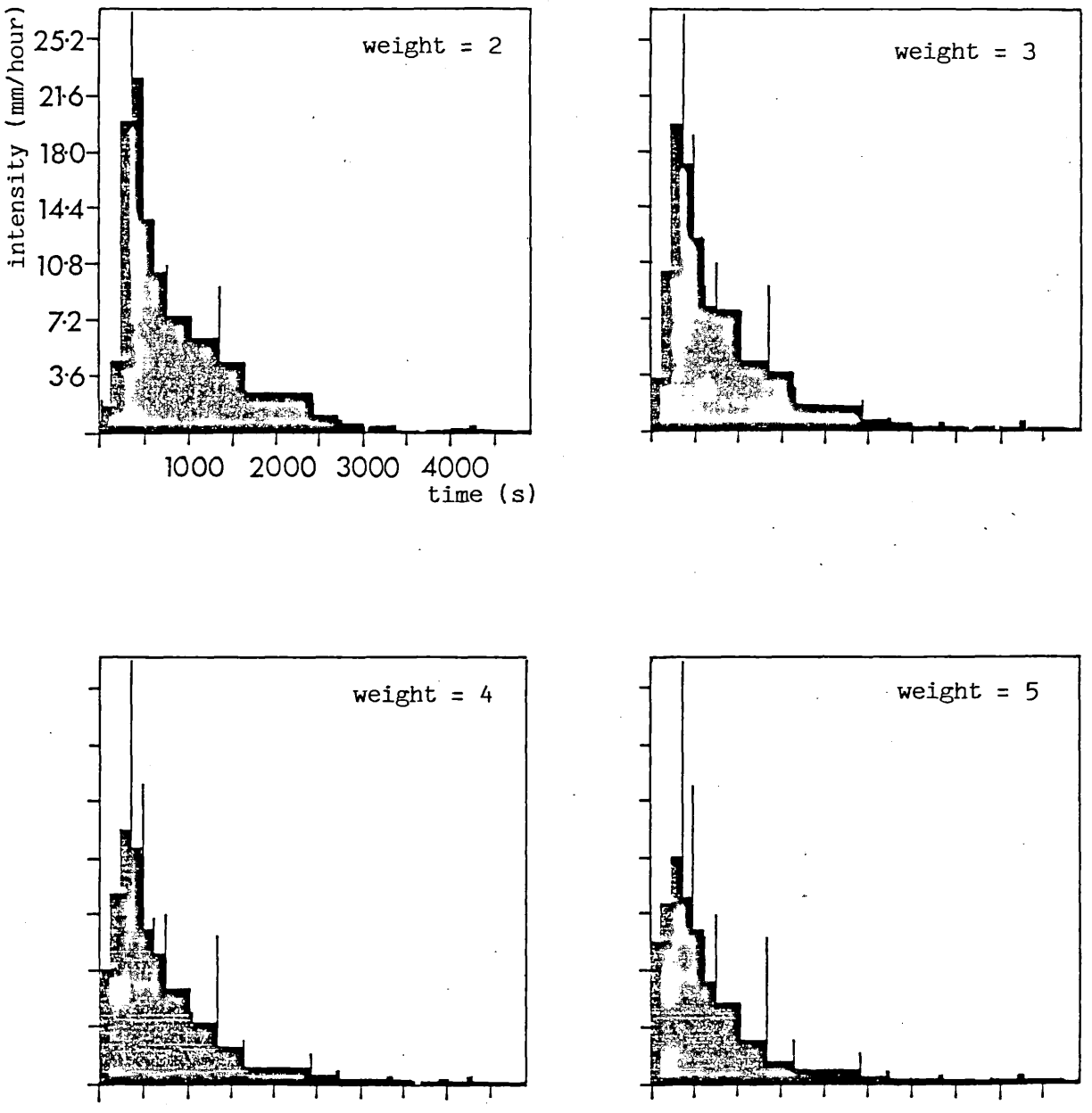

Table 5.5 Values for measured depth (Dm) and calculated depth of samples and gaps (Dc) from all interpolations and weights, the difference between Dc and Dm being expressed as a percentage of Dm.

storm		(a) intensity interpolation (b) depth interpolation							
	Dm (mm)	Dc for each weight (mm)							
		2	%	3	%	4	%	5	%
j10a	0.2	0.325	63	0.318	59	0.300	50	0.287	44
		0.255	28	0.234	17	0.211	11	0.220	10
j10b	3.7	5.152	39	4.841	31	4.436	20	4.016	9
		4.821	30	4.331	17	3.765	2	3.300	11
j11	12.7	20.562	62	19.285	52	17.482	38	16.175	27
		17.023	34	13.817	9	11.343	11	9.902	22
j12	1.41	2.944	109	2.679	90	2.152	53	1.792	27
		2.467	75	1.740	23	1.217	14	0.851	40
j13	0.11	0.631	474	0.626	469	0.588	435	0.594	440
		0.515	368	0.480	336	0.447	306	0.458	316
j14a	0.10	0.080	20	0.057	43	0.045	55	0.037	63
		0.077	23	0.046	54	0.046	54	0.046	54
j15	2.83	1.704	40	1.527	46	1.421	50	1.343	53
		1.233	56	0.682	76	0.546	81	0.524	81
j16b	0.36	0.507	41	0.483	34	0.427	19	0.380	6
		0.492	37	0.458	27	0.400	11	0.354	2
j20	2.93	5.099	74	4.474	53	3.926	34	3.454	18
		4.147	42	3.391	16	2.723	7	1.944	32

successive weights reduces the estimate of Dc, sometimes to a value smaller than Dm. The smallest storms (j13 and j14a) had fewer samples taken than the larger storms and therefore the initial estimates are little changed by increasing the weighting.

The differences between Dc and Dm have been expressed as a percentage of Dm to assess the errors of the interpolations. The smaller the percentage difference, the closer the estimate to the measured depth. From Figure 5.8 it can be seen that the "intensity" interpolation consistently reduced the difference between Dc and Dm with each additional weight. In contrast Figure 5.9 shows that the "depth" interpolation with a weight of 2 gives too high an estimate and with each additional weight is lowered to a minimum percentage difference with a weight of 4. A weight of 5 gave an estimate for Dc lower than Dm and consequently the percentage difference increased. Generally the percentage differences given by the depth interpolation were lower than the differences from the intensity interpolation.

iii) The sensitivity of calculations for kinetic energy to the choice of interpolation

The total kinetic energy of each storm is calculated from the drop-size distribution and depth of each sample and gap. It has been shown that the drop-size distribution changes throughout storms and that kinetic energy is strongly dependent on the drop-size distribution. Therefore if the interpolation allocated an erroneous amount of water to any part of the storm the total kinetic energy would be altered. To investigate the sensitivity of the kinetic energy to the interpolation the energy for each sample and gap was calculated for all interpolations and weights for storm j11. The results are presented in Table 5.6. All values for Dc have been corrected to equal Dm and therefore differences in the total kinetic energy recorded on the sample area are due to the different distributions of rainfall depth throughout the storm by the interpolations.

Figure 5.8 The difference between Dc and Dm expressed as a percentage of Dm for all weights of the "intensity" interpolation for each storm (omitting j13)

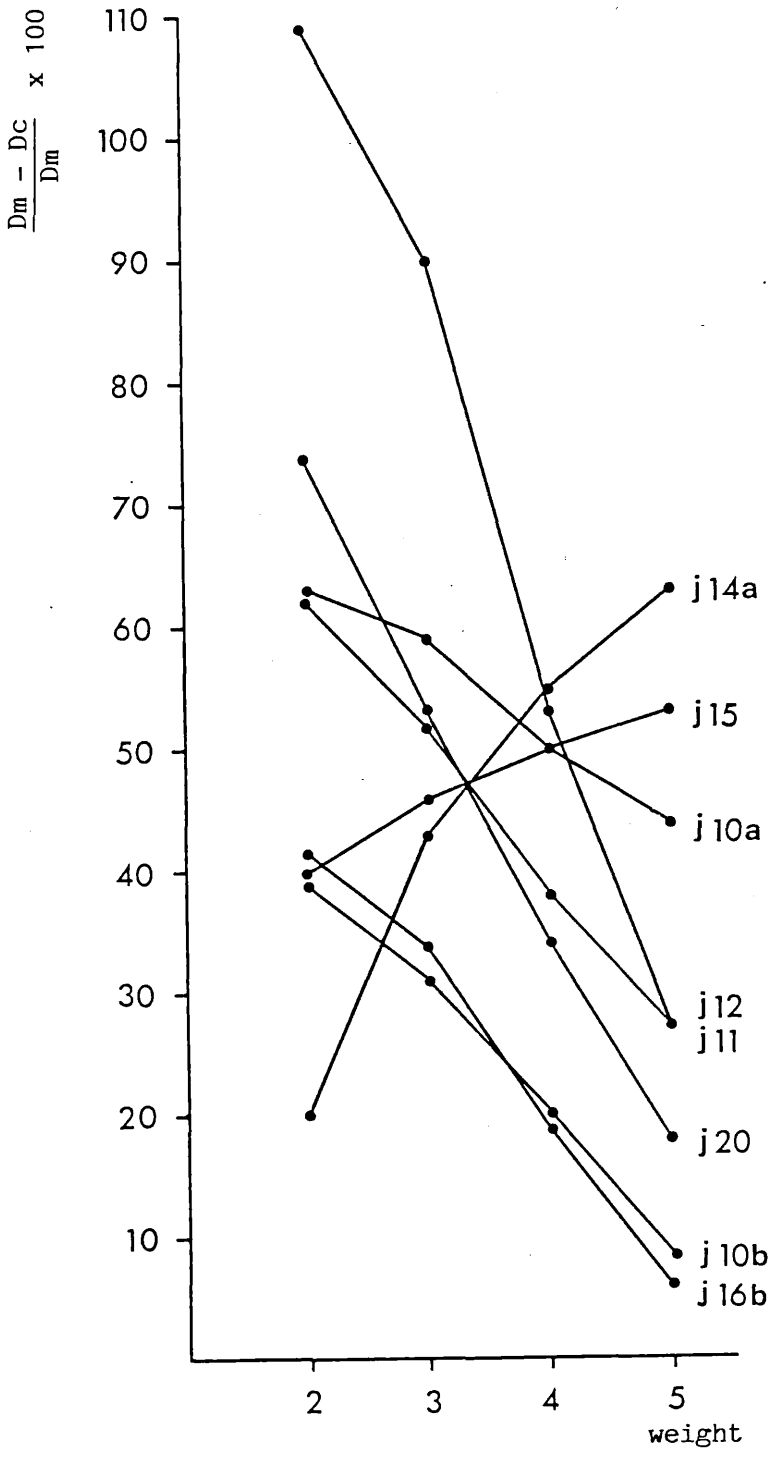

Figure 5.9 The difference between Dc and Dm expressed as a percentage of Dm for all weights of the "depth" interpolation for each storm (omitting j13)

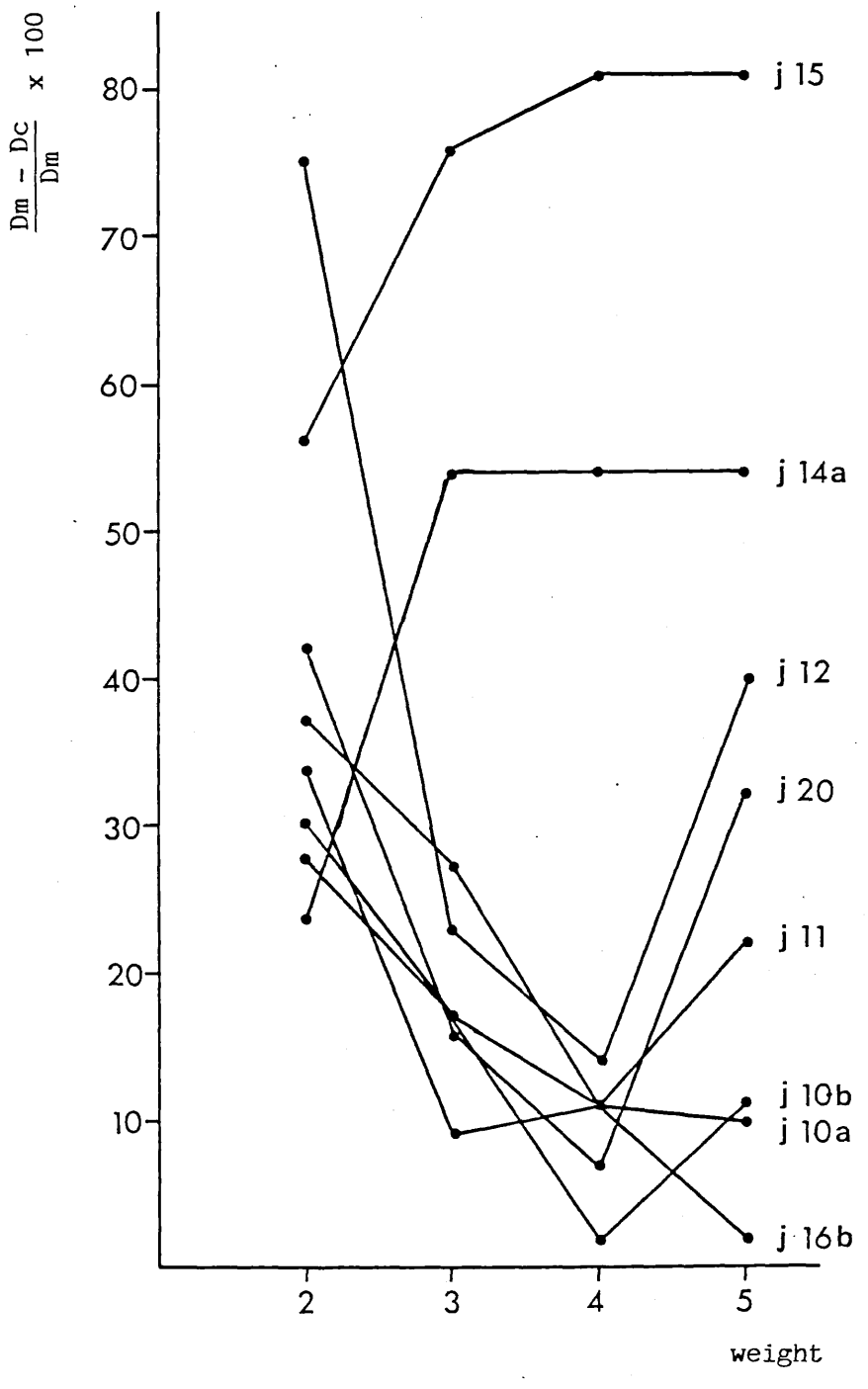

Table 5.6 A comparison between the energy (J) calculated for each sample and gap of storm j11, using the different interpolations and weights.

Number	Depth interpolation				Intensity interpolation			
	2	3	4	5	2	3	4	5
1	3.86e-4	4.76e-4	5.80e-4	6.64e-4	3.20e-4	3.41e-4	3.76e-4	4.07e-4
g1	2.90e-3	1.12e-2	2.16e-2	3.60e-2	2.50e-3	1.36e-1	1.47e-1	1.84e-1
2	3.58e-4	4.40e-4	5.37e-4	6.15e-4	2.96e-4	3.16e-4	3.48e-4	3.77e-4
g2	5.89e-2	1.08e-1	1.91e-1	2.94e-1	5.67e-1	5.30e-1	6.33e-1	6.66e-1
3	7.05e-3	8.69e-3	1.06e-2	1.21e-2	5.84e-3	6.22e-3	6.87e-3	7.42e-3
g3	3.74e-1	4.93e-1	5.52e-1	5.77e-1	4.19e-1	4.30e-1	4.34e-1	4.29e-1
4	5.53e-3	6.82e-3	8.30e-3	9.51e-3	4.58e-3	4.88e-3	5.39e-3	5.82e-3
g4	4.62e-1	5.63e-1	6.43e-1	7.26e-1	4.07e-1	4.22e-1	4.38e-1	4.62e-1
5	7.56e-3	9.31e-3	1.13e-2	2.30e-2	6.26e-3	6.67e-3	7.36e-3	7.95e-3
g5	2.40e-1	2.61e-1	3.09e-1	3.97e-1	2.11e-1	2.00e-1	2.10e-1	2.48e-1
6	1.18e-2	1.45e-2	1.77e-2	2.02e-2	9.73e-3	1.04e-2	1.15e-2	1.24e-2
g6	7.98e-1	9.77e-1	1.40e-0	1.50e-0	6.60e-1	6.99e-1	8.96e-1	9.21e-1
7	1.18e-2	1.45e-2	1.77e-2	2.02e-2	9.75e-3	1.04e-2	1.15e-2	t.24e-2
g7	7.47e-2	1.18e-1	1.31e-1	1.30e-1	6.22e-2	8.30e-2	8.56e-2	7.64e-2
8	6.73e-3	8.29e-3	1.01e-2	1.16e-2	5.57e-3	5.94e-3	9.59e-3	7.08e-3
g8	9.08e-1	9.51e-1	7.21e-1	5.99e-1	7.25e-1	6.86e-1	5.90e-1	5.25e-1
9	1.78e-2	2.19e-2	2.67e-2	3.06e-2	1.47e-2	1.57e-2	1.73e-2	1.87e-2
g9	1.31e-0	8.98e-1	7.64e-1	3.80e-1	1.12e-0	8.41e-1	7.24e-1	6.29e-1
10	9.59e-3	1.18e-2	1.44e-2	1.65e-2	7.94e-3	8.46e-3	9.36e-3	1.01e-2
g10	6.70e-1	5.72e-1	7.86e-1	3.28e-1	7.00e-1	5.50e-1	4.60e-1	3.98e-1
11	2.22e-3	2.74e-3	3.34e-3	3.82e-3	1.84e-3	1.96e-3	2.16e-3	2.34e-3
g11	7.35e-2	3.63e-2	4.43e-2	5.07e-2	6.12e-2	4.59e-2	3.80e-2	3.28e-2
12	1.23e-3	1.51e-3	1.84e-3	2.11e-3	1.02e-3	1.08e-3	1.20e-3	1.29e-3
g12	2.40e-2	2.96e-2	3.60e-2	4.13e-2	3.68e-2	2.62e-2	2.16e-2	1.87e-2
13	5.82e-4	7.17e-4	8.74e-4	1.00e-3	4.82e-4	5.14e-4	5.67e-4	6.13e-4
sum	5.07407	5.11971	5.22293	5.17093	5.04223	4.72192	4.75817	4.67602

The mean kinetic energy for all eight interpolations is 4.97575 J (s.d. = 0.222), with a potential variation of 8.9% ($\pm$ 2 s.d.) about the mean. A similar comparison between the total kinetic energies (J) calculated for storm j20 gave values of 0.83541, 0.83918, 0.84733, 0.85948, 0.85505, 0.85427, 0.87252 and 0.88456 for the "depth" interpolation weights 2, 3, 4, and 5 and "intensity" interpolation weights 2, 3, 4, and 5 respectively. The mean of these estimates in 0.85598 J $\pm$ 3.8% ($\pm$ 2 s.d.).

To examine the effect of the interpolations on the kinetic energy during the storm, the values for kinetic energy from Table 5.6 have been cumulated and expressed as a percentage of the total energy. Figure 5.10 shows that the "intensity" interpolations allow the kinetic energy to accumulate more rapidly at the beginning of the storm. For both interpolations the increase in weight allows more rapid accumulation of energy at the beginning of the storm.

To test the significance of the differences between the curves a Kolomorogov-Smirnov test for two independent samples was carried out. This test may be used to determine whether two samples are drawn from the same or different populations by focusing attention on the maximum difference (D) between two empirical cumulative distributions. The two interpolations which have been identified for use, the "depth" interpolation with a weight of 2 (D2) and the "depth" interpolation with a weight of 4 (D4), were each compared with the seven other interpolations.

For the given number of samples the critical value for D at the 99% confidence limit is given as 0.46 (Norcliffe 1977). The maximum difference for all curves from D4 was D2 with a value of 0.23. The maximum difference of all curves from D2 was D5 with a value of 0.31. Since the experimental values for D were in all cases less than the critical value for D it was assumed that, relative to the chosen interpolations, all other interpolations could be considered to come from the same population and that variation was due to random effects.

Figure 5.10 Cumulated kinetic energy of each sample and gap for storm j11 for both intensity and depth interpolations and all weights, expressed as a percentage of total calculated energy

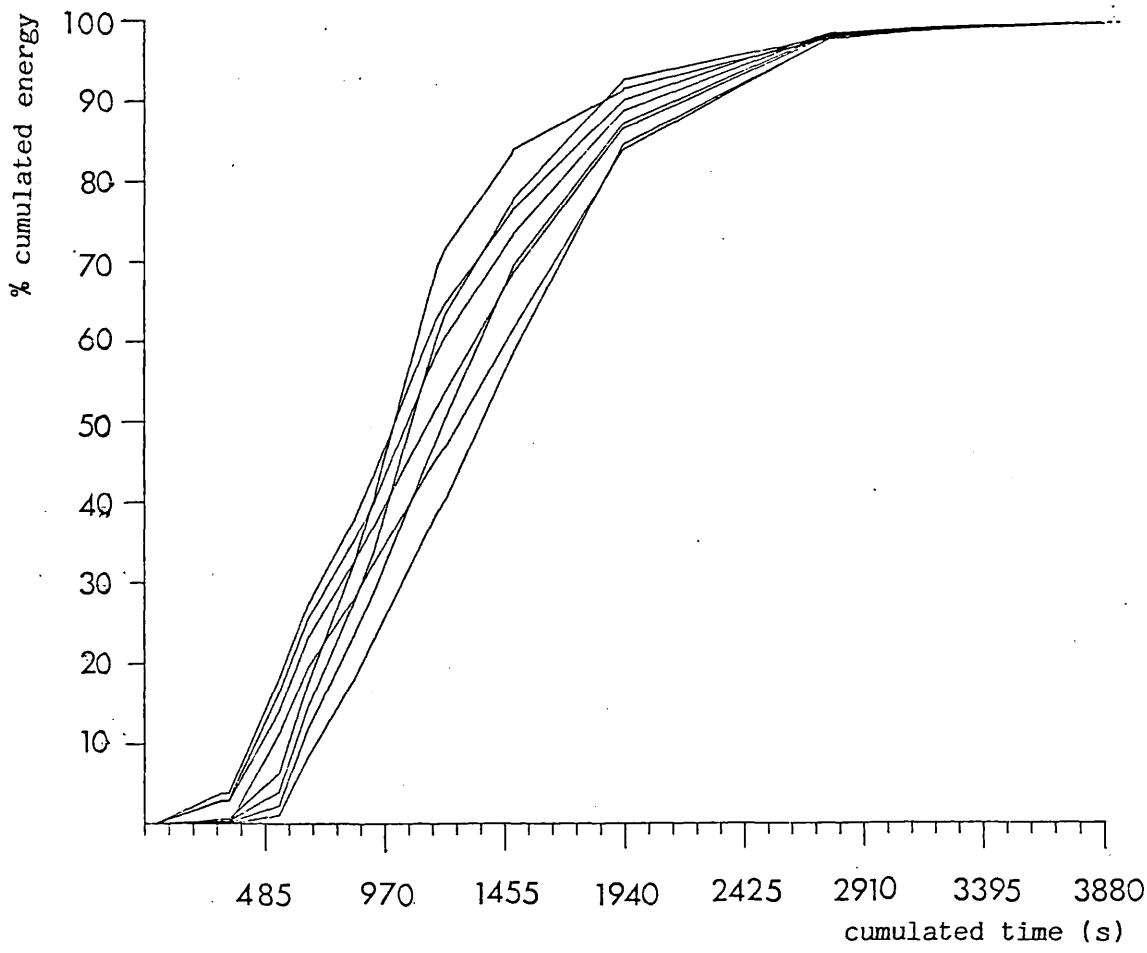

This test shows that the choice of interpolation has no statistically significant effect on the distribution of kinetic energy during the storm, although there may be variation in the total kinetic energy calculated. The comparison with j20 suggests that the variation of total kinetic energy about the mean of $\pm$ 8.9% may be larger with storms of more depth.

iv) Selection of the interpolation

The two main criteria for the selection of the interpolation method were the comparison between the interpolated and continuously recorded profiles and the comparison between Dc and Dm. The two types of interpolation have different effects on the intensity of rain particularly in the end portion of the storm. Where data is available for comparison the "depth" interpolation imitates the rapid decay more effectively. Similarly the depth interpolation gives lower percentage differences between Dc and Dm, particularly for the 4th weight. However the accentuation of the decaying tail is not appropiate where the storm intensity profile does not show an initially high intensity burst followed by a gradual decay. Some of the tropical storms and all the temperate storms show irregular profiles with no clearly defined peak. In these cases it is suggested that a lower weighting of the "depth" interpolation should be used so that the patterns of the 4th weight are not imposed on the results.

v) Discussion of the errors

There are several possible causes for the difference between Dc and Dm. Attention has already been paid to the values of Dm and it has been shown that with the information available these values cannot be improved upon.

Dc is calculated from the drop-size distributions of the samples of raindrop and systematic errors in the calibration between stain and

drop sizes may account for the difference. Errors compounded at each stage of the analysis could lead to a systematic overestimate of Dc. Conversley large stains obscuring smaller ones on the sheets may have lead to an underestimate of sample depth. The final possible cause of the difference is that the interpolation is at fault. However techniques are limited by the extent of the data available. It is assumed that the errors are equally distributed over all drops and that the most accurate process is to take the best fitting interpolation and distribute the errors proportionally to the depth of water in each sample and gap.

Section Four The derivation of a paired data set for coincident rainfall input to the canopy and throughfall output from the canopy from the interpolated continuous record

1) Method

Rainfall and throughfall were not sampled simultaneously and therefore no immediate comparisons may be made between the kinetic energy or depth of either for a given period. Figure 5.11 shows a schematic illustration of the problem. For each of the throughfall samples a rainfall sample for the same time period was derived from the continuous record. For each throughfall sample the paired rainfall sample was composed of parts of samples and gaps so that it represented a sample taken over the same time as the throughfall sample.

The calculation of numbers of drops of a given size (F') for each sample and gap has been given in Section 2. It was assumed that the numbers of raindrops of any given size were distributed evenly throughout the sample or gap period. Let the number of drops of a given size falling in the paired sample open for the same period as

Figure 5.11 A schematic illustration of the derivation of simultaneously paired rainfall and throughfall samples from the continuous record

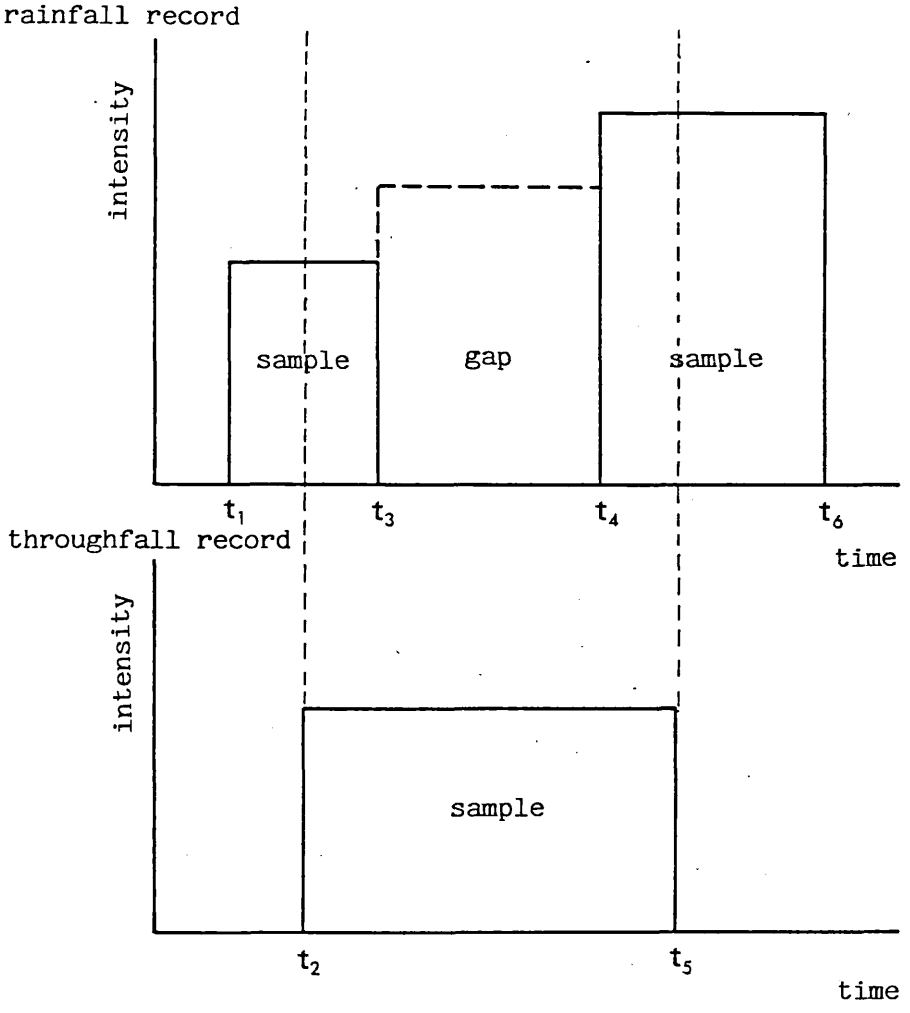

the canopy sample be $P_{i(t2t5)}$ and be calculated thus

$$P_{i(t2t5)} = P_{i(t2t3)} + P_{i(t3t4)} + P_{i(t4t5)} \qquad [5.34]$$

where, for the period t2 to t3

$$P_{i(t2t3)} = F'_{i(t2t3)} \frac{t3 - t2}{t3 - t1} \qquad [5.31]$$

for the period t3 to t4

$$P_{i(t4t5)} = F'_{i(t3t4)} \qquad [5.32]$$

for the period t4 to t5

$$P_{i(t4t5)} = F'_{i(t4t6)} \frac{t5 - t4}{t6 - t4} \qquad [5.33]$$

The depth (Pd) and kinetic energy (Pj) for the paired sample may be calculated from equation [5.20]

$$Pd = \frac{1}{pi\ k^2} \sum_{i=1}^{n} P_i v_i$$

and from [5.5]

$$Pj = \sum_{i=1}^{n} P_i\ j_i$$

Hence for different periods during the storm which may be related to the amount of water held in storage the effect of the canopy on changing the drop-size distribution of rainfall may be quantified.

CHAPTER SIX THE ANALYSIS OF THROUGHFALL FROM THE OAK CANOPY

Introduction

The basic plan for the analysis of both the oak canopy and the tropical rain forest data sets has been outlined in Chapter Three. A number of statements were made which were designed to investigate the links between qualitative models of canopy storage change and the change in drop-size distribution of throughfall. This chapter will examine the first four statements which were

i) The canopy changes the drop-size distribution of rain.
ii) The kinetic energy changes as a result of the change in drop-size distribution and as a result of the change in the height of fall.
iii) There is a sequence of changes in the drop-size distribution through a storm, and hence the storm may be divided into a series of stages each with a particular change in drop-size distribution.
iv) Each stage of the sequence has a different balance between the kinetic energy of the rainfall and the kinetic energy of the throughfall.

Appendix 1(a) shows the number of drops in each size class for each sample and the duration of each sample and gap of rain and throughfall for all the oak forest storms. The drop-size distributions of simultaneously paired sets of rainfall and throughfall have been derived from these samples using the methods described in Chapter Five. The drop-size distributions of both falling rain and throughfall at specific times varies with the type of rain and with the effect of the canopy. It is assumed that the differences between paired data sets are due to the presence of the canopy.

Section One The change in the drop-size distribution of rain by a canopy

1) Description of the distributions

i) Graphical descriptions

There is insufficient space available to allow the graphical illustration of each of the drop-size distributions of the rainfall and throughfall, so the majority of the descriptions will be numerical. However the percentage of the total number of drops in each size class for throughfall and rainfall of storm d3(1) and d3(5) have been plotted in Figures 6.1 and 6.2 to illustrate a few general points. It should be noted that the class interval between the smallest drop sizes is half that of the rest. All the calculations were made using the stain diameters of the drops to minimise the errors in converting stain diameter to drop diameter. However where stain diameters are referred to in the text the equivalent drop diameter is also given.

The number of drops in each sample ranged between several hundred and a thousand, depending on the duration of the sample and the adjustments to drop numbers by the interpolation. The drop-size distribution of rainfall tended to have a continuous range of drop sizes from 0.25 mm (0.14 mm) in increments of 0.5 mm (0.23 mm) up to 5.0 or 5.5 mm (1.23 or 1.32) mm with single incidences of larger drops at irregular intervals above that. The distributions tended to be slightly positively skewed with a modal size with several hundred drops per sample at a drop diameter between 1.5 and 2.5 mm (0.51 and 0.74 mm).

The drop-size distribution of throughfall included uninterrupted rain drops and tended to reflect the range of drop sizes occurring in the rainfall. However Figure 6.1 shows an important difference in the drop-size distribution. The peak of the distribution was reduced and the range spread to include equal numbers of drops of diameter 0.38,

Figure 6.1 The percentage of total numbers of drops in size classes in rainfall and throughfall paired sample d3(1)

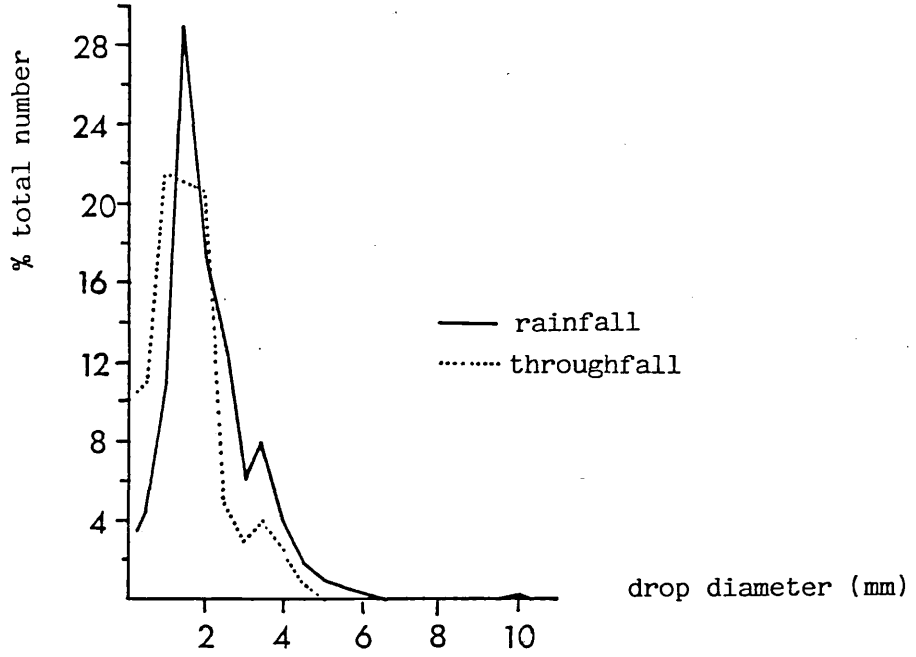

Figure 6.2 The percentage of total numbers of drops in size classes in rainfall and throughfall paired sample d3(5)

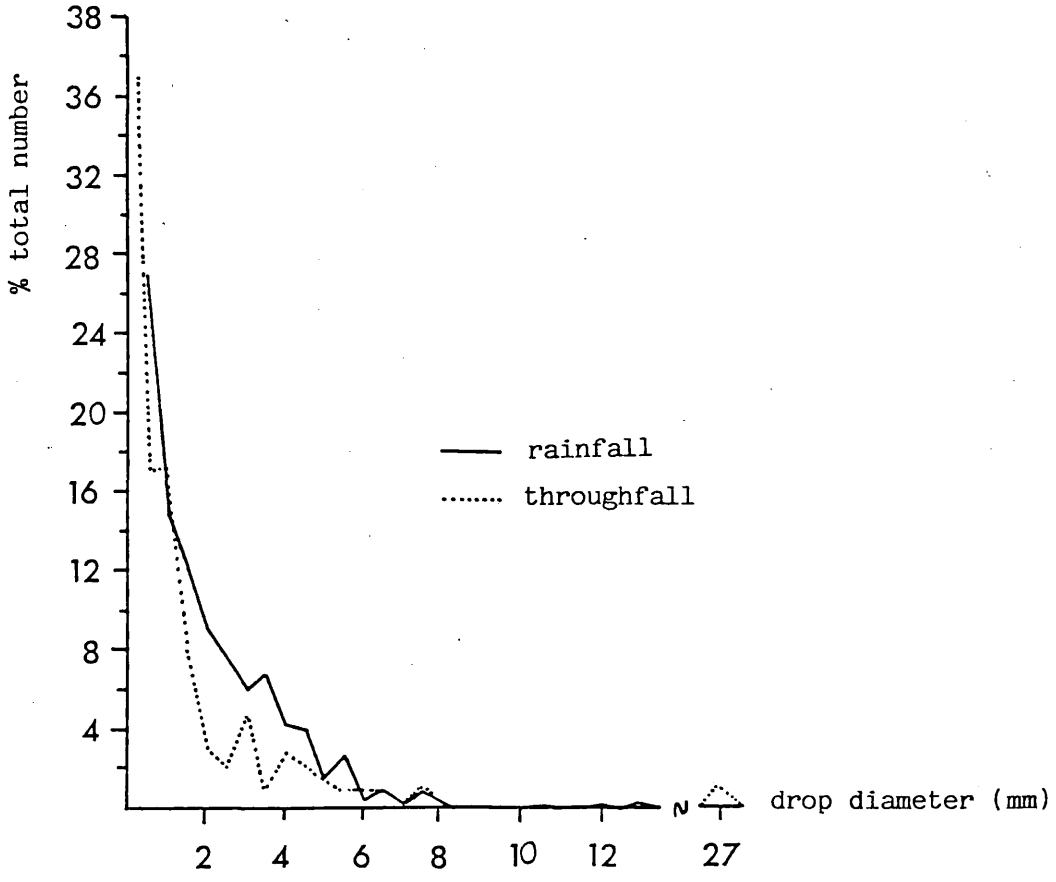

0.51 and 0.63 mm. In this example nearly 70% of the drops were concentrated over this range in comparison to 53% of the rainfall drops. Figure 6.2, and on inspection Appendix 1(a), reveal that the number of drops larger than those in the rainfall is usually only 2 or 3 per sample.

Hence the canopy appears to have the effect of increasing and evenly distributing the number of drops over the peak size classes as suggested by Ovington (1954) while giving, for each sample, single occurrences of drops larger than those in the rain.

ii) Numerical descriptions

The qualitative model of drop-size distribution change stressed the importance of the high-energy large drops and a description which reflects the incidence of these was sought. Numerical descriptions of the distributions concentrated on the mean and standard deviation. Table 6.1 lists the mean stain size and standard deviation for each paired sample of rainfall and throughfall.

The mean of each sample was not found to be particularly sensitive to the range in drop sizes because of the relatively low frequency of large drops. There were commonly several hundred drops within the range 1.5 to 2.5 mm (0.51 to 0.74 mm) and the mean reflects this most frequently occurring drop size.

In contrast the standard deviation of any distribution is sensitive to the tails. It was suggested that sample distributions with higher values of standard deviation tended to be those with a higher relative frequence of larger drops. Large drops were interpreted as those with a diameter greater than or equal to 5.5 mm (1.32 mm). This drop size lies just outside the range of the mean plus two standard deviations, 1.8 + 3.6 mm (0.58 + 0.97 mm) averaged for all rainfall samples. For each sample, the standard deviation ($s.d._r$) was plotted against the percentage of drops >5.5 mm (1.32 mm)

Table 6.1 Mean stain diameter ($\bar{x}$) (mm) and standard deviation (s.d.) (mm) for each paired sample of rainfall (R) and throughfall (T)

Sample	$\bar{x}$		s.d.		Sample	$\bar{x}$		s.d.	
	R	T	R	T		R	T	R	T
d3(1)	2.06	1.52	1.15	0.94	d125(12)	1.58	1.94	1.94	3.10
(2)	2.01	1.62	1.28	1.29	(13)	1.38	1.09	1.84	2.78
(3)	1.95	1.55	1.35	1.20	d178a(1)	1.96	1.54	1.22	0.90
(4)	2.00	1.50	1.73	1.33	(2)	1.90	1.61	1.91	1.71
(5)	2.03	1.33	1.73	2.31	(3)	2.75	2.11	3.02	2.60
(6)	1.88	1.31	1.81	1.28	(4)	1.93	1.55	2.95	3.02
(7)	1.84	1.60	1.37	1.54	(5)	1.45	1.47	2.33	1.67
(8)	1.73	1.23	1.16	1.05	(6)	1.16	3.34	2.07	4.25
(9)	1.87	1.72	1.46	2.07	(7)	1.33	1.57	1.86	2.00
(10)	2.00	1.32	1.78	1.32	(8)	1.99	1.20	1.84	1.18
(11)	1.86	1.37	1.90	1.23	(9)	2.53	2.51	2.06	2.24
(12)	1.14	1.26	1.33	1.53	(10)	1.12	1.13	0.83	1.47
d52(1)	0.64	0.52	0.61	0.46	d178d(1)	1.96	1.64	1.37	1.19
(2)	2.00	1.06	1.49	0.70	(2)	1.82	1.06	2.37	1.50
(3)	2.15	1.42	1.71	1.32	(3)	2.66	1.36	3.14	1.77
(4)	2.09	1.53	1.71	1.46	(4)	1.96	1.82	2.99	2.41
(5)	2.06	1.68	1.87	2.02	(5)	1.43	1.53	2.28	1.84
(6)	2.34	1.61	1.90	1.90	(6)	1.19	1.45	2.15	3.51
(7)	1.79	1.47	1.32	1.59	(7)	1.30	1.39	1.80	2.14
(8)	2.16	1.60	1.16	2.44	(8)	1.99	1.63	1.84	3.72
(9)	1.71	1.44	1.06	1.10	(9)	1.87	1.58	1.76	2.96
(10)	1.72	1.42	1.11	0.87	d211(1)	1.91	1.98	1.78	1.44
(11)	1.55	1.64	0.75	2.02	(2)	2.16	1.74	2.08	1.60
(12)	1.45	1.40	0.67	1.50	(3)	1.50	2.26	2.39	3.01
(13)	1.53	1.51	1.05	1.78	(4)	1.48	1.81	2.16	1.52
d125(1)	1.72	1.25	1.59	1.02	(5)	2.12	1.51	2.60	1.57
(2)	1.72	1.46	2.03	1.70	(6)	1.90	1.08	2.64	2.28
(3)	1.90	1.70	2.01	1.80	d237(1)	2.52	1.82	1.35	1.20
(4)	1.76	1.81	1.98	1.44	(2)	2.46	1.55	1.19	1.11
(5)	1.54	1.63	2.51	2.30	(3)	1.80	1.59	0.79	0.91
(6)	1.49	1.47	1.91	1.61	(4)	1.43	1.28	0.65	1.08
(7)	1.74	1.25	2.08	1.31	(5)	0.62	0.54	0.51	1.04
(8)	2.25	1.94	2.96	2.36	(6)	0.67	0.62	0.49	0.65
(9)	1.53	1.63	2.26	1.99	(7)	0.73	0.77	0.46	1.93
(10)	2.33	1.62	1.82	2.34	(8)	0.90	0.82	0.55	1.17
(11)	2.06	2.08	2.29	2.75					

(%L) (Figure 6.3). The regression of standard deviation of stain diameter on the percentage of large drops had an equation of

$$s.d._r = 1.01 + 0.142\ \%L \quad (r = 0.89) \qquad [6.1]$$

The percentage of incidence of single large drops in all samples varies according to the total number of drops in the sample and the scatter of points in Figure 6.3 may be due to this.

A similar regression of standard deviation of throughfall stain sizes ($s.d._t$) against the percentage of large drops (%L) was carried out for the throughfall data set (Figure 6.4) producing an equation of regression of

$$(s.d._t) = 1.25 + 0.142\ \%L \quad (r = 0.70) \qquad [6.2]$$

Although the gradient of this second equation was the same as the first, the y intercept was higher indicating that for a given standard deviation the number of large drops in a rainfall sample was expected to be higher than in a throughfall sample. Hence an increase in standard deviation was not solely due to an increase in large drops. The r value indicated a generally poorer relationship and there were frequently points where low incidences of large drops were associated with high values for standard deviation.

For rainfall drop-size distributions with a single peak of drop sizes, an increase in standard deviation by the canopy may be associated with an increase in the occurrence of large drops. For throughfall an increase in standard deviation may also be associated with the more even spread of drops over the lower sizes noted in Figure 6.1.

Figure 6.3 The standard deviation of stain diameters (mm) plotted against the percentage of drops with a diameter ⩾ 5.5 mm for each rainfall sample

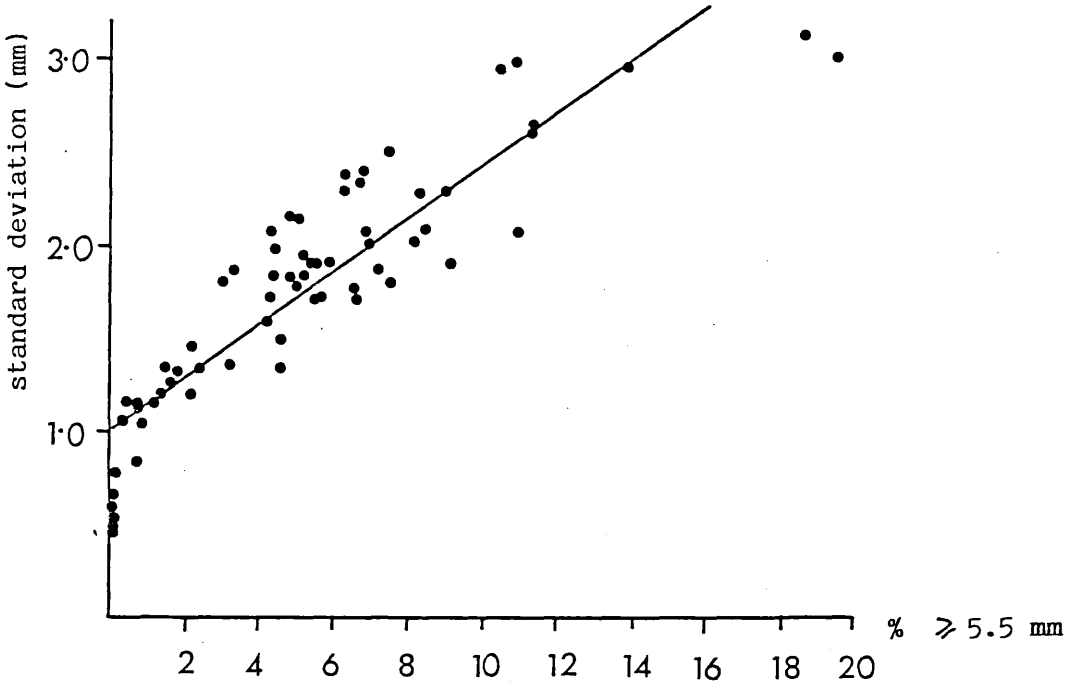

Figure 6.4 The standard deviation of stain diameters (mm) plotted against the percentage of drops with a diameter ⩾ 5.5 mm for each throughfall sample

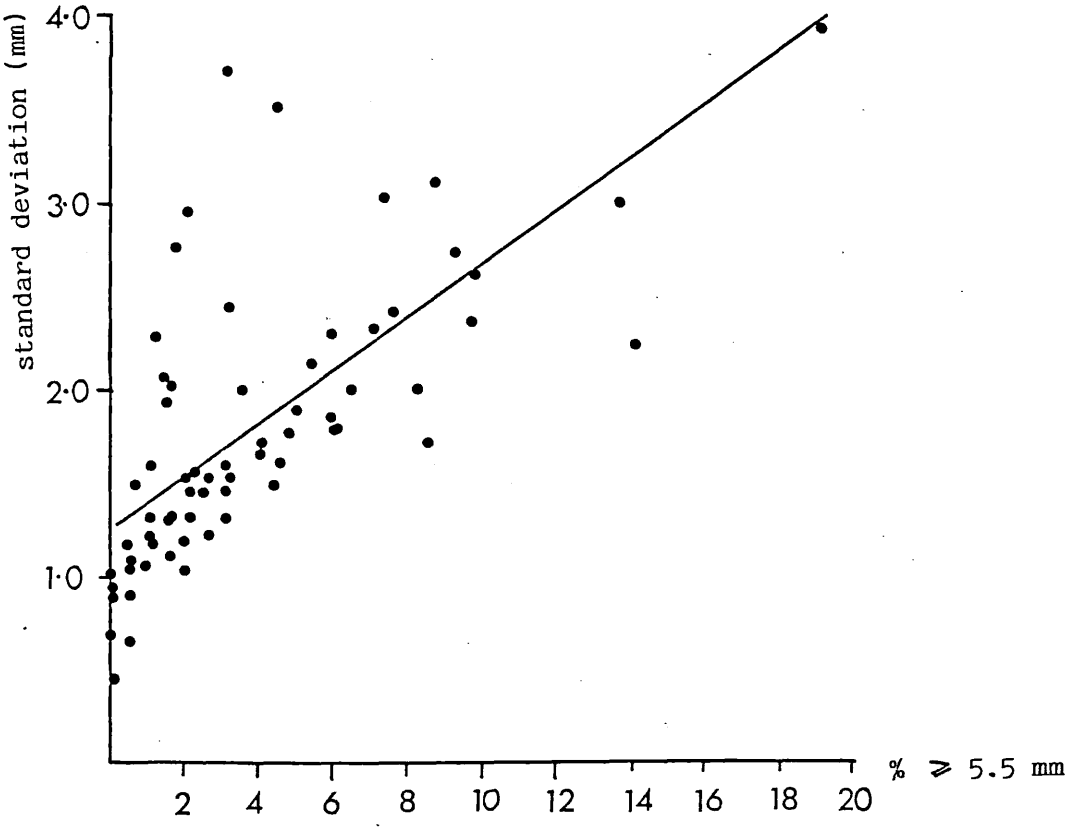

2) A comparison between the rainfall and throughfall drop-size distributions

The mean and standard deviation of all paired data sets (Table 6.1) were compared to assess the general impact of the canopy on the drop-size distribution. It should be noted that there may be time-related variation concealed within the general pattern which has not been identified yet.

The mean stain size for each throughfall distribution ($\bar{x}_t$) was regressed against the mean rainfall stain size ($\bar{x}_r$) of the paired rainfall distributions (Figure 6.5) and the two were compared by a t-test. Table 6.2 reveals that the presence of a canopy lowered the mean stain size for each distribution from 1.76 to 1.51 mm (0.57 to 0.51 mm), that the values for the mean size are statistically distinct and that the relationship between the two was such that

$$\bar{x}_t = 0.614 + 0.492\ \bar{x}_r \quad (r = 0.62) \qquad [6.3]$$

In contrast the mean standard deviation of stain diameter for all distributions was raised from 1.71 to 1.77 mm (0.59 to 0.60 mm) although the two data sets were not statistically distinct. The equation of the regression line

$$s.d._t = 0.758 + 0.590\ s.d._r \quad (r = 0.51) \qquad [6.4]$$

emphasised the wide scatter of the data by indicating a decrease in standard deviation by the canopy. The qualitative model of drop-size distribution change has suggested that the canopy may have different effects on the drop-size distribution of the rain at different periods during the storm. Figure 6.6 shows that in 31 out of the 71 cases the standard deviation was greater under the canopy than in the open.

Figure 6.5 The mean throughfall stain diameter (mm) plotted against the mean rainfall stain diameter (mm) for all paired samples

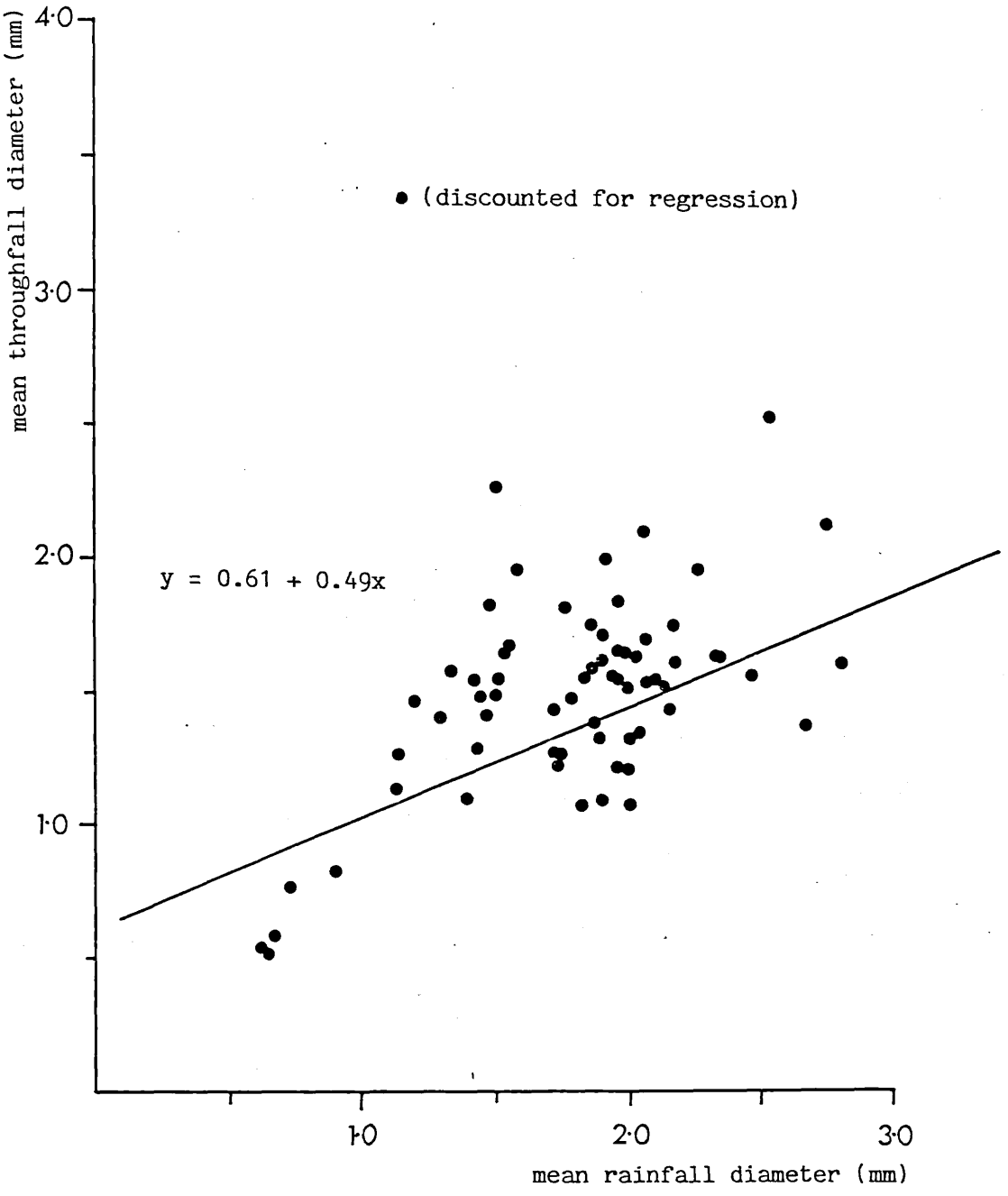

Table 6.2 Analysis of means of the mean stain diameter ($\bar{x}$) (mm) and standard deviation (s.d.) (mm) for each paired sample of rainfall and throughfall

	mean	95% confidence intervals	t-test results	
			t	p
rainfall ($\bar{x}$)	1.76	1.65, 1.87		
throughfall ($\bar{x}$)	1.51	1.41, 1.61	4.54	<0.001
rainfall (s.d.)	1.71	1.55, 1.86		
throughfall (s.d.)	1.77	1.59, 1.95	0.72	0.47

(The t-test tested the probability (p) of the mean of the rainfall data equalling the mean of the throughfall data, with 70 degrees of freedom)

Figure 6.6 The standard deviation of throughfall stain diameters (mm) plotted against the standard deviation of rainfall stain diameters (mm) for all paired samples

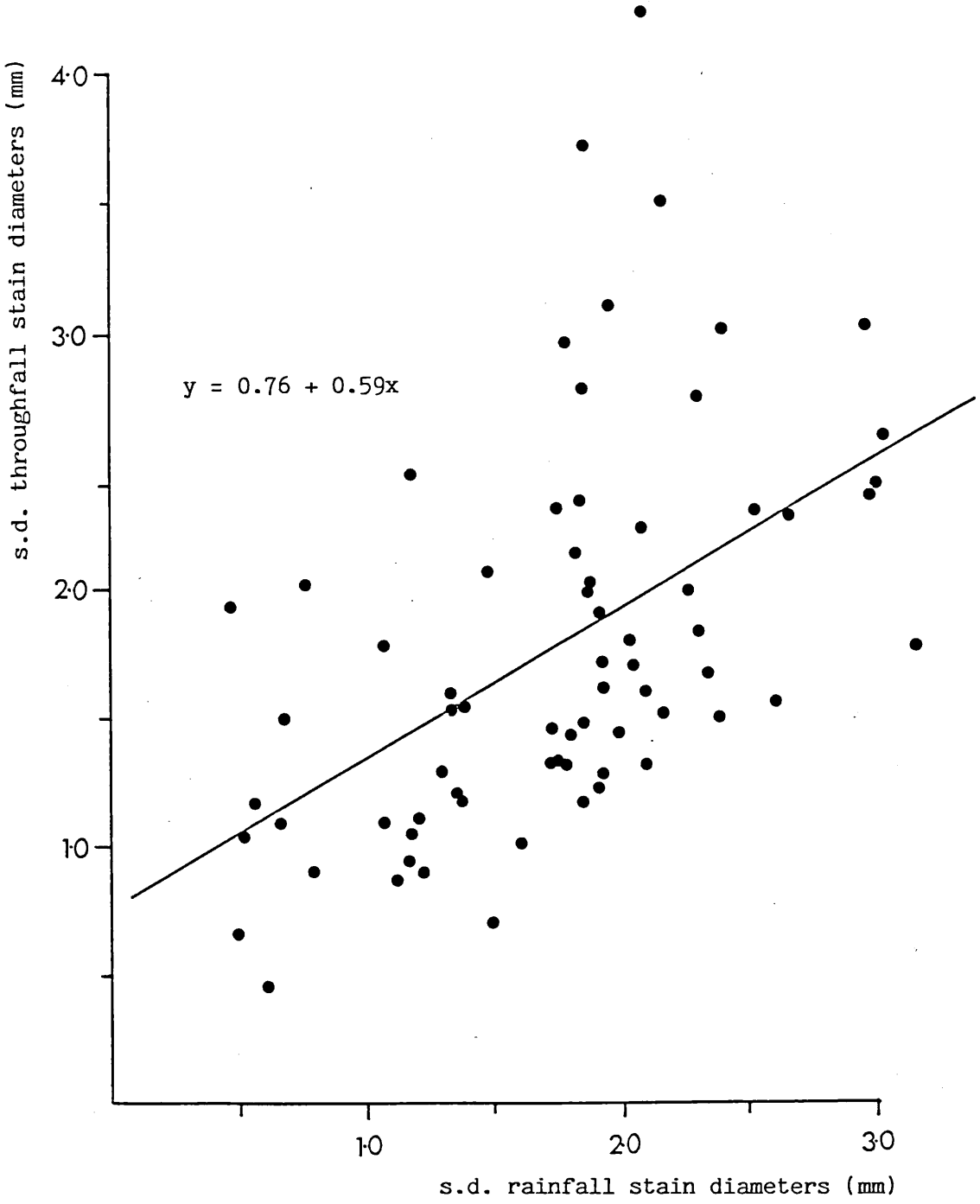

Since the data points contain examples for all parts of the storm the wide scatter is consistent with the ideas of the model.

It may be concluded that the presence of a canopy will change the drop-size distribution of rain. In the data sets examined here the mean drop size tended to be reduced and the concentration of drop sizes spread out more. The standard deviation tended to increase as a result of the spread of small drop sizes but also as a result of the incidence of larger drops.

Section Two Change in the kinetic energy as a result of the change in drop-size distribution and the change in fall height

The second proposition of the model is that as a consequence of the change in drop-size distribution of the rain by the canopy there is a change in the kinetic energy of the drops. The aim here is to establish a relationship between the standard deviation of the distribution and the kinetic energy it possesses. Secondly the effect of the canopy in changing the kinetic energy by changing the fall height will be examined.

The kinetic energy of each paired sample has been standardised as the energy/mm/m^2 and is presented in Table 6.3. The almost exponential increase in kinetic energy with increase in drop diameter has been described in Chapter Two, and samples with a number of large drops will possess more kinetic energy/mm than the equivalent depth of water falling as smaller drops. A decrease in the canopy height will affect the kinetic energy on impact of samples containing larger drops proportionally more than samples containing small drops. The sampling area has been standardised to 1 m^2 for comparison with the results of previous research.

Table 6.3 The kinetic energy of each paired sample of rainfall (R) and throughfall (T) (calculated for fall heights of 8 m and 3 m) standardised to J/mm/m²

Sample	R	T(8 m)	T(3 m)	Sample	R	T(8 m)	T(3 m)
d3(1)	7.56	5.21	5.15	d125(12)	14.23	28.47	16.81
(2)	8.55	7.19	6.92	(13)	14.60	34.99	19.09
(3)	8.65	7.45	6.81	d178a(1)	7.26	5.03	4.96
(4)	11.34	8.01	7.48	(2)	15.70	13.57	10.61
(5)	10.81	28.00	16.34	(3)	18.07	19.66	13.68
(6)	12.41	9.37	8.09	(4)	21.85	25.92	16.42
(7)	9.38	11.60	9.34	(5)	19.21	11.31	9.64
(8)	7.11	6.16	5.97	(6)	20.77	26.97	16.75
(9)	9.56	21.74	13.59	(7)	17.54	15.25	11.79
(10)	11.40	8.23	7.58	(8)	11.83	7.92	7.36
(11)	12.08	7.13	6.83	(9)	11.91	13.40	11.37
(12)	8.85	11.66	9.78	(10)	5.20	15.76	11.65
d52(1)	4.17	2.86	2.86	d178d(1)	8.75	6.80	6.52
(2)	8.61	3.31	3.29	(2)	20.51	14.25	11.28
(3)	10.46	8.43	7.90	(3)	19.50	14.12	11.41
(4)	10.81	8.73	8.10	(4)	21.93	17.81	13.19
(5)	11.93	13.50	11.40	(5)	18.83	14.41	10.87
(6)	11.84	14.97	11.41	(6)	21.21	34.76	19.36
(7)	7.57	17.14	11 44	(7)	16.88	20.51	14.18
(8)	6.76	29.16	16.91	(8)	11.79	37.63	22.19
(9)	5.94	9.23	7.56	(9)	11.00	35.44	20.33
(10)	6.26	4.93	4.83	d211(1)	11.26	8.78	8.05
(11)	4.20	27.98	15.86	(2)	13.77	9.87	8.83
(12)	3.60	19.23	12.06	(3)	21.09	21.19	14.72
(13)	6.51	11.62	10.36	(4)	18.98	10.35	8.83
d125(1)	9.87	5.76	5.63	(5)	19.38	13.17	10.23
(2)	13.26	11.70	10.02	(6)	20.64	34.52	18.98
(3)	13.60	11.66	10.06	d237(1)	8.45	7.01	6.73
(4)	14.84	8.26	7.83	(2)	7.60	6.08	5.90
(5)	21.20	17.57	13.02	(3)	5.03	4.82	4.67
(6)	16.54	11.85	9.66	(4)	3.30	6.83	6.56
(7)	15.76	9.33	8.51	(5)	2.41	14.24	11.98
(8)	20.04	17.32	12.73	(6)	2.24	6.28	5.92
(9)	17.33	16.35	11.93	(7)	2.09	32.66	18.10
(10)	11.63	20.06	13.85	(8)	2.61	20.96	12.78
(11)	15.75	23.57	14.97				

1) The relationship between the drop-size distribution and the kinetic energy

i) Rainfall

The kinetic energy/mm/m² of rainfall ($k.e._r$) for each sample has been plotted against the standard deviation of the stain size ($s.d._r$) (Figure 6.7) and an equation of regression obtained where

$$k.e._r = 8.16\ s.d._r - 1.90 \quad (r = 0.94) \qquad [6.5]$$

It will be noted from Figure 6.7 that the increase in kinetic energy with standard deviation suddenly became more scattered above a standard deviation of 2.0 mm (0.63 mm). It is suggested that these higher standard deviation values are produced by the incidence of a few drips much larger than the rest. Similarly the value for kinetic energy/mm/m² will be weighted by the large drops. Hence the scatter of the points may be caused by the relative effect on the standard deviation and kinetic energy of single drops.

ii) Throughfall

Because the relationship between the standard deviation and the incidence of large drops was clouded by the increase in standard deviation also being caused by a levelling of the frequency of smaller drops, the kinetic energy of throughfall ($k.e._t$) of the paired samples was plotted separately against the standard deviation of the stain diameters ($s.d._t$) (Figure 6.8) and a regression calculated such that

$$k.e._t = 10.1\ s.d._t - 2.89 \quad (r = 0.84) \qquad [6.6]$$

Figure 6.7 The kinetic energy (J/mm/m²) of paired oak canopy throughfall samples plotted against the standard deviation of stain diameter (mm) of each drop-size distribution

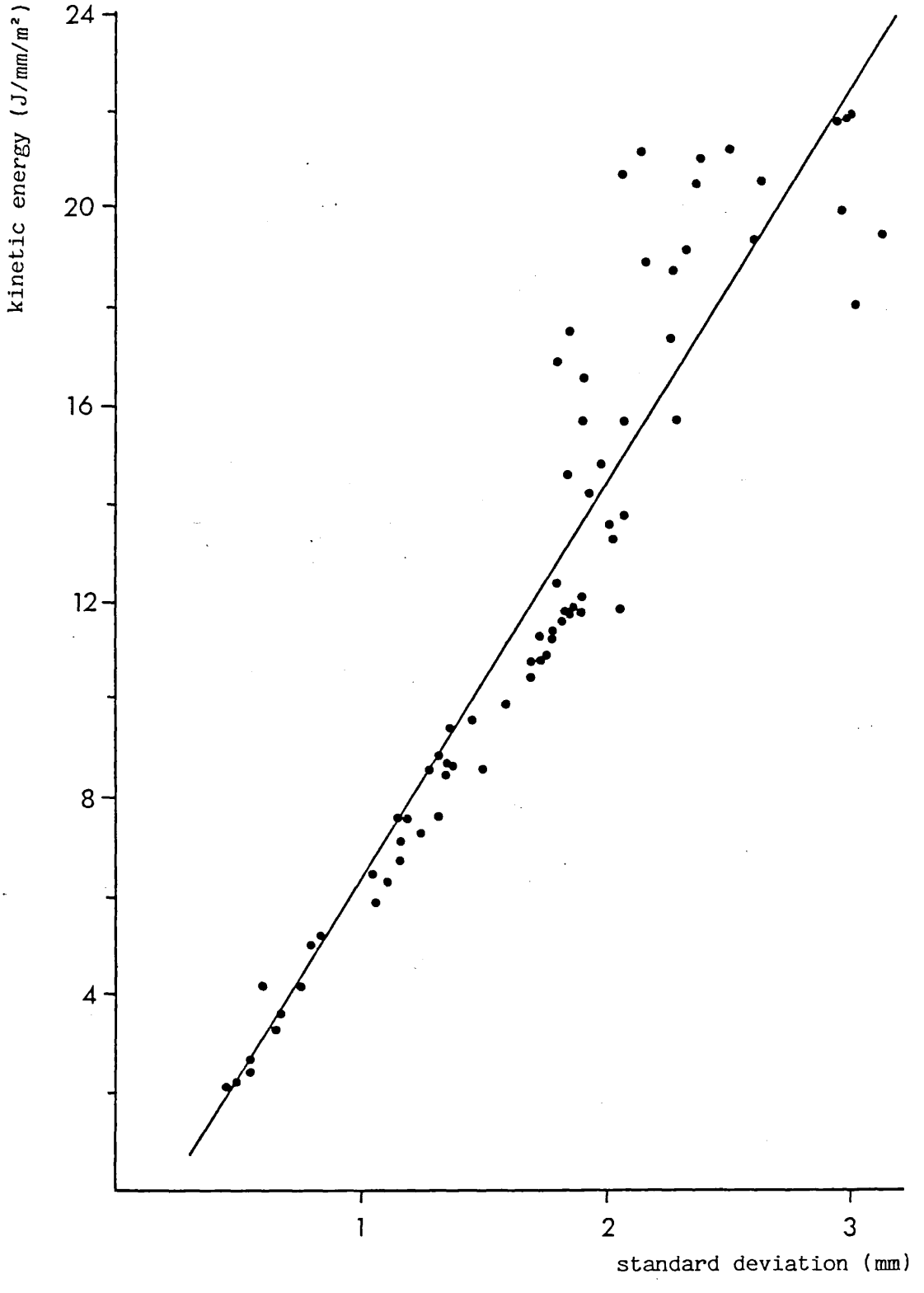

Figure 6.8 Kinetic energy (J/mm/m²) of throughfall samples plotted against the standard deviation of the stain diameters (mm)

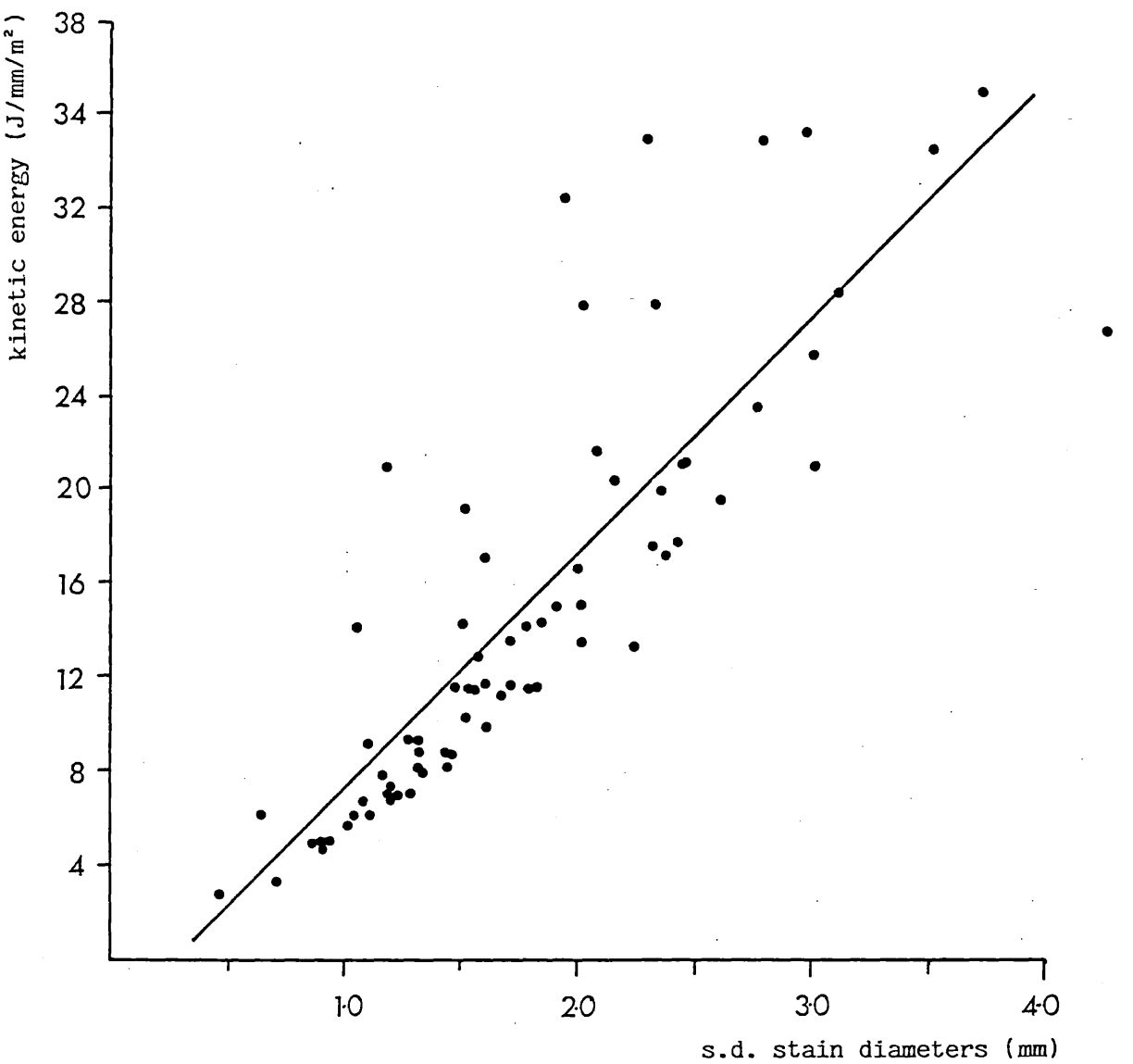

The plot reveals more scatter than for rainfall. Most of the scatter is for points where the kinetic energy/mm/m² is higher for a given standard deviation than would be expected.

A positive relationship between the standard deviation and kinetic energy/mm/m² has been established for both the rainfall and throughfall samples. Hence kinetic energy/mm/m² has been related to the incidence of larger drops.

iii) The extent of the change in kinetic energy by the canopy

Table 6.4 presents the analysis of the means of rainfall and throughfall kinetic energy and the analysis of the difference. The mean of the kinetic energy of rainfall is 12.02 J/mm/m² and the mean of the throughfall is 14.97 J/mm/m². The difference between them is significant at the 99.5% level.

Figure 6.9 plots the kinetic energy/mm/m² of throughfall against rainfall for all samples. As has been stated before, this analysis is expected to include examples of rainfall and throughfall pairs from all stages of the storms including examples of energy reduction and enhancement by the canopy. An inspection of Figure 6.9 tends to confirm this expectation. There are some points below the line $y = x$ where the kinetic energy of the throughfall is less than that of the rainfall but most are above. From the difference in the range of scattering below and above the line $y = x$ it appears that the ability of the canopy to enhance the kinetic energy is far greater than its ability to reduce it.

2) The effect of the canopy height on the throughfall energy

To test the affect the canopy height has on the kinetic energy/mm/m² of throughfall, the kinetic energy was recalculated for all throughfall samples assuming a maximum height of fall of 3 m.

Table 6.4 Analysis of means of the kinetic energy (J/mm/m²) of paired samples of rainfall and throughfall (calculated for a fall height of 8 m)

	mean	95% confidence intervals	t-test results	
			t	p
rainfall	12.02	10.68, 13.37		
throughfall	14.97	12.8, 17.1	2.72	0.008

(The t-test tested the probability (p) of the mean of the rainfall data equalling the mean of the throughfall data with 70 degrees of freedom)

Figure 6.9 The kinetic energy (J/mm/m²) of paired samples of oak canopy throughfall (calculated using a fall height of 8 m) plotted against the energy of paired samples of rainfall

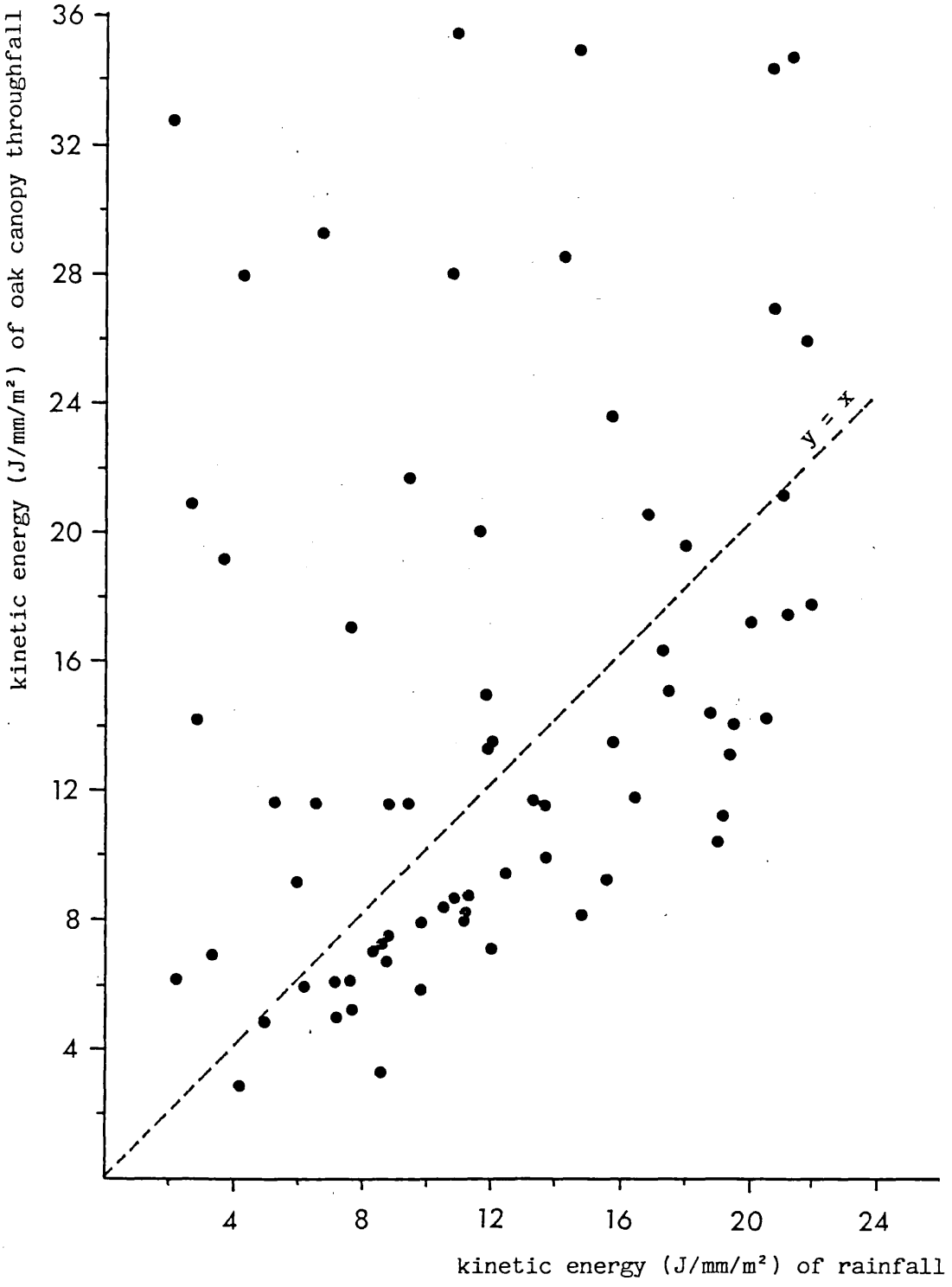

Usually it may be expected that the drop-size distributions of throughfall from lower plant canopies will be different from the distributions from trees because of difference in the leaf structures. However by holding the drop-size distribution constant in this way it is possible to examine the affect of height reduction on distributions with proportionally larger numbers of large drops.

i) The effect of drop-size distribution on the change in energy

The change in fall height to 3 m will not affect the kinetic energy of all drop sizes equally, since drops of less than about 1 mm diameter will have attained their terminal velocity already. The change in height will decrease the kinetic energy of the larger drops proportionally more. Hence the kinetic energy of distributions composed mainly of smaller drops will be altered less than distributions with large drops. To illustrate this the kinetic energy of each sample calculated using a 3 m fall height has been expressed as a percentage of the kinetic energy of drops at terminal velocity ($\%k.e._{8m}$) and plotted against the standard deviation of the distribution ($s.d._t$) (Figure 6.10). The equation of regression is such that

$$\%k.e._{8m} = 107 - 15.0\ s.d._t \quad (r = 0.79) \qquad [6.7]$$

Hence those samples with a high standard deviation, which are those with larger drops, are more affected by a decrease in canopy height than distributions made up of smaller drops.

ii) Absolute difference between rainfall and throughfall energy

Table 6.5 examines the difference between the kinetic energy/mm/m^2 of all paired rainfall and throughfall samples after 3 m fall. The

Figure 6.10 The kinetic energy (J/mm/m²) of samples of oak canopy throughfall calculated with a fall height of 3 m expressed as a percentage of the kinetic energy (J/mm/m²) of the same throughfall sample calculated with a fall height of 8 m, plotted against the standard deviation of the stain diameters (mm) of each sample

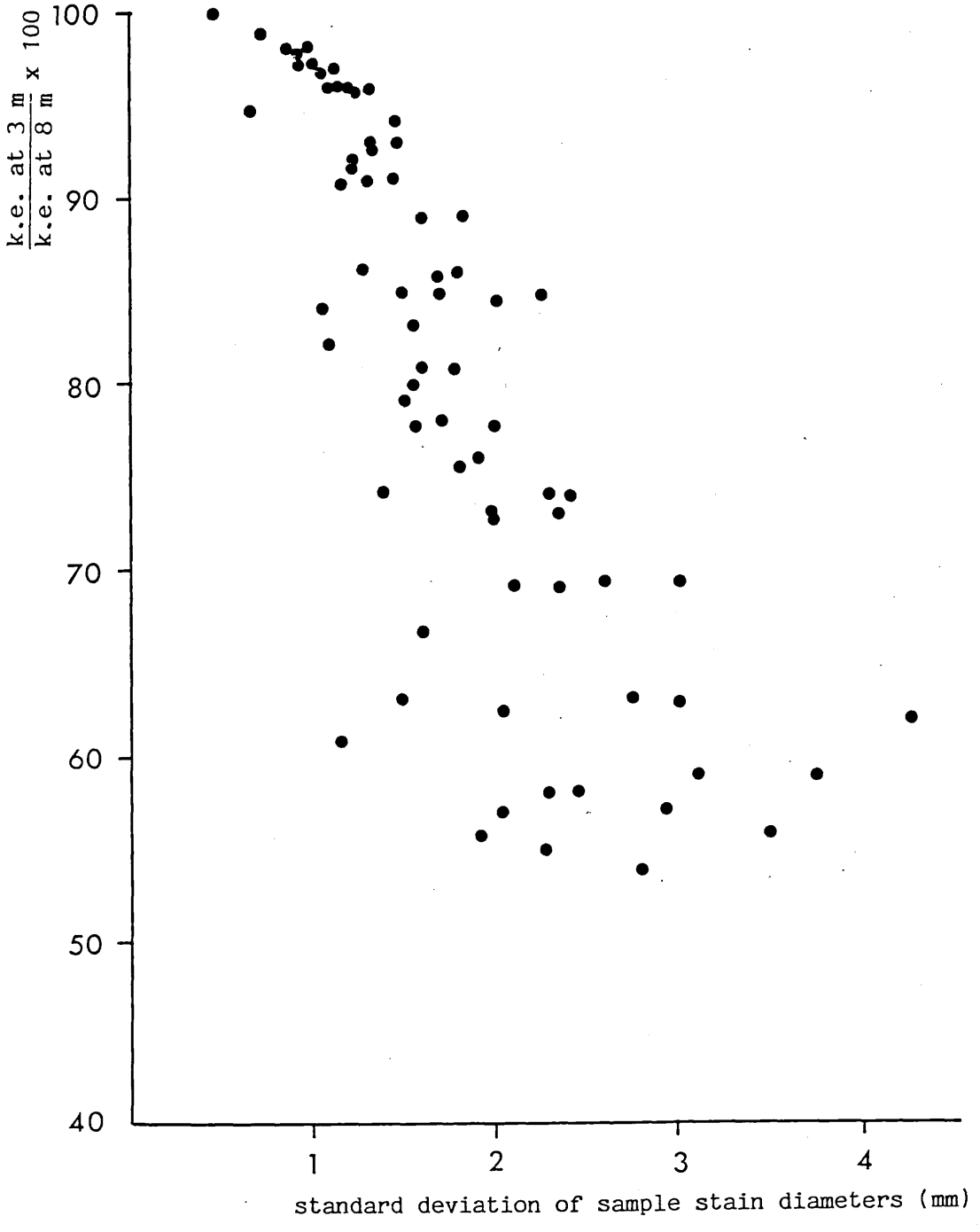

Table 6.5 Analysis of means of the kinetic energy (J/mm/m²) of paired samples of rainfall and throughfall (calculated for a fall height of 3 m)

	mean	95% confidence intervals	t-test results	
			t	p
rainfall	12.02	10.68, 13.37		
throughfall	10.87	9.83, 11.92	1.65	0.10

(The t-test tested the probability (p) of the mean of the rainfall data equalling the mean of the throughfall data with 70 degrees of freedom)

mean kinetic energy is lowered by the canopy form 12.02 J/mm/m² to 10.87 J/mm/m², although the 95% confidence intervals over lap leaving the probability of the two distributions being different only at the 90% level. Figure 6.11 illustrates that the scatter of points is much closer to y = x. While there are still samples where the kinetic energy of the throughfall is greater than the rainfall, the scatter is much less.

Section Three Canopy storage and the sequence of kinetic energy change

The third of the statements derived from the qualitative model proposes a sequence of changes to the rainfall by the canopy which is linked to the depth of water stored in the canopy. For this project there was no data collected on the change in storage during the storms with which to compare the drop-size distributions. The examination of the validity of the statement has to depend on the construction of canopy storage curves from the drop samples and the comparison between general features of these curves and those of the general model illustrated in Figure 3.1. Where the canopy reduces the standard deviation of the drop-size distribution, it is expected that there will be an increase in canopy storage, while where the canopy shows an increase in large drops it is expected that there will be a decrease in canopy storage.

The data was examined in two ways. From the interpolated continuous record of change in intensity and drop-size distribution the cumulated canopy storage was calculated for each storm. Each curve was compared qualitatively with the general canopy storage curve (Figure 3.1), account being taken of whether the canopy was expected to be filled to capacity or not. Secondly, using all the paired data sets, a storm was simulated to provide a new canopy storage model, the phases of which could be identified with specific ratios of rainfall

Figure 6.11 Kinetic energy (J/mm/m²) of throughfall samples calculated using a maximum 3 m height of fall, plotted against the kinetic energy (J/mm/m²) of paired samples of rainfall

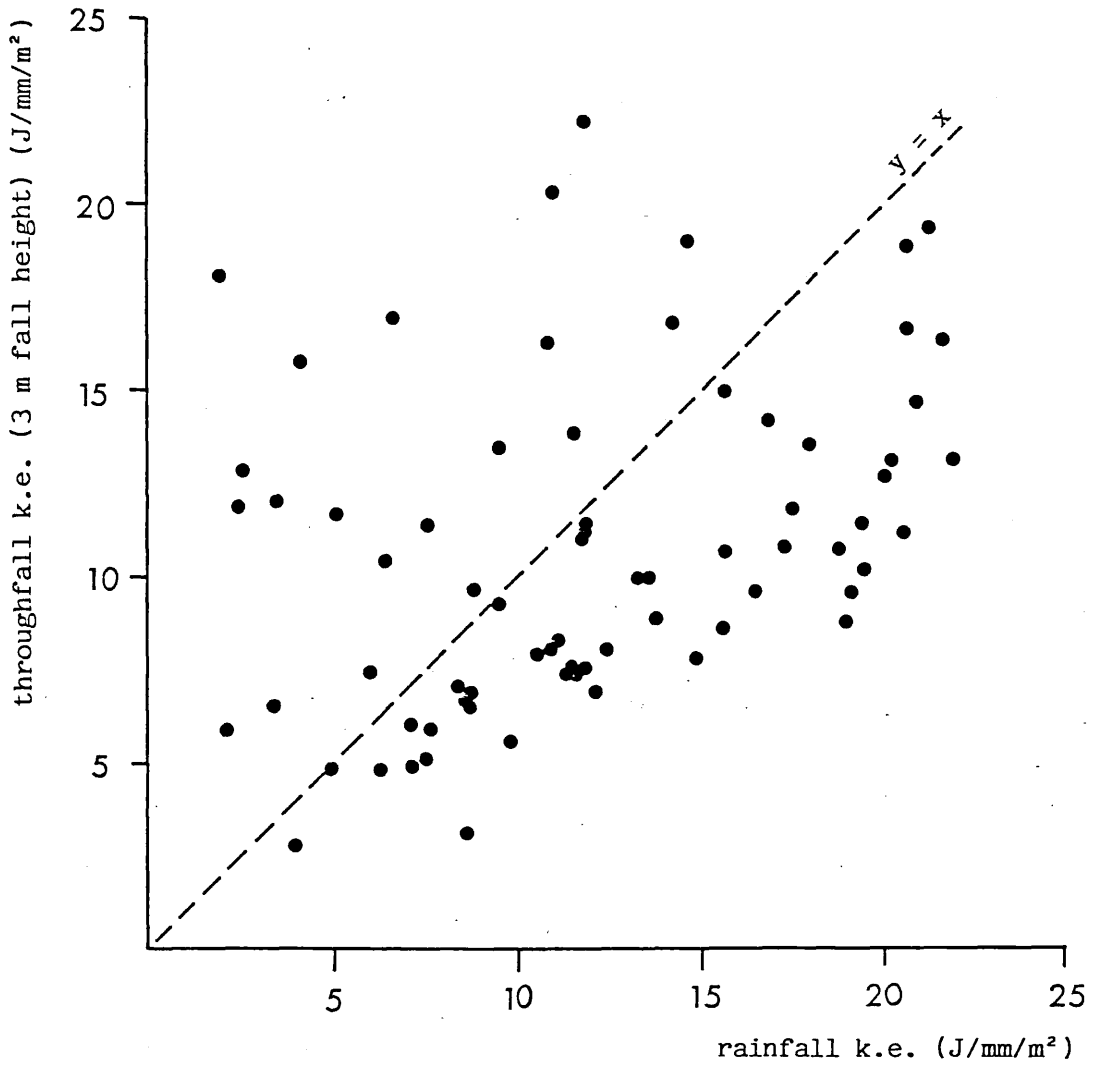

and throughfall drop-size distributions and kinetic energy.

1) Canopy storage curves from individual storms

i) Descriptions of the curves

The cumulated depth of rainfall (R) and throughfall (T) was calculated from the interpolated continuous record of samples and gaps. The difference between cumulated rainfall and throughfall at any point represents the amount of water lost to evaporation, diverted to stemflow or held in storage (S). It was assumed that the first two losses were negligible and that the depth of storage for any instant could be calculated from

$$S = R - T \qquad [6.8]$$

Graphs of the cumulative storage were constructed (Figures 6.12 to 6.18). Storm d178 was sampled at two places under the canopy throughout the storm, about 5 m apart and hence there are two storage curves. In each figure the ratio of the standard deviation of the throughfall to rainfall distributions calculated from the paired data has also been plotted against cumulative time. Where the ratio is greater than 1.0 it is assumed that the drop-size distribution is being spread by the canopy and there is an increased incidence of large drops.

In storms d3, d52 and d211 (Figures 6.12, 6.13 and 6.17) there was insufficient rain to fill the canopy which during d3 and d52 was at its densest (Table 5.4). For all three graphs the sample drop-size distributions produced a storage level which rose continuously although during d52 and d211 there were a few occasions when the occurrance of large drops in the throughfall caused halts to the rising curve.

Figure 6.12 Rainfall, throughfall and canopy storage (mm) cumulated with time for storm d3

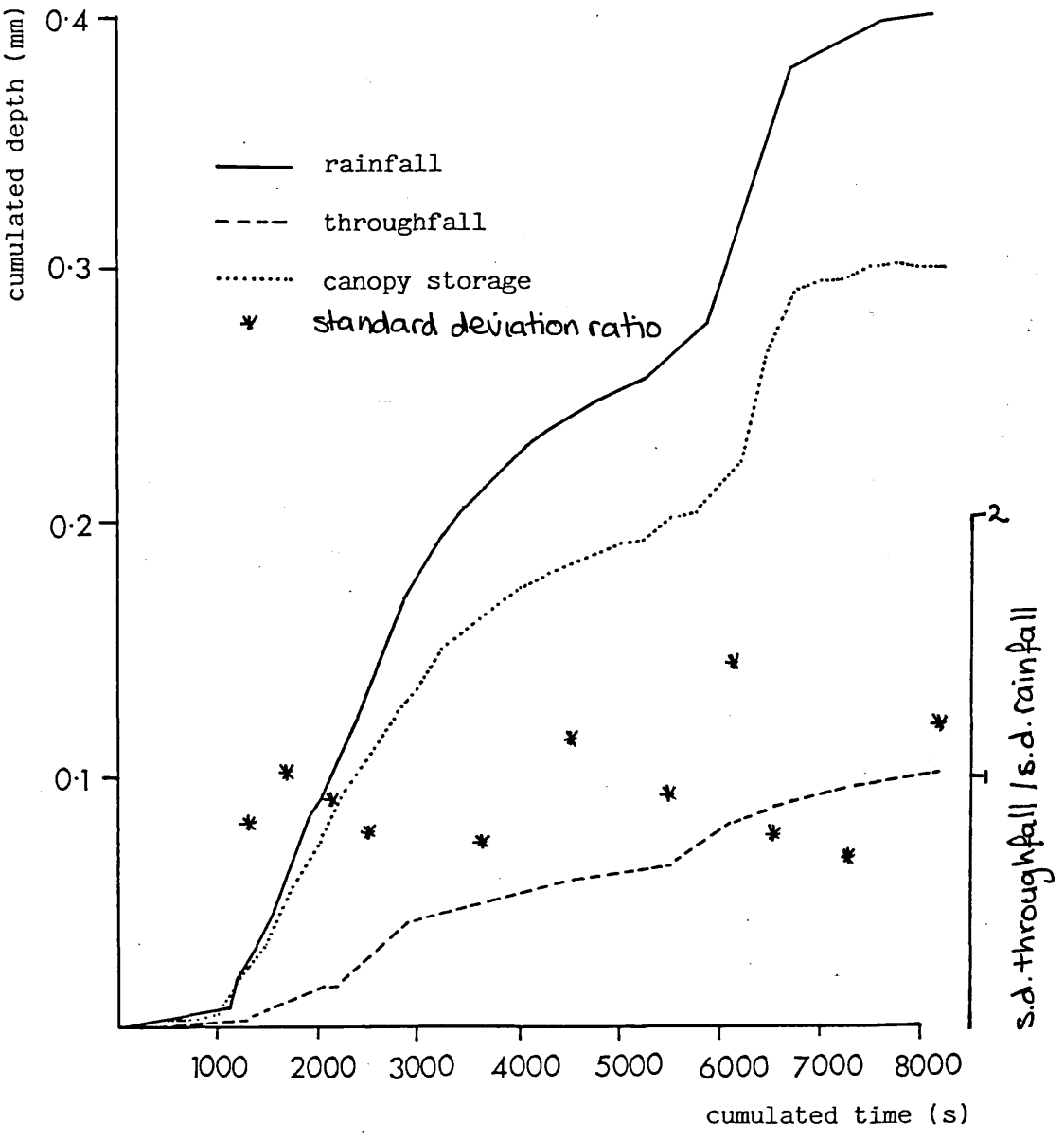

Figure 6.13 Rainfall, throughfall and canopy storage (mm) cumulated with time for storm d52

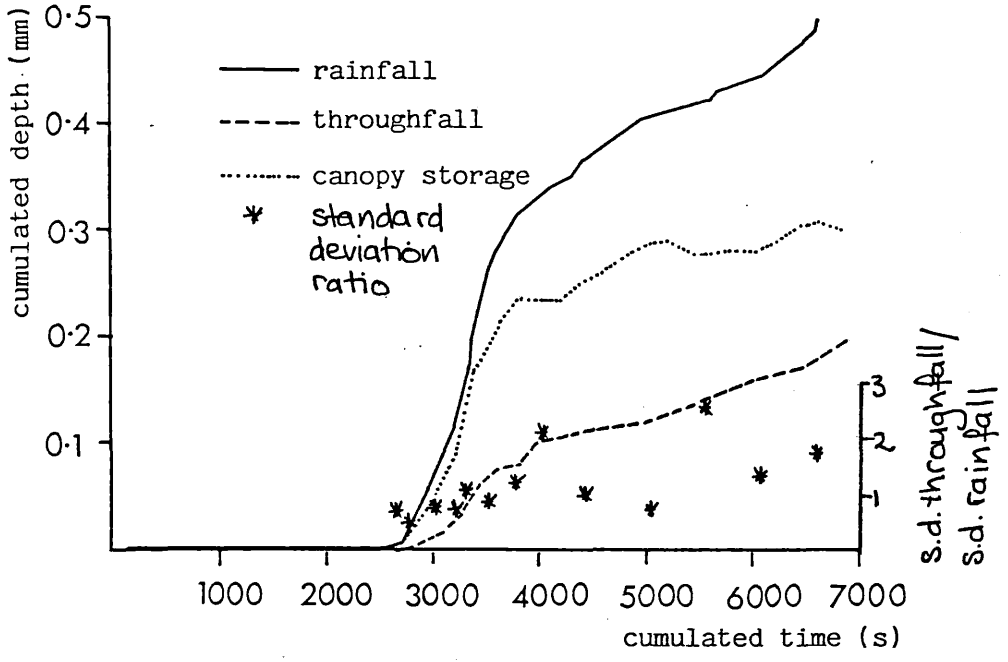

Figure 6.14 Rainfall, throughfall and canopy storage (mm) cumulated with time for storm d125

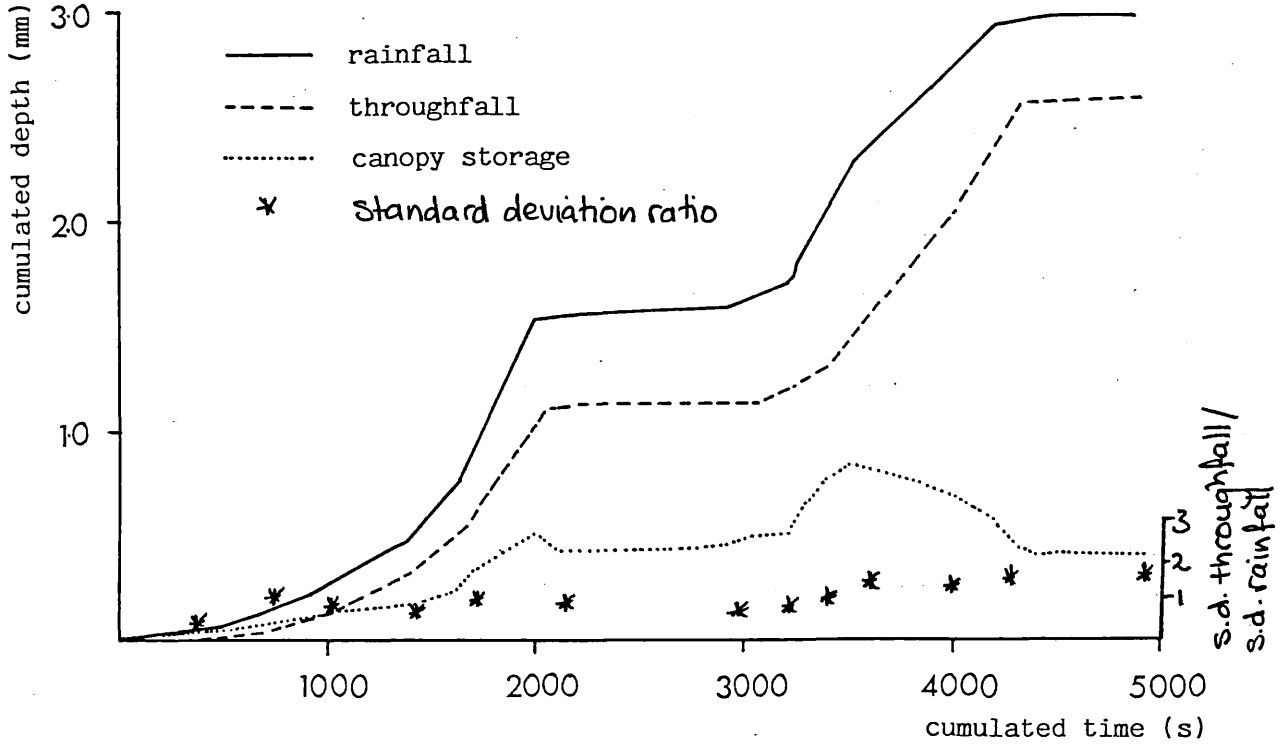

Figure 6.15 Rainfall, throughfall and canopy storage (mm) cumulated with time for storm d178a

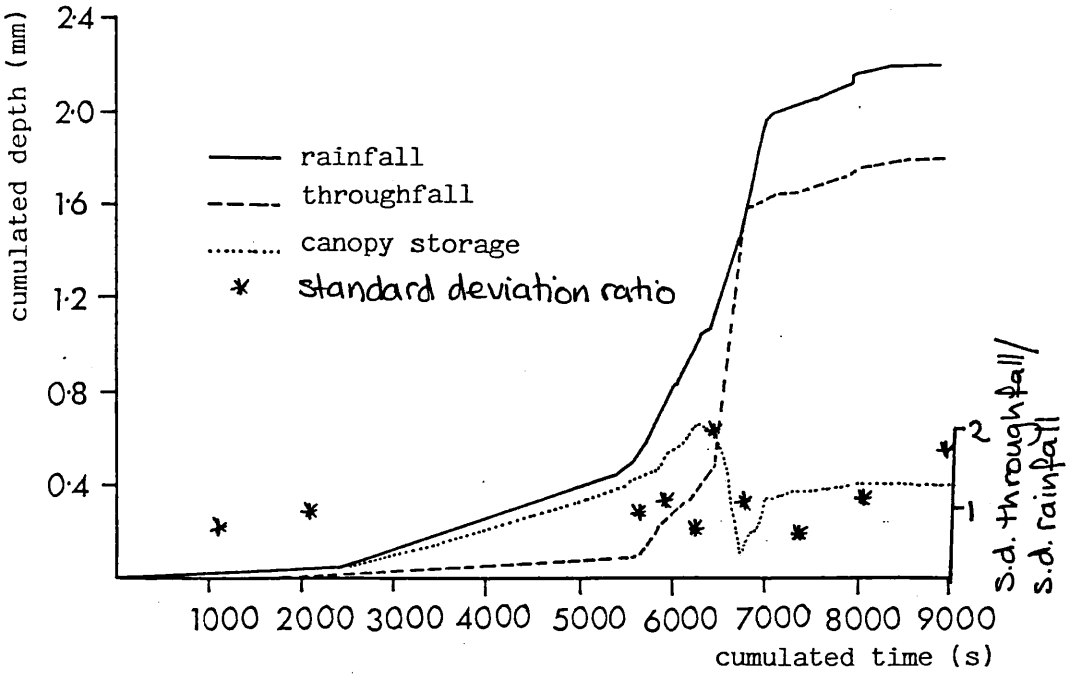

Figure 6.16 Rainfall, throughfall and canopy storage (mm) cumulated with time for storm d178d

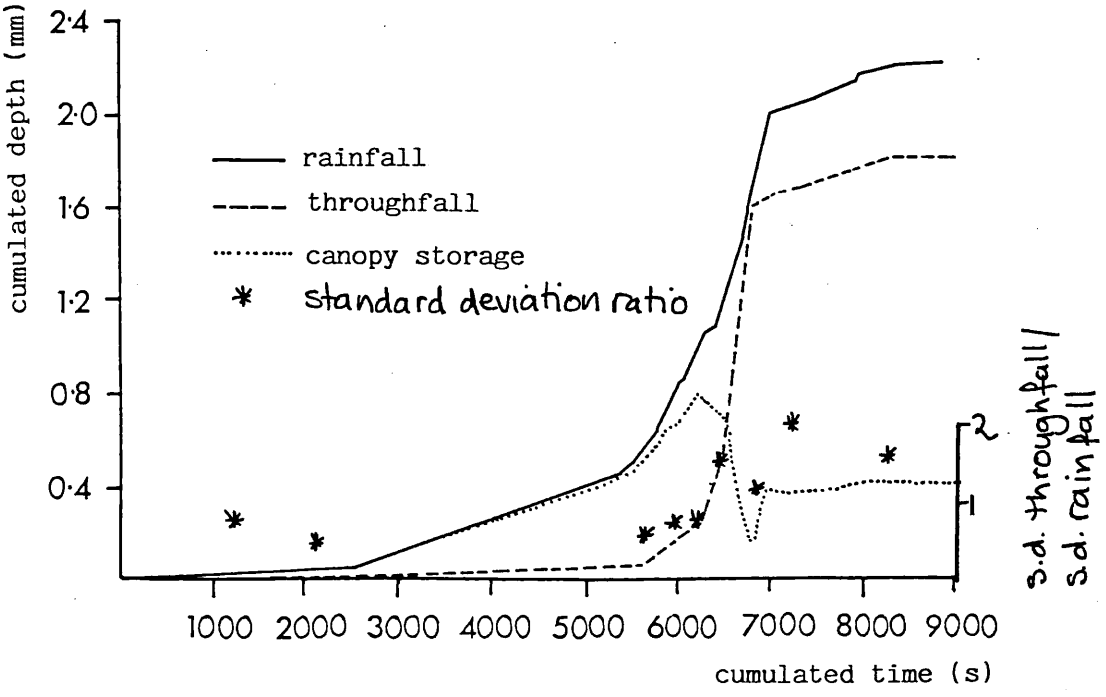

Figure 6.17 Rainfall, throughfall and canopy storage (mm) cumulated with time for storm d211

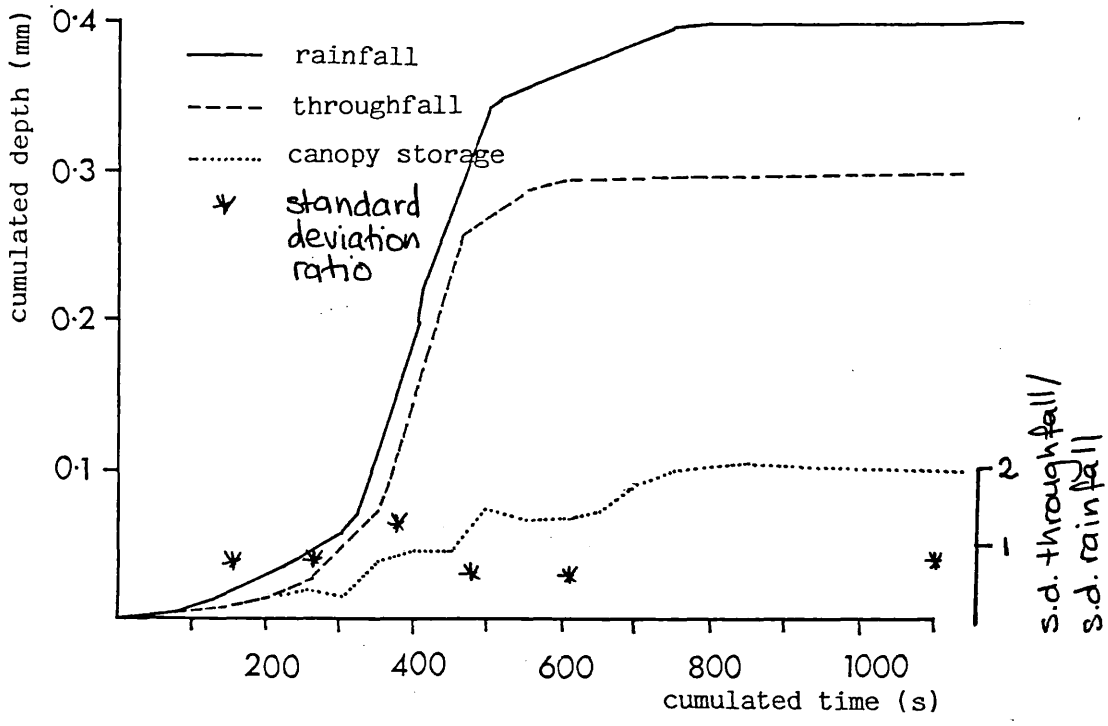

Figure 6.18 Rainfall, throughfall and canopy storage (mm) cumulated with time for storm d237

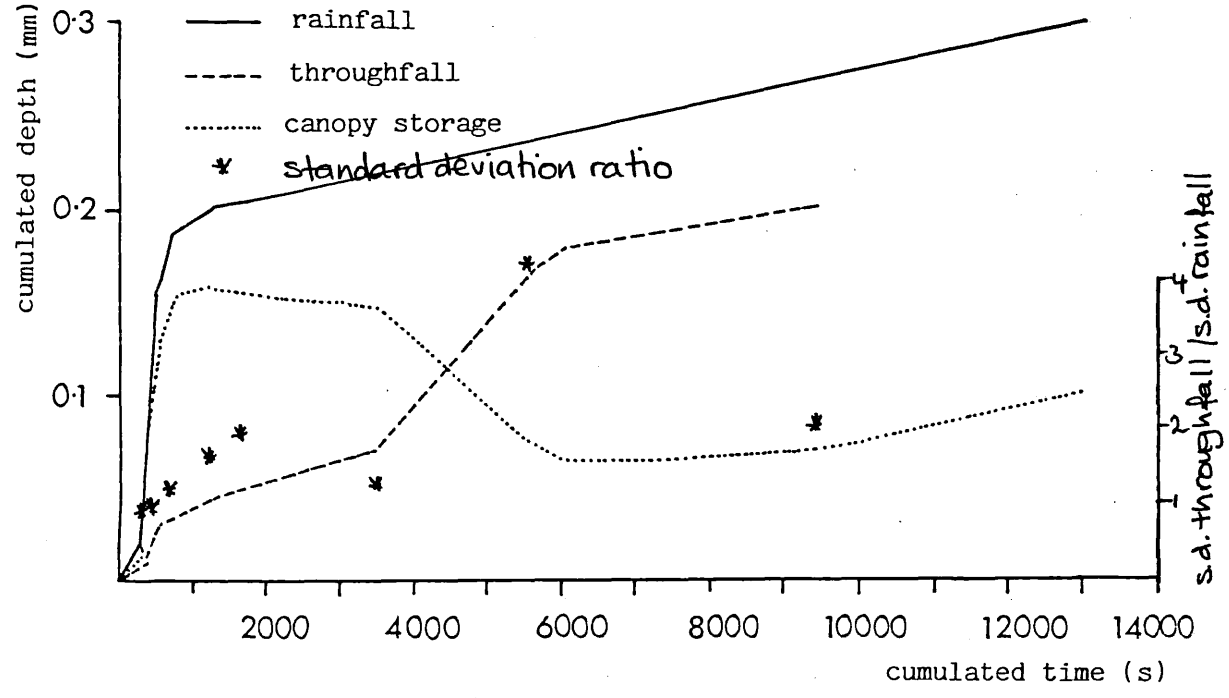

In contrast the drop-size distributions of the three other storms d125, d178a, d178d and d237 (Figures 6.14, 6.15, 6.16 and 6.18) produced storage curves which showed periods of increase in storage followed by a large decrease sustained in the cases of d178a, d178d and d237 over several samples. Afterwards in the cases of d178a, d178d and d237 the canopy filled again.

ii) Comparison of the graphs produced with the general model

The shapes of the canopy storage graphs calculated for each storm should correspond to one of the family of canopy storage curves presented in Figure 3.1. The particular general curve depends on the length of storm, the amount of water and the canopy cover. However such comparisons are of necessity qualitative since there is no empirical base for the general model nor an explicit mathematical function for the experimentally derived curves. Differences between the general and measured curves may be because the model curves illustrate a net accumulation over the whole canopy. These storm-specific curves are derived from the throughfall at a point and general trends may be obscured by individually draining stores and seasonal variation in the canopy. The approximated values for total rainfall and throughfall depth make it impossible to link the changes in drop-size distribution to specific levels of storage.

The depth of storms d3, d52 and d211 (Figures 6.12, 6.13 and 6.17) relative to the amount of canopy cover suggest that the canopy was never filled and the storage curve produced was expected to be similar to the lowest in Figure 3.1. All three curves show continuous accumulations of stored water. In storm d52 there were two instances where the ratio between the standard deviation of the throughfall and rainfall exceeded 2.0, causing steps in the curve. In both cases this was caused by stains of 29.0 mm (4.42 mm) in the throughfall drop-size distribution. These three storms may be considered to represent stages [a] and [b] in the qualitative drop-size distribution model, showing an initial decrease in the drop sizes by the canopy

followed by the dripping from a few point stores.

Storms d125 and d178 (Figures 6.14, 6.15 and 6.16) were assumed to be sufficient to fill the canopy capacity and for drainage to take place on a wider scale. Storm d237 (Figure 6.18) was estimated not to have filled the capacity but 6 of the 8 paired samples have standard deviation ratios of more than 1.0. The shape of each of these four graphs is varied but one general point can be made. Sampling of both rainfall and throughfall continued until rain and dripping from the canopy ceased. In all cases throughfall continued at most only a few minutes after the cease of rainfall, although the rainfall intensity decreased towards the end of the storm, and the logarithmical decaying drainage curve after the cease of rainfall suggested by Rutter et al. (1971) was not observed.

Both canopy storage curves for storm d178 (Figures 6.15 and 6.16) show a peak of storage followed by several samples where the standard deviation ratio was greater than 1.0, causing a sharp decrease in storage and after which the water accumulated again. This curve is not similar to any of the general curves. At the time of this storm, the canopy cover was at its least dense (17%). It is suggested that most of the individual storms were full when a disturbance of the canopy by wind or a cascade of overflowing stores almost emptied the canopy and left it below saturation point again. However confirmation of this suggestion cannot be made because this pulse of throughfall was not repeated during the storm as might have been suspected. This is an important observation in light of points raised in Chapter Four concerning the restriction of throughfall drop size sampling to one only one location despite proven spatial variability of throughfall kinetic energy. The rapid drainage, perhaps caused by wind disturbance of the canopy, was recorded at both sample locations about 5 m apart and hence the same drop-size distributions could have been sampled at any location within the plot.

No sudden cascading drops can account for the prolonged draining of the canopy in storms d125 and d237 (Figures 6.14 and 6.18) which

show a build up of stored water and then a decline sustained over several samples. The curve of d125 is complicated by a temporary lull in rainfall in the middle of the storm. These curves were similar to the general model curves which reach a peak in storage, although subsequent drainage takes place, while it is still raining. Although the canopy was only slightly denser than in d178, 20% in d125 and it had reached 35% in d237. It is suggested that with an increase in the number and variety of stored depths in individual stores a cascade of drops through the canopy may not be observed.

To conclude, storms which were assumed not to fill the canopy reproduced curves similar in form to those of the general model. The standard deviation ratios of d52 showed that similar features to stage [b] of the qualitative drop-size distribution model where there are individual draining stores within a filling canopy. The repeated occurrence of large drops in successive samples suggested by later stages reduced the canopy storage levels. However more specific points cannot be made and the differences in percentage cover make the curves respond differently.

iii) Sensitivity of the canopy storage curve to relative rainfall and throughfall depths

To examine the sensitivity of the canopy storage curves to the choice of throughfall depth relative to rainfall depth for the interpolation a total throughfall depth of 0.3 mm instead of 0.1 mm was assumed for storm d3 with a rainfall depth of 0.4 mm (Figure 6.19). While the same trend of increasing storage may be observed it will be noted that the samples with a standard deviation ratio of more than 1.0 mm now cause a decrease in the storage curve, accentuating the importance of the large drops in samples d3c(5) and d3c(9) and causing drainage which before was unobserved. Therefore the choice of interpolation depths may either repress or enhance drop-size distributions which could place that part of the storm in a different stage of the succession of drop-size distribution changes.

Figure 6.19 Contrasting the cumulated canopy storage (mm), for storm d3, calculated assuming interception capacities of 0.1 and 0.3 mm

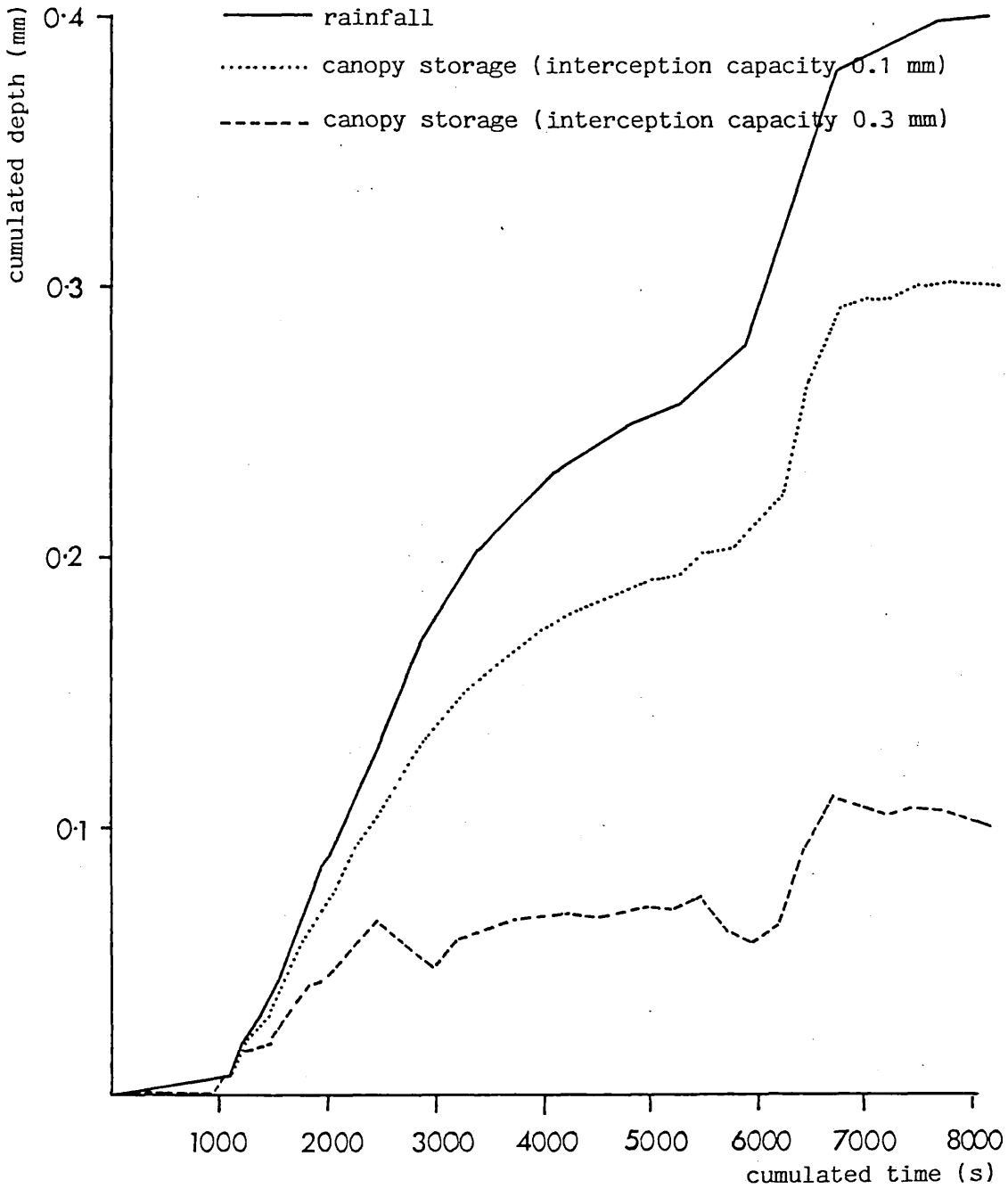

2) A canopy storage curve from a simulated storm

A series of changes in the drop-size distribution of the throughfall through a storm has been suggested by the model. As a logical extension, the canopy storage curve is assumed to match its periods of increase and decrease with the changes in distribution. Attempts to reproduce this curve from the sampled sequence of drop-size distribution changes for individual storms have met with limited success. Consequently a simulated storm was produced by listing all rainfall and throughfall pairs of distributions for all storms in the sequence of change suggested by the model. The object was to produce a general canopy storage curve similar to that suggested by the models of Massman (1980) and Rutter et al. (1971) to see if the changes in distribution may produce periods of filling and emptying in the canopy storage.

i) Creation of the simulated storm

The qualitative model suggested a progressive increase in the occurrence of large drops in the throughfall from the canopy and hence an increase in the ratio of the standard deviation of the paired samples of rainfall and throughfall through the storm. Hence all the rainfall and throughfall pairs of distributions for all storms were listed in order in increasing standard deviation ratio regardless of their order in the original storm. All pairs were placed in a continuous string as if they has been sampled consecutively from the same storm.

The array of data was examined to select a suitable depth for the storm. The existence of many samples where the standard deviation ratio exceeded 1.0 suggested that the canopy storage capacity may be considered to have been exceeded and a stage reached where dripping occurred from many stores.

A storm depth of 3.0 mm was chosen. A canopy capacity of 1.0 mm

for an oak tree in summer, leaves a total throughfall depth of 2.0 mm. The depth of each sample was corrected proportionally using equation [5.18] so that the total rainfall and the total throughfall were 3.0 and 2.0 mm respectively. The relative depth of throughfall to rainfall for each paired sample determined the shape of the general storage curve produced. The cumulative depth of simulated throughfall from the canopy has been plotted against the cumulative depth of simulated rain (Figure 6.20).

A visual inspection suggested that the curve in Figure 6.20 could be divided into three sections, each with a different linear relationship between throughfall and rainfall depth. The original division between sections was made by eye then points were successively included or excluded on either side of the division to choose the best-fit regressions to establish the gradients of each section of the curve. In practice a couple of points either way on any section made very little difference to the gradients. The gradient of the line reflects the rate of canopy filling. Gradients less than 1.0 show a filling canopy, gradients greater than 1.0 an emptying canopy. The gradients of each line were tested to see if they were statistically different from each other.

The equations of regression and the analysis of the gradients are presented in Table 6.6. The difference between all three is highly significant statistically. Hence the simulated storm may be divided into three distinct sections.

ii) Discussion of the simulated storm

The simulated storm used simultaneously sampled pairs of rainfall and throughfall drop-size distributions. The relative depths of water in each sample have produced three distinct relationships between throughfall and rainfall depth. From [6.8] the general relationship between cumulative canopy storage depth (S) and cumulative rainfall depth (R) for each phase may be written thus

Figure 6.20 Cumulated throughfall depth (T mm) plotted against cumulated rainfall depth (R mm) using all paired samples in order of increasing ratio of the standard deviations of throughfall to rainfall drop sizes

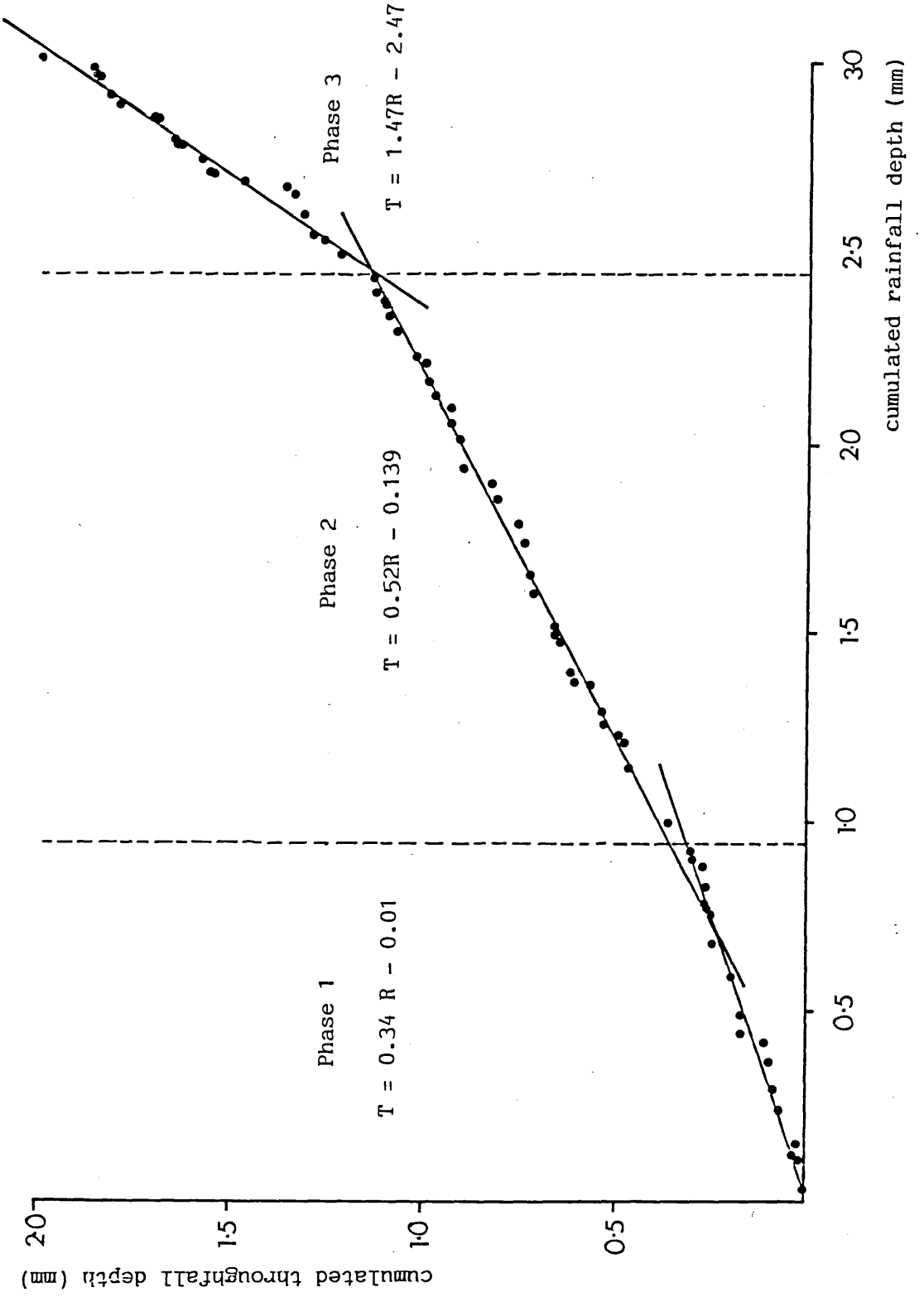

Table 6.6 Analysis of the simulated storm by the fitting of regression lines to the three different phases in the relationship between rainfall depth (R) and throughfall depth (T)

Phase	Equation of regression	r	t-test	
			t	p
1	T = 0.244 R - 0.0123	0.99		
2	T = 0.522 R - 0.139	0.98	* 16.68	<0.001
3	T = 1.47 R - 2.47	1.00	** 7.69	<0.001

* testing the probability that the gradient of the regression for Phase 2 is the same as that for Phase 1

** testing the probability that the gradient of the regression for Phase 3 in the same as that for Phase2

Phase 1	$S = 0.0123 + 0.656\ R$	[6.9]
Phase 2	$S = 0.139 + 0.478\ R$	[6.10]
Phase 3	$S = 2.47 - 0.47\ R$	[6.11]

Figure 6.21 illustrates the storage curve generated from the simulated storm using these general relationships between cumulated rainfall and storage. Comparisons between the simulated storage curve and the models of Massman (1980) and Rutter et al. (1971) are again of necessity qualitative. The simulated storm shows three phases in the canopy storage change, the first with a higher rate of filling than the second, followed by a period of emptying and as such is similar in form to the model curves.

The model storage curve suggests that only the lowest rising limb should be linear. Although more complex curves could have been fitted to the relationship between throughfall and rainfall in Figure 6.20 the information as to their shape is insufficiently detailed. A curve might be fitted to the graph at the junctions of the different regression lines. The steeply decaying falling limb suggested by Rutter et al. (1971) is not observable in the upper limb of the Figure 6.20, of all the phases this has the most scattered data.

Section Four The kinetic energy of each stage in the sequence of change in throughfall through the simulated storm

1) Relation of the qualitative model of drop-size distribution change to the rates of canopy filling

The different phases in the relationship between throughfall depth and rainfall depth have been related to the hypothesised stages of drop-size distribution in the qualitative model. The simulated sequence of drop-size distribution change has been divided into the

Figure 6.21 Cumulated storage curve generated from the simulated storm

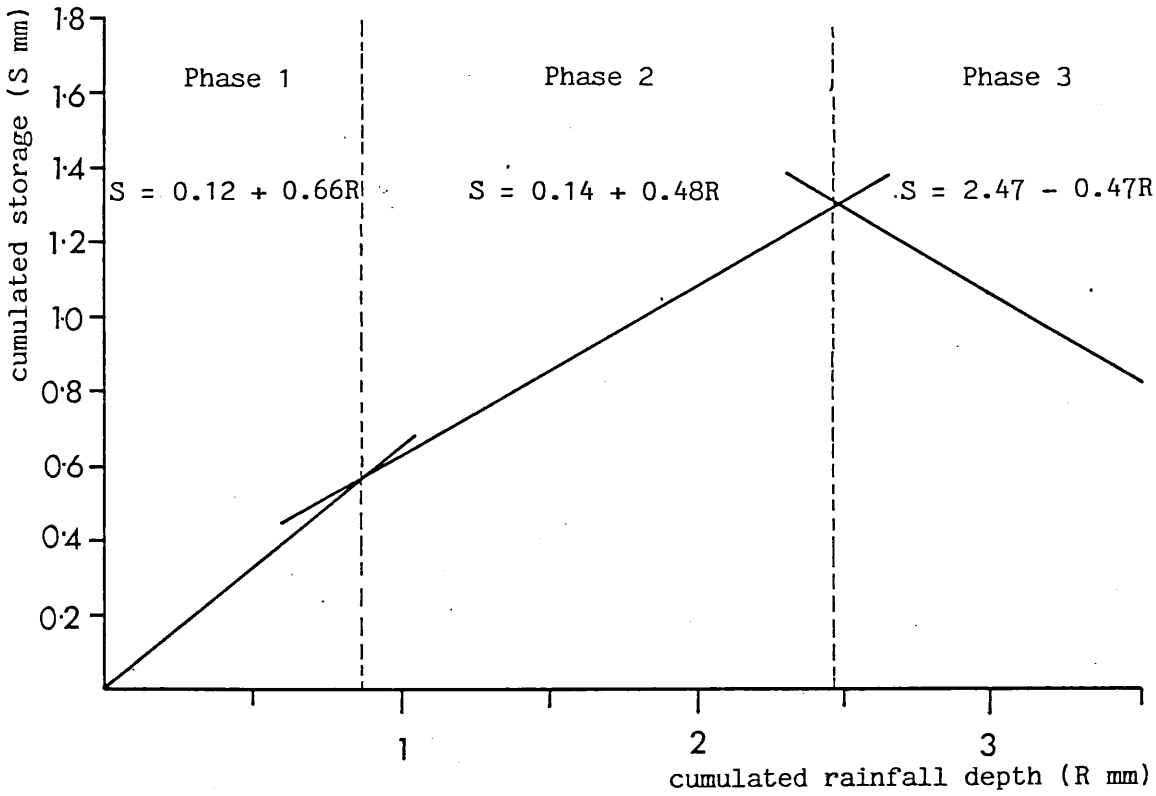

three different phases of the storm. To examine the hypothesis that there is an increased incidence of larger drops in the throughfall as the storm progresses, the standard deviation of the throughfall samples in each phase have been analysed and the results are presented in Table 6.7.

The standard deviation of the samples increases from Phase 1 to Phase 3, confirming that the samples at the end of the storm have a higher incidence of larger drops than those at the beginning. The difference between the distributions in Phase 1 and Phase 2 is significant at the 99.9% level and at the 95% level between Phases 2 and 3.

Table 6.8 summarises the range of standard deviation ratios in each phase of the simulated storm and links it to the stages of the qualitative model of drop size distribution change. The table shows that several of the model stages are indistinguishable from each other in the data collected. However periods of increase in canopy storage with no dripping, periods of increase with dripping and periods of storage decrease due to extensive dripping can be determined.

2) Relation of stage to the change in kinetic energy of throughfall and rainfall

i) Analysis of kinetic energy/mm/m² in each phase

It was suggested by the model that the total kinetic energy under the canopy is a function of the balance between the different stages. The kinetic energy/mm/m² of all paired samples of throughfall and rainfall falling in each phase of the simulated storm have been analysed and the results are presented in Table 6.9.

In Phase 1, the mean kinetic energy of throughfall was significantly reduced by the canopy, from 13.04 J/mm/m² to 8.51 J/mm/m². In Phase 2 the mean kinetic energies of rainfall and

Table 6.7 Analysis of means of the standard deviation of throughfall samples in each phase of the simulated storm

	mean	95% confidence interval		t-test		
				t	p	DF
Phase 1	1.26	1.10, 1.43				
Phase 2	1.76	1.56, 1.96	*	3.94	<0.001	49
Phase 3	2.26	1.80, 2.71	**	2.10	0.05	27

* t-test tests the probability that the mean of the distribution of standard deviations in Phase 1 is the same as that in Phase 2

** t-test tests the probability that the mean of the distribution of standard deviations in Phase 2 is the same as that in Phase 3

Table 6.8 The relationship between the three phases of the simulated storm and the stages of the qualitative model of drop-size distribution change in terms of the ratio of the standard deviation (s.d.) of the throughfall (T) to rainfall (R) for paired samples

Phase	Equivalent stage	Canopy state	s.d. (T/R)
1	Stage 1	Rapidly increasing canopy storage	0 - 0.78
2	Stages 2 and 3	Reduced canopy filling due to water loss from point stores	0.78 - 1.20
3	Stages 4 and 5	Canopy emptying	1.20 - ∞

Table 6.9 Analysis of means of the kinetic energy/mm/m² of rainfall (R) and throughfall (T) for each of the three canopy storage phases of the simulated storm

		mean (J/mm/m²)	95.0% confidence interval	t-test		
				t	p	d.f.
Phase 1	rainfall	13.04	10.7, 15.4			
	throughfall	8.51	6.92, 10.09	3.36	0.002	31.6
Phase 2	rainfall	13.14	11.27, 15.00			
	throughfall	13.48	11.1, 15.9	0.23	0.82	58.6
Phase 3	rainfall	9.28	6.2, 12.3			
	throughfall	23.49	19.0, 28.0	5.45	<0.001	33.2

(The two sample t-test tested the probability of the mean of the rainfall data equalling the mean of the throughfall data)

throughfall were 13.14 and 13.48 J/mm/m^2 respectively and the two data sets were statistically indistinct. In Phase 3 of the storm the canopy increased the mean kinetic energy of the rainfall from 9.28 J/mm/m^2 to 23.49 J/mm/m^2 and once again the difference was highly statistically significant.

ii) Analysis of total kinetic energy in each phase

The total kinetic energy of rainfall and throughfall for each phase of the simulated storm has been calculated and is presented in Table 6.10. In the open the total kinetic energy of the rainfall was 38.81 J while under the canopy the total was 39.74 J. It may be assumed that if the storm had stopped after the end of Phase 1, while the size and range of the rainfall drops was being decreased there would have been a 5-fold decrease in the amount of the kinetic energy reaching the ground. If the storm stopped after the end of Phase 2, by which time the canopy was sufficiently full to allow dripping although the storage level was still rising, the reduction would have been 2-fold. It might be expected that had the storm continued for longer in its last phase with the rainfall energy reduced and the throughfall energy at a maximum the total kinetic energy under the canopy might be still greater than that in the open.

Conclusions

Samples of rainfall and throughfall were taken for seven storms under an oak canopy. Estimates of rainfall depth were made from Meteorological Office daily rainfall records and from a continuous raingauge sited nearby. Throughfall depth was estimated from the measurements of percentage canopy cover. A continuous record of drop-size distribution change was interpolated from the drop-size distribution samples and total depths. From the continuous record simultaneously paired samples of rainfall and throughfall were derived.

Table 6.10 The total kinetic energy (J/m^2) of rainfall (R) and throughfall (T) for each phase of the simulated storm

	Rainfall energy (J/m^2)	Throughfall energy (J/m^2)
Phase 1	12.53	2.51
Phase 2	20.22	12.91
Phase 3	6.06	24.32
Total	38.88	39.74

Comparison between the drop-size distributions of the paired samples revealed that the canopy effectively changed the drop-size distribution of rainfall, concentrating the numbers of drops between 0.51 mm and 0.74 mm diameter and increasing the incidence of large drops. The changes in drop-size distribution were related to changes in the kinetic energy/mm/m^2 of the paired samples.

The cumulated rainfall and throughfall depths and the cumulated canopy storage for each storm were calculated from the continuous record of drop-size distributions. The storage curves were compared with the model curves of Massman (1980) and Rutter et al. (1971) to assess the link between the changes in drop-size distribution and storage. Secondly a storm was simulated from all the paired samples of rainfall and throughfall. All paired samples were ordered in terms of the ratio between the standard deviation of the drop-size distributions of throughfall and rainfall to simulate the hypothesised changes in drop-size distribution through a storm. Three distinct relationships between throughfall and rainfall depth were found with increasing value of the standard deviation ratio. A general curve for canopy storage compared favourably with the model curves.

Further analysis showed that the relative kinetic energy/mm/m^2 of the paired samples of rainfall and throughfall depended on the phase of the simulated storm, with a decrease in energy by the canopy in Phase 1 and an increase in Phase 2. The total kinetic energy of each phase was calculated. It was revealed that the balance of throughfall and rainfall energy for a storm depended on the change in the drop-size distributions by the canopy. Throughfall for storms which included little dripping from the canopy had less energy than in storms where dripping became widespread.

CHAPTER SEVEN THE ANALYSIS OF THROUGHFALL FROM THE TROPICAL RAIN FOREST CANOPIES

Introduction

The aims of this chapter are three-fold. Firstly it aims to examine, in a different environment, the link between canopy storage and throughfall drop-size distribution change which was established under the temperate oak forest. Secondly this chapter continues the examination of the statements outlined in Chapter Three. The availability, in this data set, of additional accurate information on storm depths and splash amounts together with a constantly evergreen and unchanging canopy cover allow the relationship between storm depth, intensity and canopy storage change to be examined in detail. The statements for examination are that:

v) The sequence of changes in the drop-size distribution and hence in the kinetic energy/mm/m^2 is predictable (i.e. the same for each storm),

vi) The predictable sequence of changes in the drop-size distributions can be related to constants in

   a) rainfall intensity
   b) the depth of canopy storage,

vii) The total difference between the kinetic energy of the rainfall and throughfall depends on the amount of water falling during the different stages of the storm.

Finally by contrasting the results from managed and unmanaged forest sites the impact of a particular vegetation change may be assessed.

Data is presented from seven tropical storms. The field location

and sites have been described in detail in Chapter Four. The parameters of each storm were measured in an open site (o) and under two different rain forest canopies, a low multiple-layered canopy (mc) which, although it was probably secondary regeneration, was chosen to reflect conditions of unfelled rain forest and a high, single-layered canopy (sc) from which the undergrowth had been removed, chosen to reflect some form of forest management and assumed to be the same as the upper layer of the multiple canopy.

Appendix 1(b) shows the number of drops in each size class for each sample of rain and throughfall and the duration of each sample and gap. The drop-size distributions and depth of water in the unsampled gaps were interpolated from the samples to provide a continuous record of drop-size distribution change. Instantaneously paired samples of rainfall and throughfall for each storm and site were derived from the continuous record of drop-size distribution change using methods described in Chapter Five. As was assumed for the oak canopy results the differences between rainfall and throughfall depth and drop-size distribution are considered to be due to the presence of the canopy.

Section One Descriptions of rainfall and throughfall drop-size distributions and changes by the canopy

The first section of this chapter describes the drop-size distributions of the rainfall and both throughfall samples and assesses the extent of the change by the canopy. The methods of description are the same as those of Chapter Six and are intended to re-examine the first statement derived from the qualitative models, that the presence of the canopy changes the drop-size distribution of the rain, by describing the rainfall and throughfall drop-size distributions separately and then comparing them. As in Chapter Six, the analysis of the drop sizes uses the stain diameters rather than the drop diameters derived from the calibration, to reduce errors due to the conversion. However, wherever stain diameters are referred to,

the equivalent drop diameter is given in brackets.

1) Numerical descriptions of rainfall and throughfall paired samples

Visual inspection of Appendix 1(b) reveals that as with the oak data, the majority of the stains in any sample are clustered over a small size range although the range of sizes is wider in the rain forest data. Hence the mean stain size will reflect this majority of drops, while the standard deviation will be sensitive to the incidence of larger drops.

The mean stain size and standard deviation of every paired sample are presented in Table 7.1. An analysis of the means of each data set is given in Table 7.2. Two sets of paired samples were derived from the continuous record of rainfall, one simultaneously paired with the single canopy throughfall and the other paired with the multiple canopy throughfall.

i) Mean stain sizes

For both paired samples derived from the continuous record of rainfall, the mean stain size varied from 0.49 mm (an equivalent drop diameter of 0.23 mm) to 5.15 mm (1.26 mm). Table 7.2 shows that the mean, mean stain size for all samples paired with single canopy throughfall samples, is 2.58 mm (0.76 mm), while those paired with the multiple canopy throughfalls is 2.57 mm (0.76 mm). There is a 99% probability that the means of the two rainfall data sets are drawn from the same distribution.

The mean stain sizes for single canopy throughfall samples range from 0.51 mm (0.23 mm) to 2.92 mm (0.84 mm) with a mean of 1.48 mm (0.51 mm). For the mean stain sizes of the multiple canopy throughfall the range is from 0.52 mm (0.23 mm) to 3.41 mm (0.93 mm)

Table 7.1 The mean diameter ($\bar{x}$ mm) and standard deviation (s.d. mm) of stain sizes for each paired sample of rainfall (R) and throughfall (T) for all storms

a) Single canopy site

Sample	$\bar{x}$		s.d.		Sample	$\bar{x}$		s.d.	
	R	T	R	T		R	T	R	T
j10b(1)	4.03	1.37	2.45	3.04	j15(4)	1.29	1.09	1.73	1.23
(2)	4.00	2.51	2.41	4.88	(5)	1.30	1.90	1.74	4.27
(3)	3.67	1.50	2.62	4.42	(6)	1.66	0.85	1.91	1.68
(4)	2.45	1.67	1.85	3.53	(7)	4.02	1.09	2.57	3.20
(5)	2.48	1.80	1.90	4.39	(8)	2.70	1.55	2.00	3.03
(6)	2.31	1.51	1.71	3.28	(9)	2.86	1.58	2.43	4.41
(7)	2.02	1.16	1.33	2.10	(10)	2.95	1.80	2.49	4.67
(8)	1.77	1.12	1.28	1.29	(11)	2.42	2.21	1.68	4.97
(9)	1.90	1.12	1.16	1.33	(12)	2.17	1.93	1.38	4.05
(10)	2.41	0.76	2.23	1.07	(13)	2.06	1.07	1.96	1.15
(11)	0.93	0.96	0.37	1.23	(14)	3.10	1.43	2.51	2.63
j11 (1)	1.73	1.62	1.60	0.74	(15)	3.06	1.70	2.64	4.34
(2)	2.82	1.52	3.77	1.38	(16)	3.65	1.54	2.73	3.78
(3)	4.39	2.92	4.19	6.90	(17)	3.38	1.37	2.30	3.10
(4)	1.14	1.43	2.98	2.44	j16b(1)	2.76	1.13	2.84	2.42
(5)	1.10	1.47	2.82	3.86	(2)	3.00	2.20	3.37	5.45
(6)	2.45	1.48	3.77	3.58	(3)	3.00	1.11	2.78	1.53
(7)	2.28	2.46	3.64	5.80	(4)	2.77	2.34	1.88	5.21
(8)	3.45	1.45	2.51	2.62	(5)	2.47	1.74	1.45	3.80
(9)	3.26	1.27	2.19	1.37	(6)	2.42	1.43	1.47	2.24
j12(1)	2.53	0.89	5.48	0.99	(7)	2.43	1.37	1.38	1.98
(2)	2.23	1.71	4.78	3.76	(8)	1.82	1.00	1.22	1.06
(3)	2.68	1.34	3.59	2.27	j20(1)	2.68	0.78	3.95	0.88
(4)	2.87	0.99	2.46	1.48	(2)	2.02	1.94	2.85	3.24
(5)	2.11	1.54	1.27	3.18	(3)	2.16	1.25	3.13	2.74
(6)	1.15	1.72	1.71	3.73	(4)	2.52	1.74	3.69	3.38
(7)	4.00	1.82	3.14	3.68	(5)	3.03	1.37	3.43	2.88
(8)	2.91	1.08	1.67	1.82	(6)	3.49	1.29	2.74	2.15
j13(1)	2.39	1.83	1.11	1.25	(7)	3.04	2.09	2.25	5.57
(2)	2.86	1.00	2.52	0.58	(8)	2.70	2.04	1.60	4.22
(3)	2.92	0.51	2.14	0.32	(9)	2.57	1.47	1.56	3.63
j15(1)	4.55	1.28	3.58	3.05	(10)	2.19	1.48	1.38	3.56
(2)	3.13	1.55	3.05	4.13	(11)	1.96	1.34	1.47	2.80
(3)	0.49	1.17	0.31	2.57	(12)	2.10	0.88	1.63	0.73

Table 7.1 (cont'd) The mean diameter ($\bar{x}$ mm) and standard deviation (s.d. mm) of stain sizes for each paired sample of rainfall (R) and throughfall (T) for all storms

b) Multiple canopy site

Sample	$\bar{x}$		s.d.		Sample	$\bar{x}$		s.d.	
	R	T	R	T		R	T	R	T
j10b(9)	3.65	2.25	2.59	5.23	j15(8)	3.74	0.52	4.10	0.60
(10)	2.52	2.09	1.98	5.07	(9)	3.34	1.33	2.46	3.57
(11)	2.48	1,47	1.90	2.82	(10)	2.86	1.25	2.45	3.26
(12)	2.02	1.89	1.30	2.74	(11)	2.69	1.10	2.18	0.89
(13)	1.84	2.31	1.26	5.91	(12)	2.16	0.66	1.38	0.86
(14)	1.70	2.24	1.61	5.10	(13)	2.17	0.89	1.37	0.83
(15)	1.66	1.81	1.44	2.82	(14)	1.62	0.65	1.52	0.57
j11(1)	1.93	0.91	2.21	1.13	(15)	2.00	0.71	1.86	0.46
(2)	4.72	1.75	4.40	4.01	(16)	2.08	2.78	1.99	6.77
(3)	4.73	2.09	4.62	7.61	(17)	3.11	0.53	2.44	0.52
(4)	2.49	2.18	3.83	4.98	(18)	3.09	0.79	2.69	0.83
(5)	1.11	1.34	2.87	3.02	(19)	3.64	1.15	2.69	1.15
(6)	2.48	1.98	3.77	7.88	(20)	3.27	0.94	2.13	0.63
(7)	2.34	2.00	3.73	6.42	(21)	3.31	0.76	2.13	0.80
(8)	3.02	1.34	3.44	4.72	j16b(1)	2.00	0.69	2.93	0.68
(9)	3.07	1.90	3.51	4.50	(2)	2.85	0.85	2.26	0.81
(10)	3.02	2.33	3.44	5.99	(3)	2.47	0.69	1.47	0.72
(11)	3.48	1.46	2.57	3.24	(4)	2.43	0.87	1.42	0.93
j12(1)	3.26	0.96	7.15	3.31	(5)	2.10	0.78	1.30	0.61
(2)	2.39	1.29	3.98	2.55	j20(1)	2.41	0.88	3.62	0.65
(3)	2.83	2.11	2.47	5.14	(2)	2.00	0.78	2.81	1.14
(4)	2.46	1.47	1.44	3.61	(3)	2.10	1.32	3.00	3.08
(5)	1.24	3.22	0.89	6.90	(4)	2.41	2.54	3.51	5.48
(6)	2.54	2.47	3.37	4.87	(5)	2.79	1.60	3.15	4.31
(7)	2.92	2.19	1.65	4.62	(6)	3.01	2.02	3.39	4.64
j13(1)	2.82	1.08	2.43	0.87	(7)	3.61	3.41	2.86	7.36
(2)	2.86	0.69	2.12	0.56	(8)	2.93	1.20	2.05	2.28
j15(2)	5.15	1.34	2.61	2.51	(9)	2.59	2.29	1.56	5.36
(3)	3.06	0.82	2.98	0.74	(10)	2.10	3.12	1.34	6.40
(4)	0.49	0.84	0.32	0.79	(11)	1.98	1.54	1.28	2.20
(5)	1.30	0.85	1.74	0.73	(12)	2.09	2.11	1.62	5.42
(6)	1.28	1.21	1.72	0.95	(13)	2.11	2.38	1.63	5.56
(7)	1.29	0.83	1.73	0.87	(14)	2.66	2.03	1.98	4.98

Table 7.2 Analysis of means of mean stain diameter (mm) for each paired sample of rainfall and throughfall from single and multiple canopies

	n	mean	95% confidence intervals
rainfall	68	2.58	2.38, 2.78
single canopy throughfall	68	1.48	1.37, 1.59
rainfall	66	2.57	2.37, 2.78
multiple canopy throughfall	66	1.51	1.34, 1.69

t-test results	t	p
rainfall and single canopy throughfall	10.69	<0.0001
rainfall and multiple canopy throughfall	7.91	<0.0001
single canopy throughfall and multiple canopy throughfall	0.32	0.75

t-test tests the hypothesis that the mean stain diameters are the same

with a mean of 1.51 mm (0.51 mm).

To examine the extent to which both canopies changed the mean stain size, a paired sample t-test was carried out on all rainfall and throughfall paired samples (Table 7.2). The t-tests reveal that for both multiple and single canopy sites, the differences between the mean stain sizes of rainfall and throughfall was highly significant. An examination of the mean values reveals that the average mean stain size of throughfall samples was lower than that of the rainfall.

A two sample t-test was used to assess the significance of the difference between the mean stain sizes of the throughfall samples from both canopies (Table 7.2). Although the mean stain size from the single canopy was 1.48 mm (0.51 mm) and that from the multiple canopy was 1.51 mm (0.51 mm) there was a 75% probability that the two means were drawn from the same distribution.

Figures 7.1 and 7.2 illustrate plots of mean stain diameter of throughfall against the mean stain diameter of rainfall for all paired samples. Figure 7.1 shows that the range of mean stain sizes of all single canopy throughfall samples is compressed from a range of 1.0 to 4.0 mm (0.38 to 1.05 mm), with most occurring between 1.0 and 2.0 mm (0.38 and 0.63 mm). Since the mean is sensitive to that size class in which the majority of drops occur, it may be concluded that the single canopy regulates the drop sizes by reducing the size of the majority of the drops. Figure 7.2 shows that the majority of multiple canopy throughfall drops are between 0.5 and 3.0 mm (0.23 and 1.23 mm) for a similar rainfall range. It it is assumed that the single canopy layer is contained within the multiple canopy it is suggested that although the higher layers of the canopy may regulate the majority of drop sizes to within a narrow range, the range is increased by the lower canopy.

ii) Standard deviations of stain sizes in paired samples

It has been demonstrated in Chapter Six that the standard

Figure 7.1 Plot of mean stain diameter (mm) of single canopy throughfall samples against mean stain diameter (mm) of rainfall samples, for all paired samples

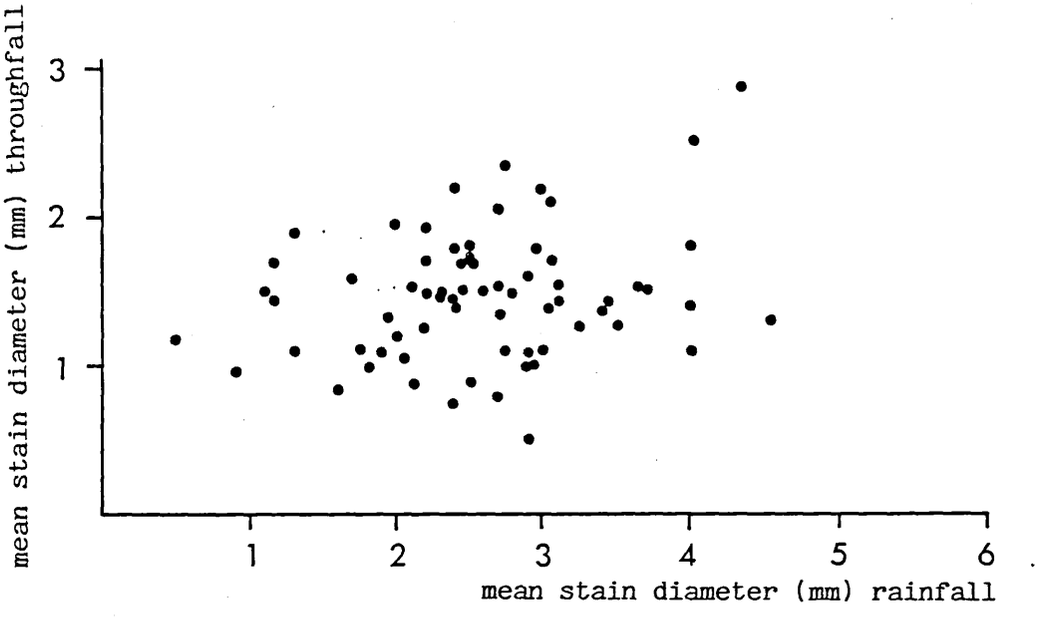

Figure 7.2 Plot of mean stain diameter (mm) of multiple canopy throughfall samples against mean stain diameter (mm) of rainfall samples, for all paired samples

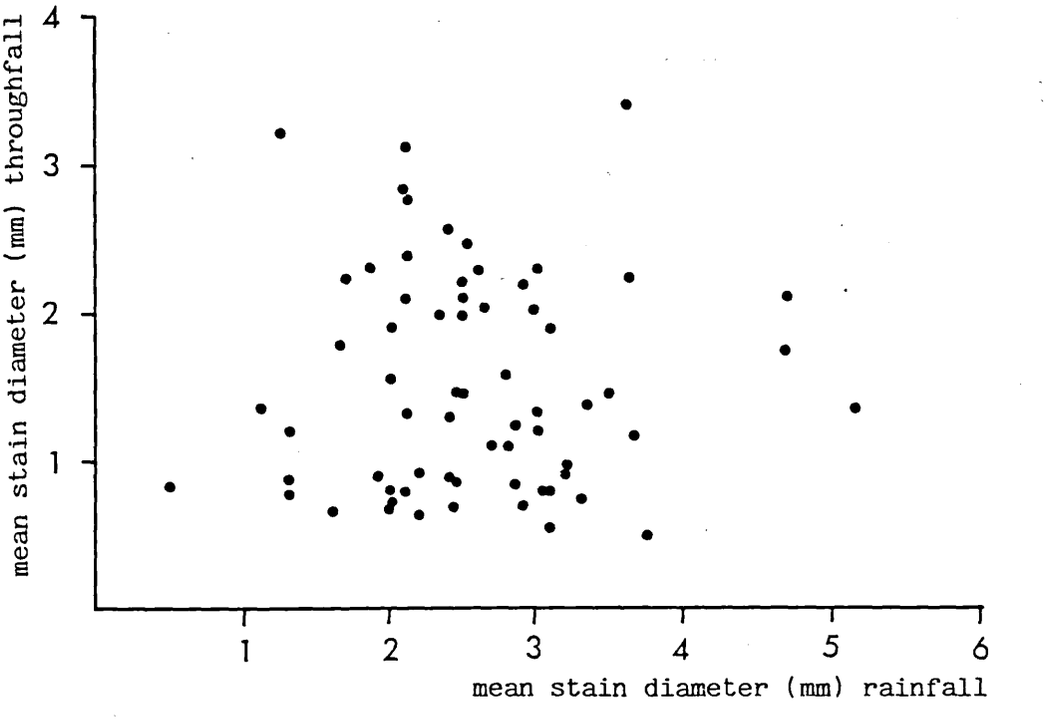

deviation of any sample is sensitive to the number of large drops included. The same series of comparisons was made between the standard deviations of all the paired samples (Table 7.3). For all rainfall samples the standard deviation varied between 0.31 mm (0.17 mm) and 7.15 mm (1.59 mm), with a mean of 2.35 mm (0.71 mm) for rainfall paired with the single canopy throughfall samples and a mean of 2.45 mm (0.73 mm) for samples paired with the multiple canopy throughfall samples. A two sample t-test showed that the means of the two distributions were not statistically distinct.

The standard deviation of throughfall samples from the single canopy ranged from 0.32 mm (0.17 mm) to 6.90 mm (1.55 mm) with a mean of 2.91 mm (0.84 mm). The standard deviation of multiple canopy throughfall samples ranged from 0.46 mm (0.22 mm) to 7.88 mm (1.70 mm) with a mean of 3.12 mm (0.87 mm).

Paired sample t-tests (Table 7.3) showed that the difference between the standard deviations in the paired samples of single canopy throughfall and rainfall, and multiple canopy throughfall and rainfall were both significant at the 99% level. A two sample t-test comparing the standard deviation of the two throughfall data sets (that is the single and multiple canopy throughfall) show that the means are statistically indistinct ($p = 0.52$). Therefore while it can be demonstrated that both canopies change the drop-size distribution of rain, increasing the number of large drops, the sizes of throughfall from both canopies are similar.

Figures 7.3 and 7.4 illustrate plots of the standard deviation of throughfall from both canopies against that of the paired rainfall samples. Figure 7.3 shows a wide scatter of points, with 26 samples showing a reduction in the standard deviation by the single canopy and the rest an increase. Figure 7.4 shows that in 30 of the multiple canopy samples the standard deviation was reduced. There is a clustering of the points below 1.0 mm (0.38 mm). There are more throughfall samples with a standard deviation of greater than 6.0 mm (1.41 mm) than in the single canopy. It was shown in Chapter Six that

Table 7.3 Analysis of means of standard deviations of stain diameters (mm) for each paired sample of rainfall and throughfall from single and multiple canopies

	n	mean	95% confidence intervals
rainfall	68	2.35	2.11, 2.59
single canopy throughfall	68	2.91	2.56, 3.27
rainfall	66	2.45	2.18, 2.72
multiple canopy throughfall	66	3.12	2.57, 3.68

t-test results	t	p
rainfall and single canopy throughfall	2.90	0.005
rainfall and multiple canopy throughfall	2.39	0.02
single canopy throughfall and multiple canopy throughfall	0.64	0.52

t-test tests the probability tant the mean standard deviations are the same

Figure 7.3 Plot of standard deviation of stain diameters (mm) of single canopy throughfall samples, against standard deviation (mm) of stain diameters of rainfall samples, for all paired samples

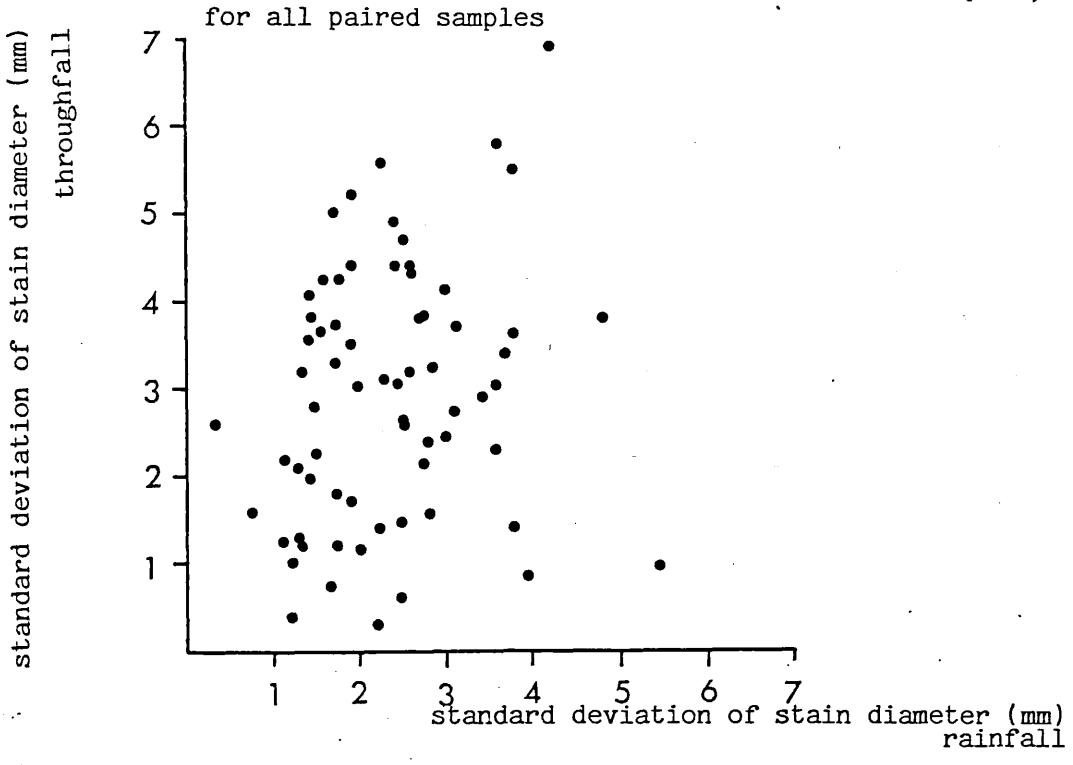

Figure 7.4 Plot of standard deviation of stain diameters (mm) of multiple canopy throughfall samples, against standard deviation (mm) of stain diameters of rainfall samples, for all paired samples

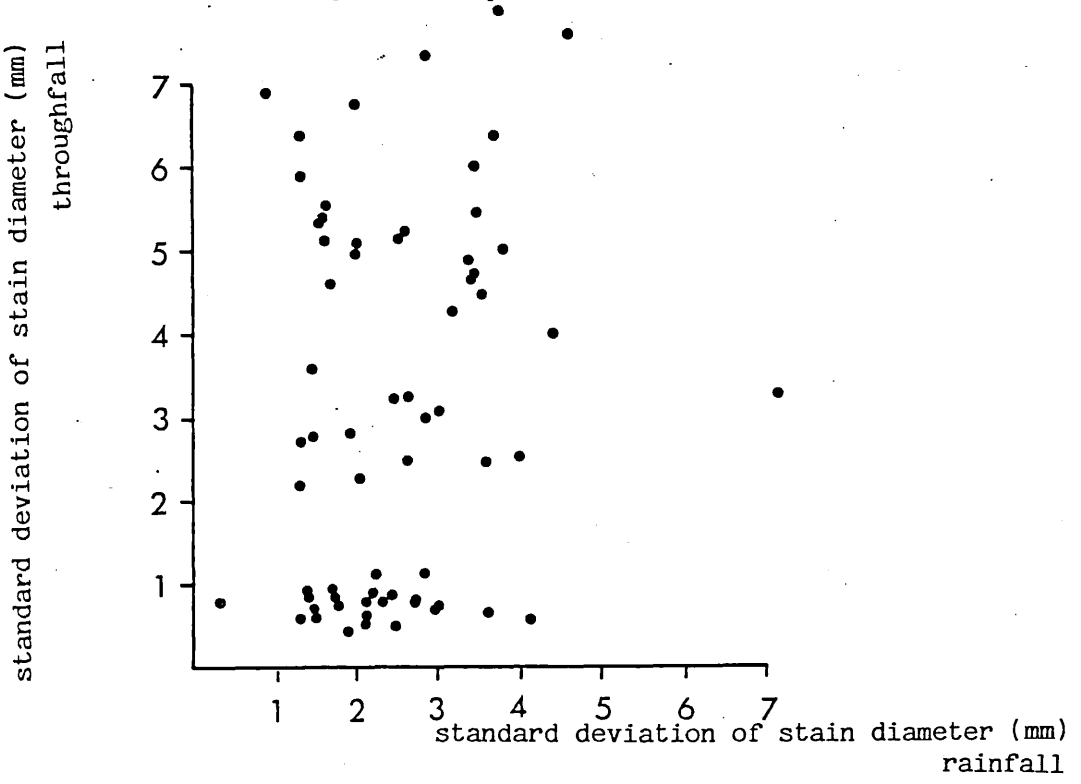

there was a positive correlation between the kinetic energy of a sample and the standard deviation of the stain sizes, and hence a positive correlation between the kinetic energy and the incidence of large drops.

iii) A summary of the effect of the canopies on the drop-size distribution

It is suggested that the single canopy acts as an effective regulator of the majority of drop sizes, concentrating the range of stain sizes to between 1.0 or 2.0 mm (0.38 or 0.63 mm). However the standard deviations show that while the majority of drop sizes may be decreased there is also an increase in the incidence of larger drops of a low frequency. The undergrowth layers of the multiple canopy tend to increase the range of mean drop sizes. For half the paired samples the standard deviation is lowered with the range of stain sizes restricted. The other half show a wide range of mean stain sizes with a higher incidence of large drops. As shown for the oak canopy, the tropical rain forest canopies change the drop-size distribution of the rainfall although the extent of the change by both canopies is different. It was demonstrated in Chapter Six that changes in the drop-size distribution could result in the changes in the kinetic energy/mm/m^2 of the rainfall by the canopy.

Section 2 An examination of the sequence of kinetic energy changes in rainfall and throughfall for all storms

The fifth statement derived from the qualitative model of drop-size distribution and canopy storage changes is that the sequence of changes in drop-size distribution (and hence in kinetic energy) is predictable, that there is a discernable pattern of increase or decrease in the kinetic energy/mm/m^2 of rainfall and throughfall which

holds for all storms and depends on rainfall intensity and canopy storage. The model suggests an initial phase where the effect of a canopy is to reduce the sizes of rain drops by splitting them when by inference, the kinetic energy/mm/m^2 is lowered. Later the dripping of large drops from the canopy increases the range of sizes and also the kinetic energy/mm/m^2. It is suggested that the relative proportions of each phase is related to the canopy storage. The model does not describe changes in the rainfall energy/mm/m^2, however field observations have suggested that the initial burst of high intensity described above has large drops followed by a period of less intense rain with smaller drops. This pattern would bring about a decrease in the kinetic energy/mm/m^2 through the storm.

The kinetic energy/mm/m^2 of each paired sample of rainfall and throughfall for all sites is listed in Table 7.4. For the multiple canopy throughfall samples the kinetic energy was calculated using both terminal velocities and velocity after a fall height of 3 m. The value for energy calculated using terminal velocity may be used for comparison with the single canopy data to assess differences in the drop-size distributions between sites.

1) Presentation of the data

Figure 7.5 illustrates the frequency of occurrence of values of kinetic energy/mm/m^2 for rainfall and throughfall samples from both canopies. The figure shows that while the kinetic energy of rainfall samples appear to be normally distributed, the distribution of values from the canopies are bimodal and this is more marked under the single than the multiple canopy.

For the multiple canopy, Figure 7.5 shows the concentration of the majority of samples, normally distributed, between the range of 16 and 26 J/mm/m^2 with a few outliers forming a lower group betwen 2 and 8 J/mm/m^2. Under the single canopy both groups appear normally distributed, the lower group including samples with an energy between

Table 7.4 The kinetic energy of all paired samples of rainfall (R) and throughfall (T) from the single and multiple canopies (assuming heights of fall of 3 m and 8 m), standardised to J/mm/m²

a) Single canopy site

Sample	R	T	Sample	R	T
j10b(1)	14.17	32.79	j15(4)	10.96	8.97
(2)	13.91	36.11	(5)	11.00	34.40
(3)	14.77	38.57	(6)	11.20	28.54
(4)	12.04	32.87	(7)	15.02	37.38
(5)	12.44	36.53	(8)	11.46	27.90
(6)	11.63	32.58	(9)	13.36	38.01
(7)	8.11	28.21	(10)	13.37	38.21
(8)	7.20	11.31	(11)	9.88	36.67
(9)	6.44	9.24	(12)	7.52	32.97
(10)	13.87	15.39	(13)	11.87	7.75
(11)	1.62	10.08	(14)	14.24	28.97
j11(1)	14.52	4.02	(15)	15.45	36.93
(2)	27.08	9.34	(16)	15.51	34.01
(3)	23.05	39.29	(17)	13.63	34.39
(4)	33.72	27.15	j16b(1)	17.23	32.81
(5)	33.17	36.87	(2)	20.00	37.24
(6)	26.66	35.44	(3)	16.64	12.83
(7)	25.83	38.66	(4)	11.47	35.07
(8)	16.64	29.99	(5)	8.75	35.03
(9)	12.35	14.31	(6)	8.50	22.09
j12(1)	34.40	8.60	(7)	8.09	18.56
(2)	31.72	33.38	(8)	6.96	30.85
(3)	19.48	25.55	j20(1)	25.54	9.89
(4)	13.80	18.38	(2)	18.01	25.58
(5)	7.34	33.16	(3)	20.17	30.23
(6)	15.78	34.95	(4)	22.44	32.25
(7)	18.50	32.52	(5)	19.12	32.58
(8)	10.37	25.46	(6)	14.86	25.67
j13(1)	6.60	6.63	(7)	12.55	38.53
(2)	13.58	2.98	(8)	9.20	35.25
(3)	12.15	10.12	(9)	9.43	35.92
j15(1)	19.96	33.94	(10)	7.81	36.27
(2)	15.63	37.56	(11)	9.85	30.23
(3)	1.09	30.24	(12)	10.72	3.82

Table 7.4 (cont'd) The kinetic energy of all paired samples of rainfall (R) and throughfall (T) from the single and multiple canopies (assuming heights of fall of 3 m and 8 m), standardised to J/mm/m²

b) Multiple canopy site

Sample	R	T (8 m)	T (3 m)	Sample	R	T (8 m)	T (3 m)
j10b(9)	14.59	39.92	25.04	j15(8)	25.62	37.06	20.34
(10)	13.08	38.45	22.16	(9)	14.47	38.31	21.33
(11)	12.44	32.59	19.01	(10)	13.50	34.13	19.13
(12)	8.13	27.64	16.60	(11)	12.07	39.68	21.76
(13)	6.98	39.86	23.56	(12)	7.50	36.16	20.10
(14)	11.40	37.26	22.36	(13)	7.49	39.93	22.61
(15)	10.44	32.57	18.80	(14)	9.74	37.97	20.75
j11(1)	20.76	10.12	8.79	(15)	11.01	39.02	21.23
(2)	23.66	36.55	21.37	(16)	12.02	37.36	20.36
(3)	25.08	42.06	26.52	(17)	13.67	37.99	21.11
(4)	25.62	36.68	20.52	(18)	15.76	37.49	20.77
(5)	33.31	32.58	18.43	(19)	15.26	39.13	21.79
(6)	26.38	42.04	25.36	(20)	12.23	36.04	20.13
(7)	26.25	40.01	23.45	(21)	12.29	32.54	18.71
(8)	21.93	40.59	24.08	j16b(1)	17.63	37.91	21.81
(9)	22.26	36.25	20.51	(2)	13.92	40.26	23.69
(10)	21.93	38.42	22.06	(3)	8.88	36.99	20.60
(11)	17.02	36.38	21.31	(4)	8.29	37.07	20.43
j12(1)	36.94	38.30	20.79	(5)	7.49	40.72	22.66
(2)	24.37	29.06	16.82	j20(1)	24.86	4.06	3.93
(3)	13.78	36.81	20.32	(2)	17.97	10.97	9.29
(4)	8.08	36.25	21.21	(3)	19.17	41.26	23.73
(5)	4.48	37.25	21.26	(4)	21.33	35.72	20.05
(6)	20.50	33.32	18.91	(5)	17.11	40.98	23.47
(7)	10.13	34.80	20.07	(6)	18.70	37.63	20.82
j13(1)	13.68	4.81	4.79	(7)	15.79	37.45	20.70
(2)	11.89	7.08	6.32	(8)	11.79	28.41	16.99
j15(2)	16.24	38.55	21.64	(9)	9.46	36.68	20.62
(3)	15.35	39.39	20.81	(10)	7.76	36.10	20.12
(4)	1.20	38.42	20.97	(11)	7.37	32.91	19.08
(5)	11.05	37.93	20.82	(12)	10.57	38.18	21.53
(6)	10.89	36.69	20.16	(13)	10.76	35.84	20.86
(7)	10.10	38.09	20.94	(14)	12.06	36.68	20.20

Figure 7.5 Frequency of occurrence of values of kinetic energy/mm/m² for all samples of rainfall and throughfall from the single and multiple canopies (fall height, 3m)

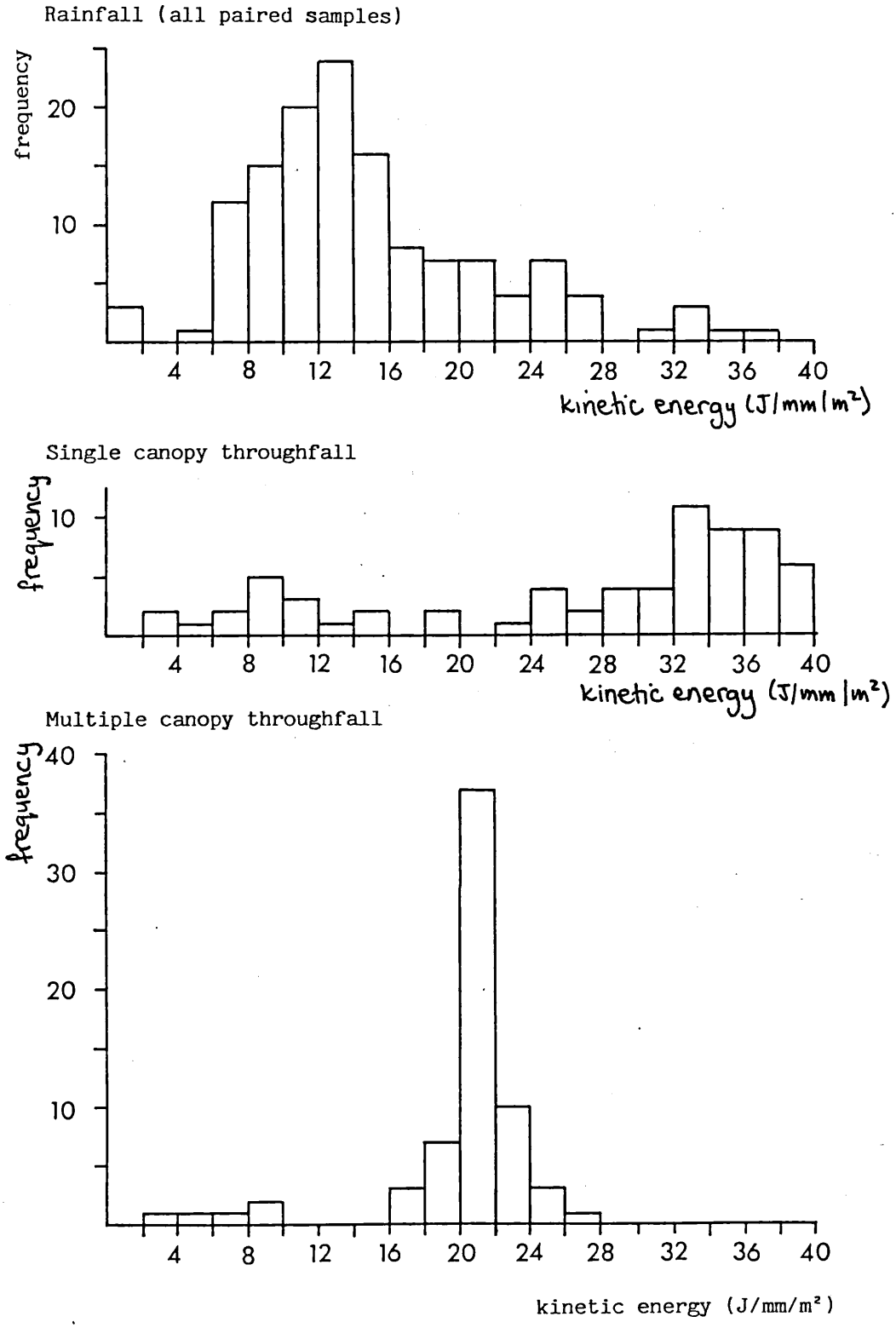

2 and 20 J/mm/m² and the upper group, including the maximum number of samples, between 22 and 40 J/mm/m². Table 7.5 shows the analysis of means of kinetic energy/mm/m² of all paired samples of rainfall and throughfall for all the samples taken together and the throughfall data divided into the upper and lower groups. For both canopies the two groups are statistically distinct.

All values of rainfall and throughfall kinetic energy/mm/m² have been considered together for each site to pick out some general trends in the changes by the canopy. Graphs plotting kinetic energy/mm/m² of throughfall against that of rainfall for all paired samples are given in Figures 7.6, 7.7 and 7.8 and the statistical analysis in Table 7.5.

The analysis shows an increase in mean kinetic energy/mm/m² for rainfall of from 14.75 J/mm/m² (s.d. = 7.15) to an average 27.02 J/mm/m² (s.d. = 11.04) by the single canopy and to 19.96 J/mm/m² (s.d. = 4.29) by the multiple canopy. The paired sample t-test shows that in both cases the difference between rainfall and throughfall samples was highly significant ($p < 0.0001$). Figure 7.6 shows that the majority of the rainfall samples had a kinetic energy/mm/m² between 6.5 and 19.5 J/mm/m², while that of the majority of the single canopy throughfall samples lies between 26.0 and 39.0 J/mm/m². Figure 7.7 illustrates that the throughfall energies from the multiple canopy samples are markedly more concentrated between 17.86 and 22.74 J/mm/m².

Figure 7.8 plots throughfall kinetic energy/mm/m² for the multiple canopy throughfall against rainfall assuming that all drops were at terminal velocity. When this is compared with Figure 7.6 it will be observed that the regulation of throughfall energy from the multiple canopy is more marked than from the single canopy. Table 7.5 shows the mean kinetic energy/mm/m² to be 34.75 J/mm/m² (s.d. = 8.44) which is highly significantly different from the mean energies of throughfall from the single canopy.

The concentration of the kinetic energy of the majority of

Table 7.5 Analysis of means of kinetic energy/mm/m² of all paired samples of rainfall, single canopy throughfall and multiple canopy throughfall (assuming heights of fall of 3 m and 8 m) and the throughfall samples divided into the two kinetic energy groups

	mean (J/mm/m²)	standard deviation	95% confidence intervals
rainfall	14.73	7.15	13.00, 16.45
single canopy throughfall (all)	27.02	11.04	24.40, 29.70
single canopy upper group	33.12	4.18	
single canopy lower group	10.12	4.50	
rainfall	15.06	7.15	13.37, 16.76
multiple canopy throughfall (3m)	19.96	4.30	18.90, 21.02
multiple canopy upper group (3m)	21.05	1.89	
multiple canopy lower group (3m)	6.62	2.37	
multiple canopy throughfall (8m)	34.78	8.44	32.70, 36.90

t-test results	t	p
rainfall and single canopy throughfall	8.09	<0.0001
rainfall and multiple canopy throughfall (3m)	4.80	<0.0001
single canopy throughfall and multiple canopy throughfall (8m)	4.90	<0.0001

Paired sample t-test testing the probability that the mean of the two samples is the same.

Figure 7.6 Kinetic energy (J/mm/m²) of single canopy throughfall samples plotted against the kinetic energy (J/mm/m²) of rainfall, for all paired samples

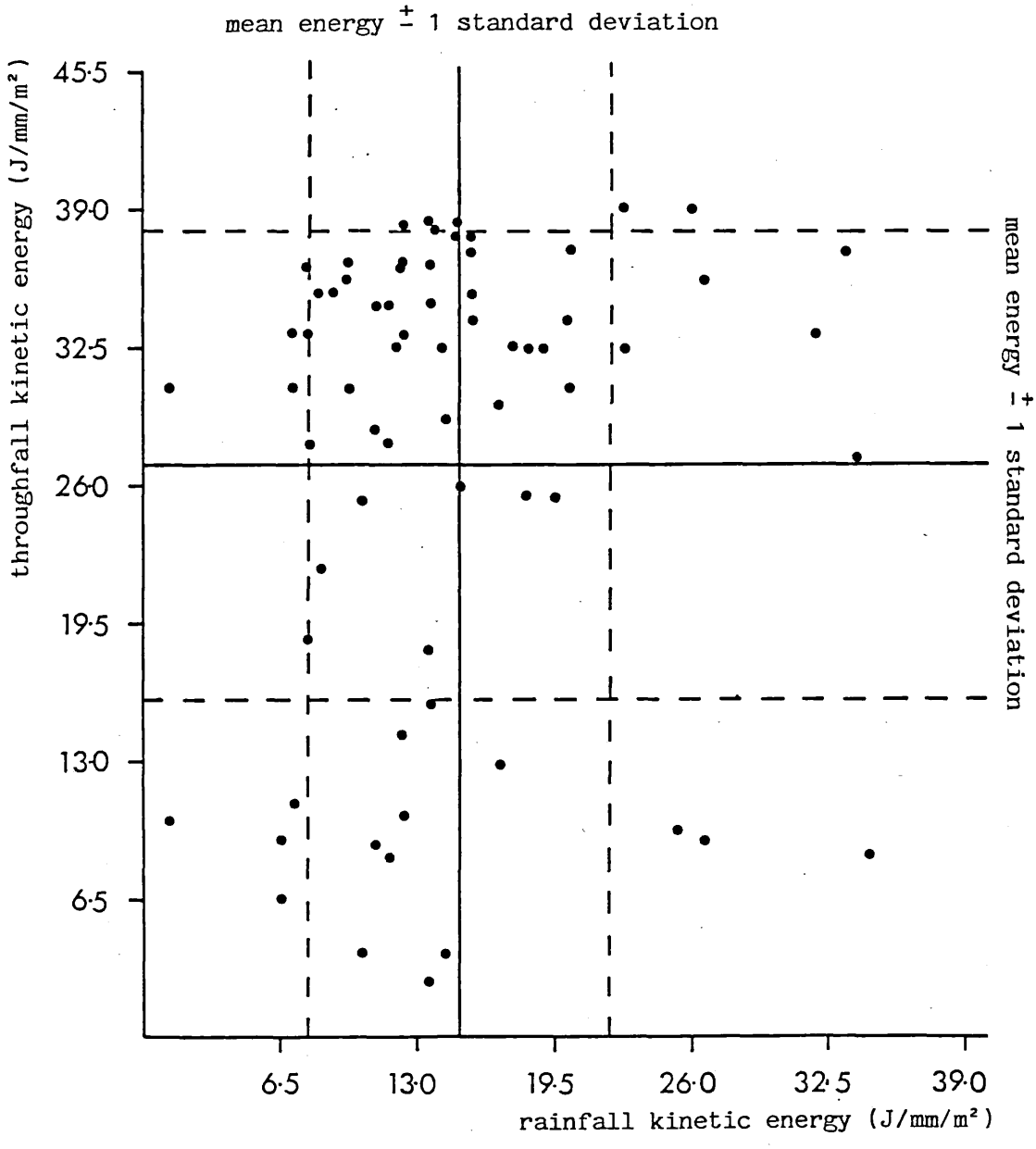

Figure 7.7 Kinetic energy (J/mm/m²) of throughfall samples from the multiple canopy (calculated using a fall height of 3 m) plotted against the kinetic energy (J/mm/m²) of rainfall, for all paired samples

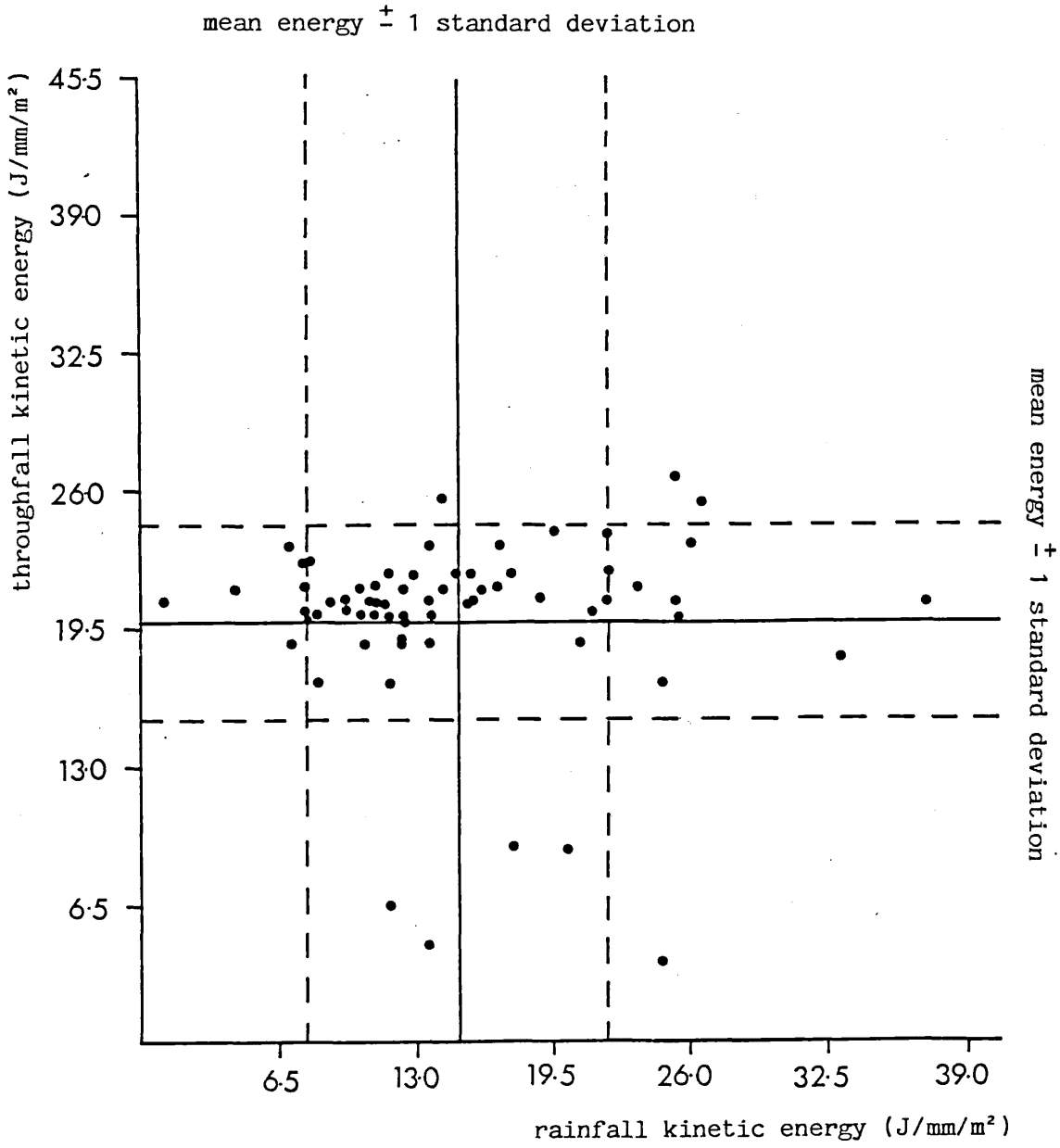

Figure 7.8 Kinetic energy (J/mm/m²) of throughfall samples from the multiple canopy (calculated using a fall height of 8 m) plotted against the kinetic energy (J/mm/m²) of rainfall, for all paired samples

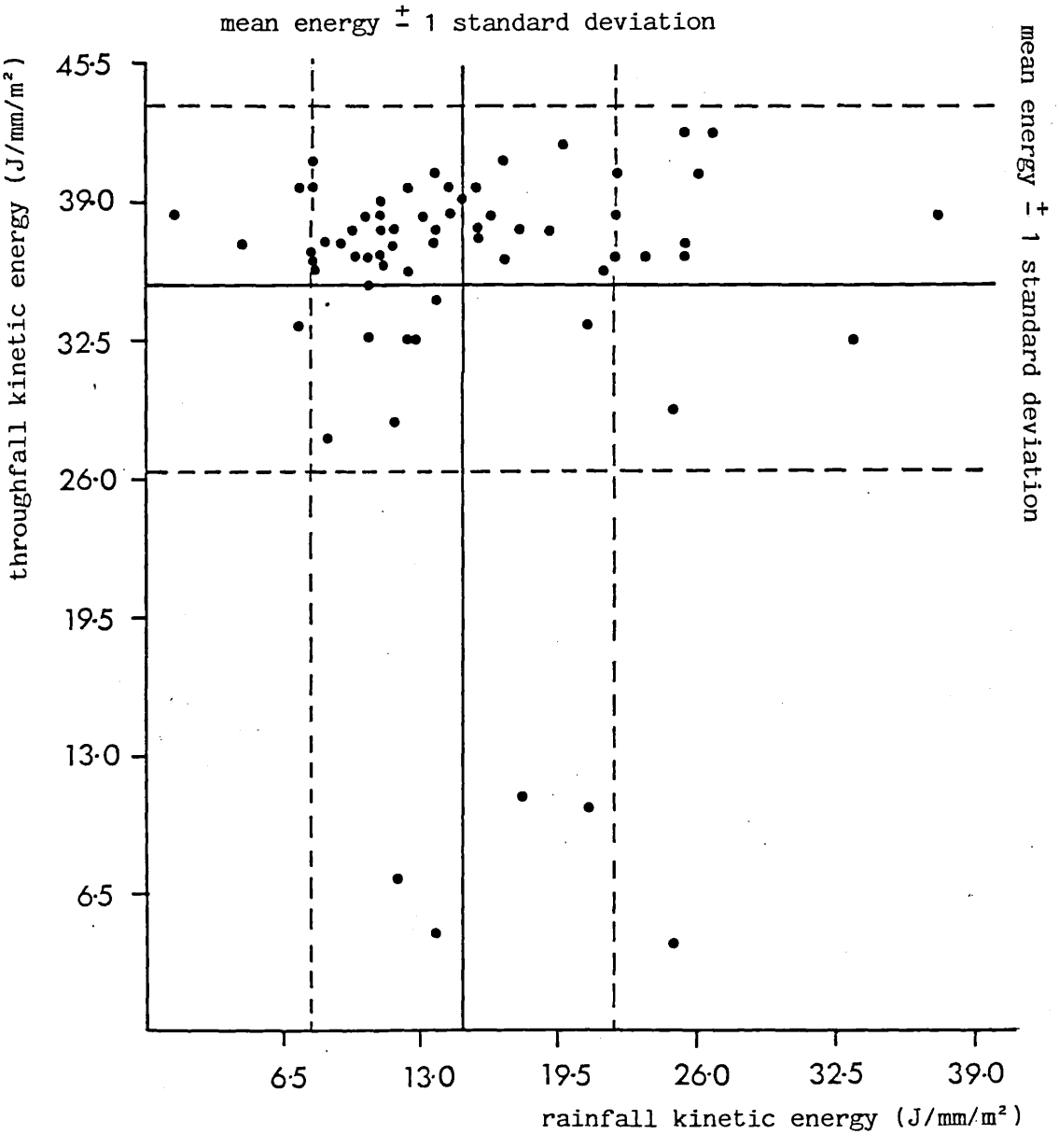

throughfall samples into a more limited range of values than the rainfall, together with the statistical independence of the data sets, are important observations. They suggest that both canopies regulate the kinetic energy of rainfall, producing throughfall of constant energy per unit volume from a variable rainfall energy. The regulation is more marked under the multiple than single canopy. However under both canopies there are samples where the kinetic energy/mm/m^2 of rainfall was reduced and not increased to the upper energy group. These are identified in Figures 7.6, 7.7 and 7.8 as lying below the line $y = x$. From the qualitative model of kinetic energy change it is expected that these low energy samples occur at the start of the storms. This will be discussed in greater detail later.

2) Changes in the kinetic energy of rainfall and througfall during all storms

To look for systematic changes in the kinetic energy/mm/m^2 of both rainfall and throughfall from both canopies with rainfall intensity, the kinetic energy has been plotted against the rainfall intensity for each sample (Figures 7.9, 7.10 and 7.11). Among others Kinnel et al. (1971) reported a logarithmic increase in kinetic energy with an increase in rainfall intensity. Figure 5.5 illustrates graphically the change in intensity of rain and throughfall through each storm and an inspection of these graphs reveals, generally, an initial intense burst of rain followed by a decrease. However changes in intensity for all storms and sites will be examined in more detail later.

Figure 7.9 illustrates the relationship between the kinetic energy and intensity of rainfall for the rainfall samples derived to be simultaneous with both single canopy and multiple canopy throughfall samples. The analysis of the regression line is given in Table 7.6 and shows that although the r value is 0.76, the slope of the regression is significantly different from 0 at the 99.9% level. Hence the kinetic energy/mm/m^2 of rainfall increases with an increase

Figure 7.9 Kinetic energy (J/mm/m²) of all rainfall samples plotted against rainfall intensity (mm/hour)

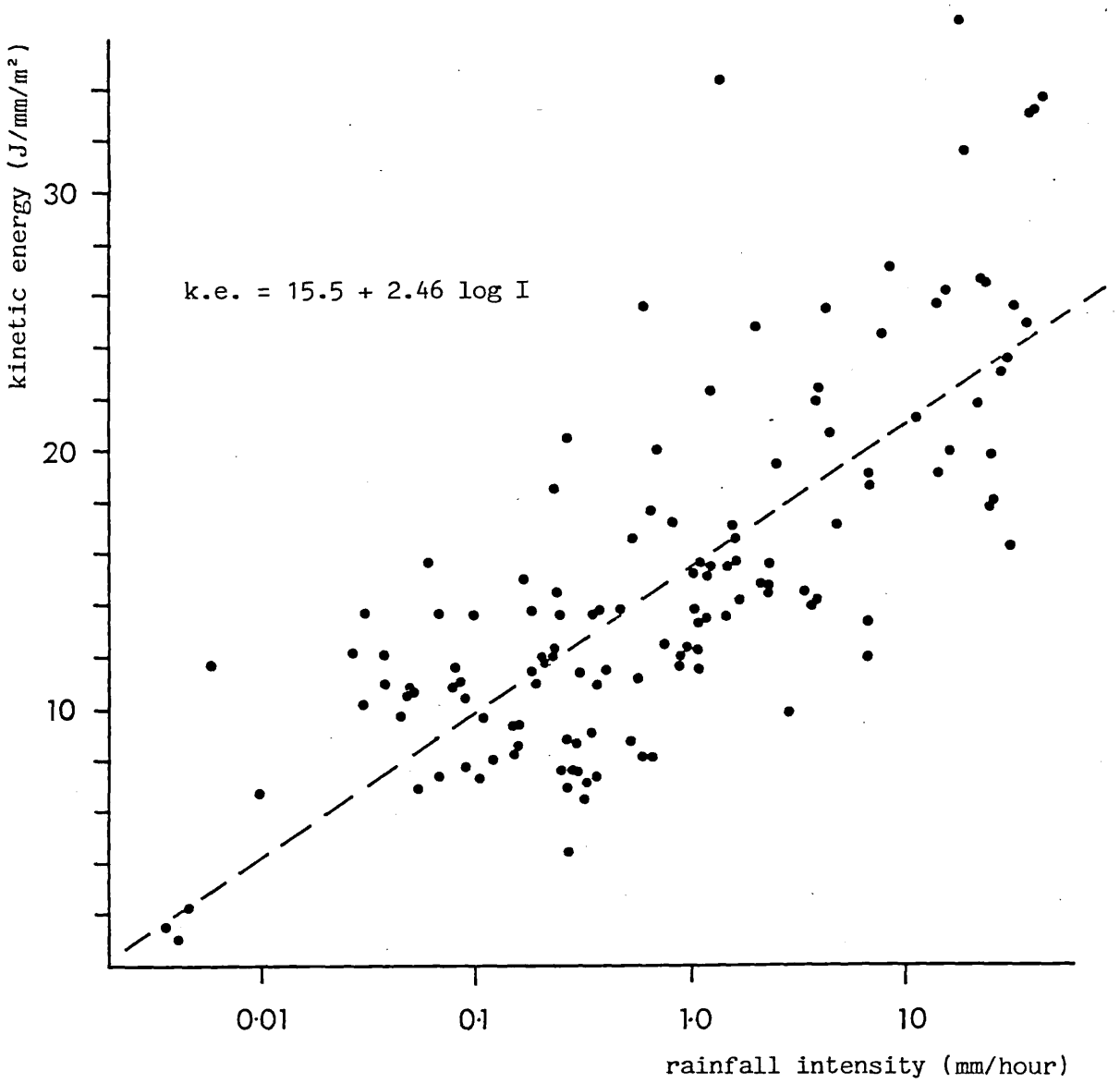

Figure 7.10 Kinetic energy (J/mm/m²) of multiple canopy throughfall samples plotted against simultaneous rainfall intensity (mm/hour)

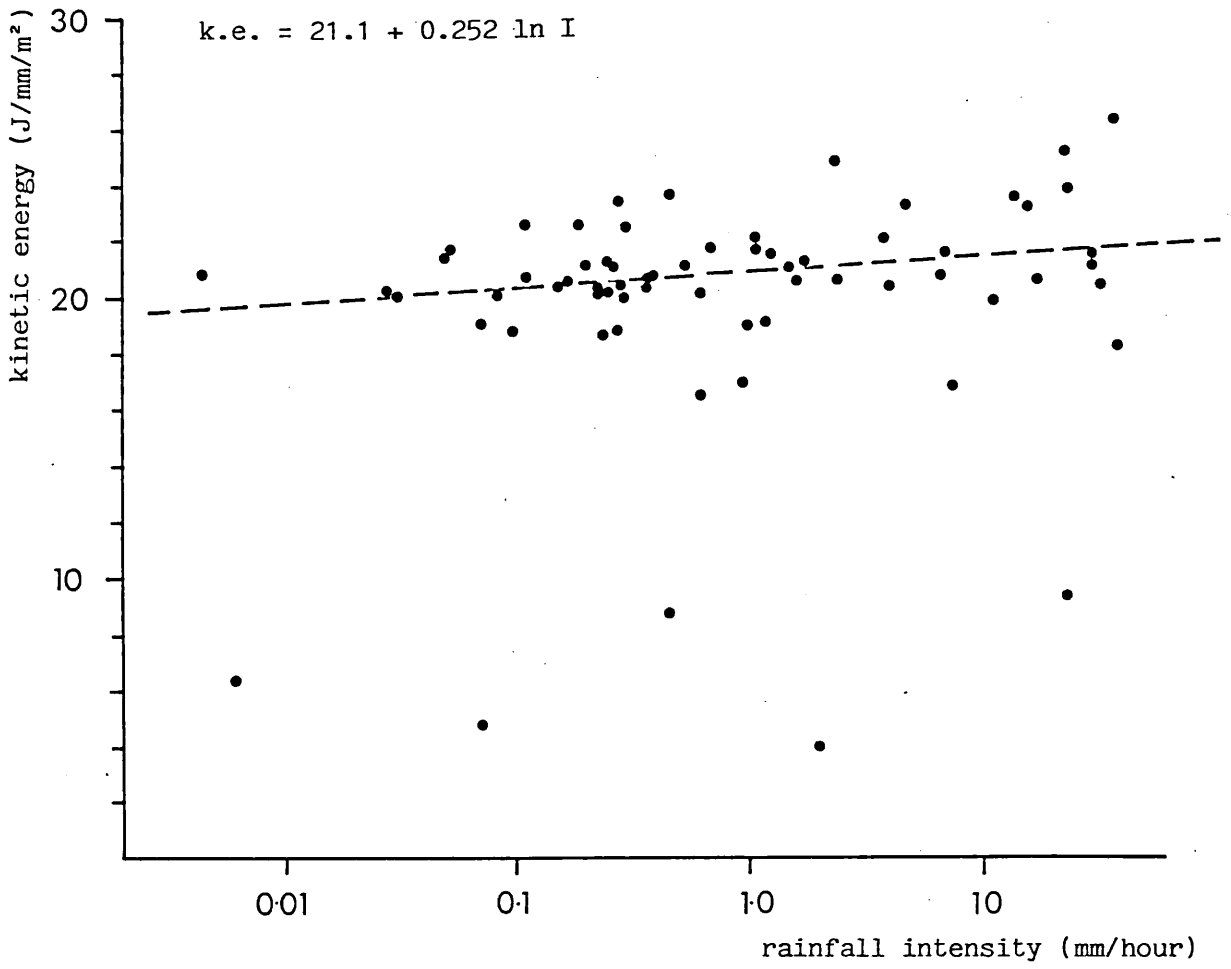

Figure 7.11 Kinetic energy (J/mm/m²) of single canopy throughfall samples plotted against simultaneous rainfall intensity (mm/hour)

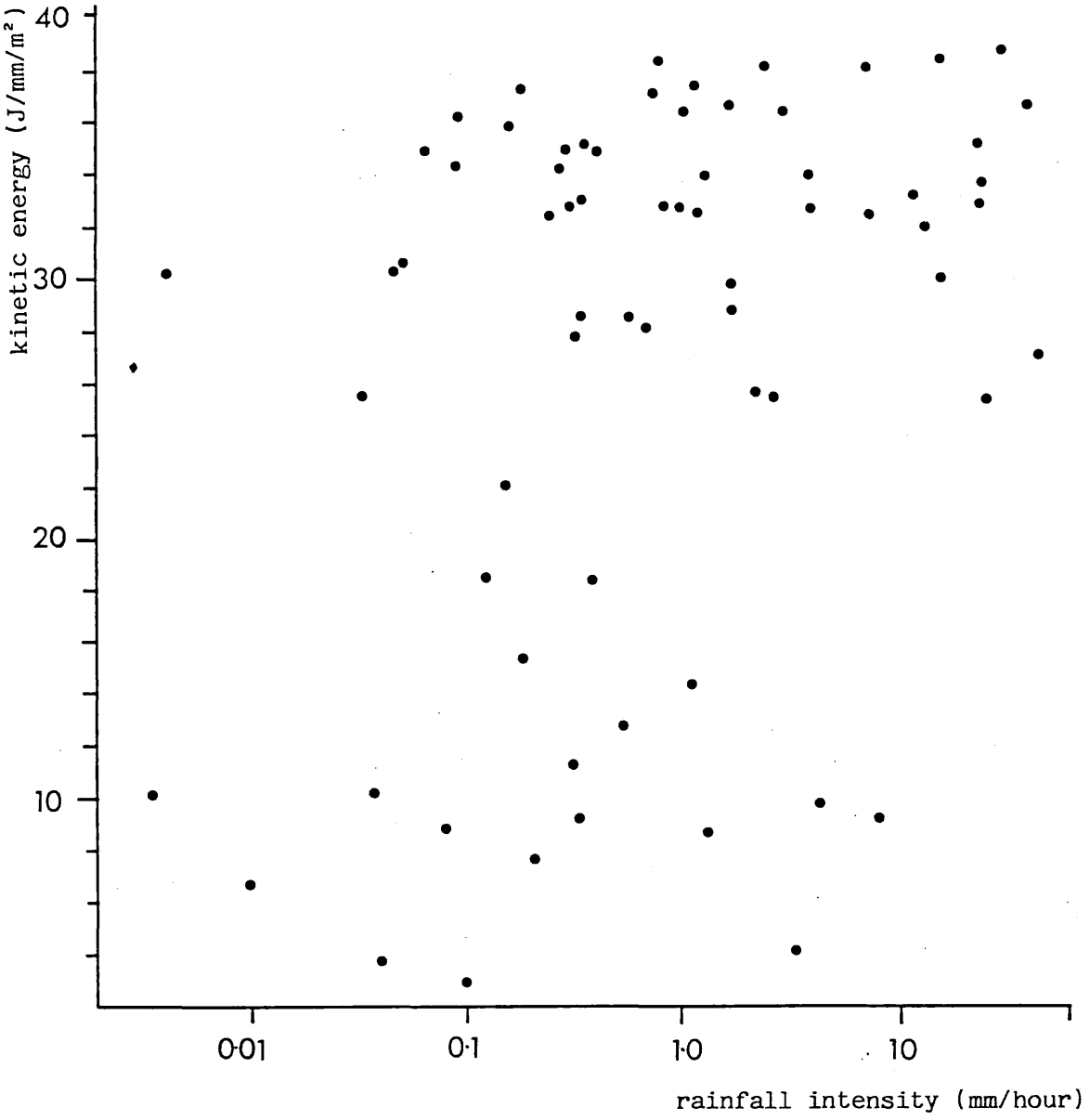

Table 7.6 Regression equations of kinetic energy/mm/m² (k.e.) against rainfall intensity (I) for paired samples of rainfall and multiple canopy throughfall (assuming a fall height of 3 m) for all storms

	regression equation	r	t value	p
rainfall	k.e. = 15.5 + 2.46 ln I	0.76	13.45	<0.001
multiple canopy upper group (>10.0 J/mm/m²)	k.e. = 21.1 + 0.252 ln I	0.25	2.24	0.05
single canopy upper group (>20.0 J/mm/m²)	k.e. = 33.1 + 0.287 ln I	0.00	1.0	
single canopy lower group (<20.0 J/mm/m²)	k.e. = 10.4 + 0.165 log I	0.00	0.30	

t-test tests the probability that the slope coefficient = 0

in rainfall intensity. Based on the work of Laws and Parsons (1943) Wischmeier and Smith (1958) obtained a similar equation, KE = 13.32 + 5.66 ln I.

Figure 7.10 shows a similar plot of kinetic energy (calculated for a fall height of 3 m) against the intensity of the simultaneously paired rainfall sample and the results are strikingly different from those for rainfall. Discounting the low energy outliers, the kinetic energy/mm/m^2 of throughfall appears to be almost independent of the rainfall intensity. Table 7.6 shows a gradual increase in kinetic energy with intensity and the slope coefficient is significantly different from 0 at the 95% level. Thus it appears that like the rainfall, the kinetic energy of the throughfall does vary with rainfall intensity. However the rate of increase is much lower, an increase in rainfall energy of 1000 times increases the throughfall kinetic energy only by 1.1 times and it is suggested that the increase may be ignored.

In contrast to the two other sites, Figure 7.11 illustrates for the single canopy site neither a clear increase in kinetic energy with rainfall intensity nor a clear constant value for all the samples. However, if the kinetic energy values are divided into the two distinct energy groups with a break point at 20 J/mm/m^2, as suggested by Figure 7.5, each group may be separately regressed against rainfall intensity (Table 7.6). Both regressions show that the kinetic energy of throughfall in each group is independent of rainfall, with a correlation of 0 and slope coefficients not significantly different from 0. The relationships between rainfall and throughfall kinetic energy/mm/m^2 and rainfall intensity are summarised in Figure 7.12.

Hence for the throughfall samples from both the single and multiple canopies, the kinetic energy falls into one of two groups with either a relatively high or a low energy value. For all groups the kinetic energy of the throughfall samples appear to be independent of the intensity of the rainfall at that time. In Section 4 the groups will be examined to establish any links between the high or low

Figure 7.12 A summary of the relationships between rainfall, single and multiple canopy throughfall kinetic energy and rainfall intensity

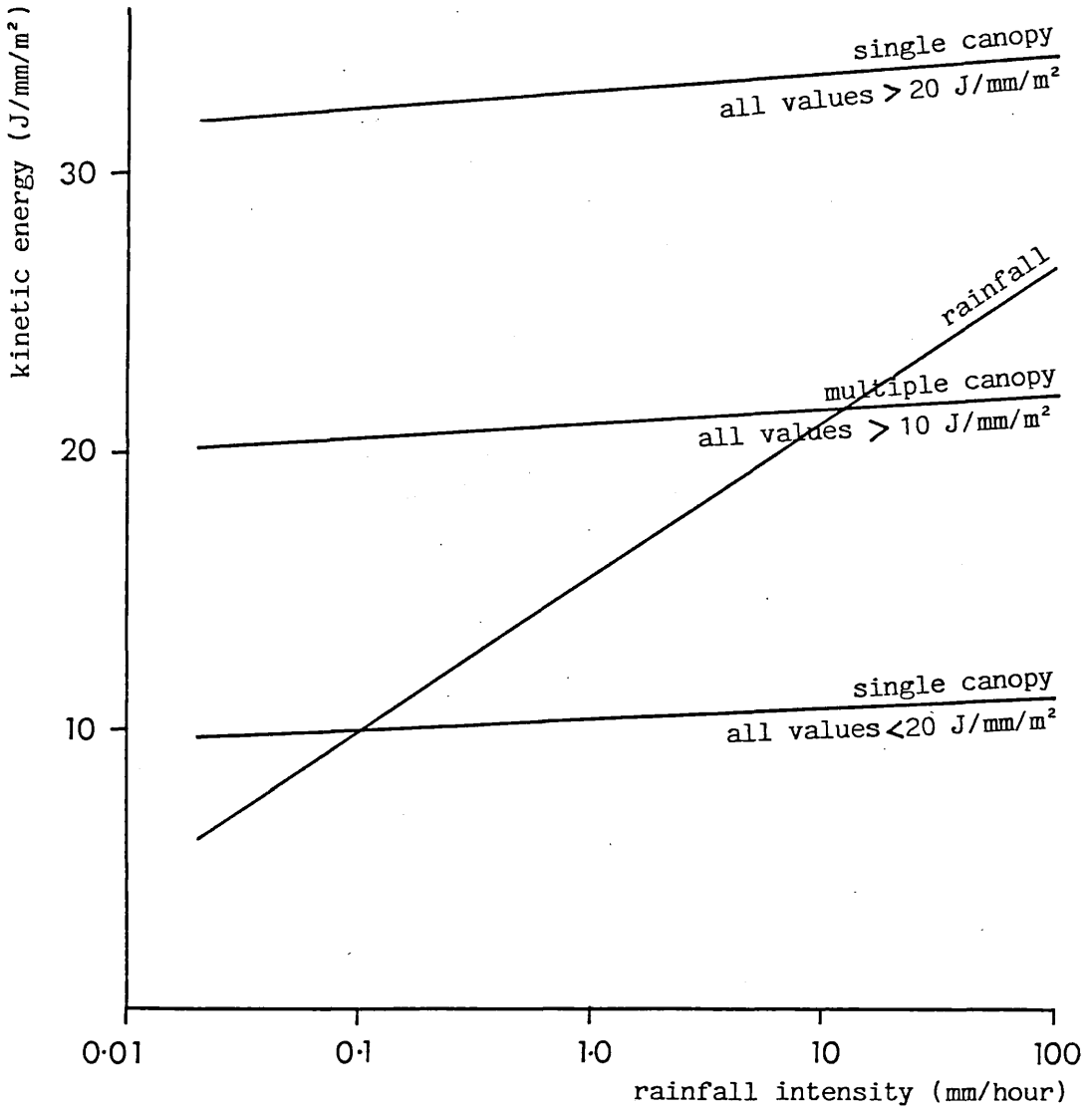

energy value, the time at which the sample was taken and the amount of water held in the canopy storage at that time.

Section Three Descriptions of changes in the canopy storage during the storms and comparisons with kinetic energy changes

The sixth statement derived from the model is that the predictable sequence of changes in the drop-size distributions can be related to constants in a) rainfall depth and b) the depth of canopy storage. In Chapter Six it was demonstrated that by placing the paired samples in an order of drop-size distribution change suggested by the model, an interception curve could be simulated which showed two phases of increasing interception and a period of drainage. This Chapter will look for this sequence of changes in actual storms. Changes in the canopy storage for each canopy and storm will be described in this section and compared with the kinetic energy changes.

1) Presentation of the cumulative rainfall and throughfall data

i) Summary of rainfall and throughfall depths

Details of rainfall depths measured by the funnel and continuously recording gauges and the derivation of the mean throughfall depth have been given in Chapter Five. A summary of these measured depths (Dm), the times of the start and end of sampling for each storm and the capacities estimated for the canopy above each site are given in Table 7.7.

ii) Presentation of cumulated interception curves

Details of the interpolation procedure to determine cumulative

Table 7.7 A summary of measured depths (mm) of rainfall and throughfall for all storms, the times of the start and end of drop size sampling, sampling duration (hours) and the estimated canopy capacities (mm)

storm	site	sampling times			measured depth
		start	end	duration	
j10b	open	12-10-46	13-24-00	1-13-14	3.7
	single canopy	12-30-30	13-34-30	1-04-00	3.11
	multiple canopy	12-35-30	14-06-20	1-30-50	1.67
j11	open	10-26-00	11-30-39	1-04-39	12.7
	single canopy	10-28-09	12-25-00	1-56-51	11.53
	multiple canopy	10-25-30	12-34-45	2-09-15	4.63
j12	open	15-45-45	16-20-56	0-35-11	1.41
	single canopy	15-45-45	16-25-00	0-39-15	0.97
	multiple canopy	15-49-15	16-45-46	0-56-31	0.17
j13	open	13-20-50	13-37-24	0-16-34	0.11
	single canopy	13-20-50	15-36-00	2-15-00	0.01
	multiple canopy	13-23-35	15-59-00	2-35-25	trace
j15	open	12-15-10	14-28-00	2-12-50	2.83
	single canopy	12-15-42	14-51-18	2-35-36	2.22
	multiple canopy	12-14-42	15-17-00	3-02-18	0.99
j16b	open	12-54-16	13-49-49	0-55-33	0.36
	single canopy	12-56-27	14-05-29	1-09-02	0.12
	multiple canopy	12-52-10	14-19-00	1-26-50	0.03
j20	open	14-56-25	16-35-30	1-39-05	2.93
	single canopy	14-58-33	16-26-00	1-27-27	2.39
	multiple canopy	14-56-15	16-43-20	1-47-50	0.84
Estimates of canopy capacity from Table 5.2					
	single canopy				0.13
	multiple canopy				0.21

depth of rainfall and throughfall from the samples of drop sizes have already been given in Chapter Five. For any given time the difference between the cumulated depth of rainfall and the cumulated depth of throughfall may be considered to be the depth of water held in storage on the canopy, the amount lost to evaporation during the storm plus the amount diverted to stemflow. Evaporation of intercepted water during the storm has been considered in Chapter Five and is estimated to be 0.25 mm/hr. Stemflow has not been quantified but it is suspected that it could be important in the multiple canopy site where it might account for the very high interception losses.

Curves of the difference between cumulated rainfall and throughfall for both canopy sites have been drawn (Figures 7.13 and 7.14). Several points arising from an initial inspection of Table 7.7 and the interception curves will be discussed before the description of the curves is given. The process of the derivation of the cumulated depth curves is complex and the effect of the interpolations and other data manipulation procedures on the resultant curves will be discussed in detail where the results were different from those expected.

2) Discussion of the derivation of cumulated rainfall and throughfall curves

i) Summary of interpolation methods

Although the interpolation methods have already been described in detail they will be summarised here to aid the discussion. The drop-size distribution, and hence the depth of rainfall and throughfall was recorded in discrete samples through each storm. To calculate the depth of water unsampled in the gaps between samples (dg), intermediate values were interpolated according to the depth (d) of rain in succeeding samples. Different interpolations were used according to the approximation of the pattern of sampled intensity

Figure 7.13 Cumulated interception (mm) curves for the tropical rain forest single canopy during all storms

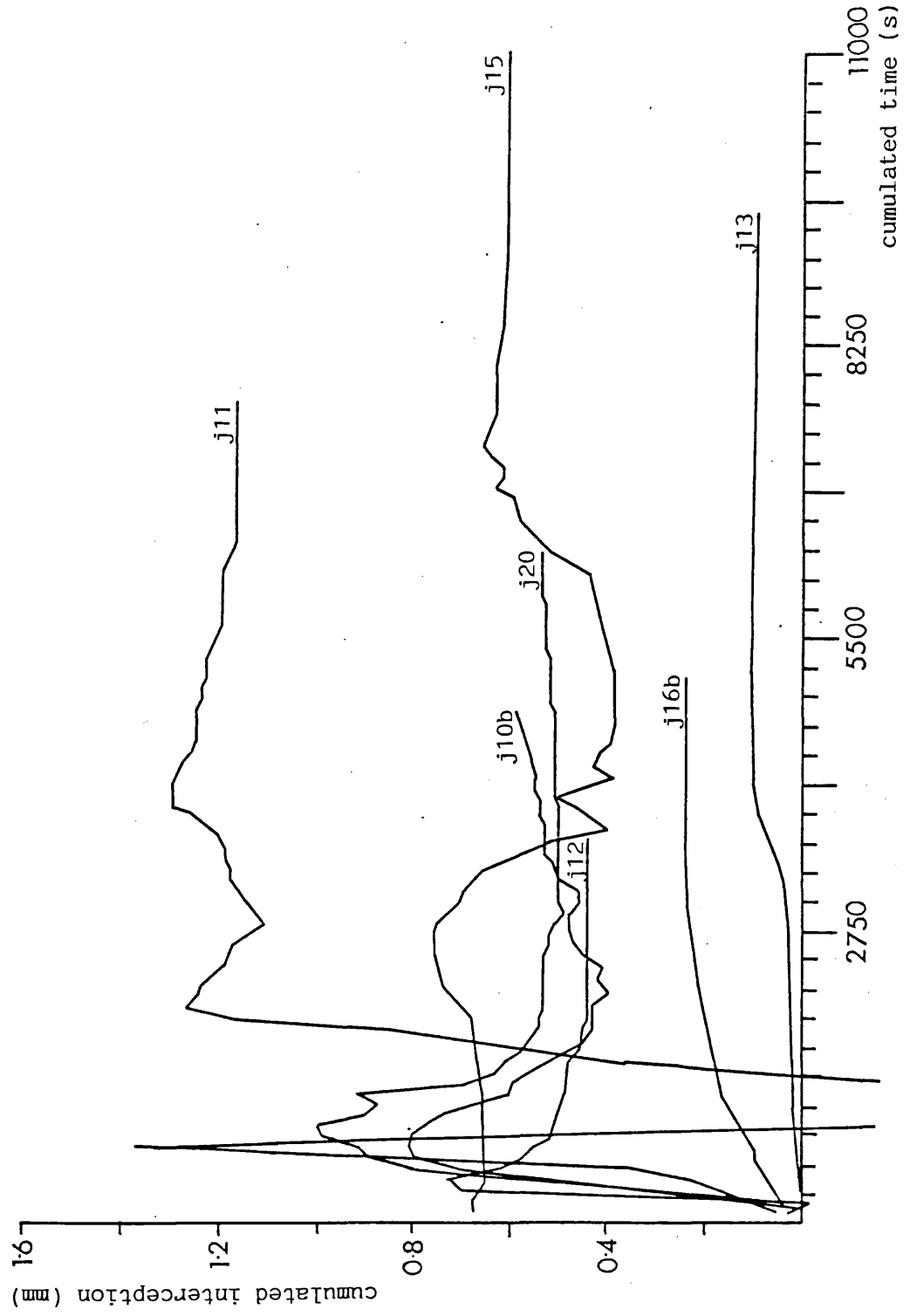

Figure 7.14 Cumulated interception curves for the tropical rain forest multiple canopy, during all storms

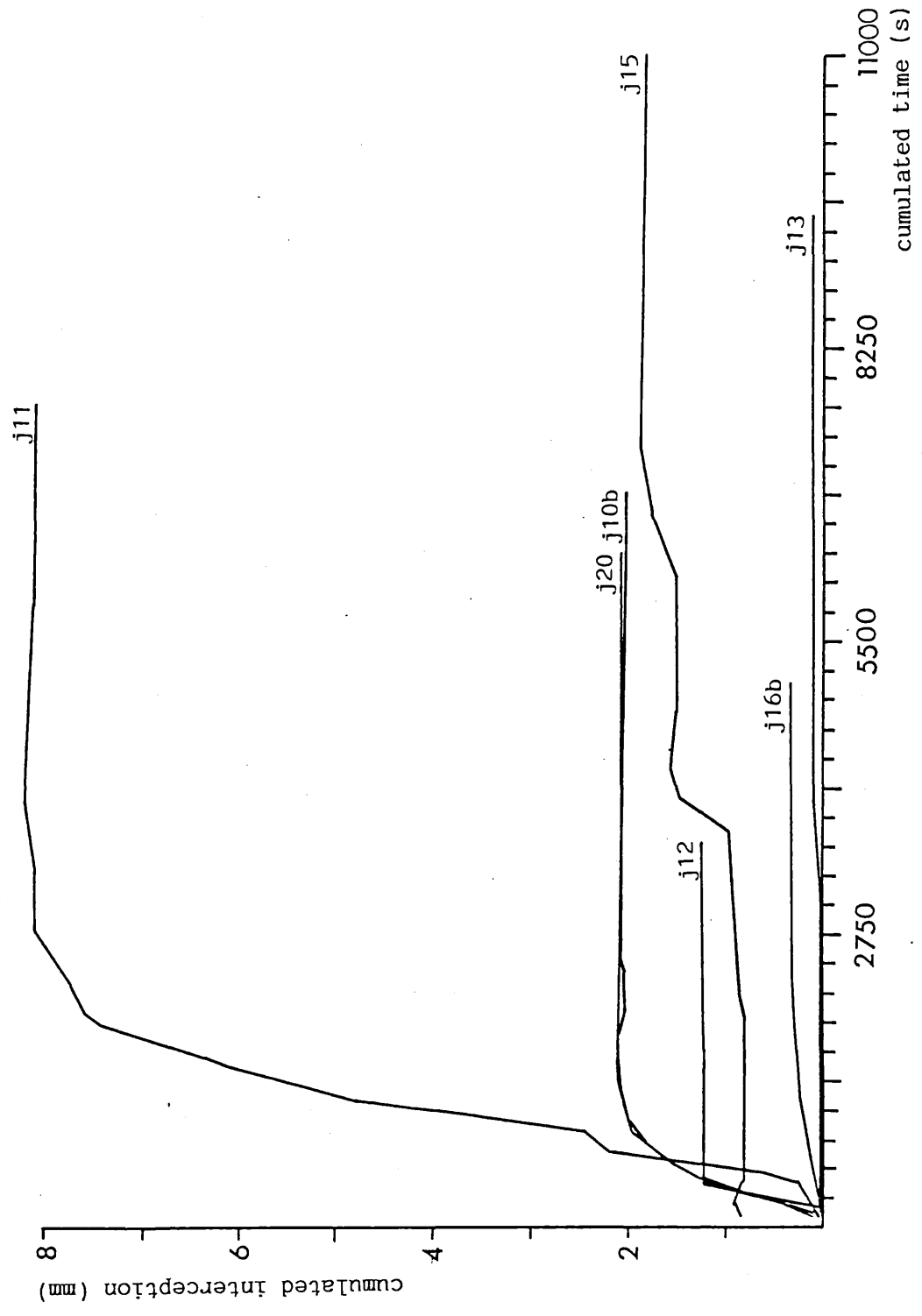

change to an initial single high intensity peak with a logarithmically decaying tail. The sampled and interpolated depths were totalled (Dc) and the total compared with the mean depth of water collected in a grid of raingauges on each site (Dm). Each sample depth and interoplated gap depth was altered in proportion to its size so that Dc equalled Dm. It was assumed that the raindrop sampling started when the storm started and finished as the last raindrop fell and consequently the drop samples and raingauges recorded rain over the same period. The same assumption was made for the throughfall samples and raingauges.

ii) Analytical procedure when the start of rainfall and throughfall sampling were not coincident

In very few of the storms did drop sampling under the canopies start at the precise instant that it did in the open, there was usually a delay of up to two minutes (Table 7.7). However in one storm under both canopies the delay was very much longer. For storm j10bsc there was a delay of 19.67 minutes and for j10bmc the delay was 24.67 minutes in a storm lasting 81.23 minutes. To compensate for these delays the following methods were adopted.

In storm j10bsc the total rainfall measured was 3.7 mm, total throughfall 3.11 mm and hence the loss to storage and evaporation was 0.59 mm. Loss to stemflow was not considered in the single canopy site. It was assumed that the canopy capacity was filled during the first 20 unsampled minutes of the storm and that all losses to interception occurred during this time, as did all evaporation losses. From the interpolated samples and gaps, cumulated rainfall after 19.67 minutes was calculated to be 2.92 mm. Therefore, if throughfall is rainfall less interception loss, cumulated throughfall was 2.33 mm. Hence a sample of 2.33 mm was assumed to have fallen during the unsampled period and all depths were corrected so that Dc equalled Dm.

For storm j10bmc the same rainfall depth, 3.7 mm, applied but the

total throughfall measured 1.67 mm leaving a net loss to evaporation, canopy storage and stemflow of 2.03 mm. After 24.67 minutes the cumulated rainfall was 3.19 mm. If it is assumed again that all interception loss was in the unsampled period, the depth of throughfall was 1.16 mm, 69% of the total throughfall. However, points raised in Chapter Five suggest that loss to evaporation and especially stemflow play a greater role in the multiple than the single canopy. Thus it was decided that the assumption that all the interception loss occurred in the initial unsampled period may not be valid and an alternative method was used which did not make this assumption.

The changes in intensity of throughfall were examined and compared with other multiple canopy throughfall profiles. It was decided that the first recorded sample should be repeated at the beginning of the unsampled period and the gap depth interpolated in the usual way. The depth of throughfall calculated to have fallen in the unsampled period was 1.08 mm, 65% of the total value. The similarity of the two estimates lessened the importance of the choice of method. Under the impression that water loss to stemflow continued throughout the storm and not only at the beginning, the second method yielding a lower interception loss during the unsampled start of the throughfall was used.

The interpolation procedure to cumulate rain fallen during the storm may be adapted to cover large gaps in the sampling as in storms j10bsc and j10bmc by estimating the depth of water fallen during the gap. However results drawn from the interpolated period should be treated with caution.

iii) Analytical procedure when cumulative throughfall exceeded rainfall

Unlike all the other storms the cumulative rainfall and single canopy throughfall curves intersect in storm j11 to produce a negative

cumulated interception (Figure 7.13) implying that more rain was falling through the canopy than was falling onto it. It is possible that the canopy above the sample point could be acting as a funnel, collecting water from a larger sampling area. This is not observed on any of the other storms except for brief instances at the beginning of some storms and there are a number of possible causes arising from the analytical methodology which should also be examined.

The interpolation used for j11 calculated the depth of throughfall in the gaps from the four succeeding samples. In some of the other storms only two samples were used. The different interpolations produce a different Dc to be corrected to Dm. When the interpolation using two succeeding samples was used in this data set, Dc changed from 5.8 mm to 14.2 mm, to be compared with a Dm of 11.5 mm. However despite the difference in interpolation and amount of correction needed to obtain the total depth the two curves still intersected.

The intersection of the depth curves coincides with an intense burst of rainfall of an intensity of 252 mm/hr in the canopy sample (3), recorded between 739 and 741 s from the start of the storm. At this time there was a gap in the open site samples from 666 to 843 s. It is possible that there was a similarly intense burst of rain in the open but it went unrecorded.

The mean depth of rain recorded in the open is 12.7 mm and the mean depth of throughfall was 11.5 mm, leaving a loss to interception of 1.2 mm. This is higher than other storms which have shown interception losses ranging from 0.5 to 0.6 mm (Table 7.7). Within the throughfall gauge readings there was an abnormally low value of 3.2 mm which when removed from the data set changed the throughfall depth to 11.9 mm and the interception loss to 0.9 mm. However even when this higher throughfall value is introduced the cumulated depth curves still intersect.

There was a period of some 18 minutes, 28 minutes after the start of the storm in which drops were not sampled under the canopy,

representing a loss of some three or four samples. During interpolation the depth of each sample (d) is corrected in proportion to its relative size to (d') [5.18]. It is possible that the absence of several samples of similar depth meant that the adjustment was incorrect and d' was too high. During the time when there was no sampling an estimated 1.85 mm fell in the open. Since the canopy capacity is assumed to have been filled by this time, and excluding evaporation, the depth of throughfall was expected to have been of a similar order. In fact the interpolation calculates a depth of 1.32 mm under the canopy. Even the alteration of this unsampled depth does not affect the intersection of the two cumulated depth curves.

After examining different possible causes of the intersection of the rainfall and throughfall curves for storm j11sc two explanations are feasible. Firstly the canopy could indeed be funneling water from a large catchment area onto the sampling sheet. However it is most probable that the burst of rain recorded under the canopy was matched by a similar, but unrecorded burst above it.

The shape of the interpolated curves determined from the mean depth of rain measured over a wide area is sensitive to freak values in the depths recorded. Because the rain was not monitored constantly, missing recordings of high intensity bursts of rain may also alter the shape of the curve.

iv) Draining of stored water from the multiple canopy

Although the actual shapes of the cumulative depth for rainfall and throughfall curves and the resultant interception curves have yet to be discussed the implications of the analytical procedure on the curves will be discussed here.

On inspection the curves showing water loss to canopy storage and evaporation in both rain forest sites (Figures 7.13 and 7.14) differ in one main respect. The multiple canopy shows no evidence of

draining on the scale seen under the single canopy. The differences between measured rainfall and throughfall depths are several times far above the interception capacity suggested by Franken et al. (1982) of 0.8 mm.

It will be noted that in many instances throughfall was still being measured under the canopy long after it has ceased in the open. However the gradient of the cumulative depth curve is very shallow at the end of the storms suggesting perhaps that the interpolation was tending to reduce the tail of the storm too much.

To investigate the effects of the interpolation on the throughfall at the tail of the storm, an example from storm j20mc was worked through. Originally the cumulative depths for j20mc were calculated using an interpolation between four succeeding values. During the interpolation it is only the depths for the unsampled gaps which are calculated, the sample depths remain as they are. Where there are less than four succeeding samples the interpolation is made from those that remain. Hence the last few gaps are calculated from the same number of samples regardless of the number used earlier in the storm. The cumulative depth under the canoy resulting from just the interpolation are compared with those where the total depth has been corrected (Figure 7.15). It can be seen that those values at the tail of the storm are in fact low and that the interpolation is not suppressing a steady rise.

Thus, assuming the values of Dm for multiple canopy throughfall are correct, the interpolation is not suppressing any evidence of drainage from the canopy on the scale of that of the single canopy.

3) Descriptions of cumulative rainfall, throughfall and interception curves

The effect of the analytical procedure on the cumulative depth data has been discussed and error due to sampling and interpolation

Figure 7.15 Comparing the shapes of the corrected and uncorrected cumulated throughfall curves for the multiple canopy during storm j20

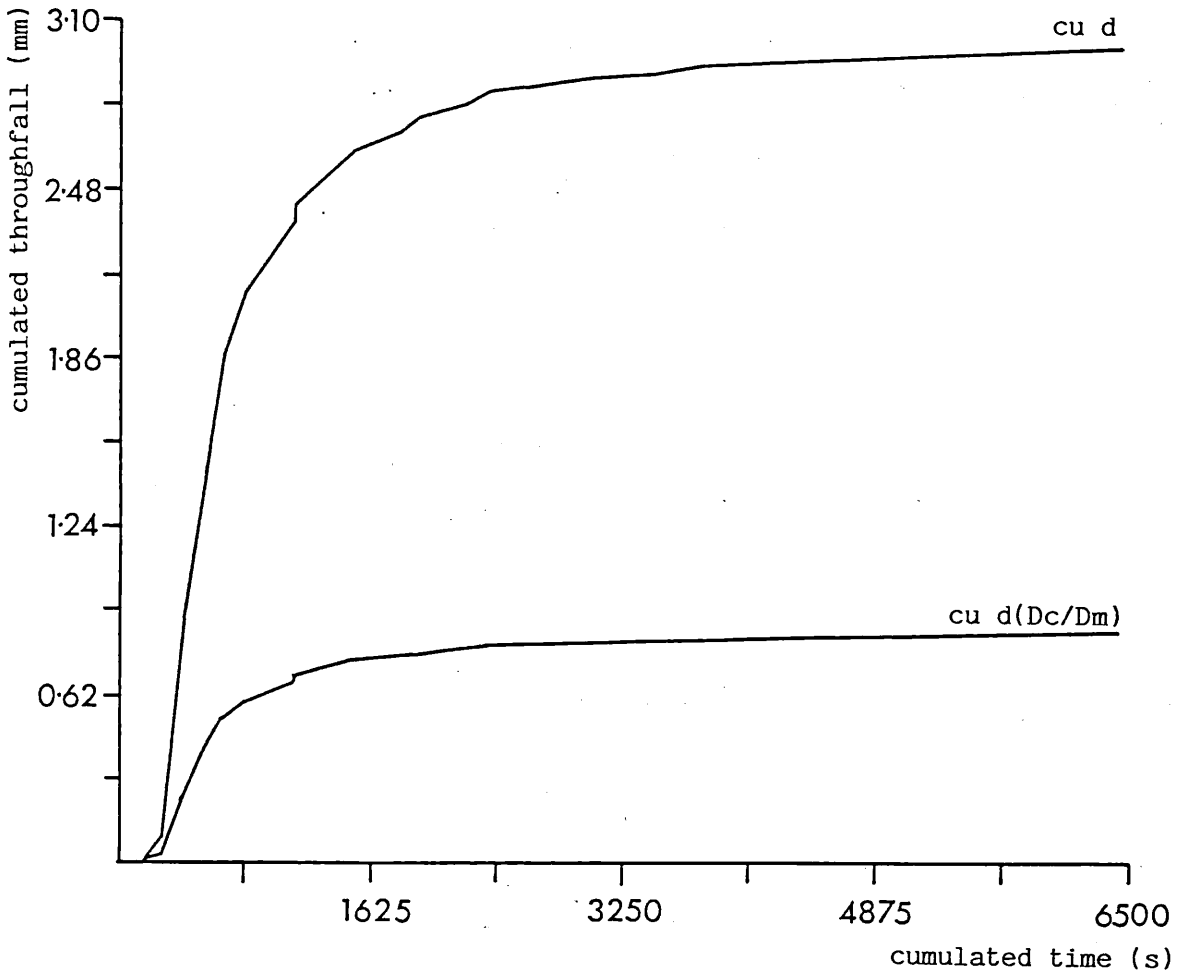

methods limited as far as possible. The interception curves are derived from the cumulative rainfall and throughfall curves (Figures 7.13 and 7.14) which will now be examined to provide a background for later discussion.

i) Rainfall and throughfall curves

It has been observed before that the majority of the storms started with a 10 minute burst of intense rain and thereafter the intensity gradually declined. Two exceptions to this were storms j13 and j15, the former which was a very small storm (0.11 mm total depth) and the latter which although larger (2.8 mm total depth) was made up of three bursts of rain over a period of 2.2 hours.

In order to standardise changes in rainfall intensity for all storms the cumulative depths and cumulative times were expressed as a fraction of total depth and total time over which sampling occurred (Figures 7.16, 7.17 and 7.18). From storms j10b, j11, j12, j16b and j20 a general curve has been constructed from the mean of times taken to reach 10% increments in depth (Table 7.8).

Storms in all sites had accumulated 50% of the water by 20% of the time, then 95% of water by 60% of the time. The rate of accumulation was remarkably similar in all three sites. Any distinction between the rates must be treated cautiously as the data is averaged from only a few storms with, in the open and multiple canopy sites, widely differing rates of accumulation. Also slight differences in the start of the sampling times, for storms where compensation has not been made in the interpolation, may cause the whole curve to be shifted along the time axis. However averaging all the storms will tend to minimise this error.

A delay in accumulation of throughfall would indicate that water which was falling in the open at the start of the storm was not falling under the canopy; that the fall of throughfall is being

Figure 7.16 Standardised cumulated rainfall depth-time curves for all storms

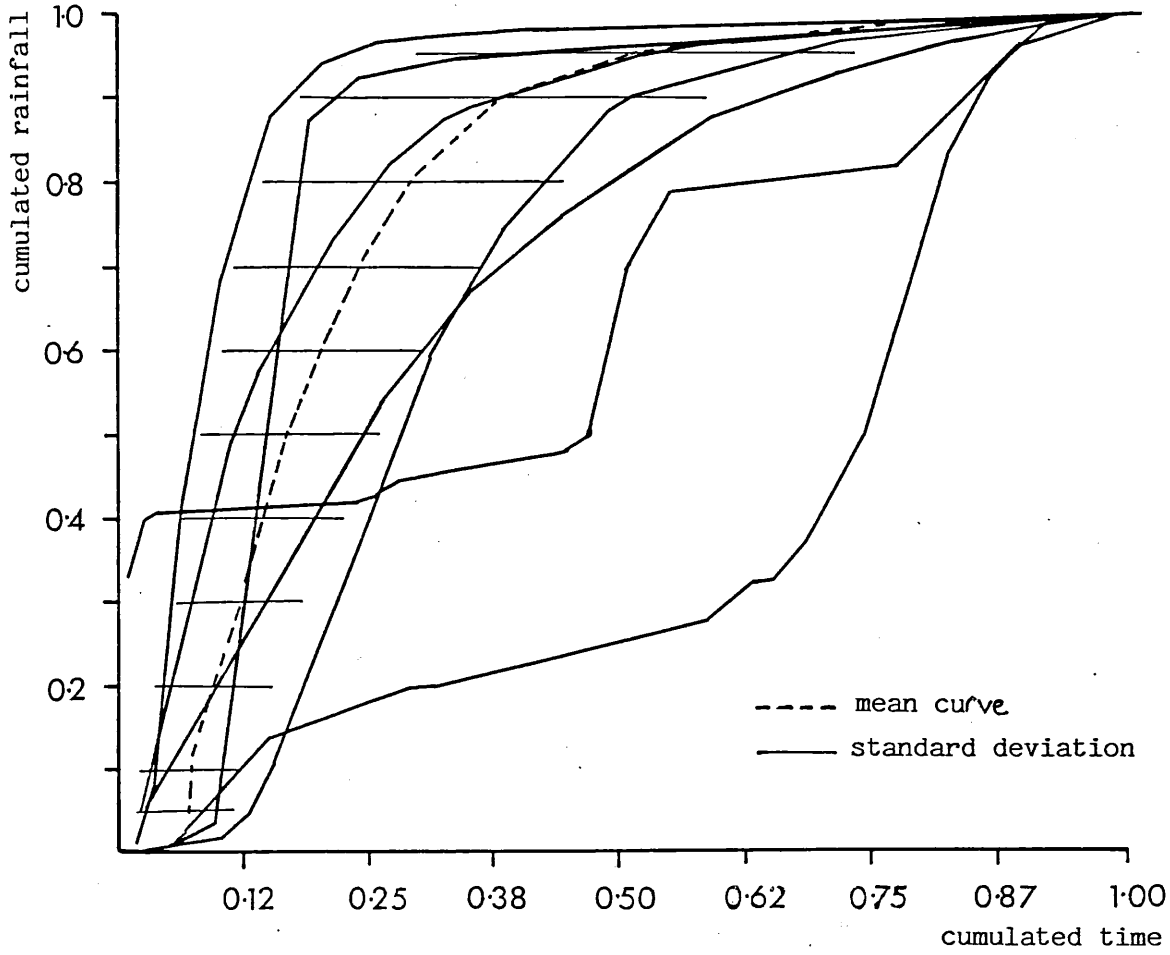

Figure 7.17 Standardised cumulated single canopy throughfall depth-time curves for all storms

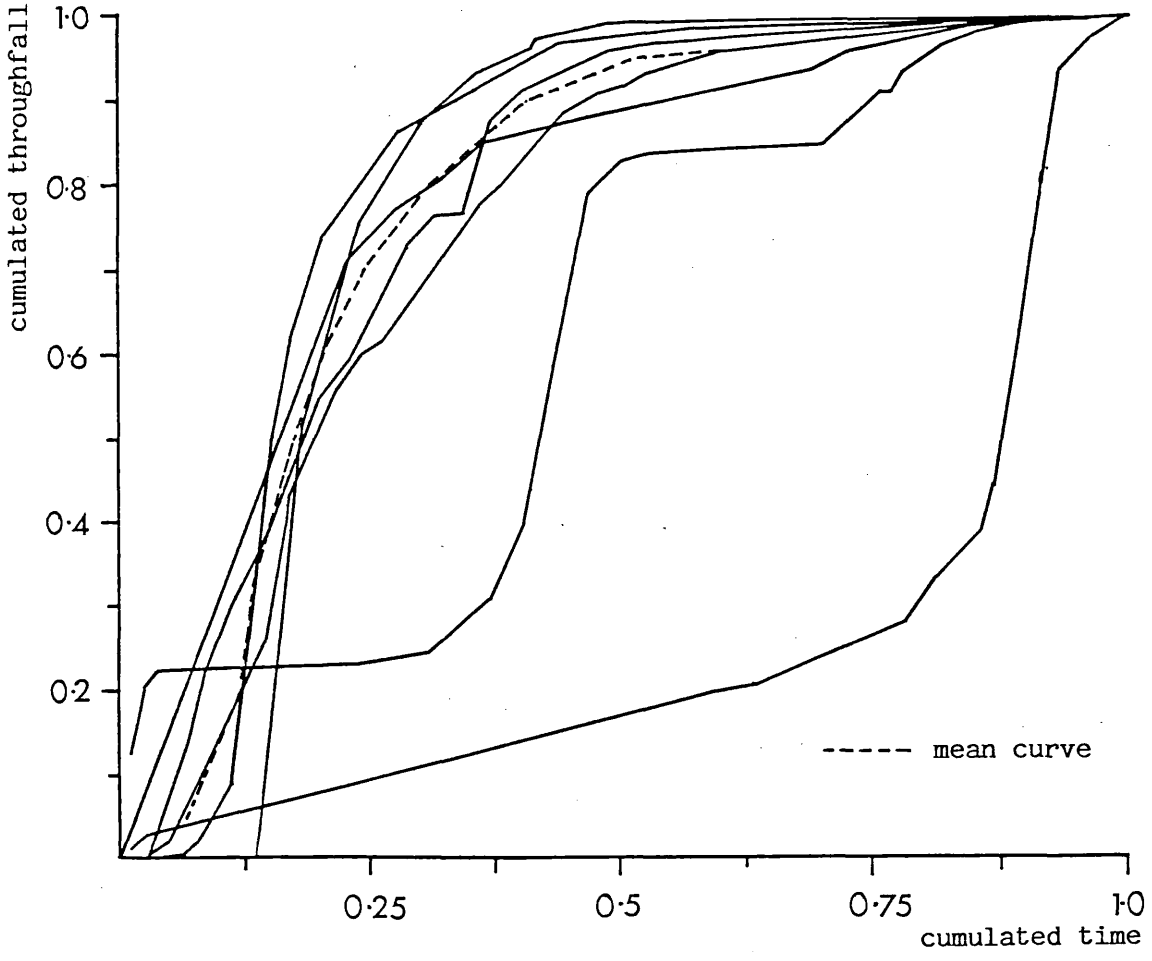

Figure 7.18 Standardised cumulated multiple canopy throughfall depth-time curves for all storms

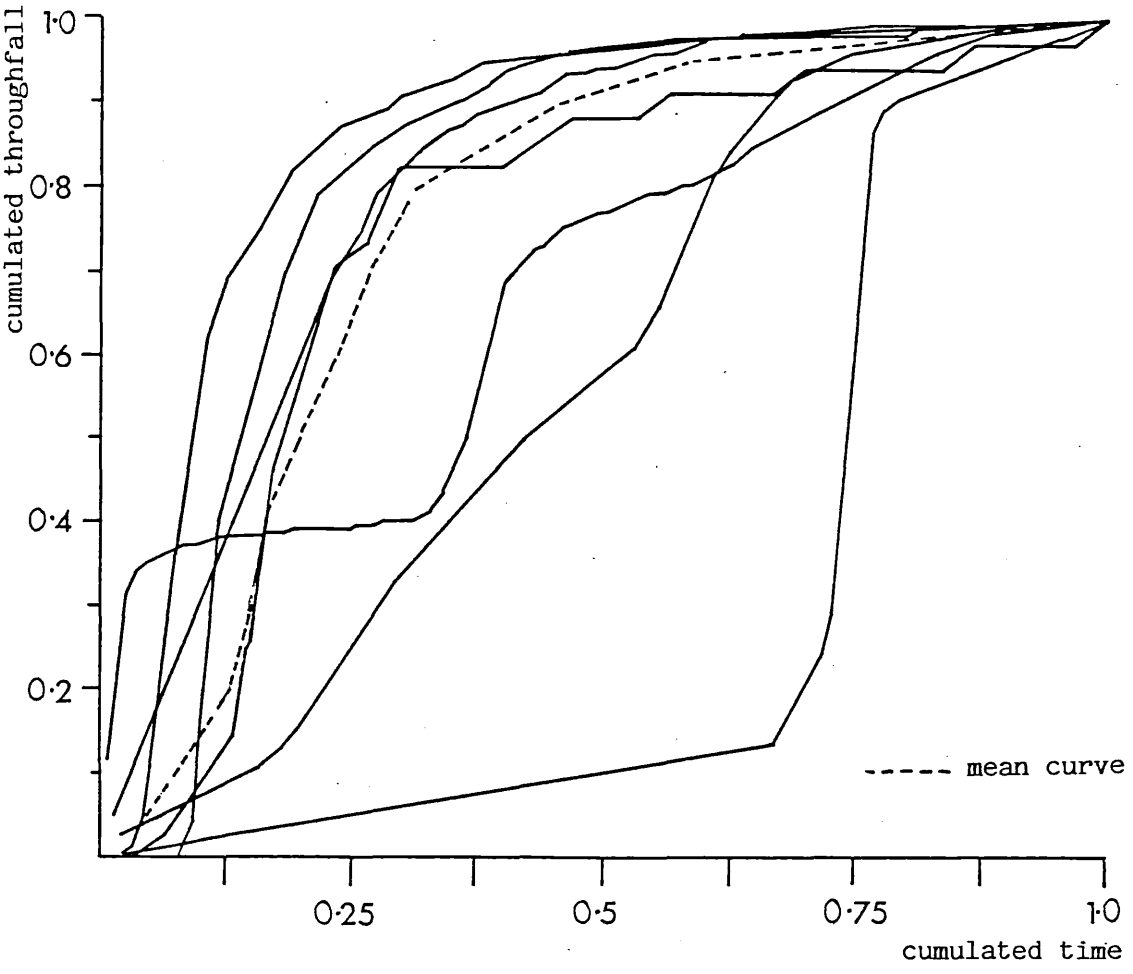

Table 7.8 Mean times, expressed as a percentage of storm duration, to accumulate 10% increments in depth for rainfall, single canopy throughfall and multiple canopy throughfall for storms j10b, j11, j12, j16b and j20

	% of total storm duration					
% cumulative depth	open		single canopy		multiple canopy	
	mean	s.d.	mean	s.d.	mean	s.d.
5	7	(5)	7	(5)	5	(4)
10	7	(5)	8	(5)	8	(4)
20	9	(6)	12	(3)	13	(7)
30	12	(6)	13	(3)	15	(9)
40	14	(8)	15	(2)	17	(10)
50	17	(9)	17	(2)	20	(13)
60	20	(10)	21	(3)	24	(16)
70	24	(12)	24	(5)	27	(17)
80	29	(15)	31	(6)	31	(17)
90	38	(20)	41	(9)	45	(15)
95	51		51	(13)	58	(20)

delayed by incident rain being intercepted by the canopy. Such a delay is not visible in the rates of accumulation under the single canopy but a slight delay may be discerned under the multiple canopy. This indicates that there is not a period of no throughfall prior to canopy filling under the single canopy, throughfall starts immediately. There is however a period of less throughfall under the much larger multiple canopy when some of the canopy storage capacity may be being filled.

The interception curves (Figures 7.13 and 7.14) have already been introduced and are derived from the difference between the cumulative rainfall and the cumulative throughfall for both single and multiple canopies. When the curve rises, the cumulative depth of the rainfall is greater than the depth of throughfall falling from the canopy above the sampling point and the canopy is assumed to be filling. There may be dripping from the canopy during periods of accumulation. It was observed by Herwitz (1985) that less than 35% of intercepted rain is detained on rain forest leaves in the first 30s of rain. When the curve falls there is more water coming from the canopy than is going into it at that moment and the canopy is assumed to be emptying. It is assumed that for storms with an intensity sufficiently high to exceed rates of evaporation and rates of stemflow, the canopy will fill and large scale drainage will be observed.

The shape of the interception curves is determined by the shape of both of the other two curves, any irregularities in either will be reflected in the resultant curve. The curves can be divided into two broad sets, those which show an accumulation of water followed by a net drainage and those which show accumulated water with no evidence of draining.

ii) Description of the interception curves where there is drainage

The storms which exhibited filling then draining all occurred at

the single canopy site in storms number j10bsc, j12sc, j15sc and j20sc (Figure 7.13). Generally the curves show a rapid accumulation followed in some instances by an irregular plateau indicating (except j15sc) a state of dynamic equilibrium between rainfall input and throughfall output. In the case of j15sc the equilibrium was static because there was a long period of no rain after the start of sampling. The plateau is followed by a draining period, the logarithmic decay of Rutter et al. (1971) being best exhibited by j20sc. Several of the storms (j10bsc, j15sc, j20sc) show a final, slight increase of intercepted water towards the end of the sampling.

Table 7.9 indicates for those storms in which there were identifiable periods of canopy filling then emptying, the time taken for the peak interception to be reached, the cumulative depth of rainfall at the peak and the amount of interception at the peak. The table shows that the same canopy responded differently between storms and that the cumulative depths of between 1.23 and 2.58 mm were needed before large scale drainage. Similarly the amount of water intercepted varied from between 0.68 and 1.0 mm. However all these storms had intensities in excess of 10.3 mm/hr from the start of the storm to the period of peak.

iii) Description of interception curves where there was no drainage

The single canopy in storms j13 and j16b and the multiple canopy in all storms show no periods of wide scale drainage from the canopy as revealed by the relative cumulative depths of rainfall and throughfall. With the exception of j15mc and apart from some very brief decreases, they show an inverse logarithmic increase in intercepted water. For j15mc the irregularity of the rainfall pattern superimposes itself on the interception curve causing a series of steps.

Table 7.10 summarises the total depths of intercepted water and

Table 7.9 Description of the interception curves for all storms where there was an observed decrease in canopy storage

	time to peak (s)	cumulative depth at peak (mm)	depth of peak (mm)	average intensity before peak (mm/hr)
j10bsc	720	2.27	0.80	11.35
j11sc	sampling recorded negative storage			
j12sc	400	1.23	0.73	11.07
j15sc	200	1.13	0.68	20.34
j20sc	900	2.58	1.00	10.32

Table 7.10 Summary of total interception depths (mm) at the end of all storms for the single and multiple canopy sites

storm	total storm depth (mm)	single canopy interception	multiple canopy interception
j10b	3.7	* 0.58	2.02
j11	12.7	1.17 (0.90)	8.04
j12	1.41	* 0.44	1.24
j13	0.11	0.10	0.10
j15	2.83	* 0.61	1.83
j16b	0.36	0.24	0.33
j20	2.93	* 0.54	2.08

* storms for which a period of canopy drainage was recorded
(0.90) adjusted mean depth without freak value

identifies those storms in which wide scale drainage was recorded. The two storms which did not fill the single canopy sufficiently for it to drain, j13sc and j16bsc, had total interceptions of 0.10 and 0.24 mm respectively, well below the canopy capacity. For the majority of the storms the multiple canopy response was not what was expected from the rainfall depths and the storm intensities. In particular storm j11mc in which there was a total rainfall of 12.7 mm and a throughfall depth of 4.63 mm leaving a total interception depth of 8.04 mm far in excess of the canopy capacity.

Other aspects of the relationship between rainfall depth and throughfall depth have been discussed already. In Chapter Five the derivation of an average value for throughfall from the 25 rain gauge values was examined. The values for throughfall depth obtained were considered to be low when compared to those measured by Gash (unpublished) at a nearby site. However it was concluded that the throughfall measurements were sufficiently accurate to suggest that the differences were due to differences in the canopy structure between the sites. In this chapter the effects of the interpolation on the derivation of the cumulative interception curve have been considered and it has been concluded that the interpolation is not causing any evidence of wide scale drainage to be suppressed.

The relative depths of rainfall and throughfall measured in the raingauges constrain the cumulative depths of intercepted water calculated from the drop samples. The accuracy of the measured depths has been examined and it must be concluded that the rate of accumulation of throughfall was always less than that of the rainfall under the multiple canopy. It may be suggested that the rate of removal from the canopy by stemflow in plants lower in the canopy especially palms, conduct the water away from the free fall space and to the ground along the stems. The energy of such water may be used in scouring the ground around the palms instead of causing splash.

4) Linking kinetic energy changes to changes in cumulated rainfall and interception depths

i) General trends in changes in kinetic energy of rainfall and throughfall with cumulative rainfall depth

It was suggested by the qualitative model that the initial effect of the canopy on falling rain is to shatter the raindrops into smaller sizes thereby reducing the kinetic energy of the throughfall to less than that of the rainfall. Thereafter the canopy increases the incidence of larger drops and the kinetic energy of the throughfall to greater than that of the rain. Analysis in Section 2 has shown that the kinetic energy of the throughfall falls into one of two groups with either a high or low energy value. Hence it is expected that the low energy samples occur either at the start of rain when there is little water stored on the leaves or at the end when the rainfall ceases to provide any impetus for knocking stored water off the leaves.

The suggestion of a constant value of rainfall or throughfall at which cumulated kinetic energy under the canopy exceeds that of the rainfall depends on the relative changes in kinetic energy. The general regressions of kinetic energy/mm/m^2 for all paired samples in each site have been plotted in Figure 7.12. The general trends indicate constant levels of throughfall energy above a declining level of rainfall energy. Therefore from the start of the storm the kinetic energy of throughfall should be greater than that of the rainfall implying that there is no critical depth of rain, and consequent storage, at which the canopy starts increasing kinetic energy.

ii) Identification of the throughfall samples which occur in the lower energy groups

In Section 2 it was stated that the kinetic energy of throughfall samples appeared to fall in either a lower or a higher energy group

and that the energy was independent of rainfall intensity and hence rainfall energy. It is suggested that the kinetic energy of any throughfall sample depends on the time at which it was taken and consequently the canopy storage. Table 7.11 lists all single and multiple canopy samples and the percentage of total storm duration lapsed by the end of each sample. Those samples where the kinetic energy falls in the low energy groups are marked. For the single canopy whether or not the sample was taken during a stage of canopy filling has also been noted. For the multiple canopy all samples appeared to have been taken during a phase of canopy filling.

Under the multiple canopy, the five samples which occurred in the lower energy groups were all either at the start or at the end of the storms. The variation in percentage time elapsed at the end of the initial samples suggests that the rate of penetration of the rainfall through the canopy varied between storms. Storm j13 was the smallest and least intense and consequently there was probably a delay in the penetration of the rain.

Under the single canopy the picture is more complex as there are samples from the lower energy group occurring part way through the storms in addition to those occurring at the beginning and ends. However it may be seen from Table 7.11 that the majority of the samples with low energy were taken during a phase of canopy filling, even when the filling took place at the end of the storm as in storm j10bsc. Samples j15sc(4) and j15sc(13) which occurred apparently in the middle of the storm and not during canopy filling were the last samples before each of the two lulls during the storm and hence may represent a situation similar to the end of storm samples.

iii) Discussion of the relationship between throughfall energy and the canopy storage level

It has been concluded that the kinetic energy of throughfall is independent of the kinetic energy of rainfall but depends on the

Table 7.11 The percentage of total storm duration elapsed by the end of each throughfall sample and the identification of those samples (*) whose kinetic energy/mm/m² is in the lower energy group (single canopy <20 J/mm/m², multiple canopy (3 m) <10 J/mm/m²).

single canopy				multiple canopy			
j10b(1)	24.60	j15(4)	10.18* f	j10b(9)	31.17	j15(8)	28.80
(2)	27.37	(5)	19.45	(10)	38.49	(9)	41.99
(3)	31.06	(6)	29.61	(11)	47.07	(10)	46.26
(4)	37.01	(7)	35.11	(12)	55.38	(11)	50.39
(5)	42.96	(8)	41.44	(13)	66.15	(12)	54.77
(6)	49.96	(9)	45.33	(14)	85.64	(13)	59.10
(7)	56.05	(10)	49.00	(15)	98.77	(14)	63.40
(8)	62.76* r	(11)	52.92	j11(1)	14.05*	(15)	67.84
(9)	69.37* r	(12)	58.44	(2)	17.20	(16)	72.81
(10)	85.76* r	(13)	69.92* f	(3)	20.39	(17)	78.95
(11)	103.08* r	(14)	79.59	(4)	23.59	(18)	83.04
j11(1)	9.74* r	(15)	84.23	(5)	26.94	(19)	88.28
(2)	12.74* r	(16)	89.50	(6)	34.80	(20)	92.56
(3)	19.10	(17)	95.33	(7)	42.97	(21)	96.81
(4)	24.23	j16b(1)	7.08	(8)	50.99	j16b(1)	24.72
(5)	29.39	(2)	20.76	(9)	59.60	(2)	42.51
(6)	33.51	(3)	32.19* r	(10)	68.86	(3)	61.63
(7)	44.32	(4)	43.11	(11)	77.26	(4)	78.73
(8)	73.42	(5)	55.48	j12(1)	12.84	(5)	92.38
(9)	92.55* f	(6)	66.88* r	(2)	19.59	j20(1)	2.60*
j12(1)	10.70* r	(7)	81.25* r	(3)	26.15	(2)	4.71*
(2)	15.22	(8)	102.49	(4)	33.57	(3)	6.81
(3)	21.16	j20(1)	2.43* r	(5)	43.03	(4)	9.05
(4)	27.58* f	(2)	4.41	(6)	71.94	(5)	11.18
(5)	34.95	(3)	6.27	(7)	125.58	(6)	13.46
(6)	57.77	(4)	8.77	j13(1)	26.83*	(7)	18.86
(7)	77.75	(5)	12.46	(2)	138.39*	(8)	24.90
(8)	111.98	(6)	16.60	j15(2)	1.46	(9)	31.89
j13(1)	4.56* r	(7)	21.88	(3)	3.10	(10)	39.82
(2)	15.86* r	(8)	27.24	(4)	4.98	(11)	50.68
(3)	96.68* r	(9)	33.61	(5)	7.03	(12)	60.11
j15(1)	0.41	(10)	44.67	(6)	12.86	(13)	87.68
(2)	2.08	(11)	60.77	(7)	18.82	(14)	107.54
(3)	4.62	(12)	90.95* f				

r rising limb of storage curve
f falling or level limb of storage curve

canopy structure and on the time lapse since the start of the storm, hence on the level of water held in storage. It appears from the analysis of the kinetic energy samples taken throughout a number of storms that the canopy acts as an energy regulator.

The energy of the throughfall falls in one of two groups, at a relatively high or a relatively low level. The majority of the samples (70% under the single canopy and 92% under the multiple canopy) fall at the high level. The average value for the high level appears to depend on the thickness of the canopy, a value of 33.12 $J/mm/m^2$ was recorded from the single canopy while if it is assumed that the water fell from the multiple canopy at terminal velocity the average value is a higher 37.02 $J/mm/m^2$. It is assumed that the difference is due to the amount of drop-size distribution change brought about by the canopy. The energy values in the high group are commonly higher that those of the rainfall, implying that the kinetic energy of the rainfall is increased by the canopy. There is insufficient evidence to suggest that the regulation of the kinetic energy by the canopy would serve to reduce the kinetic energy of rainfall should it be higher than the canopy energy for a prolonged time.

From the analysis of the time elapsed since the start of the storm at the end of each sample it appears that while throughfall may be at the high energy level throughout the storm it is most likely to fall from a moderately saturated or draining canopy in the middle of the storm. This coincides with the stages of the qualitative drop-size distribution model at which the coalescence of water drops on the leaves is at a maximum.

Within the first 30% of the duration of a storm and during the final 40%, samples with energy in the lower group have been recorded for both sites. On average the kinetic energy of these samples is half to one third of the kinetic energy in the higher groups. It is suggested that at the beginning of some storms the canopy may only split the raindrops into smaller droplets, with coalescence only

occurring after there has been an accumulation of water on the leaves. This would correspond with early stages of the qualitative drop-size distribution model. However the repetition of throughfall samples of low energy at the end of the storm has not been accounted for by the model. It is suggested that the leaves rapidly shed the accumulated water either because the leaves are especially adapted for doing so or the percussion of the impacting rainfrops knocks the water off. Once rainfall intensity has declined at the end of the storm, water which is already intercepted will tend not to drain, leaving only raindrops or shattered smaller drops in the throughfall.

The values for kinetic energy of samples of througfall taken throughout the storms appear not to be sensitive to all the stages of drop-size distribution change proposed by the qualitative model. Instead two distinct groups of energy values have been identified. Similarly an identical progression of energy change throughout each storm has not been found. In storms j10b, j15 and j16b the kinetic energy of throughfall was at the high level from the start of sampling. However it is possible that the probability of a sample being in the lower kinetic energy group declined from the start of the storm until about 30% of the duration and increases again after 60% of storm duration. During the middle of the storm it is probable that all samples recorded will be in the high energy group. The use of this information in predicting the change in rainfall energy by a canopy will be discussed in Chapter 8.

iv) Discussion of the implications of the frequency distribution of throughfall kinetic energy/mm/m^2 has on the number of sampling points

If it is assumed that the canopy configuration above each sampling point may be slighty different either during the storms or between storms, then the variability of throughfall kinetic energy/mm/m^2 particularly under the multiple canopy has useful implications for the number of throughfall drop-size distribution sampling points needed.

The low variability in kinetic energy/mm/m² both within and between storms reported in this and other studies (for instance Mosley (1982) and Chapman (1948)) where drop samples were taken at a single point, implies that similar results may be obtained were simultaneous samples to be taken at a number of different locations. It has been shown that for any depth of canopy storage there is a given probability of throughfall energy being either in the high or low energy group. Hence it is possible to re-interpret the results presented in Table 4.3 which examined the kinetic energy/mm/m² of a number of simultaneous samples under a sycamore canopy.

For storm A when the tree was in full leaf, five of the eight samples are in a kinetic energy group larger than 20 J/mm/m². For storm B when the canopy cover was less complete, the distinction between groups is less well defined, but two of the six samples are in the group larger than 20 J/mm/m². Although the state of canopy storage was not recorded these results may also be interpreted as showing the same kind of variation in kinetic energy which is observed temporally as the canopy storage changes and the difference may not be due to spatial differences in the sampling locations.

Section Four Total kinetic energy of rainfall and throughfall of each storm

The sixth and final statement derived from the qualitative model is that the total difference between the kinetic energy of rainfall and throughfall depends on the amount of water fallen during the storm. While the instantaneous kinetic energy/mm/m² of rain may be higher under the canopy, the depth of water fallen relative to that in the open will be less. Therefore the ultimate balance between rainfall and throughfall energy should depend on the relative depths of rainfall and throughfall.

1) Examination of the calculated total kinetic energies

i) Presentation of the total kinetic energies for rainfall and throughfall for each storm

The total kinetic energies of rain and the throughfalls for the sample area are presented in Table 7.12, together with the depths of rain and throughfall. The derivation of kinetic energy totals from the samples of drops was described in Chapter Five ([5.29] and [5.30]). It should be noted that any errors in the original measurements are multiplied during this procedure. For all storms but one (j10b) the multiple canopy reduced the kinetic energy of rain to between 3% and 66% of the open value even when the drops were assumed to be falling at terminal velocity. The mean reduction was to 28% although variation was considerable (s.d. $\pm$22.3). It is suggested that the increase in storm j10bmc at terminal velocity might be due to the interpolation procedure compensating for missing data. In contrast the total kinetic energy of four of the storms (j10bsc, j11sc, j15sc and j20sc) was increased by the single canopy, up to 184% of the open value.

It has been demonstrated in the preceeding section that the average energy/mm/m^2 of throughfall beneath both canopies was higher than the rain. Hence the proportion of rain being intercepted in each storm must determine the balance between the total kinetic energies.

ii) Cumulated kinetic energy and cumulated rainfall depths

The kinetic energies for each sample and interpolated gap have been cumulated and plotted against cumulated rainfall depth for each storm (Figures 7.19 to 7.24). For those storms where the total throughfall energy exceeded total rainfall energy it is possible to identify the depth of rain for each specific storm needed for the cumulated throughfall energy to equal that of the rainfall (Table

Table 7.12 Total kinetic energy (J/m^2) of rainfall (R ke.) and throughfall (T ke.) for each site and storm and the energy of throughfall expressed as a percentage of the rainfall

storm	rain	single canopy		multiple canopy			
	R ke.	T ke.	%	T ke. (8 m)	%	T ke. (3 m)	%
j10b	60.36	110.81	184	64.95	108	40.04	66
j11	338.47	409.07	121	185.96	55	112.12	33
j12	47.19	29.94	63	6.03	13	3.39	7
j13	1.49	0.17	11	0.05	3	0.04	3
j15	51.05	80.17	157	37.76	74	20.96	41
j16b	5.32	4.14	78	1.17	22	0.66	12
j20	55.04	74.41	135	31.85	58	18.41	33
mean	79.85	101.24		46.82		27.94	

Figure 7.19 Cumulated kinetic energy (J/mm/m²) of rainfall and throughfall from the single (sc) and multiple (mc) canopies for storm j11

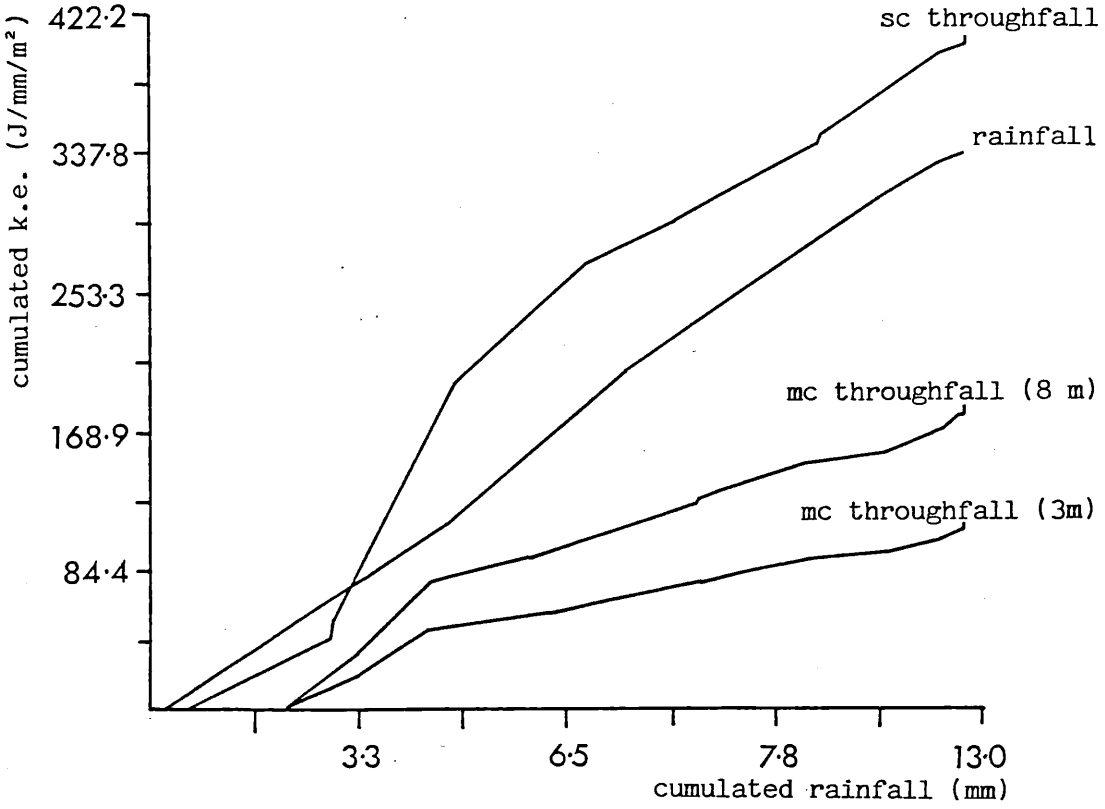

Figure 7.20 Cumulated kinetic energy (J/mm/m²) of rainfall and throughfall from the single (sc) and multiple (mc) canopies for storm j12

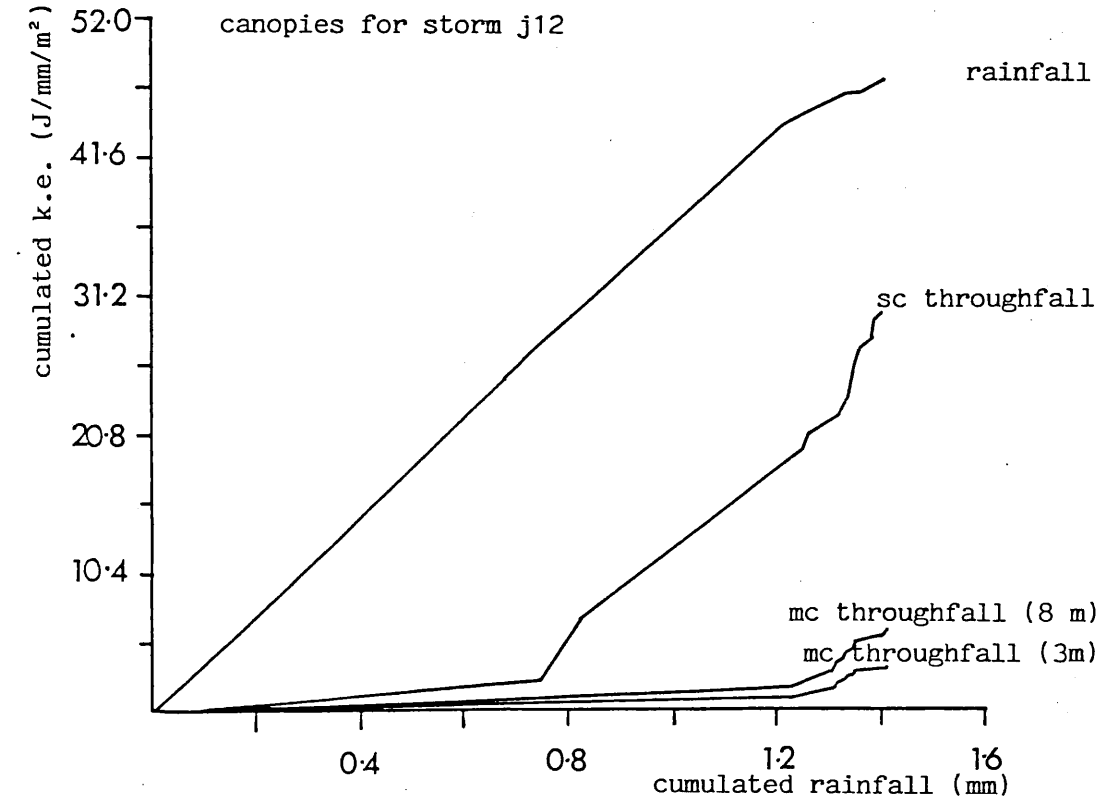

Figure 7.21 Cumulated kinetic energy (J/mm/m²) of rainfall and throughfall from the single (sc) and multiple (mc) canopies for storm j13

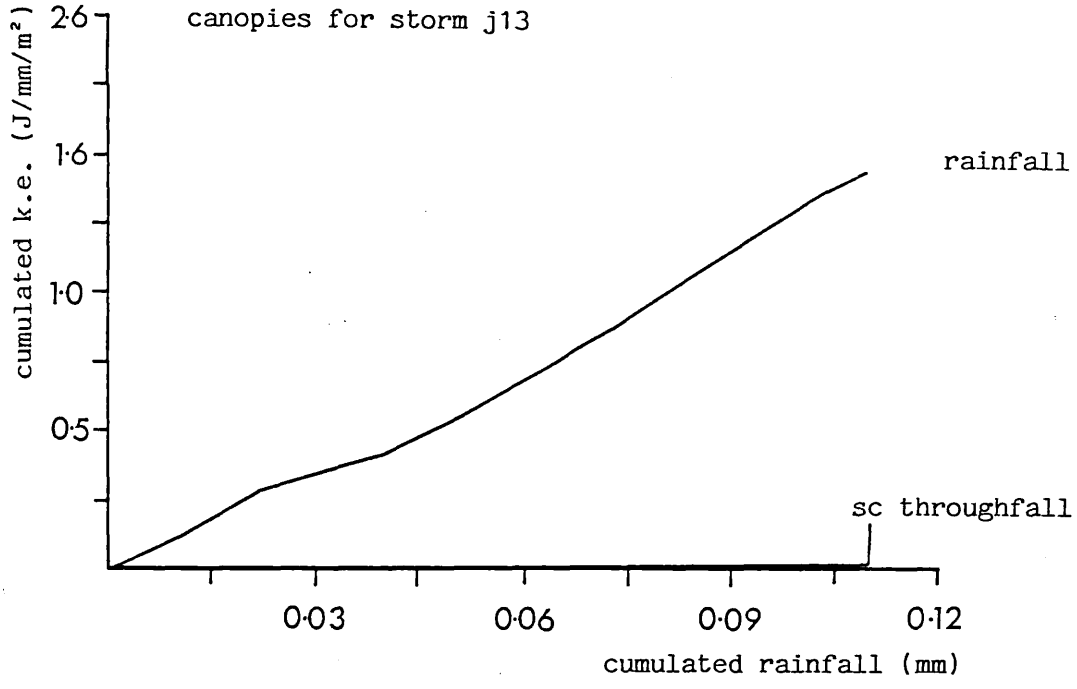

Figure 7.22 Cumulated kinetic energy (J/mm/m²) of rainfall and throughfall from the single (sc) and multiple (mc) canopies for storm j15

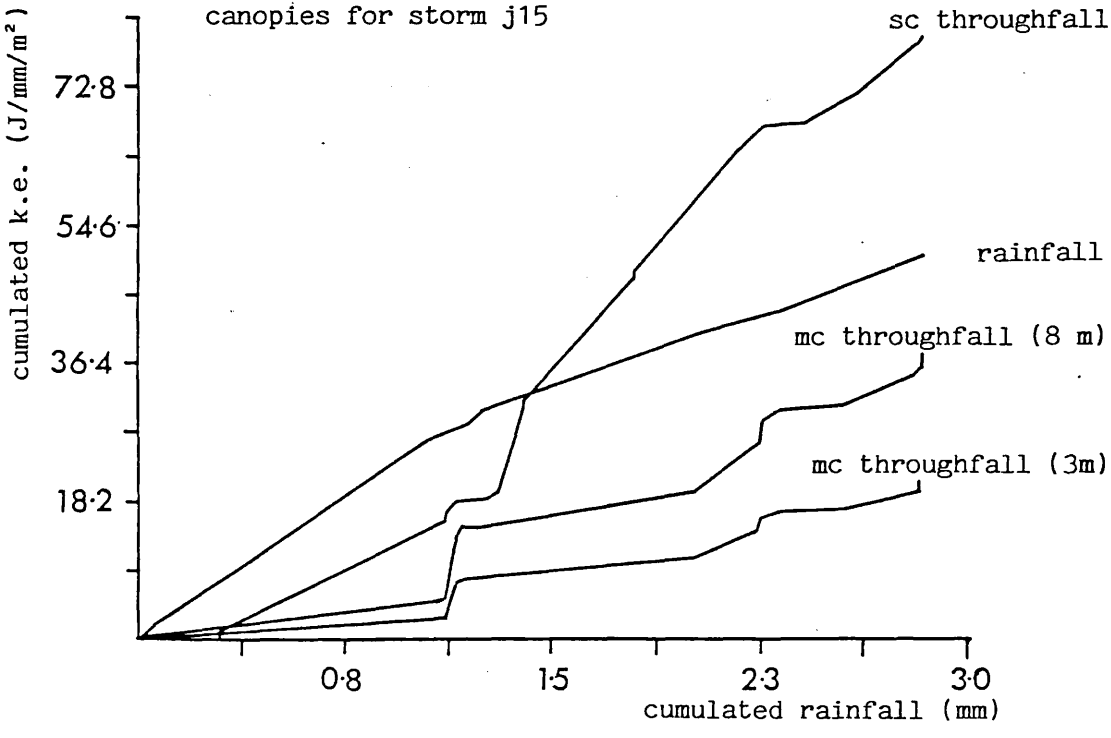

Figure 7.23 Cumulated kinetic energy (J/mm/m²) of rainfall and throughfall from the single (sc) and multiple (mc) canopies for storm j16b

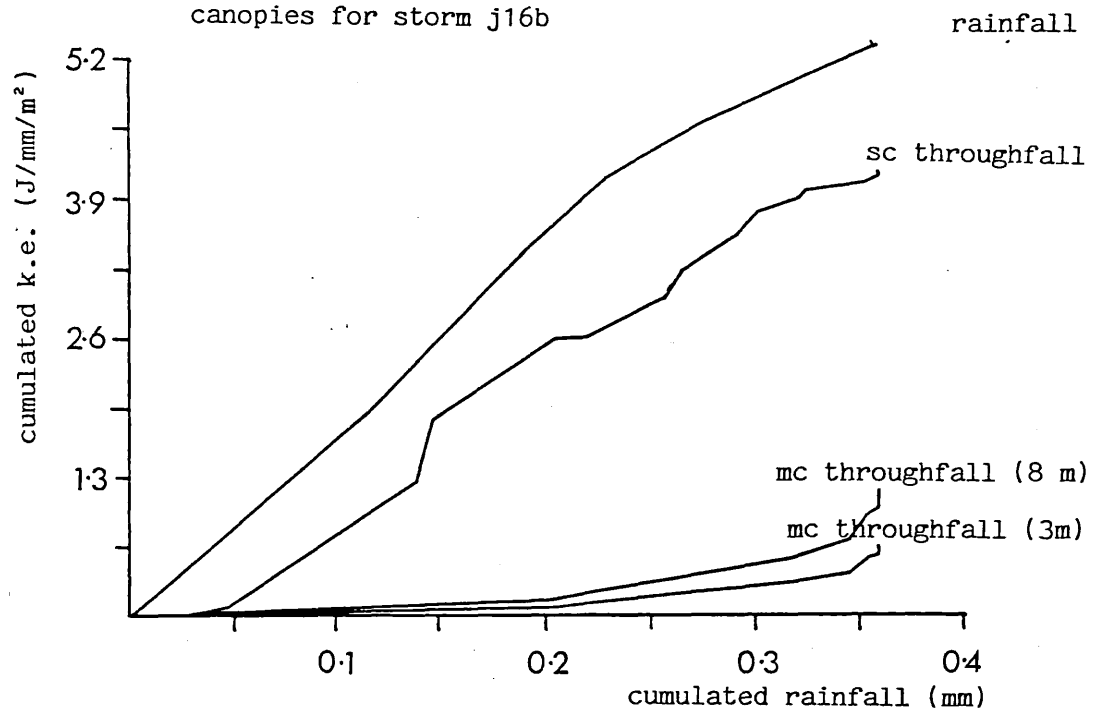

Figure 7.24 Cumulated kinetic energy (J/mm/m²) of rainfall and throughfall from the single (sc) and multiple (mc) canopies for storm j20

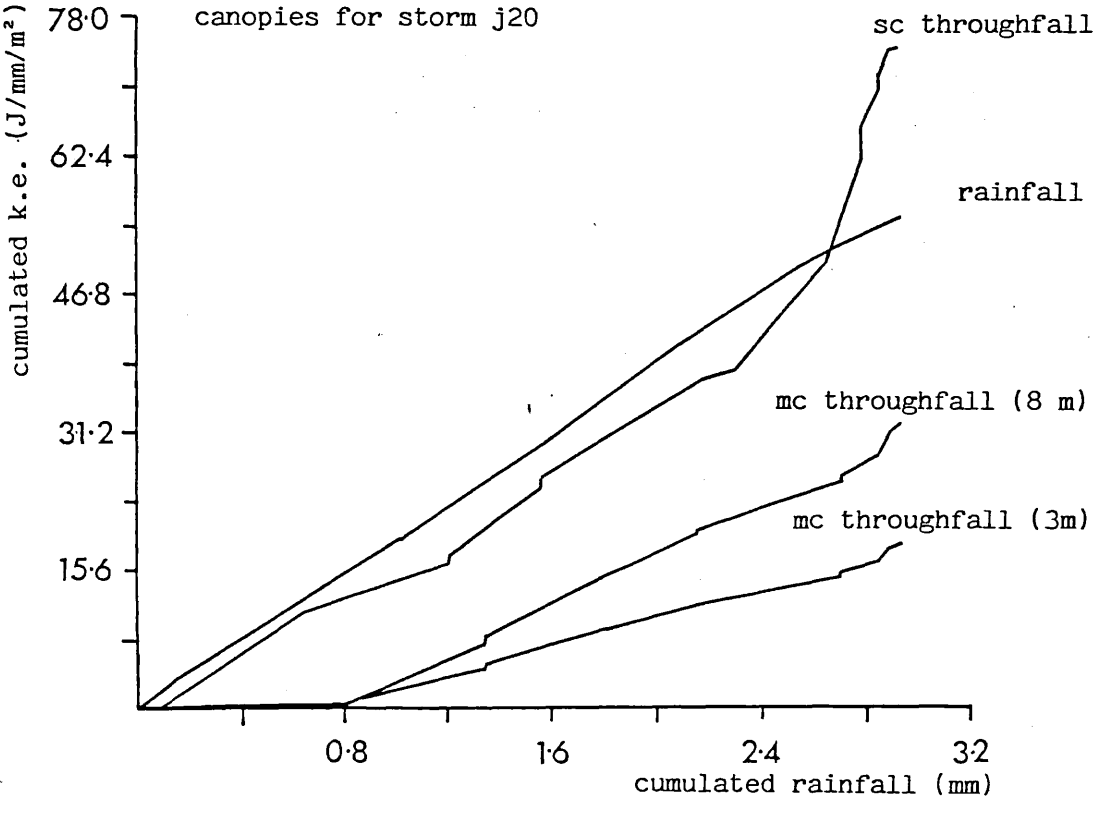

7.13). The correction for missing data at the beginning of j10bsc meant that the technique was not applicable for that storm.

The relationship between throughfall energy as a percentage of rainfall energy and storm depth has been plotted on Figure 7.25. A very weak trend of increasing output over input energy with increasing depth of storm derived from the storms of up to 3.7 mm depth would seem to grossly overestimate the energy increase for the much larger storm j11, of depth 12.7 mm.

For storms of total depth greater than 2.83 mm the transformation of the drop sizes by the single canopy was sufficient to cause the energy of throughfall to exceed the energy of rainfall. During those storms for which the thoughfall energy exceeded the open energy, j11sc, j15sc and j20sc the point at which throughfall energy exceeded rainfall energy during the storms were when 2.62 mm, 1.41 mm and 2.66 mm respectively had fallen. Hence for storms greater than about 2.5 mm, total throughfall energy tends to exceed total rainfall energy in the single canopy.

iii) The balance between total rainfall and throughfall energy with respect to the differences in drop-size distribution

As suggested above the cumulative depth is not the only indicator of kinetic energy change. A second cause of variation is the balance between the mean rainfall and throughfall instantaneous kinetic energy/mm/m^2. The throughfall energy/mm/m^2 has been shown, after a little variation, to approach a constant value through physical regulation of the drop sizes. However the mean kinetic energy/mm/m^2 of rainfall is not subject to such regulation and may be either higher or lower than that of the throughfall.

The mean values for kinetic energy/mm/m^2 for rainfall and throughfall have been calculated for each storm and the two values compared (Table 7.14). It may be assumed that the closer the mean

Table 7.13 Total storm and throughfall depths (D mm) and, for those storms where total throughfall kinetic energy exceeded total rainfall kinetic energy, the identification of critical depths (c mm) required for the cumulated energy of throughfall to equal that of the rainfall

storm	rainfall	single canopy		multiple canopy	
	D (mm)	D (mm)	c (mm)	D (mm)	c (mm)
j10b	3.7	*3.11	n/a	1.67	-
j11	12.7	*11.53	2.62	4.63	-
j12	1.41	0.97	-	0.17	-
j13	0.11	0.01	-	trace	-
j15	2.83	*2.22	1.41	0.99	-
j16b	0.36	0.12	-	0.03	-
j20	2.93	*2.39	2.66	0.84	-

* storms in which the total kinetic energy of the throughfall exceeded that of the rainfall

Figure 7.25 Total kinetic energy of throughfall ($k.e._t$) for each site and storm expressed as a percentage of total kinetic energy of rainfall ($k.e._r$), plotted against rainfall depth

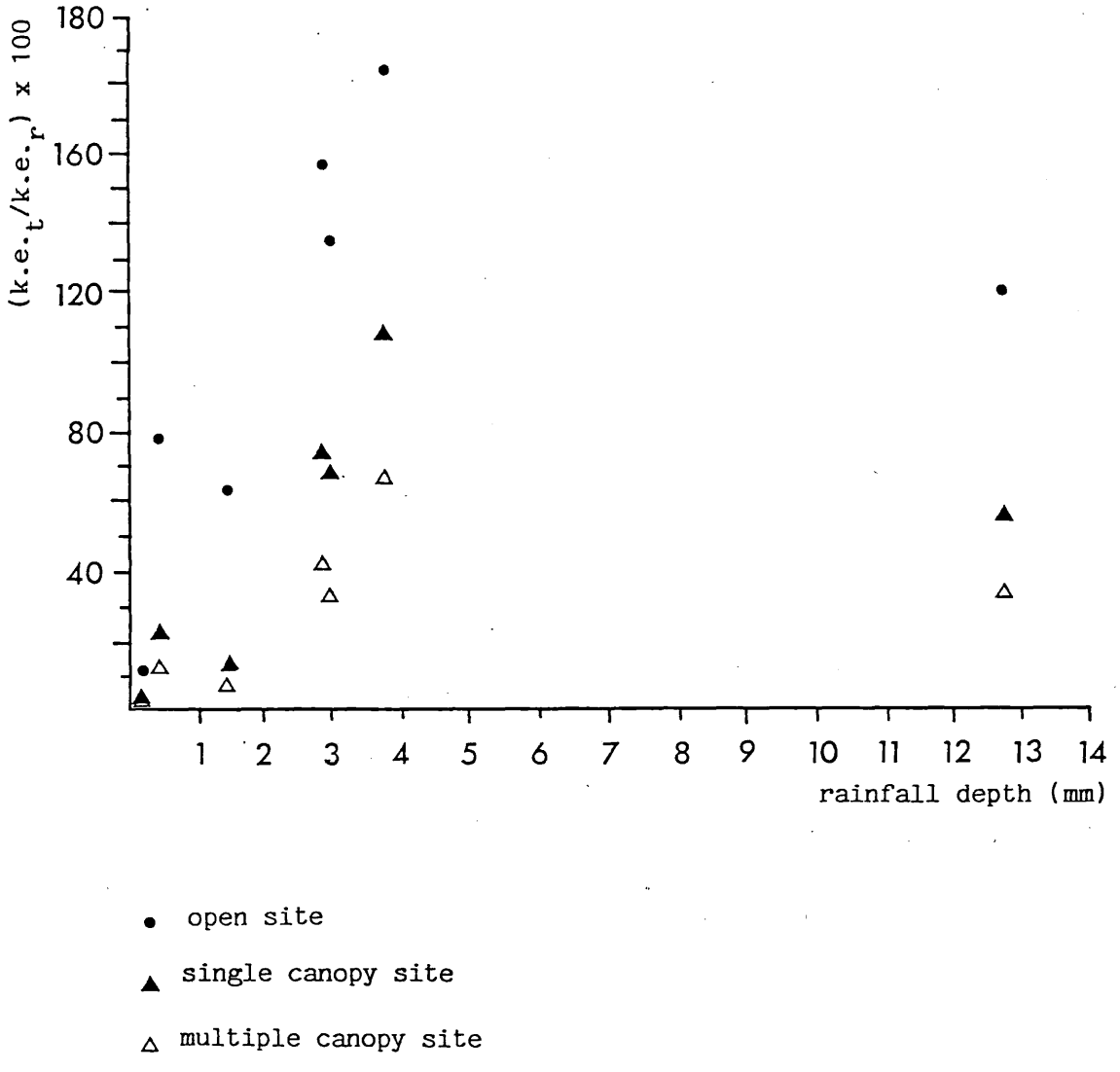

Table 7.14 Mean ($\bar{x}$) and standard deviation (s.d.) of kinetic energy (J/mm/m²) of all samples for each storm for rainfall (r) single canopy (sc) and multiple canopy (mc) throughfall canopy

	$\bar{x}_r$	$\bar{x}_{sc}$	$\bar{x}_{sc} - \bar{x}_r$
j10b	11.63 (2.99)	25.79 (11.76)	14.16
j11	23.65 (7.73)	26.11 (13.51)	2.47
j12	18.90 (9.61)	26.50 (9.16)	7.60
j13	10.78 (3.70)	6.56 (3.57)	-4.22
j15	12.41 (4.09)	30.99 (9.16)	18.58
j16b	12.21 (5.00)	28.06 (9.03)	15.85
j20	15.01 (5.91)	28.00 (10.72)	12.99

	$\bar{x}_r$	$\bar{x}_{mc}(8m)$	$\bar{x}_{mc}(3m)$	$\bar{x}_{mc}(8m)-\bar{x}_r$	$\bar{x}_{mc}(3m)-\bar{x}_r$
j10b	10.98 (2.73)	35.47 (4.61)	21.05 (2.99)	24.49	10.07
j11	24.04 (4.16)	35.60 (8.90)	27.11 (4.74)	11.56	-2.92
j12	16.89 (11.24)	35.14 (3.12)	19.94 (1.56)	18.25	3.05
j13	12.80 (1.30)	5.98 (1.62)	5.59 (1.04)	6.82	-7.21
j15	12.41 (4.68)	37.48 (1.82)	20.79 (0.91)	25.07	8.38
j16b	11.24 (4.35)	38.59 (1.75)	21.83 (1.43)	27.35	10.59
j20	14.62 (5.39)	32.35 (11.04)	18.64 (5.46)	17.73	4.03

kinetic energy/mm/m² of rainfall and throughfall the more rain will be needed to equate the total energies. If the energy of rain/mm/m² is higher than that for the canopy, if the initial energy reducing phase is not pased or if the storm should produce bigger drops than the canopy, there could be no possibility of the energies equating.

The difference in depth required during storms j11sc, j15sc and j20sc may be explained by the fact that j15sc has the largest difference between the mean kinetic energy/mm/m² of throughfall and rainfall and hence would be expected to equate the two energies with the least amount of rain. Storm j11sc has the lowest difference between the values for energy of rainfall and throughfall. Although the depth to equate rainfall and throughfall energy was similar to that of j20sc, the high mean value for kinetic energy/mm/m² of rainfall of 23.55 J/mm/m² which remained high throughout the storm, compared with throughfall which had 26.01 J/mm/m², may have lessened the increase in energy due to the canopy.

The mean kinetic energy of throughfall (assuming 3 m fall height) under the multiple canopy (20.05 J/mm/m², s.d. $\pm$ 11.00 J/mm/m²) is closer to that of the rainfall (14.88 J/mm/m², s.d. $\pm$ 11.00). The proportion of rainfall intercepted by the multiple canopy is much larger than by the single canopy. Hence on both counts the multiple canopy is very much more unlikely to ever increase the total kinetic energy of the rain.

Section Five The effect of changes in the total kinetic energy on changing the amount of splash

The ultimate point of this thesis is that the kinetic energy of incident rain controls the detachment of soil particles by splash and, by inference, the initiation of soil eroding processes. Any changes in the kinetic energy of rainfall by a vegetation canopy were thought

to change the amount of splash detachment. The methods of measuring splash detachment have been described in Chapter Four and the results are presented here. Gross comparisons between the amounts of splash in each plot for each storm are made and variation of splash amount over the plots discussed. Splash amount is related to the total kinetic energy of rain and throughfall and the relationship between splashed grain sizes and drop sizes are examined.

1) Presentation of the data

The weights of splash caught in each trap are presented in Appendix 3. Table 7.15 gives the mean and standard deviations of the measurements from the five splash traps in the open site and all 25 traps for each site and storm. The splash traps were placed in the centre of a circle of well-sorted river sand, 1 m in diameter. Sand collected in the trap thus represents cumulated movement of particles on the sand surface into an area 0.0064 m^2. It is a measure suitable for comparisons between sites which is assumed to increase as the energy available from raindrops increases.

The results show that in all storms but two there was an increased amount of splash under the single canopy up to 665% of the splash in the open for the same storm. In contrast the weight of splashed material under the multiple canopy was lower than in the open in all cases but two, down to 40% of the weight of splash in the open. In all but one case the standard deviation is higher under the single canopy than under the multiple canopy.

2) Comparisons between weight of splash and total kinetic energy

The mean weight of splash was regressed against the total kinetic energy for all sites together. In Chapter One is was stated that previous work has shown that splash detachment may be expressed as a function of kinetic energy of rainfall in the form

Table 7.15 Mean weight, $\bar{x}$ (g), of sand collected in each splash trap for all storms in the open site (n = 5) and the single and multiple canopy sites (n = 25)

	open	single canopy			multiple canopy		
	$\bar{x}$	$\bar{x}$	(s.d.)	%	$\bar{x}$	(s.d.)	%
j7a	0.0475	0.0386	(0.018)	81.3	-	-	-
j10b	0.0595	0.3959	(0.159)	665.4	0.1348	(0.124)	226.6
j11	2.0726	4.6970	(1.470)	226.6	1.4094	(1.110)	68.0
j12	0.1450	0.1366	(0.106)	94.2	0.1088	(0.086)	75.0
j13	0.0122	0.0163	(0.016)	133.6	0.0062	(0.007)	50.8
j14b	0.0306	0.1978	(0.106)	646.4	0.0913	(0.162)	298.4
j15	0.0903	0.4290	(0.265)	475.1	0.0806	(0.073)	89.3
j16b	0.0239	0.0412	(0.030)	172.4	0.0096	(0.015)	40.2
j20	0.1676	0.4711	(0.213)	281.1	0.0788	(0.120)	47.0

$$S = k\ KE^{b} \qquad [7.1]$$

where b ranges in value from 0.74 for sandy soils to 1.8 for clays (Free 1960, Bubenzer and Jones 1971, Morgan 1982, Kneale 1982). The value for k varies considerably with the method of measuring splash detachment. The results of the regression for the rain forest data are presented in Table 7.16 and k and b were found to be 0.015 and 0.71 respectively.

For each site the total weight of splash was also regressed on the total kinetic energy for each storm (Figure 7.26). With only seven points to each regression and the single large values for storm j11 to influence the slope the regressions should be treated cautiously when they are compared (Table 7.16). For the multiple canopy data the mean of the kinetic energy derived from terminal velocity and velocity of fall from 3 m was taken.

The value for k of the regression lines indicates the efficiency of the raindrops in splashing sand, such that the steeper the slope the less energy is needed to splash the same amount. Of the three sites the throughfall from the canopies transports the sand more effectively than the open rain. Table 7.16 shows that there is a 98% probability that the coefficient k slopes of the open and multiple canopy site are different. The importance of this distinction is that it implies that a threshold momentum needs to be supplied by the impacting drops before sand of a given grain size is moved. It may be that the increase in sizes of throughfall drops raises the momentum of the drops above the critical threshold for larger grain sizes.

3) Comparing changes in kinetic energy by the canopy with changes to splash

It may be expected that where the canopy leads to a reduction in the kinetic energy it will also reduce the amount of splash and that

Table 7.16 Regression of total splash, S (g), against total kinetic energy, KE (J), for all sites and for each site separately

site	regression equation	r	t	sig level	DF
all	$S = 0.015\ KE^{0.71}$	0.86			
open	$S = 0.006\ KE^{0.84}$	0.91			
single canopy	$S = 0.028\ KE^{0.66}$	0.93			
multiple canopy	$S = 0.025\ KE^{0.59}$	0.90	* 3.49	98%	6

* t-test to assess the probability that the slope coefficient k in the multiple canopy regression equation is different from that in the open regression equation

Figure 7.26 Total splash weight (S g) regressed on total kinetic energy (K.E. J/m²) for each storm and each site

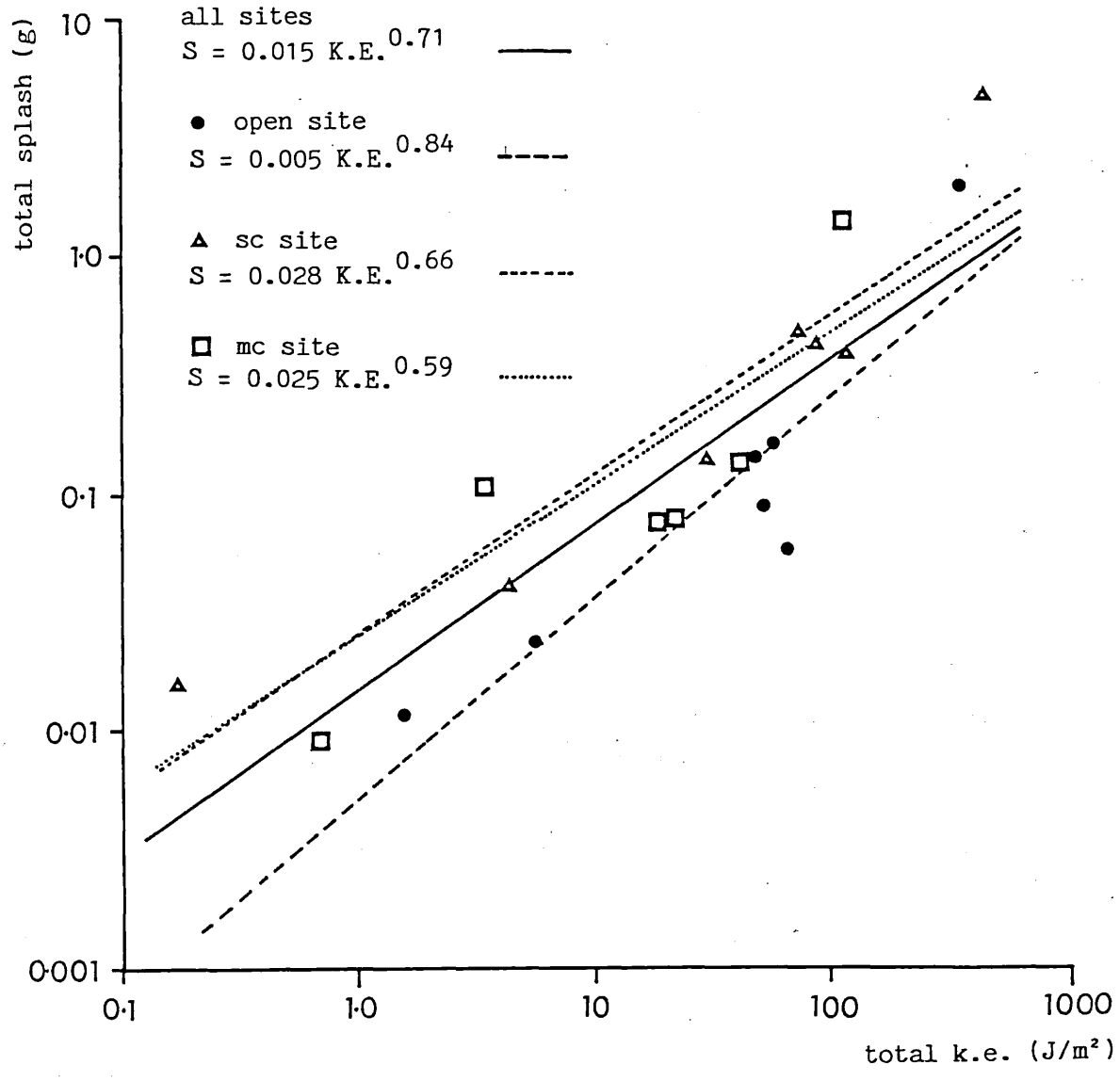

an increase in kinetic energy increases the amount of splash. Figure 7.27 shows the relationship between soil splash under the canopy as a percentage of splash in the open and kinetic energy (%S) of throughfall as a percentage of the energy of rainfall (%KE). Regressing the former on the latter yields the equation

$$\ln \%S = 3.98 + 0.013\ \%KE \qquad [7.2]$$

Again the increased efficiency of throughfall in splash is suggested. The results indicate that for three of the nine cases (marked * in Figure 7.27) where the kinetic energy of rain is reduced by the canopy, the amount of splash is greater under the canopy than in the open, implying that under some conditions the throughfall drops may exceed a critical threshold by virtue of their increased size (Park et al. 1982).

4) Relating drop-size distribution to splash particle size

To examine the hypothesis that by increasing the drop sizes of rainfall the splash particle size increases, each bulked sample of splashed material from each site and storm was sieved to examine the grain sizes. A control sample from an unsplashed sample is included for comparison. The results are presented in Table 7.17. The results are expressed as percentages of the total weight. The inclusion in the sieved samples of a few large grains, with their proportionally high weight, will skew the entire distribution to the larger grain sizes.

The mean grain sizes for the control, open, single canopy and multiple canopy are 1.83 Ø, 1.8 Ø, 1.66 Ø and 1.63 Ø respectively. There is an increase in mean size from unsplashed to splashed sand and then with increasingly large drop sizes. Figure 7.28 shows that the proportion of weight occupied by larger grains increase with the

Figure 7.27 Plotting soil splash by throughfall as a percentage of splash by rainfall (%S) against kinetic energy of throughfall as a percentage of kinetic energy of rainfall (%K.E.)

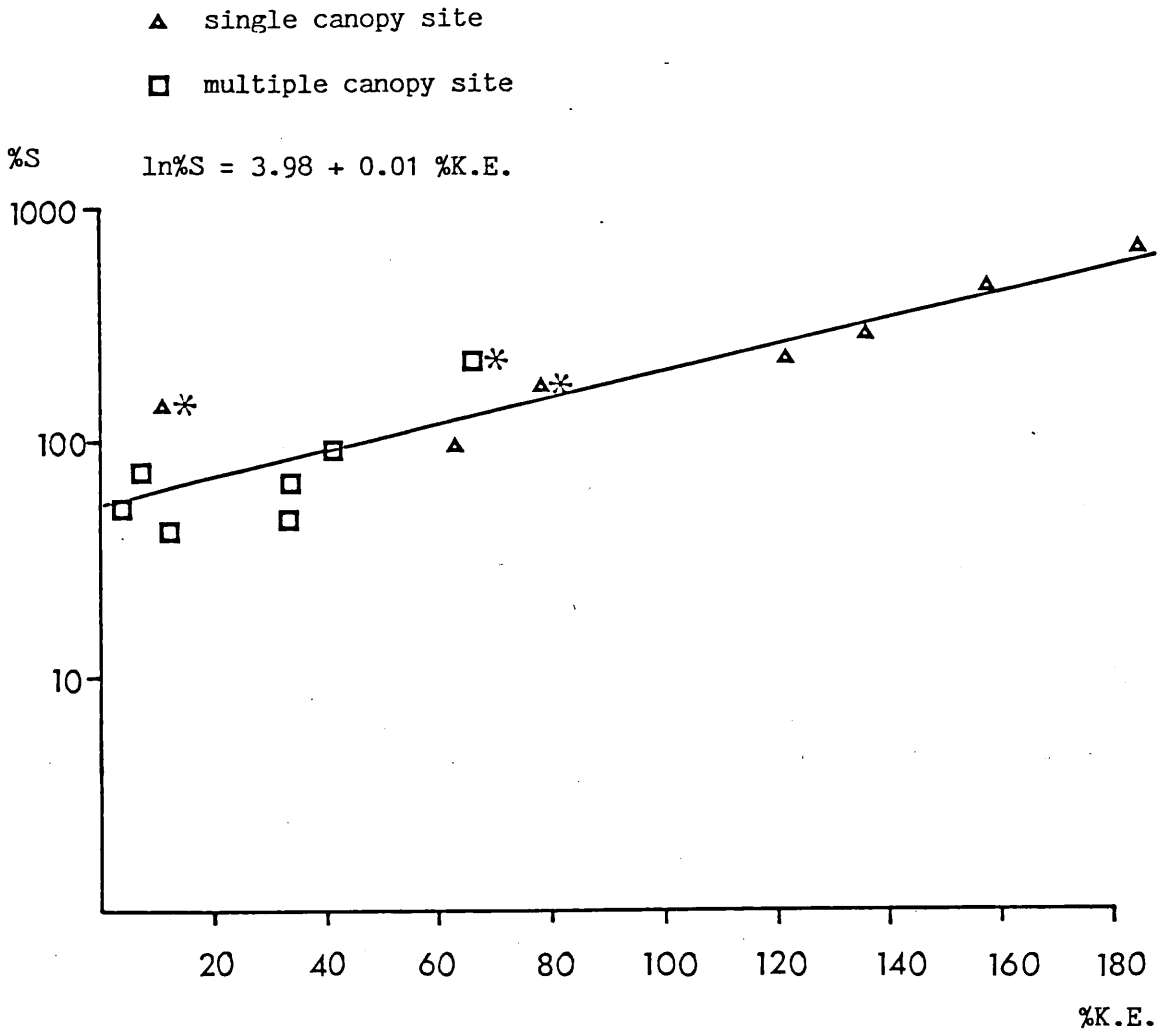

Table 7.17 Mean percentage of weight of sand splashed in each size fraction collected in the splash traps for all storms and sites and from a control site

	size fraction (Ø)						
	>0	>0.5	>1.0	>1.5	>2.0	>2.5	<2.5
open site							
j7a	0.00	8.42	19.09	27.82	21.64	11.27	11.75
j10b	3.87	6.12	14.81	26.14	24.28	12.86	11.91
j11	1.56	12.49	20.04	26.88	19.82	10.31	8.90
j12	1.41	6.06	15.10	24.71	22.47	15.38	14.87
j13	0.00	17.22	13.88	23,91	20.57	14.21	10.20
j14b	0.00	1.43	9.36	22.80	26.95	19.09	20.37
j15	0.00	5.74	14.49	26.70	24.88	16.09	12.10
j16b	0.00	8.93	17.20	34.20	21.33	13.93	4.42
j20	0.80	6.52	13.59	27.68	22.34	15.74	13.33
mean	0.85	8.10	15.28	26.76	22.70	14.32	11.98
s.d.	(1.30)	(4.53)	(3.19)	(3.27)	(2.27)	(2.66)	(4.34)
single canopy site							
j7a	0.90	8.57	14.67	26.52	22.10	13.20	14.05
j10b	1.77	11.42	18.21	27.30	20.40	11.89	9.49
j11	4.43	15.60	19.61	24.47	17.38	9.25	9.25
j12	2.31	10.58	17.15	25.84	19.97	12.44	11.71
j13	2.07	7.66	16.29	25.42	22.36	13.27	12.92
j14b	3.01	11.75	17.20	26.00	18.25	12.07	11.72
j15	3.91	3.02	19.66	27.46	21.60	12.61	11.74
j16b	4.16	12.88	16.81	26.53	19.48	10.77	9.37
j20	2.95	11.99	18.06	24.66	19.05	11.70	11.58
mean	2.83	10.39	17.52	26.02	20.07	11.91	11.31
s.d.	(1.19)	(3.60)	(1.58)	(1.05)	(1.72)	(1.26)	(1.66)
multiple canopy site							
j7a	-	-	-	-	-	-	-
j10b	1.10	10.52	18.45	26.72	20.91	12.10	10.20
j11	4.22	14.59	20.28	25.92	17.30	10.50	7.19
j12	3.85	11.52	16.19	22.16	20.41	12.64	13.23
j13	7.97	11.35	13.31	22.97	19.46	11.62	13.31
j14b	4.17	15.21	17.76	24.26	18.11	10.94	9.55
j15	3.86	13.21	18.82	28.22	17.94	9.96	7.99
j16b	0.00	7.06	14.78	23.44	22.43	15.79	16.62
j20	1.91	10.96	18.11	25.76	20.54	12.01	10.71
mean	3.39	11.80	17.21	24.93	19.64	11.95	11.10
s.d.	(2.44)	(2.58)	(2.29)	(2.07)	(1.75)	(1.79)	(3.12)
control	2.87	7.90	13.69	22.34	20.74	14.62	17.80

Figure 7.28 Plotting mean percentage of total splash sample weight (bulked for all storms) against the graded sizes to examine differences in grain sizes moved in the different sites

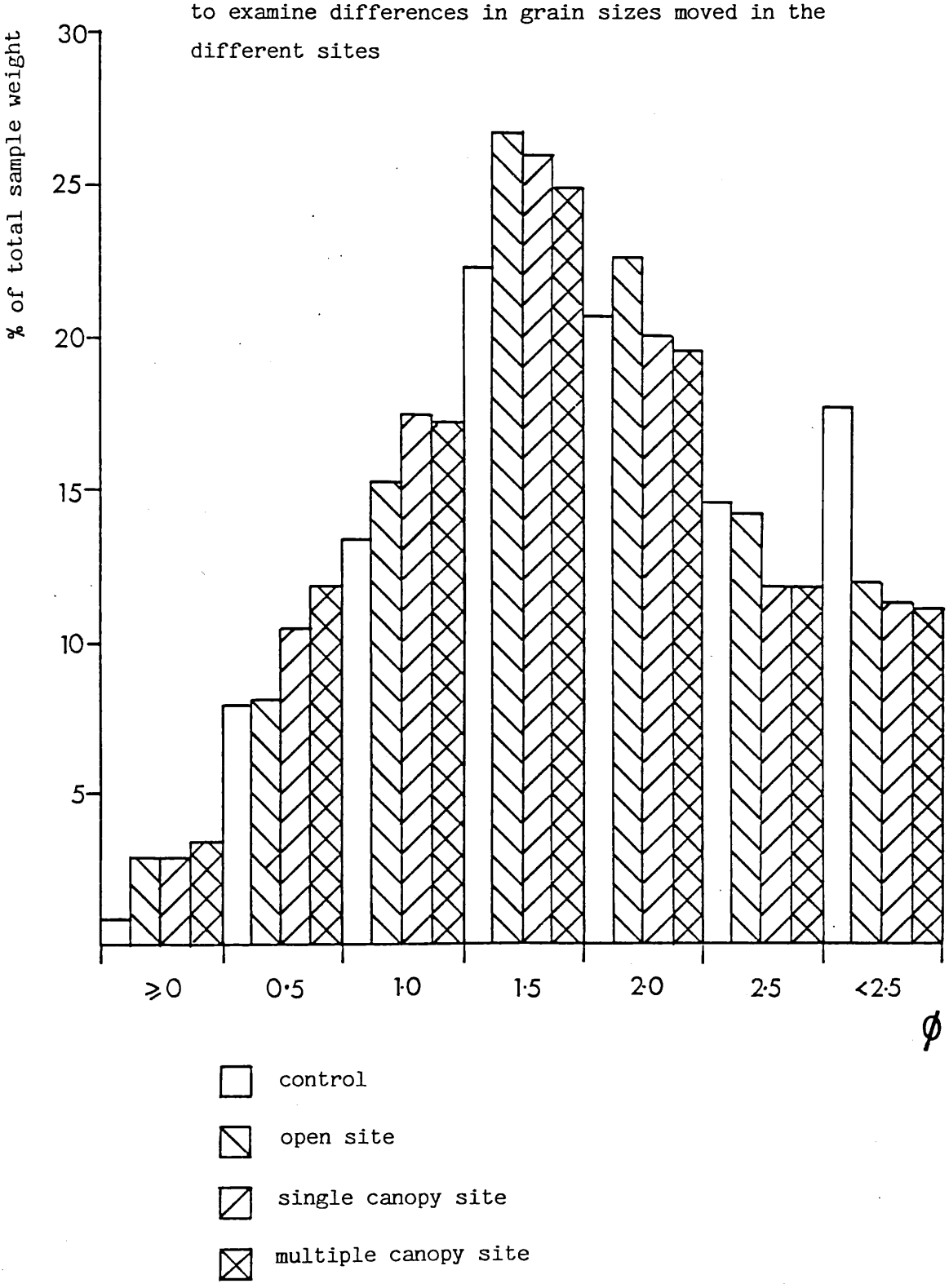

amount of cover. The expression of the values as percentages means that there is increasing incidence of larger grains from open to single to multiple canopy supporting the concept that there is a threshold for grains of given size for the amount of energy needed by a drop. This might also explain the greater variability in splash amounts in splash traps under the single canopy. The analysis of kinetic energy per mm change throughout the storm, although averaging at 27.82 J/mm/m^2 varied considerably temporally. It might be reasonably assumed that such variation also occurred spatially over the plot giving rise to the variation in splash totals observed.

Conclusions

The drop-size distributions of tropical rainfall and throughfall from contrasting canopies have been compared. The results are similar to those from temperate rain and oak canopy throughfall in that the canopy reduces the majority of the drop sizes, but increases the incidence of larger drops of a low frequency. The multiple canopy produced a wider range of throughfall drop sizes than did the single canopy. In the previous chapter it has been shown that the kinetic energy/mm/m^2 of a sample of rain or throughfall is correlated with the incidence of larger drops.

While the kinetic energy/mm/m^2 of rainfall was shown to be related to the rainfall intensity, the energy of throughfall was not. The values of kinetic energy/mm/m^2 of throughfall samples were concentrated into a more limited range than those of the rainfall, suggesting that both canopies regulate the kinetic energy of rain producing values in one of two energy groups.

The cumulative canopy storage was calculated for each canopy and storm and it was found that the kinetic energy/mm/m^2 of throughfall samples could be related to the level of storage. However it was also found to be possible to substitute the percentage of storm duration

elapsed for storage level and to relate kinetic energy/mm/m² to this more easily determined variable. Within the first 30% of the storm duration and during the final 40%, samples of the lower energy group were recorded for both sites. Throughfall at the high energy level was most likely to fall from a moderately saturated or draining canopy in the middle of the storm.

For storms of total depth greater than 2.8 mm the transformation of drop sizes by the single canopy was sufficient to cause the total kinetic energy of throughfall to exceed the energy of the rainfall. While the kinetic energy of throughfall from the multiple canopy was commonly at a higher level than that of the rainfall, the reduction in depth caused by interception, probably to stemflow, caused the total kinetic energy to be reduced. Splash from a controlled site was correlated with total kinetic energy and there is some evidence that the difference in drop-size distributions produced by the canopy increases the efficiency of the splash process.

CHAPTER EIGHT MODEL OF RAINFALL AND THROUGHFALL KINETIC ENERGY

Introduction

The purpose of this final chapter is to draw together the information built up from both the oak and tropical rain forest sites and to present the conclusions in the form of a general quantitive model. The model calculates the energy of a storm and the extent to which that rainfall energy is changed by any given canopy. The simulated values for total kinetic energy for any set of parameters is used to determine the magnitude of splash.

The model simulates the cumulated kinetic energy of a storm of any depth and pattern of intensity change. Using an experimentally determined relationship between rainfall depth and intensity and throughfall depth and intensity, the model simulates changes in throughfall energy resulting from a change in the canopy thickness (hence the uniformity of throughfall drop sizes), changes in canopy structure (resulting in different magnitudes of throughfall drops) and a change in canopy height (resulting in a change in the velocity of the falling drops). Hence for a given rainfall depth, storm duration and pattern of intensity change the total kinetic energy of the throughfall from either a natural forest canopy or a changed and managed forest may be assessed.

The basic forms of the relationships between parameters may be made to be applicable to all rainfall and vegetation types. However the conditions for which the parameters presented here were derived limit the scope of the model at present. Because of the greater detail and accuracy of the data from the tropical rain forest sites, this data set has been used to determine the parameters for the model. Hence the simulated storm depths should be within the range of storm depths measured and this precludes the simulation of storms of more than 13 mm depth, although there is no evidence that the model will not be applicable at greater depths. Similarly the relationship

between rainfall intensity and kinetic energy/mm/m² and the magnitude of the kinetic energy of throughfall have been determined specifically for tropical situations.

The results of a number of simulations will be presented representing different canopy forms and the change in kinetic energy and splash compared. With an analysis of the sensitivity of the value for kinetic energy to the different canopy parameters.

Section One Definition of the model parameters

This section will describe the set of parameters to be used in the quantitative model. The relationships between rainfall intensity and energy, the values of the two levels of throughfall energy and the relationship between total applied energy and the weight of soil splash will only be summarised here. They have already been described in Chapter Seven and will be held constant in the model. In contrast the effect of the canopy structure, thickness and height other than those measured must be simulated and the nature of the simulation is discussed in greater detail.

1) Storm depth and duration

i) Rainfall

As stated in the introduction, the simulated storms should lie within the range of measured storm depths and durations (Table 7.7). Storm depths varied between 0.11 mm and 12.7 mm, however the majority of depths were concentrated below 3.11 mm. Storm duration varied between 0.28 hours (j13) amd 2.21 hours (j15) with an average of just over an hour. For the purposes of the simulation a standard storm depth of 4 mm and duration of 1 hour was chosen. Each simulated storm was divided into 20, 3 minute increments each representing one sample and giving a sampling frequency similar to that of the

experimental work.

ii) Throughfall

The throughfall depths of the simulated storms were taken from the measured difference between rainfall and throughfall depths of storms j10b and j20 which were of similar size to the simulated 4 mm depth. On each occasion, the single canopy throughfall was about 85% of the rainfall depth. Hence a total interception loss of 0.6 mm was assumed to simulate canopies similar to the single canopy. The average loss to interception under the multiple canopy was considered in Chapter Five to be abnormally high due to the presence of a large palm in the centre of the plot. Therefore for a more general application of the model to rain forest sites, interception losses of 0.7 mm per storm were assumed, as measured by J. Gash (pers. comm.) at a nearby site and at the same time.

Using the data presented in Table 7.7 the duration of throughfall under the single canopy was an average 1.5 hours and 1.83 hours under the multiple canopy. Table 8.1 shows the depth of throughfall fallen after the end of rainfall for each storm and canopy expressed as a percentage of the total throughfall depth. Apart from storms j13 and j16b, which were the smallest storms, at most 1.7% of the total throughfall fell from the single canopy after the end of rain and 5.9% from the multiple canopy. Therefore for the purposes of the simulation it will be assumed that the end of rainfall and throughfall were coincident for both canopies. Each throughfall storm was divided into 20, 3 minute increments similar to the rainfall.

2) Intensity changes during the storm

i) Rainfall

In the previous chapter cumulated rainfall depth and cumulated

Table 8.1 The depths of throughfall, d (mm), from the single and multiple canopies after rain had ceased in the open and those depths expressed as a percentage of total throughfall depth, D

storm	single canopy		multiple canopy	
	d (mm)	% D	d (mm)	% D
j10b	0	-	0.02	1.2
j11	0.13	1.1	0.14	3.0
j12	0.005	0.5	0.01	5.9
j13	0.008	81.0	0.004	90.0
j15	0.25	1.1	0.05	5.0
j16b	0.002	1.7	0.004	13.7
j20	0	-	0.004	0.5

time were expressed as percentages of total depth (R) and storm duration (t) (Figure 7.16). Apart from storms j13 (the smallest storm) and j15 (a storm in which there were several bursts of rainfall) the figure shows that the majority of the rain fell in the first part of the storm and that through the storm the rainfall intensity declined. Visual inspection shows that the cumulated depth increased with an inverse logarithm of cumulated time. Any regular pattern of intensity change between this and a constant intensity throughout the storm may be simulated using the expression

$$pr_i = pt_i + q\ (\ln pt_i - pt_i) \qquad [8.1]$$

where pr_i is the percentage of total rain depth (R) accumulated by pt_i the percentage of storm duration elapsed and where q varies from 0 to 1. When q = 0, there is a linear increase in depth with cumulated time; the rainfall intensity remains constant through the storm. When q = 1, the depth increases with the inverse logarithm of time (Figure 8.1). To standardise the curves, so that at t=100, R=100, the following expression was added to [8.1]

$$pr_i = (pt_i + q\ (\ln pt_i - pt_i) \times \frac{100}{z} \qquad [8.2]$$

where z is the value of pr_i at t=100 in [8.1]

The percentage depth fallen in each increment was multiplied by the total storm depth of 4 mm to get the actual depth of water falling in each 3 minute increment (r_i)

$$r_i = \frac{pr_i}{100} \times 4 \qquad [8.3]$$

Figure 8.1 Illustration of the changes in rainfall intensity which may be simulated using the expression $p_{ri} = p_{ti} + q(\log_e p_{ti} - p_{ti})$ when q is varied

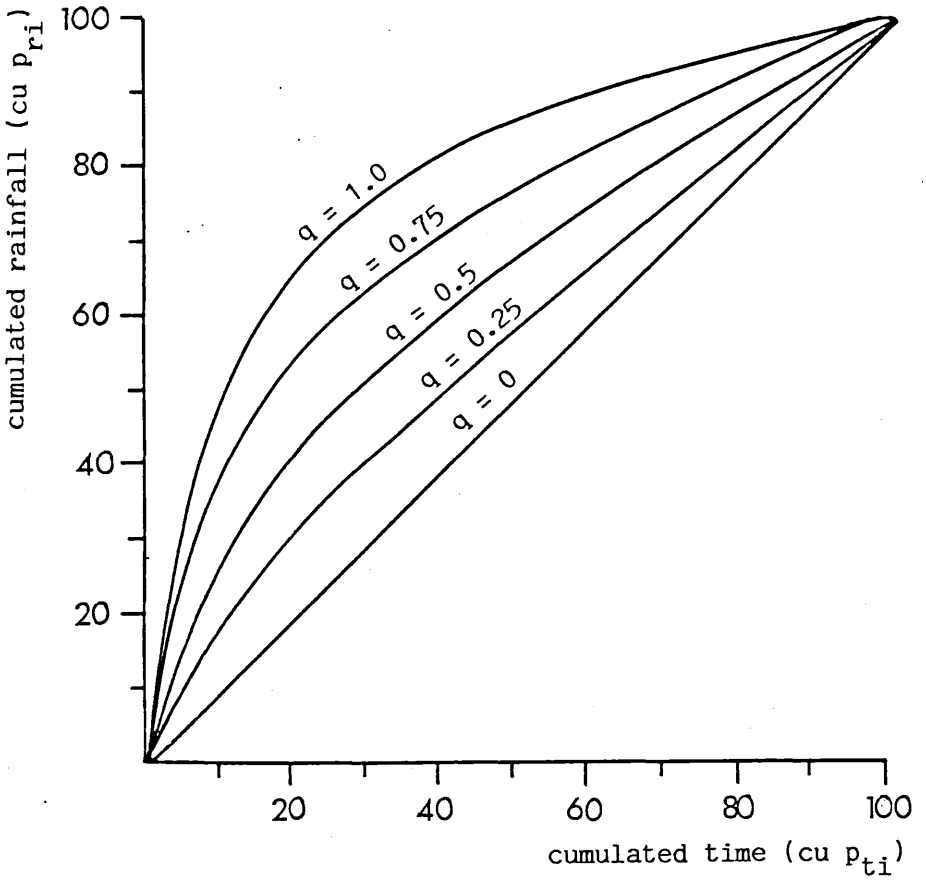

the depth of each increment was divided by 3 minutes, the duration of each sample to give the intensity (i_i mm/hour). Values for the depth and intensity of each increment of the simulated storms are presented in Table 8.2

ii) Throughfall

To calculate the total kinetic energy of the throughfall for a storm the depth of water fallen in each sample period is needed and a cumulated depth and time curve for the throughfall from any given storm must be simulated. Two cases for the timing of the loss of throughfall depth to interception were examined. The first was that interception and loss to storage occurred throughout the storm and that consequently the intensity of throughfall was consistently lower than that of the rainfall. The second case was that the intensity of throughfall would be initially lower than that of the rainfall because the canopy storage was filling but that after this the accumulation of throughfall would be similar to that of the rainfall.

Figure 7.13 illustrates the cumulated canopy storage for the single canopy and shows that for storms j10b, j12 and j20 the canopy appeared to be saturated after 15.7%, 10.8% and 14.6% respectively of the storm duration. Hence it was assumed that during the first 15% of any storm the cumulated throughfall was less than the rainfall while the canopy filled.

Figures 7.17 and 7.18 show the increase in cumulated throughfall depth with cumulated time derived from the experimental data on the single and multiple canopies. Comparisons other than visual, between the rates of accumulation of throughfall and rainfall for each storm are not possible because the amount of data is small. Figure 7.17 (apart from storms j13 and j15 again) shows a remarkable similarity between the proportions of rain falling within the same percentage of storm duration for each storm. For the multiple canopy (Figure 7.18) and excepting also j16b (another small storm) there is a similar

Table 8.2 The depth (d mm) and intensity (i mm/hour) of rainfall in 20, 3 minute increments of a 4 mm storm of 1 hour duration, for q=0, 0.5 and 1.0

increment	q=0		q=0.5		q=1.0	
	d	i	d	i	d	i
1	0.20	4.00	0.799	15.98	1.398	27.96
2	0.20	4.00	0.401	8.02	0.602	12.04
3	0.20	4.00	0.276	5.32	0.352	7.04
4	0.20	4.00	0.225	4.50	0.250	5.00
5	0.20	4.00	0.197	3.94	0.194	3.88
6	0.20	4.00	0.179	3.58	0.158	3.16
7	0.20	4.00	0.167	3.34	0.134	2.68
8	0.20	4.00	0.158	3.16	0.116	2.32
9	0.20	4.00	0.151	3.02	0.102	2.04
10	0.20	4.00	0.146	2.92	0.092	1.84
11	0.20	4.00	0.141	2.82	0.083	1.66
12	0.20	4.00	0.138	2.76	0.076	1.52
13	0.20	4.00	0.135	2.70	0.072	1.44
14	0.20	4.00	0.132	2.64	0.062	1.24
15	0.20	4.00	0.130	2.60	0.060	1.20
16	0.20	4.00	0.128	2.56	0.056	1.12
17	0.20	4.00	0.126	2.52	0.053	1.06
18	0.20	4.00	0.125	2.50	0.050	1.00
19	0.20	4.00	0.123	2.46	0.047	0.94
20	0.20	4.00	0.122	2.44	0.044	0.88

concentration of most of the throughfall depth at the start each storm. When each throughfall curve is compared with the rainfall curve there are instances of both an increase in throughfall depth at the start of the storm and of a decrease at the start and throughout the storms. There is insufficient detail in the data to define the relationship between rainfall and throughfall for any time.

The intensity of throughfall samples from both canopies were plotted against the simultaneous rainfall intensity with samples taken before 15% of the duration had elapsed being identified (Figures 8.2 and 8.3). Because of the extreme range of the values the data was plotted on a log-log scale. Throughfall intensity values were regressed against rainfall to test the relationship between the two and were found to be not significantly different from 1.0 (Table 8.3).

Considering all the throughfall samples together the throughfall intensities may be seen to be the same as rainfall intensities for any given time and not constantly lower than that of the rainfall as is suggested by the first option. Although three of the samples taken during the first 15% of the storms were below the regression line the rest were not implying that either the intensity of throughfall is not always reduced at the start of the storm, as is suggested by the second option, or the reduction was not recorded.

The regression of multiple canopy throughfall intensity on rainfall intensity again shows a high correlation but here the gradient of the line is significantly different from 1.0 and it is less than 1.0, suggesting that the intensity of the throughfall is always less than that of the rainfall. However it has been shown in Chapter Five that in this particular complete canopy rain forest site, amounts of water larger than those expected are being directed away from the throughfall space into what is supposed to be stemflow. Consequently with the recorded throughfall depths being abnormally low, the intensity of throughfall of each sample is probably abnormally low. Again those samples taken during the initial 15% of storm duration have been identified but no clear pattern of lower

Figure 8.2 Plotting the intensity of single canopy throughfall (It mm/hour) against simultaneous rainfall intensity (Ir mm/hour) for all storms

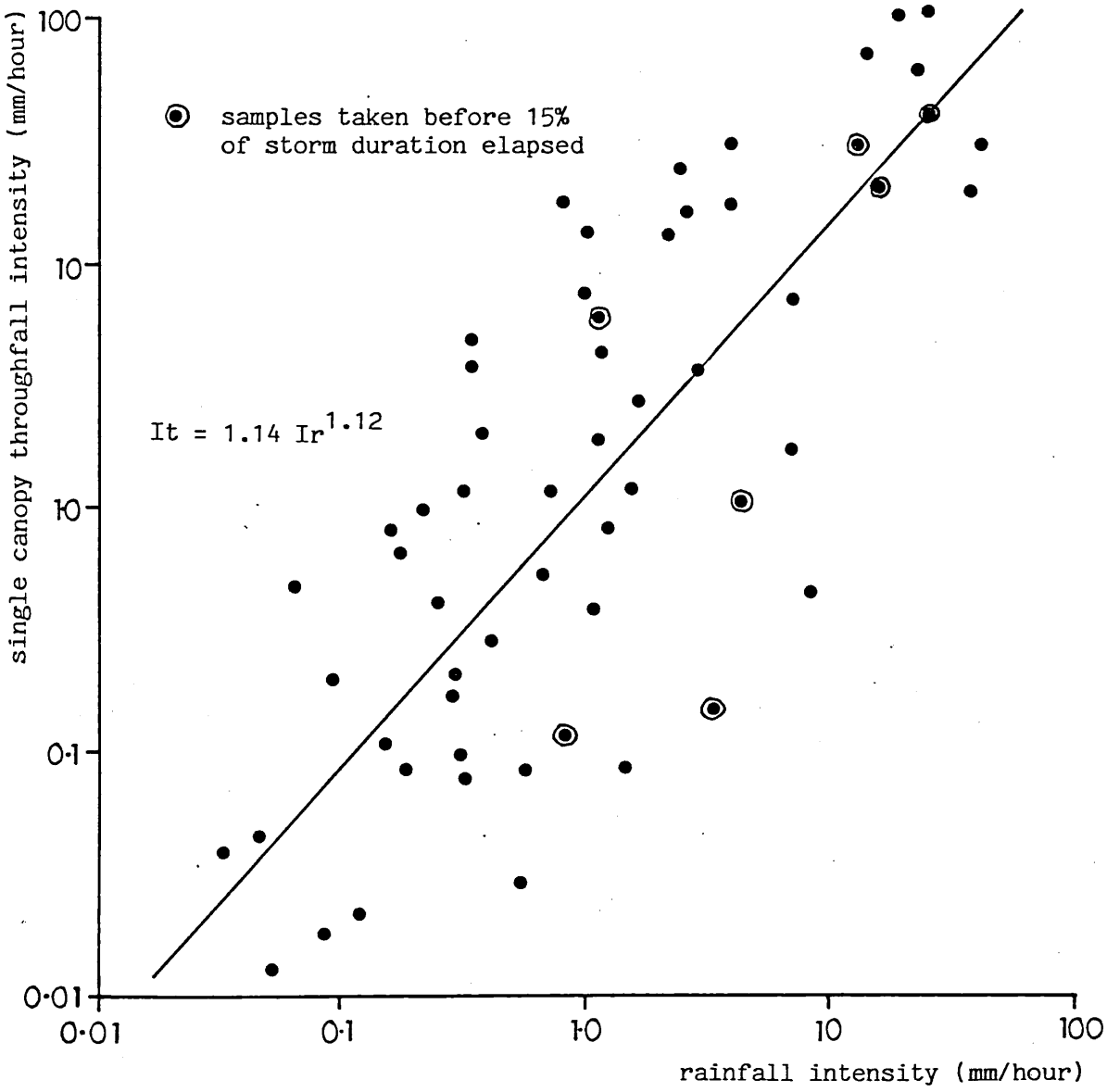

Figure 8.3 Plotting the intensity of multiple canopy throughfall (It mm/hour) against simultaneous rainfall intensity (Ir mm/hour) for all storms

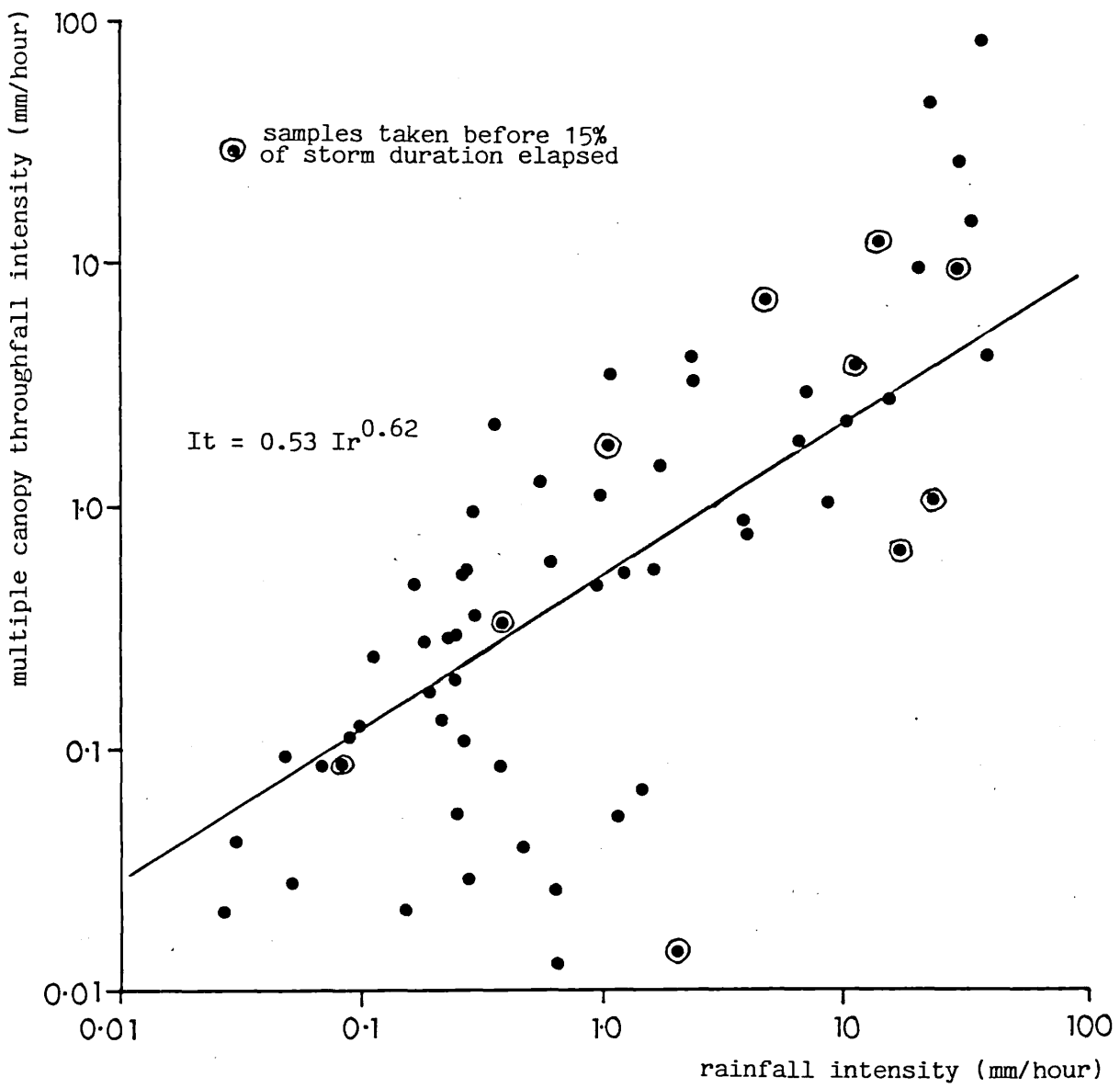

Table 8.3 Analysis of the relationship between rainfall intensity (I_r mm/hour) and coincident single and multiple canopy throughfall intensity (I_t mm/hour)

regression equation	r	t	sig. level
single canopy			
$\log_e I_t = 0.135 + 1.12 \log_e I_r$	0.79	1.12	not sig. at 95%
multiple canopy			
$\log_e I_t = 0.624 \log_e I_r - 0.642$	0.80	4.13	99.9%

t-test to test whether the slope of the regression is significantly different from 1.0

throughfall than rainfall intensities emerges.

Hence, while there is evidence under the multiple canopy that rain is lost to interception throughout the storms, there is no evidence for it under the single canopy. It was assumed that the loss to interception occurs at the start of the storm and that the intensity of simulated samples is reduced during the first 15% of the storm and thereafter it was the same as the rainfall. Hence, if R is the total depth of rain fallen during the first 3 increments each of depth r_i,

$$R = \sum_{i=1}^{3} r_i \qquad [8.4]$$

then the total depth of throughfall (T) is R less the interception capacity (I), T = R-I. Hence to calculate the depth of throughfall in each of the first three increments, T_i, the residual rainfall which has not been lost to interception is distributed in proportion to the amount of rain falling,

$$T_i = T \frac{r_i}{R} \qquad [8.5]$$

For the remainder of the increments, the throughfall intensity is the same as that of the throughfall.

When q = 0, the cumulated depth of rain in the first 15% of the storm was less than the interception capacity, therefore in these cases it was assumed that the storage capacity was filled over the first 25% of the storm duration. The depths of throughfall in each increment T_i for canopy interception capacities of 0.6 mm and 0.7 mm are given in Table 8.4.

Table 8.4 The depths of single and multiple canopy throughfall (mm) in 20, 3 minute increments of a 4 mm storm of 1 hour duration for q=0, 0.5 and 1.0

increment	single canopy			multiple canopy		
	q			q		
	0.0	0.5	1.0	0.0	0.5	1.0
1	0.08	0.474	1.041	0.06	0.420	0.982
2	0.08	0.238	0.449	0.06	0.211	0.423
3	0.08	0.164	0.262	0.06	0.145	0.247
4	0.08	0.225	0.250	0.06	0.275	0.250
5	0.08	0.197	0.194	0.06	0.197	0.194
6	0.20	0.179	0.158	0.20	0.179	0.158
7	0.20	0.167	0.134	0.20	0.167	0.134
8	0.20	0.158	0.116	0.20	0.158	0.116
9	0.20	0.151	0.102	0.20	0.151	0.102
10	0.20	0.146	0.092	0.20	0.146	0.192
11	0.20	0.141	0.083	0.20	0.141	0.083
12	0.20	0.138	0.076	0.20	0.138	0.076
13	0.20	0.135	0.072	0.20	0.135	0.072
14	0.20	0.132	0.062	0.20	0.132	0.062
15	0.20	0.130	0.060	0.20	0.130	0.060
16	0.20	0.128	0.056	0.20	0.128	0.056
17	0.20	0.126	0.053	0.20	0.126	0.153
18	0.20	0.125	0.050	0.20	0.125	0.050
19	0.20	0.123	0.047	0.20	0.123	0.047
20	0.20	0.122	0.044	0.20	0.122	0.044
total	3.4	3.4	3.4	3.3	3.3	3.3

single canopy interception loss = 0.6 mm

multiple canopy interception loss = 0.7 mm

3) Variation in throughfall kinetic energy with the height (H) of the canopy

The calculation of the kinetic energy of a throughfall sample includes the velocity of fall (s_i) of each drop in that sample (Equation [5.5]). The velocity depends on the drop diameter and hence the kinetic energy of throughfall from a canopy of any height may be simulated by varying s_i once the drop diameters have been ascertained.

i) Change in drop-size distribution with canopy height

In this study the drop-size distribution of two different canopies have been measured. The analysis of drop sizes (Figure 6.8 and Equation [6.6]) shows that the kinetic energy/mm/m^2 of any throughfall sample is higher with drop-size distributions of larger standard deviations and hence the incidence of large drop sizes. If all drops are assumed to be falling at terminal velocity the kinetic energy calculated from the multiple canopy is significantly higher than that from the single canopy (Table 7.5). This suggests that different plant structures may produce a different range of drop sizes from the water that has been intercepted. These different structures may be typical of distinct strata in the forest canopy and the accuracy of a simulation would be increased by selecting the correct drop-size distribution. In the cases studied it appears that the understorey of palms and samplings with larger leaves and different angles of inclination produce larger drops than the upper tree storey. There is not enough information to tell if the same drop-size distributions could be produced by differently structured canopies or if the drop-size distributions are specific to a particular plant form. However by using the drop-size distributions measured and changing the velocity of fall a variety of canopy heights may be simulated.

ii) Values for kinetic energy/mm/m^2 from canopies of different height

In the previous chapter it was shown that all throughfall samples

from both canopies from any storm and after any duration could be divided into two distinct groups, one with a high mean kinetic energy/mm/m² and the other with a low mean energy. The value of the mean energy for each group is determined by the height of the canopy. In addition to the two canopy heights (H) of 8 m and 3 m examined with the mean kinetic energy determined by the canopy height and particular drop-size distributions, a third canopy was simulated, where H = 5 m. The single canopy drop-size distributions were used in the simulation, the velocity of fall of each drop size class after 5 m fall being subsituted in [5.5]. This intermediate canopy thus represents a canopy of the same structure, leaf size shape and orientation as the single canopy, but of a lower height.

The descriptions of the upper and lower energy groups, the mean and standard deviation of all values, for the canopy of each height are sumarised in Table 8.5 and the distributions illustrated in Figure 8.4 where it may be seen that each group approximates a normal distribution.

4) Kinetic energy changes during the storm

i) Rainfall

A method for simulating the change in rainfall intensity through a storm has been discussed above. The relationship between rainfall intensity and kinetic energy may be taken straight from Chapter Seven (Table 7.6) where a regression of kinetic energy (k.e. J/mm/m²) for each rainfall sample against rainfall intensity (I mm/hour) produced the equation

$$\bar{k.e.}_i = 15.5 + 2.46 \log_e I_i \qquad [8.8]$$

where $\bar{k.e.}_i$ is the mean kinetic energy/mm/m² for any value of I.

Table 8.5 Descriptions of the distribution of kinetic energy ($J/mm/m^2$) values in the upper and lower energy groups for canopies of height 8 m, 5 m, and 3 m

height	upper group			lower group		
	range	mean	s.d.	range	mean	s.d.
8 m	>20 $J/mm/m^2$	33.12	4.18	<20 $J/mm/m^2$	10.12	4.50
5 m	>15 $J/mm/m^2$	22.68	4.05	<15 $J/mm/m^2$	5.04	4.72
3 m	>10 $J/mm/m^2$	21.05	1.89	<10 $J/mm/m^2$	6.62	2.37

Figure 8.4 Frequency distribution of the energy of throughfall samples (J/mm/m²) for canopy heights of 8 m, 5 m and 3 m

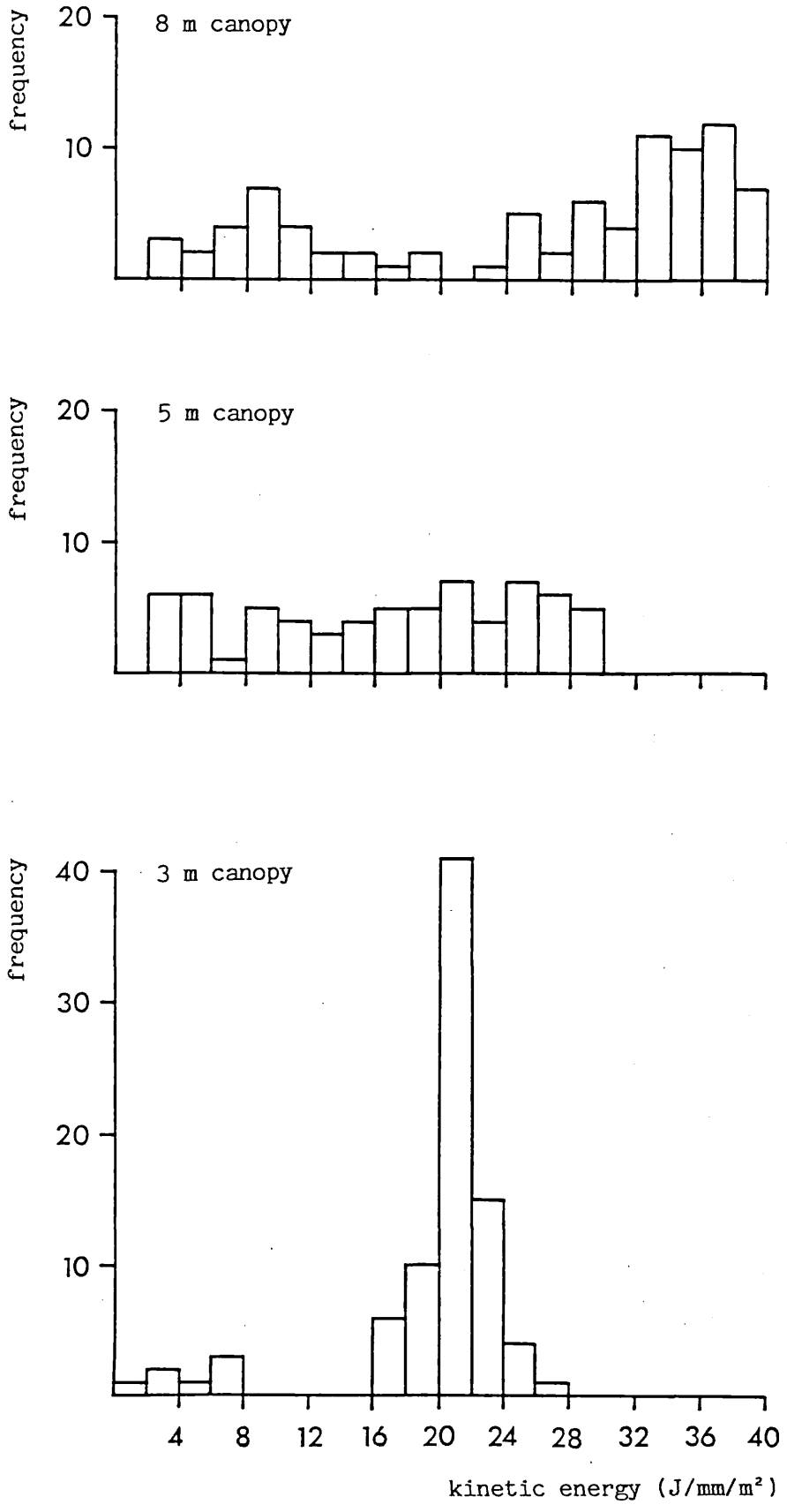

There is a good correlation between the two ($r = 0.76$) and a standard deviation about the regression line of 4.55 ($J/mm/m^2$). This sort of relationship is well documented and other workers have calculated differing values for the constants for different rainfall types. For any rainfall intensity (I_i) a distribution of values of kinetic energy/mm/m^2 may be obtained from this expression.

ii) Throughfall

Unlike rainfall, the kinetic energy of throughfall has been found to be independent of rainfall intensity and varies only between one of two distributions. It was suggested that the energy group for each canopy was dependent on the cumulated storage at the time the sample was taken. Table 7.11 showed the cumulated percentage of the total storm duration elapsed by the end of each sample and indicated those where the throughfall from the single and multiple canopies was in the lower energy group. Table 8.6 groups this data into 10% increments of storm duration and gives the probability, for a given time of the throughfall sample collected being in the high energy group. Also included are all those samples which were taken after rainfall had ceased. The probabilities of a high energy sample in each 10% time increment are plotted in Figure 8.5. From this information the time-dependent model of kinetic energy change of throughfall was developed.

It will be noted that in both sites there was a greater probability that any sample to be in the high rather than the low energy group. Under the multiple canopy 89.4% of the samples were in the high energy group and under the single canopy there were 67.7%. It is suggested that the frequency of occurrence of low energy samples reflects the thickness of the canopy, or the density of vegetation within the canopy. It was shown in Chapter Six that the kinetic energy ($J/mm/m^2$) of a sample was defined from the drop-size distribution of the sample, and that those samples of high level energy tended to be those in which large drops from the canopy had

Table 8.6 The frequency of single and multiple canopy throughfall samples in upper (U) and lower (L) energy groups for 10% increments of rainfall duration (%T)

%T	single canopy			multiple canopy		
	U	L	%U	U	L	%U
0 - 9	7	3	70	6	2	75
10 - 19	5	4	56	8	1	89
20 - 29	9	1	90	7	1	88
30 - 39	6	1	86	6	0	100
40 - 49	8	0	100	6	0	100
50 - 59	5	0	100	7	0	100
60 - 69	1	4	20	6	0	100
70 - 79	3	0	100	5	0	100
80 - 89	2	2	50	4	0	100
90 - 99	3	4	43	6	1	86
100 - 109	2	0	100	3	0	100
110 - 119	2	1	50	3	0	100
120 - 129	0	1	0	3	0	100
130 - 139	0	1	0	2	0	100
140 - 149	1	2	33	2	1	67
150 - 159	1	2	33	1	0	100
160 - 169	1	1	50	1	0	100
170 - 179	0	1	0	1	0	100
180 - 189	1	0	100	1	1	50
mean probability in each of three stages						
0 - 35%			0.77			0.86
36 - 60%			1.00			1.00
60% +			0.47			0.93

Figure 8.5 Plotting the percentage of throughfall samples in the high energy group for 10% increments of storm duration, against time elapsed

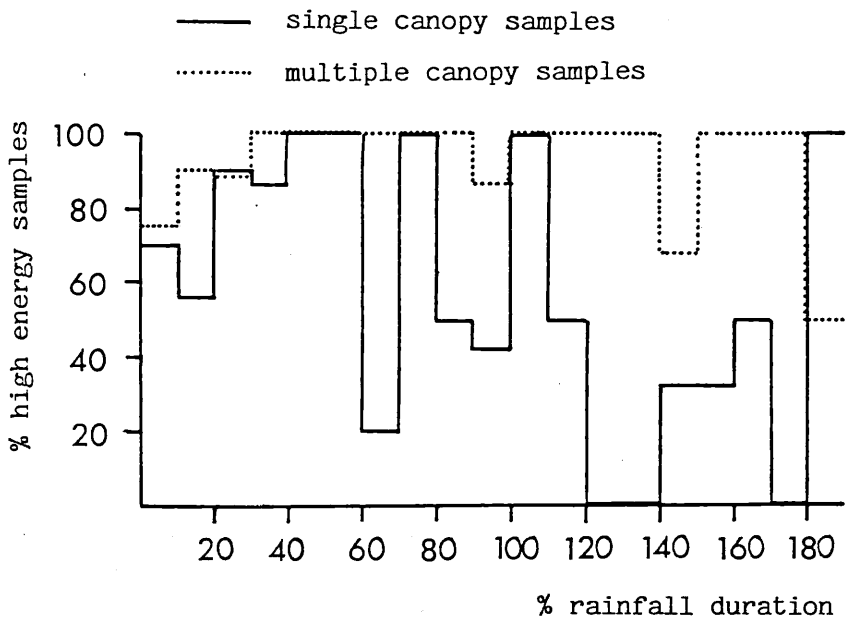

Figure 8.6 The probability of a high energy sample in each of three periods during a storm, under the single and multiple canopies

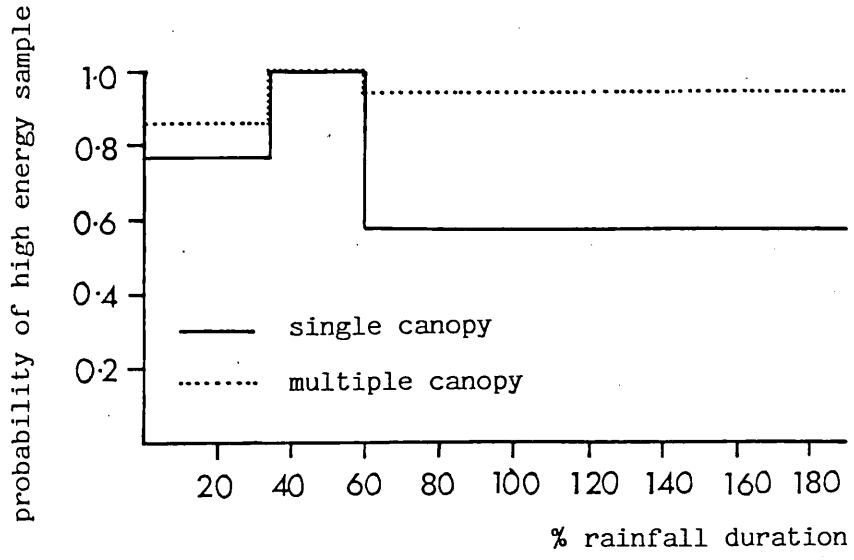

been recorded. Hence the more uniform the size of the drips of water from the canopy, the lower the probability of a low kinetic energy sample. If the single and multiple canopy sites may be taken to represent examples of moderate to high drip regulation respectively then any kind of canopy regulation may be simulated. The simulation may range from those where the only water penetrating to the ground surface has dripped off from a storage point, to those where the canopy is so thin and the interception capacity so low that the frequency of high energy drips is low.

To simulate the incidence of high and low energy increments throughout the storm there were several possible approaches. The first would have been to ignore any temporal change in the probabilities so that each increment had the same probability of a high energy level. However it was felt that previous work in this thesis justified dividing the storm into periods of differing high energy probability so that a filling, saturated and emptying canopy may produce a different range of kinetic energy values. Figure 8.5 shows that between 36 and 60% of all the storm durations all samples collected under both canopies belonged to the high energy group, but the probability of a low energy sample increased in the period 0 to 35% and in the period 60 to 100%. Unfortunately the data available is of sufficient detail for the change in probability within these begining and end periods to be ascertained in more detail. It is suggested that future evidence will show that the probability of high energy values increases as the storm progresses to canopy saturation and then decreases as the canopy drains. However on the basis of current evidence no progressive change in the probability could be detected and justified.

Each simulated storm was divided into three periods, each with a different probability of any sample being of low or high energy (P_1, P_2 and P_3) (Figure 8.6). For the single and multiple canopies the critical values for the probability in each period of the storm are given in Table 8.6. In the middle period, from 36 - 60% of the storm duration, all samples fell in the high energy group, hence $P_2 = 1.0$.

However at the beginning and the end of the storm there were differing probabilities of any sample having an energy value of the higher group. For the beginning period of the storm, P_1 from 0 to 35% of the duration there was a 0.73 probability of a high energy sample under the single canopy and a 0.86 probability under the multiple canopy. During the last 40% of the storm, the probability, P_3, of a high energy value being recorded under the single canopy was 0.47 and was 0.93 under the multiple canopy.

Differences in the probabilities of high energy values at the beginning and end of the storm may be accounted for by the idea put forward in Chapter Seven that high energy drops fell from the canopy when the canopy was saturated and water was draining from the leaves or when individual water stores could be drained by the impact of drops from above. By varying these probabilities at the beginning and end of storms it is possible to simulate any level of drop size regulation and change in regulation throughout a storm.

For the purposes of the simulation, the values taken for P_1, when the canopy was assumed to be filling, were 0.9, 0.7 and 0.5. When the canopy was assumed to be saturated, P_2 took 1.0 so that all the increments had high energy values. For the end of the storm, where the canopy was assumed to be draining, P_3 took values of 0.7, 0.5 and 0.3.

5) The relationship of total kinetic energy to soil splash

It was suggested in Chapter 7 that there was some evidence that the differences in drop sizes between sites produced different rates of increase in splash amount with an increase in kinetic energy. However the paucity of the data made the calculation of the exact differences difficult. To test the sensitivity of changes in splash amount to changes in the model parameters the relationship between total kinetic energy and mean splash weight for all sites was used. Hence when total kinetic energy (K.E. J/m^2) was regressed on mean

splash weight, S (g) (Table 7.16) the following equation was produced

$$S = 0.015\ K.E.^{0.71} \qquad [8.9]$$

where the correlation between the two parameters was 0.86.

Section Two The simulation procedure

This section describes the use of the canopy model to simulate the total kinetic energy of throughfall for a number of different canopy conditions. By comparing the kinetic energy of throughfall for each canopy with that of rainfall, it is possible to assess the sensitivity of the model to each parameter.

1) Description of the simulation method

Each realisation of the model represents either the rainfall or the throughfall of a single storm of depth 4 mm and duration 1 hour. Each storm is divided into 3 minute increments and for each increment a value for the kinetic energy ($J/mm/m^2$) is determined. The depth of water accumulated in each 3 minute increment is described by equation [8.1] with q taking values of 0, 0.5 and 1.0. By multiplying the kinetic energy ($J/mm/m^2$) by the cumulated depth in each sample and summing for the storm, a value of total kinetic energy for that realisation is reached.

There are three variables in the model describing the effect of a canopy on the energy of the throughfall. The variables are canopy height, H (and the implied the size distribution of the throughfall drops) and the probability of high energy throughfall increments

during the first 35% (P_1) and last 40% (P_3) of the storm duration. The value given for the kinetic energy of throughfall for any combination of P_1, P_3 and H is the mean of 100 realisations. The value given for the kinetic energy of rainfall for each pattern of intensity change is the mean of 40 realisations. The experimental data does not relate the incidence of high energy increments at the start of the storm to their incidence at the end in sufficient detail to discount some of the combinations and hence not all the realisations will represent realistic canopies.

The simulation is presented in diagramatic form in Figure 8.7 with each variable P_1, P_3 and H along the x, y and z axes respectively of a cube. The positions of the single and multiple canopies within the cube have been marked. It is expected that the total kinetic energy will decline along both the x and y axes as the proportion of increments with low kinetic energy increases. Similarly the kinetic energy will decrease along the z axis as the height of the canopy is reduced.

The same sequence of simulations of throughfall kinetic energy was repeated for each of the three patterns of rainfall intensity.

2) Examples of the simulation

i) Rainfall

Three different storms were simulated. The depth of water and intensity in each of the 20, 3 minute increments was given in Table 8.2. An example of the calculation of each realisation is given in Table 8.7, for a storm where q = 1. Equation [8.8] was used to determine the mean of the distribution of kinetic energies (J/mm/m²) ($\bar{k.e.}_i$) for the given intensity (I_i) of each increment. The distribution of values for kinetic energy/mm/m² for any intensity around the mean was assumed to be normal and described by the standard deviation. A Monte Carlo model drew values from the normal

Figure 8.7 A schematic illustration of the simulation of throughfall and rainfall kinetic energy using the canopy model

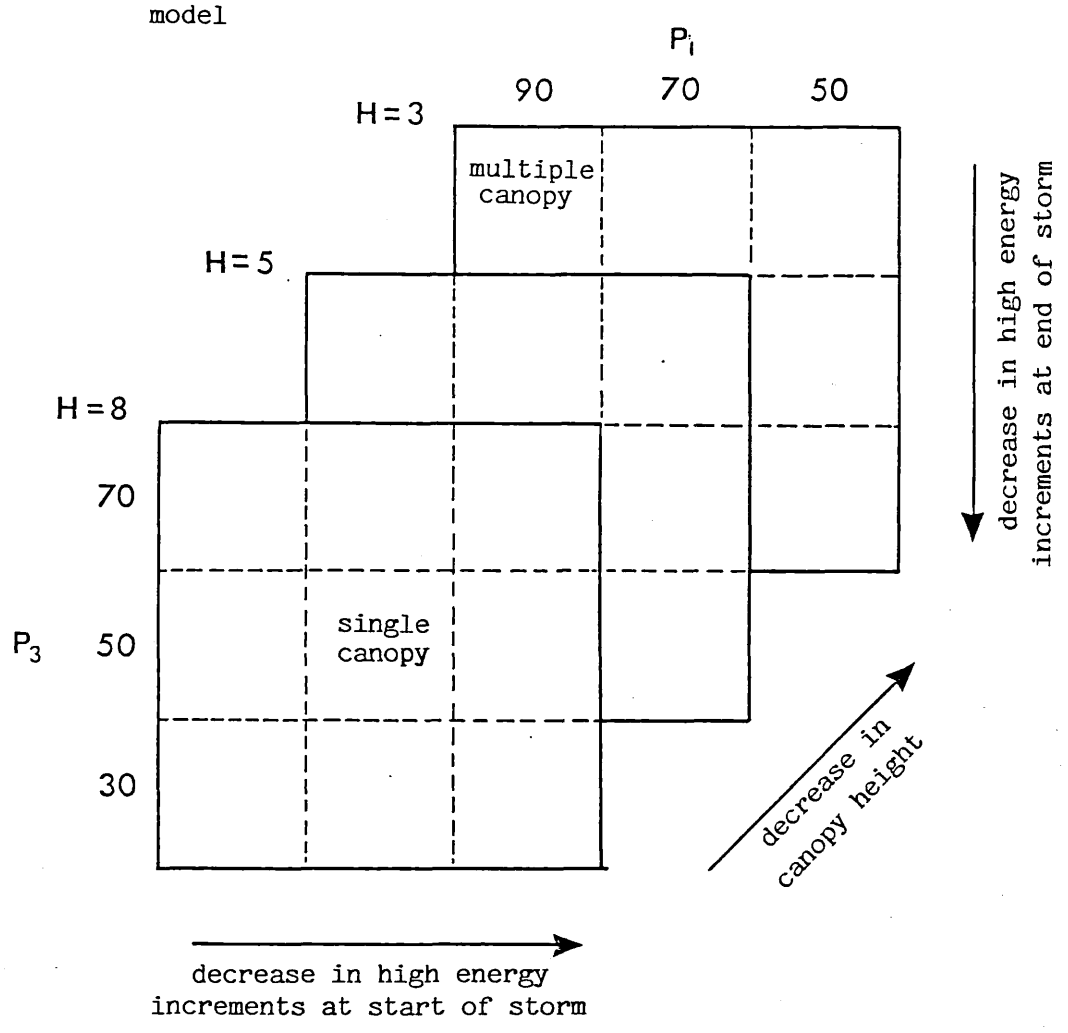

simulated for these values of q

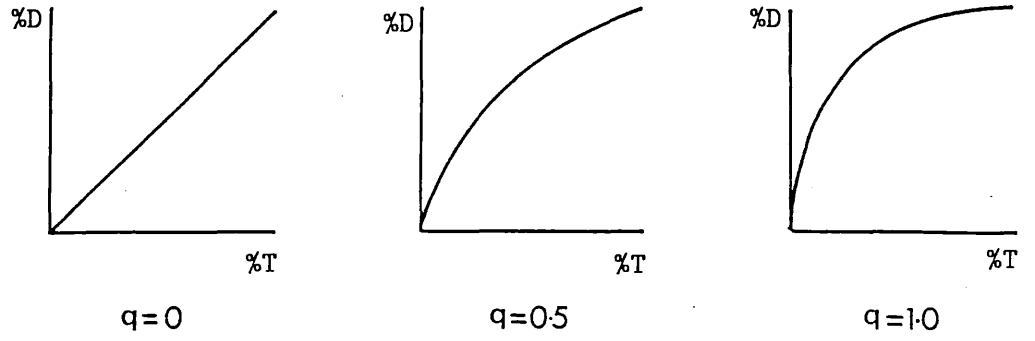

Table 8.7 A worked example of the simulation of rainfall kinetic (J/m^2) energy when q=1.0

increment	intensity (mm/hour)	$\bar{k.e.}_i$ (s.d.) ($J/mm/m^2$)	$k.e._i$ ($J/mm/m^2$)	depth (mm)	K.E. (J/m^2)
1	27.96	23.76 (4.55)	24.58	1.398	34.36
2	12.04	21.62 (4.55)	16.73	0.602	10.07
3	7.04	20.30 (4.55)	19.60	0.352	6.90
4	5.00	19.46 (4.55)	21.49	0.250	5.37
5	3.88	18.84 (4.55)	23.38	0.194	4.54
6	3.16	18.33 (4.55)	21.43	0.158	3.39
7	2.68	17.93 (4.55)	16.38	0.134	2.19
8	2.32	17.57 (4.55)	17.92	0.116	2.08
9	2.04	17.25 (4.55)	18.23	0.107	1.86
10	1.84	17.00 (4.55)	13.81	0.092	1.27
11	1.60	16.75 (4.55)	16.90	0.083	1.40
12	1.52	16.53 (4.55)	10.15	0.076	0.77
13	1.44	16.03 (4.55)	18.16	0.072	1.13
14	1.24	16.40 (4.55)	21.27	0.062	1.53
15	1.20	15.95 (4.55)	17.29	0.060	1.03
16	1.12	15.78 (4.55)	15.64	0.056	0.88
17	1.06	15.64 (4.55)	17.25	0.053	0.91
18	1.00	15.50 (4.55)	10.78	0.050	0.54
19	0.94	15.35 (4.55)	22.92	0.047	1.08
20	0.88	15.19 (4.55)	5.81	0.044	0.26
total					81.56

distribution of mean ($\bar{k.e.}_i$) and standard deviation 4.55 J/mm/m² for the cumulated kinetic energy of each increment ($k.e._i$).

To calculate the total kinetic energy (K.E.) for each realisation the values for $k.e._i$ were multiplied by the depth of rain in that increment r_i hence

$$K.E. = \sum_{i=1}^{20} k.e._i \times r_i \qquad [8.10]$$

For each value of q there were 40 different realisations of the model. The difference between the total kinetic energy of each realisation is due to the different random numbers selected by the Monte Carlo model for $k.e._i$.

ii) Throughfall

A worked example of one realisation of the throughfall simulation is given in Table 8.8, where H = 8m, P_1 = 0.9, P_3 = 0.7 and q = 1. The kinetic energy of throughfall is not determined by the rainfall intensity but depends on the time elapsed, hence the throughfall simulation has an initial step not included in the rainfall simulation. As with the rainfall simulation the storms under the canopies were divided into 20, 3 minute increments, each increment with a given probability of the throughfall being in the high energy group (P_i). To determine which energy group the increment was in, numbers between 0.0 and 1.0 were drawn at random from a uniform field. Any number up to and including the value of P_i decided a value for $\bar{k.e.}_i$ from the upper energy distribution. Any number above the critical level meant that the lower energy distribution was selected.

As in the case of the rainfall, there is a range of values in each group defined by the mean and standard deviation. The same Monte Carlo model was used to select values at random from the distribution

Table 8.8 A worked example of the simulation of throughfall kinetic energy (J/m^2) where H=8, q=1.0, P_1=0.9 and P_3=0.7

increment	P_1, P_3	$\bar{k.e.}_i$ (s.d.) ($J/mm/m^2$)	$k.e._i$ ($J/mm/m^2$)	depth (mm)	K.E. (J/m^2)
1	0.9	33.12 (4.18)	34.69	1.041	36.11
2	0.9	33.12 (4.18)	29.88	0.049	13.42
3	0.9	33.12 (4.18)	29.18	0.262	7.65
4	0.9	33.12 (4.18)	32.15	0.250	8.04
5	0.9	33.12 (4.18)	28.55	0.194	5.54
6	0.9	33.12 (4.18)	31.46	0.158	4.97
7	0.9	10.12 (4.50)	9.18	0.134	1.23
8	1.0	33.12 (4.18)	33.00	0.116	4.29
9	1.0	33.12 (4.18)	23.27	0.102	2.37
10	1.0	33.12 (4.18)	33.78	0.092	3.11
11	1.0	33.12 (4.18)	28.55	0.083	2.37
12	1.0	33.12 (4.18)	31.34	0.076	2.38
13	0.7	33.12 (4.18)	35.82	0.072	2.22
14	0.7	10.12 (4.50)	11.53	0.062	0.83
15	0.7	33.12 (4.18)	37.22	0.060	2.23
16	0.7	10.12 (4.50)	9.68	0.056	0.54
17	0.7	33.12 (4.18)	35.90	0.053	1.90
18	0.7	10.12 (4.50)	9.59	0.050	0.48
19	0.7	33.12 (4.18)	33.52	0.047	1.58
20	0.7	10.12 (4.50)	11.63	0.044	0.51
total					101.78

described ($k.e._i$). The total kinetic energy of each realisation was calculated using equation [8.10] multiplying the kinetic energy/mm/m² by the depth of each increment.

For each combination of P_1, P_3, H and q, there were 100 separate realisations of the model. Each realisation repeated the selection of ($\bar{k.e.}_i$) from P_1 and P_3. Consequently the variation in values for total kinetic energy is expected to be greater than that of the rainfall because each realisation will have a different selection of $k.\bar{e}._i$ and not just $k.e._i$.

Section Three Discussion of the simulation results

The results of the simulations are presented in Table 8.9 (where q=0), Table 8.10 (where q=0.5) and Table 8.11 (where q=1.0). For each combination of parameters, the result presented is the mean kinetic energy (J/mm/m²) of 40 realisations of the rainfall model and 100 realisations of the throughfall model. The standard deviation of each distribution is given. For each value of q, the throughfall kinetic energy is expressed as a percentage of rainfall energy to highlight the effect of different canopy parameters of the change in throughfall energy. Complete sets of combinations of P_1 and $P_3$are given for the 8 m canopy. It is assumed that the same patterns of energy change will also occur at the other two canopy heights.

1) Inherent variability of kinetic energy for any given set of paremeters

For any given combination of parameters there is a distribution of resulting kinetic energies. This variability is inherent in the model and it operates in addition to variability due to the changing parameters themselves. Variability in the rainfall kinetic energy is

Table 8.9 The results of the simulation of rainfall and throughfall kinetic energy (J/m^2) (s.d.) where q=0, and H, P_1 and P_3 are varied

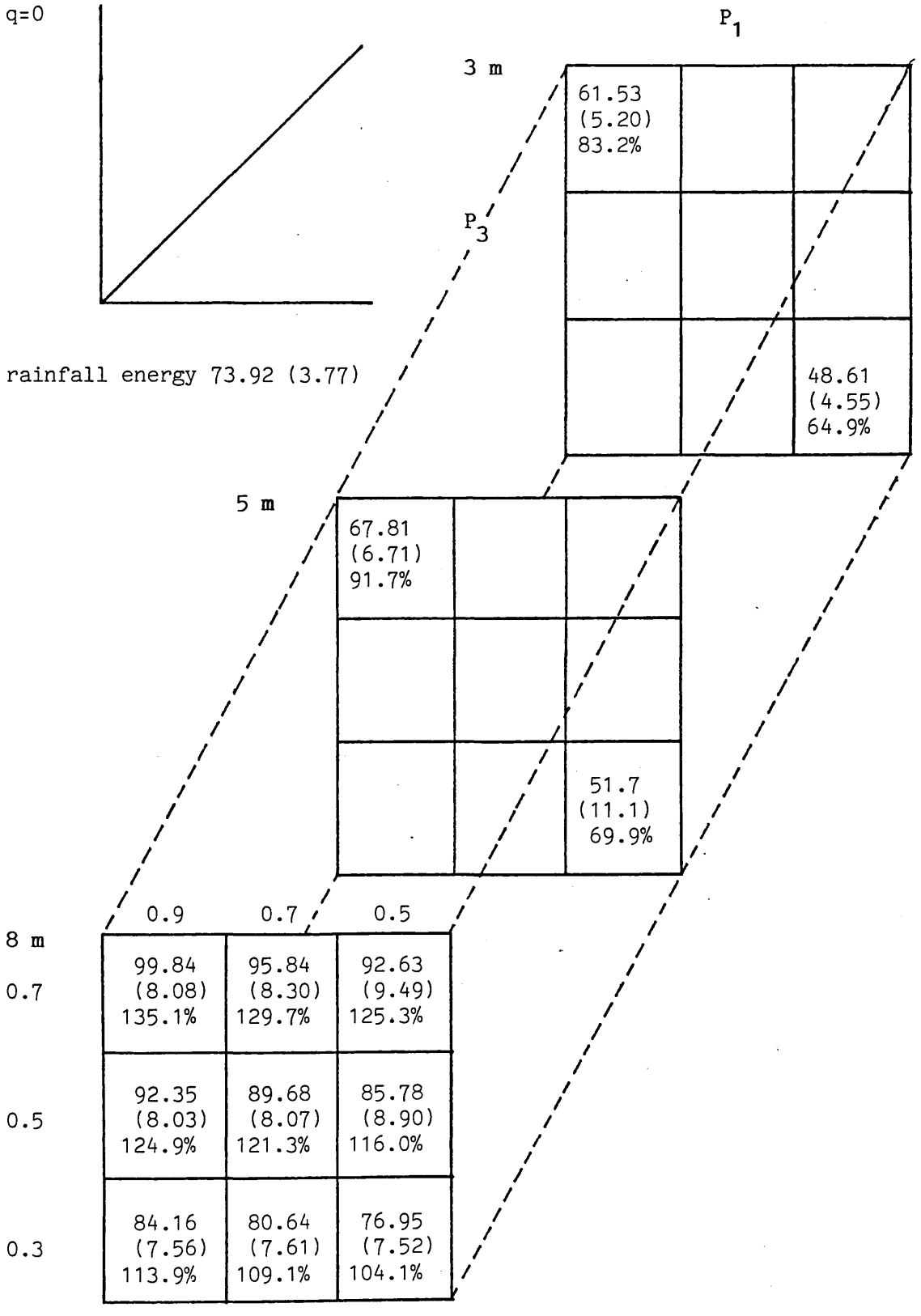

Table 8.10 The results of the simulation of rainfall and throughfall kinetic energy (J/m^2) (s.d.) where q=0.5, and H, P_1 and P_3 are varied

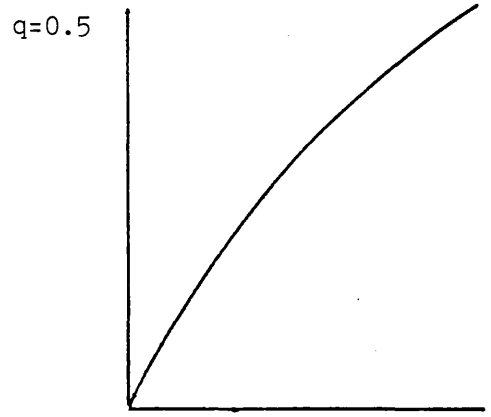

rainfall energy 76.87 (4.30)

H	P_1	P_3 = 0.9	P_3 = 0.7	P_3 = 0.5
3 m	0.7	62.76 (4.37) 81.6%		
	0.5			
	0.3			48.02 (5.55) 62.5%
5 m	0.7	69.13 (3.03) 89.9%		
	0.5			
	0.3			51.58 (7.19) 67.1%
8 m	0.7	101.63 (7.12) 132.2%	93.86 (8.10) 122.1%	87.10 (10.30) 113.3%
	0.5	96.78 (7.65) 125.9%	90.11 (8.33) 117.2%	82.99 (9.80) 108.0%
	0.3	91.55 (7.06) 119.1%	84.49 (7.93) 109.9%	77.30 (9.20) 100.6%

Table 8.11 The results of the simulation of rainfall and throughfall kinetic energy (J/m^2) (s.d.) where q=1.0, and H, P_1 and P_3 are varied

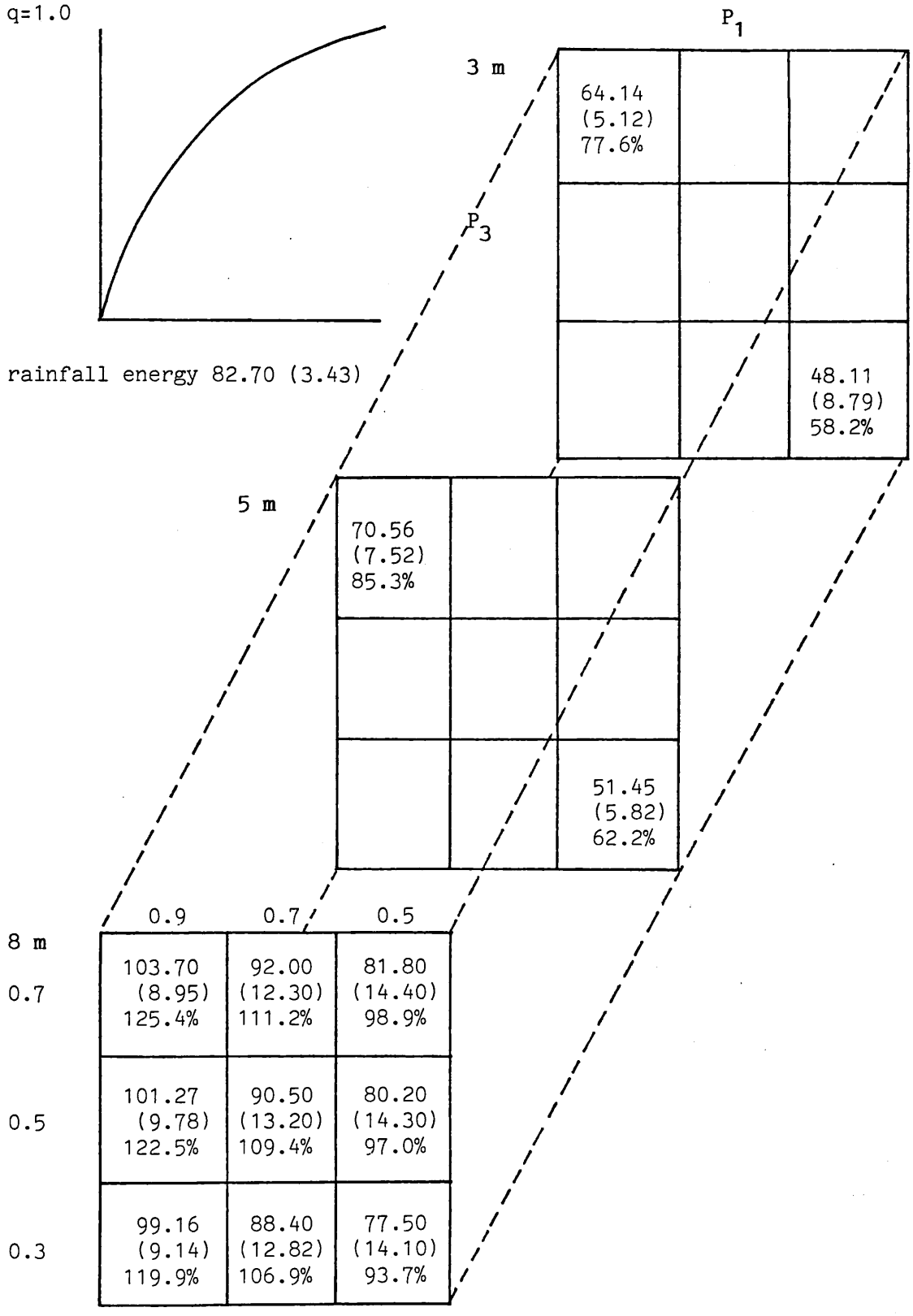

due to the random selection of simulated values for kinetic energy ($k.e._i$) from the distribution described by the mean kinetic energy ($\bar{k.e.}_i$) and standard deviation for each intensity. This selection of different values for $k.e._i$ gave standard deviations of the resulting distributions of 5.1%, 5.6% and 4.1% for values of q=0, 0.5 and 1.0 respectively.

In addition to the random selection of $k.e._i$ from the $\bar{k.e.}_i$ of each energy group, the variability of kinetic energies of throughfall for each combination of parameters depends on the selection of different energy groups for each increment dependent on P_1 and P_3. Hence for each combination of parameters, the standard deviation of the throughfall kinetic energy values are higher than those of the rainfall and are commonly between 7% and 11%. As would be expected, the spread of values for each combination is greater as P_1 decreases from 0.9 to 0.5 and as P_3 decreases from 0.7 to 0.3, hence the proportion of low and high energy increments becomes equal. The standard deviation also increases as q tends to 1 for reasons which will be discussed later.

2) Sensitivity of throughfall energy to individual parameters

i) Sensitivity of total rainfall kinetic energy to q

Despite the constant storm depth and duration of this simulation, there is an increase in the kinetic energy of throughfall as the pattern of rainfall intensity changes from uniform to inversly logarithmic. Figure 8.8 shows that when q changes from 0.0 to 0.5 there is a 4% increase in the total energy. When q changes from 0.0 to 1.0 the increase is 11.9%. The reason for this increase with the changing pattern of intensity is simple. When q=0, the depth of water is the same in each increment and all increments are of equal weight in determining the total kinetic energy. As q increases so does the depth of water in the initial increment. When q=1, 35% of the storm depth falls in the first increment, and i_1 is more than twice the

Figure 8.8 The percentage change in rainfall energy (J/m^2) resulting from a change in q

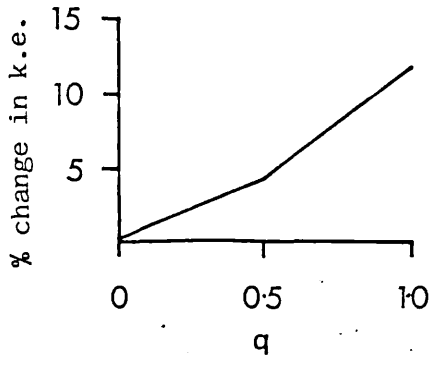

Figure 8.9 The kinetic energy of throughfall expressed as a percentage of rainfall energy, plotted against variation in P_1 for each value of P_3 and q

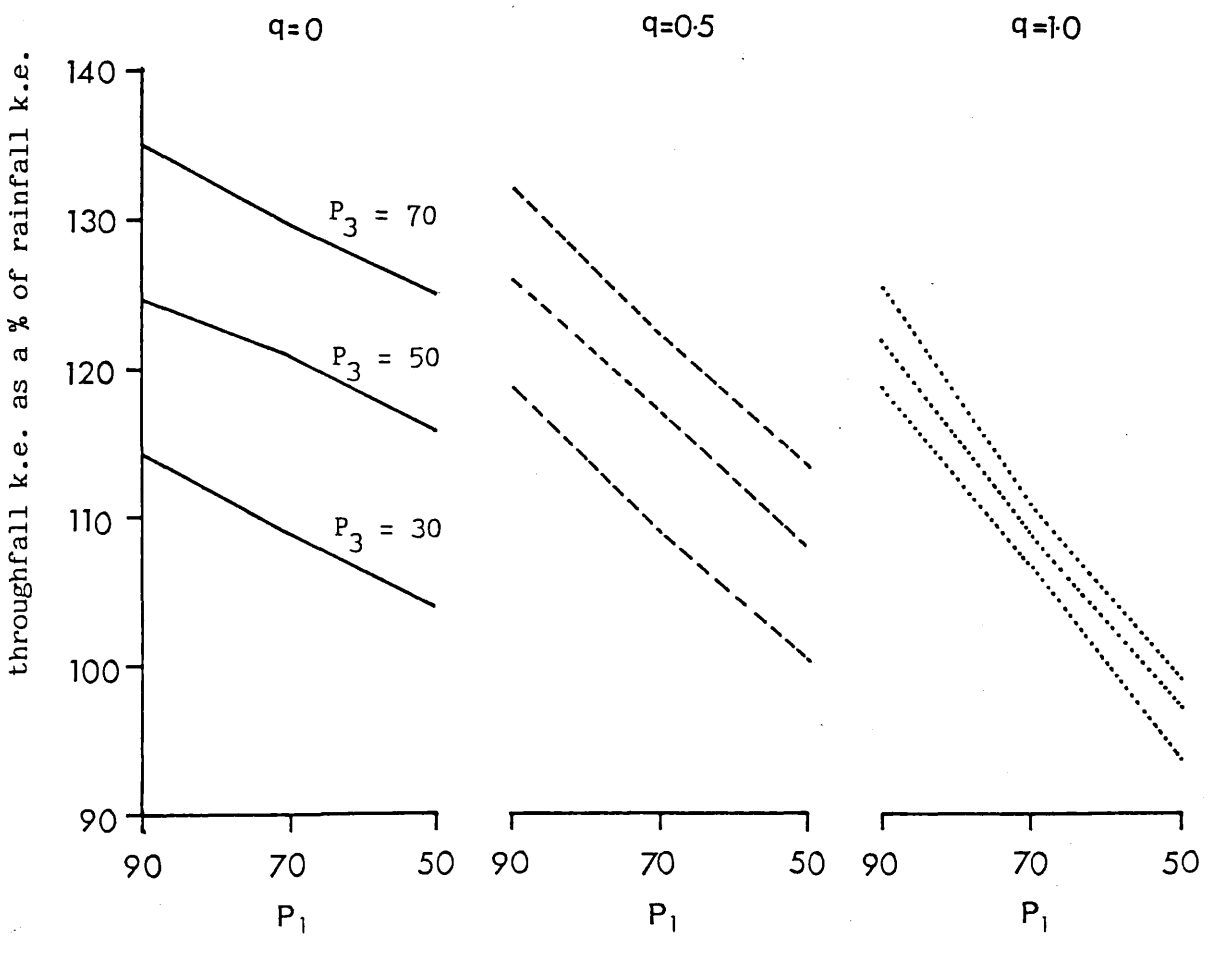

intensity of any other increment with a correspondingly high value for $\bar{k.e.}_i$. In Table 8.7 where a worked example of the calculation of kinetic energy was presented, 42% of the total kinetic energy was accounted for by the first increment.

ii) Sensitivity of throughfall kinetic energy to P_1 and P_3

Figure 8.9 shows the mean kinetic energy, when H=8 m, expressed as a percentage of rainfall energy plotted against the value of P_1 for each value of P_3 and for q=0, 0.5 and 1.0. The results are as expected, for each value of q, and with P_3 held constant, as P_1 decreases the value of the kinetic energy relative to the rainfall energy also decreases. When q=0, H=8 m and P_3=0.7, the 45% change in P_1, from 0.9 to 0.5, causes a 9.8% difference in the throughfall kinetic energy relative to rainfall energy. When q=0.5 and 1.0 the differences are 18.9% and 26.5% respectively. Similarly as P_3 decreases with P_1 held constant, so the kinetic energy also decreases. When q=0, H=8 m, and P_1 is held at 0.9 the 57% change in P_3, from 0.7 to 0.3, causes a 21.6% difference in throughfall energy relative to rainfall energy. When q=0.5 and 1.0 the differences are 13.1 and 5.5% respectively. With each decrease in P_1 or P_3, there is an increasing probability of low energy increments during the start of the storms.

iii) Sensitivity of throughfall kinetic energy to q

For a given value of P_3, and change in P_1 there is a greater change in the kinetic energy as q increases. For instance when q=0 and P_3=70, the change in P_1 causes a 9.8% decrease in the kinetic energy of throughfall relative to rainfall. When q=1 and P_3=70, the same change in P_1 causes a 26.5 change in throughfall relative to rainfall energy. These differences in the rates of change in energy with P_1 and q are due to the reasons outlined above. As q increases, so does the relative importance the kinetic energy/mm/m^2 of the first increment in determining the total kinetic energy. Therefore with a

decreasing probability of the first increment having a high energy there is an increasing probability of most of the water falling at a low energy value.

With increasing value of q the influence of P_3 on determining the total kinetic energy decreases. When all increments are of equal weight in determining kinetic energy (when q=0) the choice of P_3 is of the same importance as the choice of P_1. However as q tends to 1.0, the depth of water in each increment at the end of the storm becomes proportionlly smaller and so the choice of P_3 has less influence on the total kinetic energy. This is demonstrated by the differences in distance between the lines for each value of q in Figure 8.9.

iv) Sensitivity of throughfall energy to H

For any combination of P_1 and P_3, a reduction in the height of the canopy causes a reduction in the kinetic energy. Figure 8.10 shows the kinetic energy of throughfall expressed as a percentage of storm energy plotted against canopy height for values of P_1, P_3 of 0.9, 0.7 and 0.5, 0.3. When q=0, the change in H, from 8 m to 3 m caused for the first combination of P_1 and P_3 a reduction in the throughfall kinetic energy from 135.1% to 83.2% of rainfall energy a difference of 52%. For the other combination of P_1 and P_3 the decline was from 104.1% to 64.9%, a difference of 39.29%. A similar pattern of decrease is observed for all values of q.

3) Sensitivity of the throughfall model to each parameter

For each storm type the model has been used to simulate a variety of canopies and a range of kinetic energies for the throughfall have been calculated. For q=0, the range of throughfall energy is from 135.1% to 64% of rainfall energy, a difference of 70.2. To assess the comparative sensitivity of the model to each parameter for q=0 the given ranges of each parameter, H (8 to 3), q (0.0 to 1.0), P_1 (0.9 to

Figure 8.10 The kinetic energy of throughfall expressed as a percentage of rainfall energy, plotted against H for values of P_1,P_3 of 90,70 and 50,30

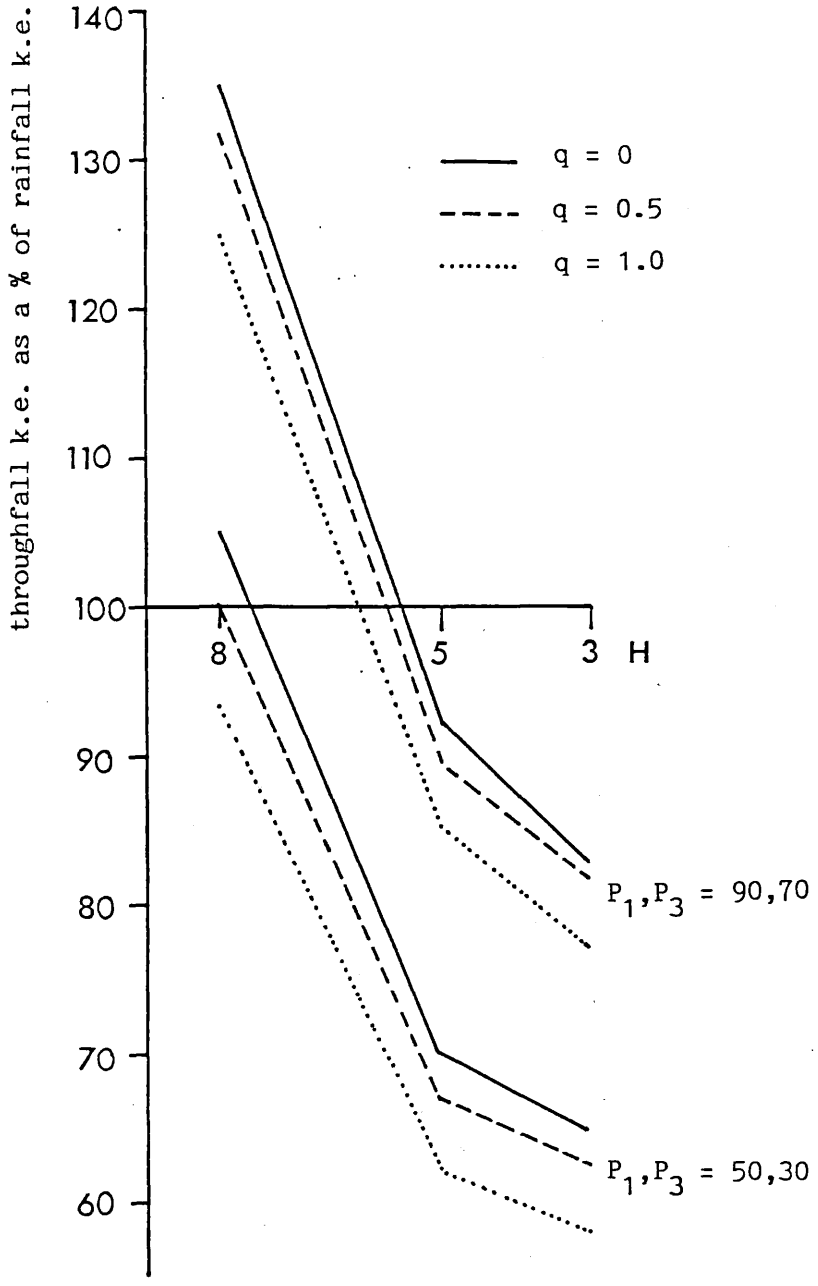

0.5) and P_3 (0.7 to 0.3) have been standardised to lie between 0 and 1.0. The combination of H=8, P_1=0.9 and P_3=0.7 was used as the reference point, with which to compare variations in H, P_1 and P_3. The difference between the relative kinetic energy of the reference point and each combination was expressed as a percentage of the range, 70.2. Hence the greater the difference between the kinetic energy of the reference point and the value of each parameter the more sensitive the model to that parameter and the greater the gradient when the difference is plotted against the percentage change in the parameter.

The results are presented in Figure 8.11 from which it is seen that most of the variability in the model predictions of throughfall kinetic energy is accounted for by H, the canopy height. The change in the gradient in the H curve, from 1.04 to 0.3, shows that the model is most sensitive the the change in canopy height from 8 to 5 m. This is an expected result in view of the rates of energy increase with height of larger drops discussed previously. The line is expected to be curvilinear although there are too few simulations to define it clearly. P_3 accounts for more of the variability in the throughfall energy with a gradient of 0.3 than does P_1 with a gradient of 0.14. Of the 20 increments in each realisation, 7 were allocated the probability P_1 and 8 the probability P_3. When q=0, the depth of water in each increment is the same and hence the total kinetic energy is more sensitive to P_3.

The assessment of sensitivity was repeated for q=1 with a range in throughfall kinetic energy as a percentage of rainfall energy from 125.4% to 58.2% and the results are presented in Figure 8.12. Again most of the variability in the throughfall kinetic energy was accounted for by the canopy height with gradients of 1.18 and 0.3 for the change in height from 8 to 5 m and 5 to 3 m. However, P_1 now accounts for more of the variability than does P_3 with gradients of 0.39 and 0.08 respectively. The reason for this change in sensitivity is the increased importance of the increments at the start of the storm when most of the depth falls.

Figure 8.11 The proportion of the range in prediction variation, plotted against the proportion of the range in parameter variability for different parameters of the model

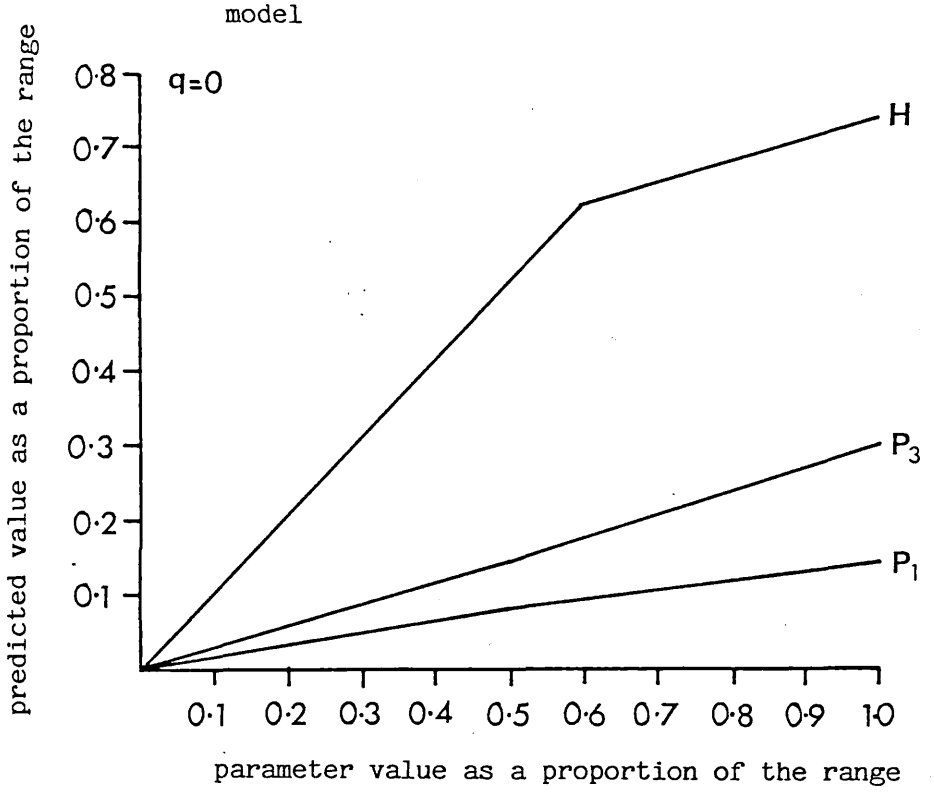

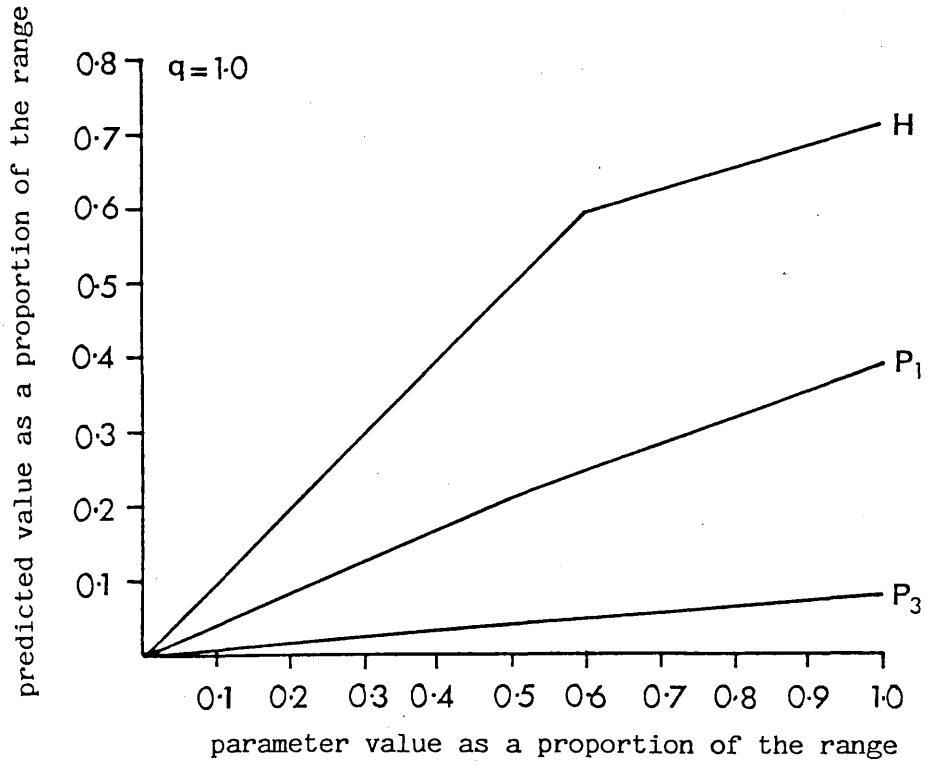

4) Sensitivity of splash to changes in the model

The splash process is a remarkably inefficient use of rainfall energy, with estimates of the mechanical efficiency around 0.2% (Morgan 1979). While the sensitivity of the general erosion process to changes in splash amount are outside the sphere of this thesis, and have not been quantified, it has been mentioned in Chapter Two that splash plays an important role in detaching soil particles and in compacting and sealing the soil surface enhancing other eroding processes.

Hence splash has been taken as an indicator of the erosivity of the rain and it has been assumed that over the range of kinetic energies simulated by the model, changes in splash would result in a change in soil loss by the whole erosion process. The relationship between mean splash weight collected in the splash traps and kinetic energy for all sites, presented above, was used to test the sensitivity of splash weight to rainfall and throughfall kinetic energy for changes in the parameters in the canopy model.

Figure 8.12 gives an example of the frequency distribution of throughfall kinetic energy values from one combination of H, q, P_1 and P_3. Over the range of kinetic energy values simulated, from 72 to 117 J/m^2, the amount of splash per storm increased from 0.312 to 0.441 g. The frequency and magnitude curve (for each value of kinetic energy, the curve is the product of frequency of the energy and magnitude of the splash) shows that most of the work done was by the kinetic energy value of most frequent occurrence. The increase in splash over the range given being insufficiently large to move the peak, so that less frequent, but higher energy storms did more work.

To examine the sensitivity of splash amount to changes in kinetic energy, the weight of sand splashed by storms of mean kinetic energy was calculated for a number of different combinations of model parameters. The amount of splash under the canopy was expressed as a percentage of rainfall splash for each value of q. The results are

Figure 8.12 The mean splash weight (g/storm) and frequency of occurrence of total storm kinetic energy for all realisations of the model when H = 8, P_1,P_3 = 90,70 and q = 1.0

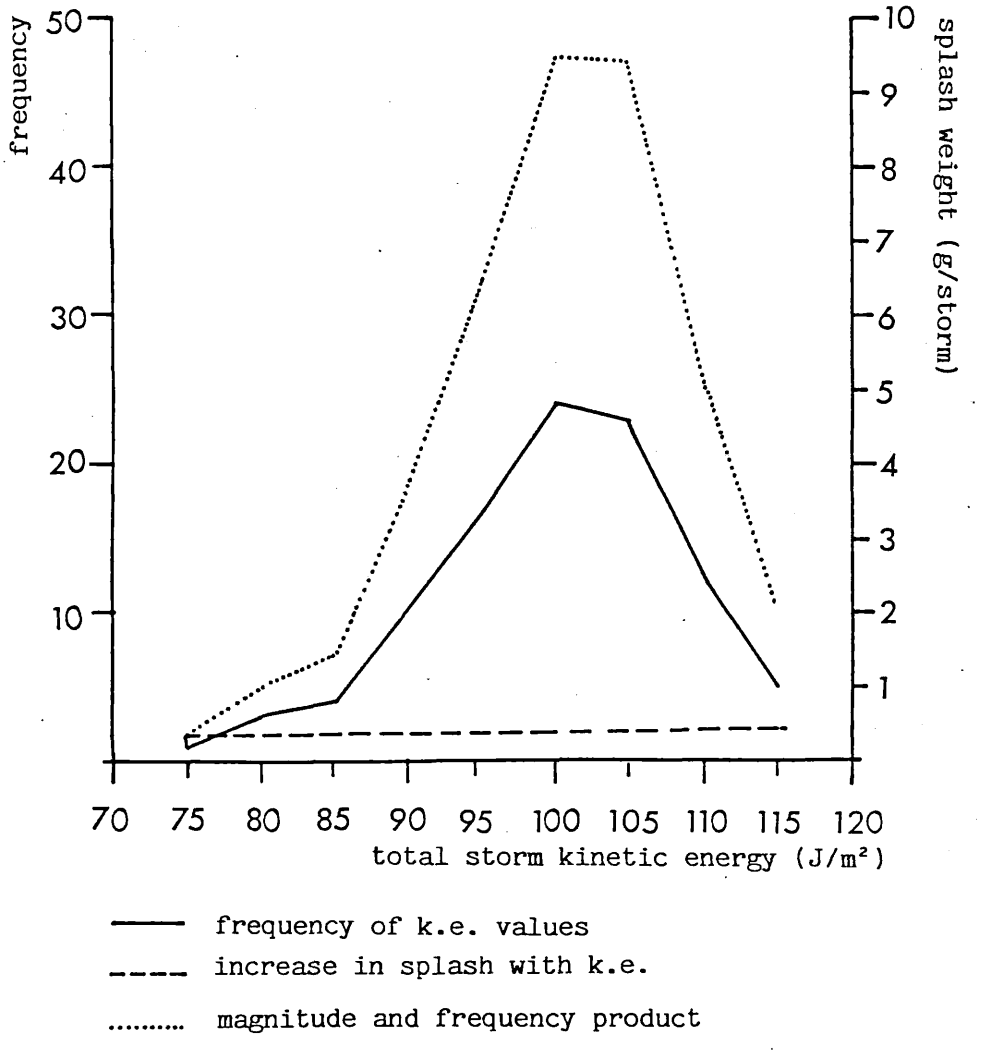

presented in Table 8.12. For each combination of parameters, the throughfall splash as a percentage of rainfall splash (%S) was regressed against the throughfall kinetic energy as a percentage of rainfall kinetic energy (%K.E.) (Figure 8.13). Hence

$$\%S = 0.725\ \%K.E. + 27.5 \qquad [8.11]$$

From this equation it can be seen that splash is less sensitive to changes in the canopy model than is the kinetic energy; that for every 1.0% increase in energy, there is an increase of 0.725% in splash.

Section Four The use of the model

1) Potential for widespread application

The physically-based model developed here may be used to predict the erosivity of throughfall from any canopy and, by comparison with rainfall erosivity, the protective role of the vegetation may be quantified. The model can also predict seasonal changes in throughfall erosivity with changes in the vegetation cover to identify seasons in which the subcanopy soil is most at risk. Information needed to run the model for any storm includes the changing intensity of rainfall, the relationship between rainfall intensity and kinetic energy/mm/m^2, the vegetation height and the frequency distribution of values of kinetic energy/mm/m^2 of a number of throughfall samples taken throughout the storm

Changing rainfall intensity is an easily measured and widely available parameter and may be used to calculate the depth of both rainfall and throughfall for any part of the storm. There is a large body of literature relating rainfall intensity to kinetic energy/mm/m^2 for a number of different environments and rainfall types. There has

Table 8.12 The weight of splash (g) predicted for the simulated rainfall kinetic energies and mean throughfall kinetic energy (S_t) for given combinations of q, H, P_1 and P_3 and throughfall splash as a percentage of rain splash ($\%S_r$)

	H	P_1, P_3			
		0.9, 0.7		0.5, 0.3	
		S_t	$\%S_r$	S_t	$\%S_r$
q=0	3	0.279	87.7	0.236	74.2
	5	0.299	94.0	0.247	77.7
	8	0.394	123.9	0.328	103.1
rain splash		0.318			
q=1.0	3	0.288	83.5	0.235	68.1
	5	0.308	89.3	0.246	71.3
	8	0.405	117.4	0.329	95.4
rain splash		0.345			

Figure 8.13 Plotting predicted soil splash by throughfall as a percentage of predicted splash by rainfall (%S) against predicted kinetic energy of throughfall as a percentage of predicted kinetic energy of rainfall (%K.E.)

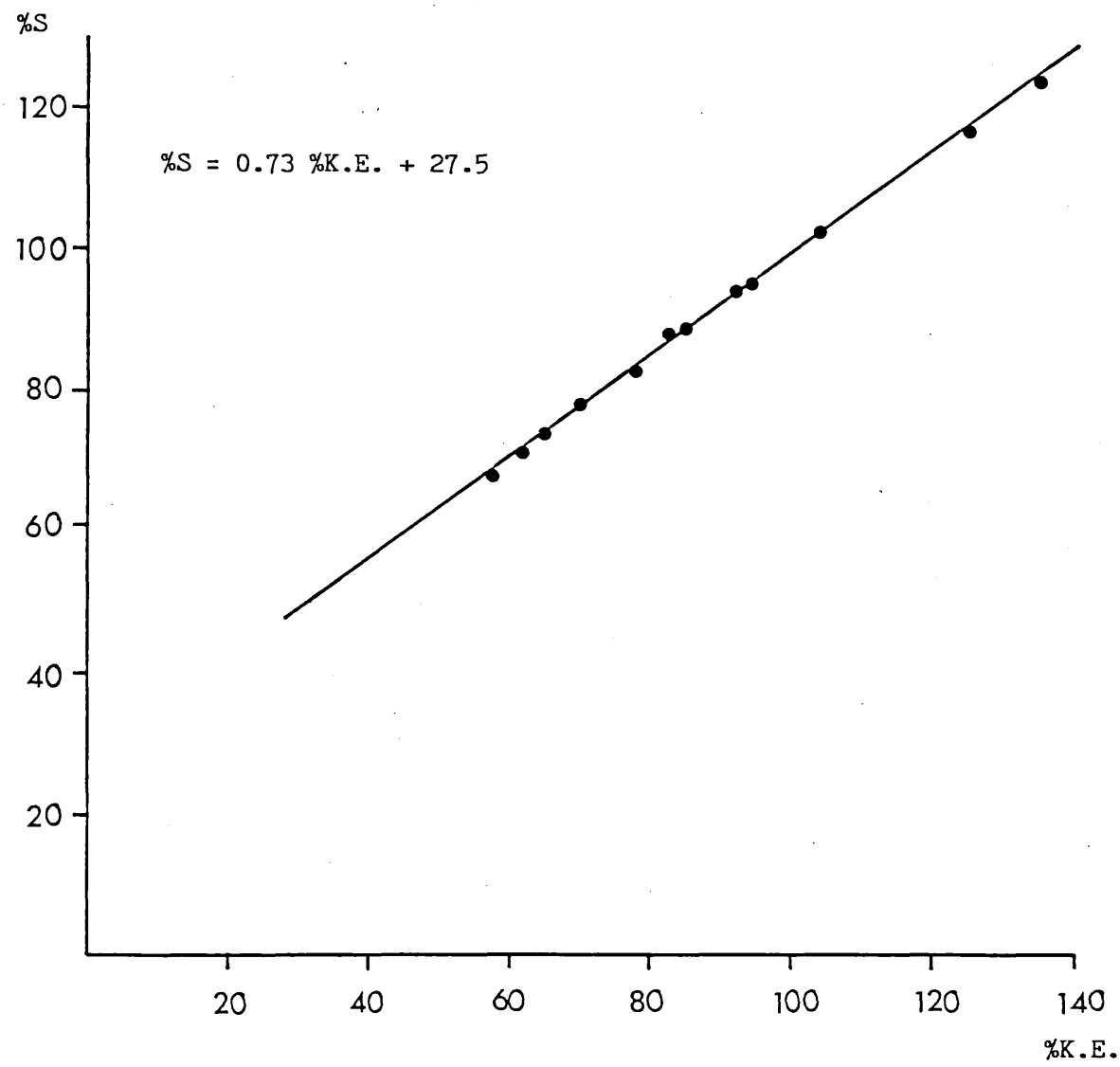

been less work on the frequency distribution of values of kinetic energy/mm/m² of throughfall for different vegetation types but there are mean values for tree canopy structures comprised broadly of needles, small leaves and large leaves and there are also values for several crops. For canopies where the throughfall drop-size distributions have not been measured it may be possible select probable values from those available.

The canopy model is most sensitive to canopy height which is the easiest parameter to obtain, although it has to be assumed that all the drops fall from the same height.

When the frequency distribution of kinetic energy/mm/m² values for throughfall are unknown the model will most successfully predict kinetic energy of throughfall from a dense canopy because the values have been shown to be constant throughout the storm. However for less dense canopies a limited number of throughfall samples may be adequate to be able to divide the values into high or low energy goups or just to describe the whole distribution. In this research there was sufficient information to justify dividing the storm into different periods each with different probabilities of samples being from a high energy group. However such a division need not be necessary and for each time increment the kinetic energy/mm/m² may be selected at random from the whole distribution.

This research has shown that the accuracy of values for kinetic energy/mm/m² calculated from samples of the drop-size distribution may be improved if they are included in an interpolation to correct the total depth calculated corrected to equal that from an independently measured source. However previous workers have not included such a correction and have taken the values for kinetic energy/mm/m² straight from the sample of drop sizes.

2) Implications of the sensitivity analysis on the use of the model

The sensitivity analysis has shown that the height of the canopy

is the most important factor in controlling the kinetic energy of the throughfall and this has implications for the use of the model. The velocity of fall of the drops depends on the height of the canopy and in the calculation fall velocity simplifying assumptions have been made on which it has now been shown the calculation of kinetic depends. Throughout this thesis, calculations of the kinetic energy of throughfall have assumed that all the drops fall from the same height. However, in reality drops may have fallen from a variety of stores higher in the canopy, the inclusion of which have proved intractable. Hence it should be noted that the calculation of kinetic energy using this method gives a a minimum value only and under plays the range of possible values.

The velocity of fall from a given height has been assumed from previously published data which record the velocity of fall of drops in still air. Measurement of vertical wind speeds both under the canopy and in the open were not made for this project and and appropiate adjustments in fall velocities have not been made. Compensation in the model for variability in wind speed would improve the accuracy of the calculations of rainfall erosivity and the assessment of the role of the canopy in changing that erosivity.

3) Concluding remarks

The research documented in this thesis has made contributions to the literature in a number of areas. It has added more information about the drop-size distribution of both temperate, frontal and tropical, convective rain storms. Further information has also been added to the literature concerning the drop-size distribution of throughfall from different canopies, oak, red pine, beech, corn and Brussels sprouts have already been considered, this research includes additional information on throughfall from an oak canopy and new information on the drop-size distribution from upper and lower stories of a tropical rain forest.

More importantly, this research has added information concerning the variation in both rainfall and throughfall drop-size distribution through storms. It has provided a technique whereby discrete samples of rainfall and throughfall may be converted into a continuous record of drop size distribution change. The results have shown that under some circumstances, the assessment of kinetic energy of throughfall by a few discrete samples may be justified because of the low variability in the results obtained from the continuous data.

This research has begun to illuminate the problem of the effect of canopy structure on the transformation of rainfall kinetic energy. It has extended Morgan's work incorporating vegetation in terms of the canopy interception capacity in a model of rainfall kinetic energy and splash detachment. This research has developed a first attempt at a new model describing the transformation of rainfall kinetic energy in terms of the change in drop-size distribution through a storm and the canopy height to simulate the effects of canopy control on splash at the ground.

To the wealth of work relating to splash and rainfall kinetic energy, this research has added another example, but it has also added to the less well investigated area of splash under different kinds of rain forest canopy, giving a characteristic range of splash for different canopy heights and storms of different kinetic energy. The research has demonstrated the importance of considering carefully forest clearance policies with respect to the relative role of the tree canopy and under-storey.

References

Al-Durrah, M. and Bradford, J. M. (1981) New methods of studying soil detachment due to raindrop impact, Journal of the Soil Science Society of America, 45, 949-953

Alexandre, D. Y. (1984) Strata in tropical rain forest at Tai (Ivory Coast), in Chadwick, A. C and Sutton S. L. (Eds) Tropical Rain-Forest: The Leeds Symposium, Special Publication of the Leeds Philosophical and Literary Society, 15-24

Ashton, P. S. (1978) Crown characteristics of tropical trees, in Tomlinson, P. B. and Zimmermann, M. H. (Eds) Tropical Trees as Living Systems, Cambridge University Press, Cambridge, 591-615

Baver, L. D., Gardner, W. H. and Gardner, W. R. (1972) (4th Ed) Soil Physics, Wiley, New York, 498 pp

Best, A. C. (1950a) The size distribution of raindrops, Quarterly Journal of the Royal Meteorological Society, 76, 16-36

Best, A. C. (1950b) Empirical formulae for the terminal velocity of water drops falling through the atmosphere, Quarterly Journal of the Royal Meteorological Society, 76, 302-311

Bevington, P. R. (1969) Data Reduction and Error Analysis for the Physical Sciences, McGraw-Hill Inc. N.Y., 336 pp

Bisal, F. (1960) The effect of raindrop size and impact velocity on sand splash, Canadian Journal of Soil Science, 40, 242-245

Blanchard, D. C. (1950) Behaviour of water drops at terminal velocity, Transactions of the American Geophysical Union, 31, 836-842

Bollinne, A. (1978) Study of the importance of splash and wash on

cultivated loamy soils of Hesbaye (Belgium), Earth Surface Processes, 3, 71-84

Brunig, E. F. (1976) Tree forms in relation to environmental conditions; an ecological viewpoint, in Cannell, M. G. R. and Last, F. T. Tree Physiology and Yield Improvement, Academic Press, London, 139-156

Bryan, R. B. (1968) The development, use and efficienty of indices of soil erodibility, Geoderma, 2, 5-26

Bryan, R. B. (1977) Assessment of soil erodibility: new approaches and directions, in Toy, T. J. (Ed) Erosion: Research Techniques, Erodibility and Sediment Delivery, Geo Books, Norwich, 57-72

Bubenzer, G. D. and Jones, B. A. (1971) Drop size and impact velocity effect on the detachment of soils under simulated rainfall, Transactions of the American Society of Agricultural Engineers, 14(4), 625-628

Chapman, G. (1948) Size of raindrops and their striking force at the soil surface in a red pine plantation, Transactions of the American Geophysical Union, 29, 664-670

Chmielowiec, S. (1977) Bombardująca działalność kropel desczczu i jej rola w modelowaniu stoków Porgórza, Manuscript in the Institute of Geography of the Jagellonian University

Clark, F. G. (1961) A hemispherical forest photocanopymeter, Journal of Forestry, 59, 103-105

Cruse, R. M. and Larson, W. E. (1977) Effect of soil shear strength on soil detachment due to raindrop impact, Journal of the Soil Science Society of America, 41, 777-781

Defant, A. (1905) Gesetzmaessigkeiten in der Verteilung der

verschiedenen Tropfengroessen bei Regenfaellen, K. Akad. Wiss., Math.-Naturw. Klasse Sitzber., No. 5, 585-646

Davies, C. N. (1942) Unpublished Ministry of Supply reports quoted by Sutton in Air Ministry report, M. R. P. No. 40

Dohrenwend, R. E. (1977) Raindrop erosion in the forest, Michigan Technological University, Ford Forestry Center L'Anse Michigan 49946, Research Note 24, 19pp

Ekern, P. G. (1950) Raindrop impact as the force initiating soil erosion, Proceedings of the Soil Science Society of America, 15, 7-10

Ekern, P. G. (1953) Problems of raindrop impact erosion, Agricultural Engineering, 34(1), 23-25

Ellison, W. D. (1944) Studies of raindrop erosion, Agricultural Engineering, 25, (4)131-136, (5)181-182

Ellison, W. D. (1947) Soil erosion studies. Parts I-V, Agricultural Engineering, 28, (I)145-146, (II)197-201, (III)245-248, (IV)297-300, (V)349-351

Elwell, H. A. and Stocking, M. A. (1975) Parameters for estimating annual runoff and soil loss from agricultural lands in Rhodesia, Water Resources Research, 11, 601-605

Evans, R. (1980) Mechanics of water erosion and their spatial and temporal controls: an experimental view point, in Kirkby, M. J. and Morgan, R. P. C. (Eds) Soil Erosion, Wiley, Chichester, 109-128

Eyre, S. R. (1968) 2nd Edition Vegetation and Soils: A World Picture, Edward Arnold, London, 328 pp

Flower, W. D. (1928) The terminal velocity of drops, Proceedings of the Physical Society of London, 40, 167-176

Franken, W., Leopoldo, P. R., Matsui, E., Nazare, M. (1982) Estudo da interceptacao da Água de chuva em coberta Florestal Amazonica do tipo firme, Acta Amazonica XII (2) 327-331

Franken, W. and Leopoldo, P. R. (1983) The Amazon - Limnology and landscape ecology of a mighty tropical river, Junk Publishers, Monog. Biol.

Free, G. R. (1960) Erosion characteristics of rainfall, Agricultural Engineering, 47(7), 447-449

Friedman, M. (1962) The interpolation of time series by related series, Journal of the Americal Statistical Association, 57, 729-757

Froehlich, W. and Slupik, J. (1980) Importance of splash in erosion process within a small flysch catchment basin, Studia Geomorphologica Carpatho-Balcanica, XIV, 77-111

Gash, J. H. C. (1979) An analytical model of rainfall interception by forests, Quarterly Journal of the Royal Meteorological Society, 105, 43-55

Gash, J. H. C., and Morton, A. J. (1978) An application of the Rutter model to the estimation of the interception loss from Thetford Forest, Journal of Hydrology, 38, 49-58

Gash, J. H. C., Lloyd, C. R. and Wright, I. R. (1980) Comparative estimates of interception loss from three coniferous forests in Great Britain, Journal of Hydrology, 48, 89-105

Gerlach, T. (1976) L'importance de l'action des gouttes de pluie pour le transport du sol sur les versants, Studia Geomorphologica

Carpatho-Balcanica, 10, 125-137

Ghadiri, H. and Payne, D. (1979) Raindrop impact and soil splash, in R. Lal and D. J. Greenland (Eds) Soil Physical Properties and Crop Production in the Tropics, Wiley-Interscience, 95-104

Grah, R. F. and Wilson, C. C. (1944) Some components of rainfall interception, Journal of Forestry, 42, 890-898

Grzés, M. (1971) Wstępne wyniki badán nad rolą kropel deszczu w procesie erozji, Zesz. Nauk. UMK w. Toruniu 26, Geografia 8, 73-80

Gunn, R. and Kinzer, G. D. (1949) The terminal velocity of fall for water droplets in stagnant air, Journal of Meteorology, 6, 243-248

Hall, M. J. (1970) Use of the stain method in determining the drop-size distribution of coarse liquid sprays, Transactions of the American Society of Agricultural Enginers, 13, 33-37,41

Hallé, F., Oldeman, R. A. A. and Tomlinson, P. B. (1978) Tropical Trees and Forests: An Architectural Analysis, Springer-Verlag, Berlin, 441 pp

Harlow, F. H. and Shannon, J. P. (1967) The splash of a liquid drop, Journal of Applied Physics, 38(10), 3855-3866

Herwitz, S. R. (1985) Interception storage capacities of tropical rain forest canopy trees, Journal of Hydrology, 77, 237-252

Horn, H. S. (1971) The Adaptive Geometry of Trees, Monographs in Population Biology 3, Princetown University Press, Princetown, 144 pp

Horton, R. E. (1919) Rainfall interception, Monthly Weather Review,

47, 603-623

Horton, R. E. (1948) Statistical distribution of drop sizes and the occurrence of dominant drop sizes in rain, Transactions of the American Geophysical Union, 29(5), 624-630

Houze, R. A., Hobbs, P. V., Parsons D. B., Hertzegh, P. H. (1979) Size distribution of precipitation particles in frontal clouds, Journal of Atmospheric Sciences, 36(1), 156-162

Huang, C., Bradford, J. M., and Cushman, J. H. (1982) A numerical study of raindrop impact phenomena: The rigid case, Journal of the Soil Science Society of America, 46, 14-19

Hudson, N. W. (1971) Soil Conservation, Batsford, London, 320 pp

Hudson, N. W. and Jackson, D. C. (1959) Results achieved in the measurement of erosion and runoff in Southern Rhodesia, Proceedings, Third Inter-African Soils Conference, Dalaba, 575-583

Jackson, I. J. (1971) Problems of throughfall and interception assessment under tropical forest, Journal of Hydrology, 12, 234-254

Jackson, I. J. (1975) Relationships between rainfall parameters and interception by tropical forest, Journal of Hydrology, 24, 215-238

Jansson, M. B. (1982) Land erosion by water in different climates, UNGI Rapport No. 57, Department of Physical Geography, Uppsala University, 151 pp

Kinnel, P. I. A. (1973) The problem of assessing the erosive power of rainfall from meteorological observations, Proceedings, Soil Science Society of America, 37(4), 617-621

Kinnel, P. I. A. (1981) Rainfall intensity-kinetic energy relationships for soil loss prediction, Journal of the Soil Science Society of America, 45, 153-155

Kirkby, M. J. (1980) Modelling water erosion processes, in Kirkby, M. J. and Morgan, R. P. C. (Eds) Soil Erosion, Wiley, Chichester, 183-216

Klett, J. D. (1971) On the break up of water in air, Journal of the Atmospheric Sciences, 28, 646-647

Klinge, H., Rodrigues, W. A., Brunig, E. and Fittkau, E. J. (1975) Biomass and structure in a central Amazonian rain forest, in Golley, F. B. and Medina, E. Tropical Ecological Systems, Trends in Terrestial and Aquatic Research, Springer-Verlag, New York - Berlin, 115-122

Kneale, W. R. (1982) Field measurements of rainfall drop-size distribution and the relationship between rainfall parameters and soil movement by rain splash, Earth Surface Processes and Landforms, 7, 499-502

Lane, W. R. (1947) A microburette for producing small liquid drops of known size, Journal of Scientific Instrumentation, 24, 98-101

Langbein, W. B. and Schumm, S. A. (1958) Yield of sediment in relation to mean annual precipitation, Transactions of the American Geophysical Union, 39(6), 1076-1084

Laws, J. O. (1941) Measurements of the fall-velocities of waterdrops and raindrops, Transactions of the American Geophysical Union, 22, 709-712

Laws, J. O. and Parsons, D. A. (1943) The relation of raindrop size to intensity, Transactions of the American Geophysical Union, 24, 452-459

Lemeur, R. and Blad, B. L. (1974) A critical review of light models for estimating the short wave radiation regime of plant canopies, Agricultural Meteorology, 14(12), 255-286

Lemon, P. E. (1956) A spherical densitometer for estimating forest overstorey density, Forest Science, 2, 314-320

Lenard, P. (1904) Uber Regen, Meteorologische Zeitschrift, 21, 248-262

Leonard, R. E. (1967) Mathematical theory of interception, in W. E. Sopper and H. W. Lull (Eds) Forest Hydrology, Pergamon Press, Oxford, 131-136

Leyton, L., Reynolds, E. R. C. and Thompson, F. B. (1967) Rainfall interception in forest and moorland, in Sopper, W. E. and Lull, H. W. (Eds) Forest Hydrology, Pergamon, Oxford, 163-178

List, R. and Gillespie, J. R. (1976) Evolution of raindrop spectra with collision-induced breakup, Journal of the Atmospheric Sciences, 33(10), 2007-2013

Marshall, J. S. and Palmer, W. McK. (1948) Relation of raindrop size to intensity, Journal of Meteorology, 5, 165-166

Mason, B. J. (1957) The Physics of Clouds, Clarendon Press, Oxford, 481 pp

Mason, B. J. and Andrews, J. B. (1960) Drop size distribution from various types of rain, Quarterly Journal of the Royal Meteorological Society, 86, 346-353

Mason, B. J. and Ramandham, R. (1953) A photoelectric spectrometer, Quarterly Journal of the Royal Meteorological Society, 79, 490-495

Massman, W. J. (1980) Water storage on forest foliage: A general model, Water Resources Research, 16(1), 210-216

McCleary, R. and Hay, R. A. (1980) Applied Time Series Analysis for the Social Sciences, Sage, London, 331 pp

McGregor, K. C. and Mutchler, C. K. (1978) The effect of crop canopy on raindrop size distribution and energy USDA Sedimentation Laboratory Annual Report Oxford, MS, 38655 USA

McIntyre, D. S. (1958) Soil splash and the formation of surface crusts by raindrop impact Soil Science, 85, 261-266

Medina, E. (1983) Adaptations of tropical trees to moisture stress, in Golley, F. B. (Ed) (1983) Tropical Rain Forest ecosystems: structure and function, Elsevier, Oxford, 225-237

Merriam, R. A. (1973) Fog drip from artificial leaves in a fog wind tunnel, Water Resources Research, 9(6), 1591-1598

Mihara, Y. (1951) Raindrops in soil erosion (English translation) National Institute of Agricultural Science, Bulletin No. 1 Tokyo, Japan, 59pp

Morgan, R. P. C. (1978) Field studies of rainsplash erosion, Earth Surface Processes, 3(3), 295-299

Morgan, R. P. C. (1979) Topics in Applied Geography: Soil Erosion, Longman, London, 114 pp

Morgan, R. P. C. (1982) Splash detachment under plant covers: Results and implications of a field study, Transactions of the American Society of Agricultural Engineers, 25(4), 987-991

Morgan, R. P. C. (1985) Establishment of plant cover parameters for modelling splash detachment, in El-Swaify, S. A., Moldenhauer,

W. C. and Lo, A. (Eds) Soil Erosion and Conservation, Soil Conservation Society of America, Iowa, 377-383

Moshovkin, V. M. and Gakhov, V. F. (1979) Physical aspects of raindrop erosion, Soviet Soil Science, 11, 716-720

Mosley, M. P. (1982) The effect of a New Zealand beech forest canopy on the kinetic energy of water drops and on surface erosion, Earth Surface Processes and Landforms, 7, 103-107

Mutchler, C. K. (1967) Parameters for describing raindrop splash, Journal of Soil Water Conservation, 22(3), 91-94

Niederdorfer, E. (1932) Messungen der Groesse der Regentropfen, Meteorologie Zeitschrift, 49, 1-14

Noble, C. A. and Morgan, R. P. C. (1983) Rainfall interception and splash detachment with a brussels sprout plant: a laboratory simulation, Earth Surface Processes and Landforms, 8, 569-577

Norcliffe, G. B. (1977) Inferential Statistics for Geographers, Hutchinson, London, 272 pp

Numerical Algorithms Group (1984) Fortran Library Manual Mark II, 2, EO

Ovington, J. D. (1954) A comparison of rainfall in different woodlands, Forestry, 27, 41-53

Palmer, R. (1963) Waterdrop impactometer, Agricultural Engineering, 44, 198-199

Palmer, R. S. (1965) Waterdrop impact forces, Transactions of the American Society of Agricultural Engineers, 8(1), 70-72

Park, S. W., Mitchell, J. K. and Bubenzer, G. D. (1982) Splash

erosion modelling: physical analysis, Transactions of the American Society of Agricultural Engineers, 25, 357-361

Pasqualucci, F. (1982) The variation of drop-size distribution in convective storms: A comparison between theory and radar measurements, Geophysical Research Letters, 9(8), 839-841

Patric, J. H. (1966) Rainfall interception by mature coniferous forests of south east Alaska, Journal of Soil and Water Conservation, 21, 229-231

Pearce, A. J. and Rowe, L. K. (1981) Rainfall interception in a multi-storied evergreen mixed forest: Estimates using Gash's analytical model, Journal of Hydrology, 49, 341-353

Pruppacher, H. R. and Pitter, R. L. (1971) A semi-empirical determination of the shape of cloud and rain drops, Journal of the Atmospheric Sciences, 28, 86-94

Quinn, N. W. and Laflen, J. M. (1981) Properties of transformed rainfall under corn canopy, American Society of Agricultural Engineers Paper No. 81-2059, 15pp

Reynolds, E. R. C. and Leyton, L. (1961) Measurement and significance of throughfall in forest stands, in Rutter, A. J. and Whitehead, F. H. (Eds) The Water Relations of Plants, Symposium of the British Ecological Society, 5-8 April 1961, 127-141

Richards, P. W. (1952) The Tropical Rain Forest (Reprinted with corrections 1979), Cambridge University Press, Cambridge, 450 pp

Richards, P. W. (1983) The three-dimensional structure of tropical rain forest, in Sutton, S. L., Whitmore, T. C. and Chadwick, A. C. Tropical Rain Forest Ecolocgy and Management, British Ecological Society Special Publication Number 2, Blackwell, Oxford, 3-10

Riezebos, H. Th. and Epema, G. F. (1985) Drop shape and erosivity, Part II: Splash detachment, transport and erosivity indices, Earth Surface Processes and Landforms, 10, 69-74

Rose, C. W. (1960) Soil detachment caused by rainfall, Soil Science, 89, 28-35

Rothacher, J. (1963) Net precipitation under a Douglas Fir forest, Forest Science, 9, 423-429

Rutter, A. J., Kershaw, K. A., Robins, P. C. and Morton, A. J. (1971) A predictive model of rainfall interception in forests. 1: Derivation of the model from observations in a plantation of Corsican Pine, Agricultural Meteorology, 9, 367-384

Savile, D. B. O. and Hayhoe, H. N. (1978) The potential effect of drop size on efficiency of splash cup and spring board dispersal devices, Canadial Journal of Botany, 56, 127-128

Schindelhauer, F. (1925) Versuch einer Registrierung der Tropfenzahl bei Regenfällen, Meteorologische Zeitschrift, 42, 25

Schmidt, W. (1909) Meteorologische Zeitschrift, 26, 183

Schottman, W. R. (1978) Estimation of the penetration of high energy raindrops through a plant canopy. Unpublished PhD Thesis. Cornell University, Ithaca, New York, 253 pp

Shuttleworth, W. J. (1978) A simplified one-dimensional theoretical description of the vegetation-atmosphere interaction, Boundary Layer Meteorology, 14, 3-27

Shuttleworth, W. J., Gash, J. H. C., Lloyd, C. R., Moore, C. J., Roberts, J., Filho, A., Fisch, G., Filho, V., Ribeiro, M., Molion, L., Sa, L., Nobre, C., Cabral, O., Patel, S. and Moraes, J. (1984) Eddy correlation measurements of energy

partition for Amazonian forest, Quarterly Journal of the Royal Meteorological Society, 110, 1143-1162

Spilhaus, A. F. (1948) Raindrop size, shape and falling speed, Journal of Meteorology, 5(3), 108-110

Sreenivas, L., Johnston, J. R. and Hill. H. O. (1947) Some relationships of vegetation and soil detachment in the erosion process, Proceedings, Soil Science Society of America, 11, 474-479

Srivastava, R. C. (1971) Size distributions of raindrops generated by their break up and coalescence, Journal of the Atmospheric Sciences, 28, 410-415

Srivastava, R. C. (1978) Parametisation of raindrop size distribution, Journal of Atmospheric Science, 35, 108-117

Thompson, F. B. (1972) Rainfall interception by oak coppice (Quercus robur), in Taylor, J. B. (Ed) Research Papers in Forest Hydrology, Aberystwyth Symposium 1970, 59-74

Thornes, J. B. (1980) Erosional processes of running water and their spatial and temporal controls: a theoretical viewpoint, in Kirkby, M. J. and Morgan, R. P. C. (Eds) Soil Erosion, Wiley, Chichester, 129-182

Tsukamoto, Y. (1966) Raindrops under forest canopies and splash erosion, Bulletin of Experimental Forestry, Tokyo University of Agricultural Technology, 5, 65-77

Voigt, G. K. (1960) Distribution of rainfall under forest stands, Forestry Science, 6, 2-10

Wiersum, K. F. (1985) Effects of various vegetation layers of an Acacia auriculiformis forest plantation on surface erosion at

Java, Indonesia, in S. A. El-Swaify, W. C. Moldenhauer and A. Lo (Eds) Soil Erosion and Conservation, Soil Conservation Society of America, 79-89

Wiesner, J. (1895) Bietraege zur kenntniss des tropischen Regens, K. Akad. Wiss., Math.-Naturw. Klasse, SitzBer., 104, 1397-1434

Williamson, G. B. (1981) Drip tips and splash erosion, Biotropica, 13(3), 228-231

Williamson, G. B. (1983) Driptips, drop size and leaf drying, Biotropica, 15(3), 232-234

Wischmeier, W. H. and Smith, D. D. (1958) Rainfall energy and its relationship to soil loss, Transactions of the American Geophysical Union, 29, 285-291

Yamatoto, T. and Anderson, H. W. (1973) Splash erosion related to soil erodibility indexes and other forest soil properties in Hawaii, Water Resources Research, 9, 336-345

Yevjevich, V. (1972) Stochastic Processes in Hydrology, Water Resources Publications, Colorado, 276 pp

Young, K. K. (1976) Erosion potential of soils, Proceedings of the Third Federal Inter-Agency Sediment Conference, Denver, Colorado

Young, R. A. and Wiersma, J. L. (1973) The role of rainfall impact in soil detachment and transport, Water Resources Research, 9, 1629-1636

Zinke, P. J. (1967) Forest interception studies in the U. S., in Sopper, W. E. and Lull, H. W. (Eds) Forest Hydrology, Pergamon Press, Oxford, 137-161

APPENDIX 1a Oak canopy site: frequency of occurrence of stain diameters (mm) on sample sheets

d3 Open Site

stain diameter	sample number												
	1	2	3	4	5	6	7	8	9	10	11	12	13
0.25	32	18	17	31	38	64	68	74	23	77	79	101	60
0.5	32	25	44	58	65	54	48	90	37	134	43	53	92
1.0	26	68	204	46	68	79	55	93	47	111	147	34	52
1.5	76	215	407	70	124	49	55	79	124	108	107	28	14
2.0	73	150	127	92	86	36	44	39	96	104	107	26	1
2.5	63	97	105	56	57	26	39	19	51	96	93	42	3
3.0	28	29	99	48	43	28	28	7	37	104	43	14	3
3.5	37	72	44	22	24	19	37	17	33	19	32	22	6
4.0	24	25	39	15	14	9	26	2	7	8	11	22	6
4.5	15	11	11	24	5	24	15	2	7	4	29	8	6
5.0	17			15	5	2	9	5	5		14	14	8
5.5	6	4	5	5	5	19	7	17				4	4
6.0					3		2	12				4	
6.5	2					11		5			4	12	
7.0						2		7				2	
7.5					3	2	4					4	
8.0						2		2					
8.5								2			4	2	
9.0										4	4	4	
10.0												2	
10.5								2					
11.5		4		2									
12.0								2					
13.0						2							

duration of each sample, t_s (s) and gap, t_g (s)

t_s	1080	60	180	60	90	93	75	186	166	407	83	77	504
t_g	30	30	180	300	280	394	398	662	616	605	668	911	

d3 Canopy Site

stain diameter	sample number											
	1	2	3	4	5	6	7	8	9	10	11	12
0.25	43	112	104	91	334	147	140	165	163	199	199	43
0.5	45	91	77	75	154	158	104	207	132	162	194	38
1.0	89	76	107	108	158	150	78	160	98	118	127	20
1.5	87	74	83	42	77	72	85	89	79	52	131	12
2.0	84	82	107	44	27	75	91	101	60	44	50	8
2.5	21	38	43	19	18	32	29	46	57	52	81	3
3.0	12	32	52	33	45	25	42	34	49	29	36	4
3.5	16	35	15	23	9	21	39	8	42	40	27	4
4.0	10	18	9	14	27	21	23	21	26	15	32	7
4.5	4	18		5	18	4			23	11	9	3
5.0		6	9	7	14			8	15	7	9	1
5.5		3			5		13	4	4		5	1
6.0		3	3	2	5					4	5	
6.5				5	5	7						
7.0							3		4			
7.5					5							
8.0										4		
8.5			3									1
9.5						4						
10.0												1
12.5							3					
23.5									4			
27.0					5							

duration of each sample, t_s (s) and gap, t_g (s)

t_s	1140	360	405	362	425	651	800	1024	568	447	756	463
t_g	30	30	28	17	41	38	5	26	23	16	397	

throughfall sampling started 120 s after rainfall sampling

d52 Open Site

stain diameter	sample number															
	1	2	3	4	5	6	7	8	9	10	11	12	13	14	15	16
0.25	858	1042	174	79	68	43	111	155	43	47	128	74	29	48	21	62
0.5	1136	982	160	159	90	91	190	99	66	31	201	130	72	31	111	161
1.0	411	230	156	202	58	67	119	28	104	106	357	215	130	130	143	146
1.5	12	121	105	238	48	79	119	81	147	192	234	232	243	270	240	81
2.0		24	133	166	58	112	70	84	75	176	84	181	127	133	104	81
2.5		24	78	130	28	70	21	77	40	106	61	136	54	41	63	48
3.0			64	94	35	40	21	25	32	39	45	45	36	14	10	59
3.5			23	101	25	21	16	60	35	31		68	25	17	3	44
4.0			5	72	25	15	12	25	20	27		17				26
4.5			9	79	23	21	25	32	12	8		11	7			11
5.0			9	29	20	30	25	14		16	56	11				4
5.5				72	5	12	21	11	3			6				
6.0				7	10		21	4		4						
6.5				7	3		21	11				6				4
7.0					3											4
7.5				7	3		4									4
8.0						3	4									
8.5							12									
9.0							8									
9.5						3										
10.0							4									
12.0					3											

duration of each sample, t_s (s) and gap, t_g (s)

t_s	169	2272	157	170	30	46	21	53	63	101	173	98	149	113	83	53
t_g	77	43	17	42	171	126	137	222	149	49	23	552	454	395	433	

d52 Canopy Site

stain diameter	sample number													
	1	2	3	4	5	6	7	8	9	10	11	12	13	14
0.25	1463	172	274	175	207	255	165	123	66	45	42	39	135	144
0.5	970	192	222	99	137	192	122	153	153	63	87	111	107	294
1.0	246	151	280	92	137	245	161	157	349	153	133	113	63	121
1.5	130	192	143	76	109	149	191	229	235	114	178	111	35	135
2.0	43	146	150	56	23	27	74	51	147	71	91	49	23	103
2.5	14	78	52	43	31	37	69	34	71	42	55	37	21	42
3.0	29	36	52	26	4	37	22	42	27	24	29	12	16	28
3.5		42	33	20	8	16	17	17	22	5	16	10	5	19
4.0		16	39	26	20	5	4	4		3	6	5	14	14
4.5		16	20	20	31	37	30	4	5	5	3	2	14	9
5.0			13	7	12	5	4	8		3			7	
5.5				3	12	16		8	11		3		7	5
6.0			20	13	8	5								
6.5				3	16	27	4						5	
7.0					4			4					7	
7.5			7		8								5	
8.0					4	5							2	
9.0					4			8						
9.5					8									
10.5									5					
13.0														5
15.5														5
16.0						5								5
17.0							4							
17.5												2		
18.5														5
28.0											3			
29.0								4						

duration of each sample, t_s (s) and gap, t_g (s)

t_s	2517	173	142	65	80	57	170	128	319	139	150	155	102	197
t_g	20	25	54	66	118	171	86	45	420	395	380	392	209	

throughfall sampling started 123 s after rainfall sampling

d125 Open Site

stain diameter	sample number												
	1	2	3	4	5	6	7	8	9	10	11	12	13
0.25	101	119	145	192	258	319	226	120	203	263	144	160	38
0.5	92	125	118	134	289	218	133	131	153	188	105	153	22
1.0	98	49	98	67	136	152	74	124	69	71	39	86	13
1.5	79	27	68	88	31	96	59	42	47	75	57	56	9
2.0	82	25	37	71	18	76	59	35	16	45	30	26	2
2.5	54	6	14	97	4	10	41	39	28	15	45	41	
3.0	32	13	54	29		25	52	21	6	11	36	67	
3.5	38	22	41	88	22	40	22	28	9	26	24	48	
4.0	22	7	14	21	9	5	33	28	6	8	36	22	
4.5	6	9	27	21		15	4	25	6	8	18	30	
5.0	9	9	7	8	22	5	4	7	6	4		4	1
5.5	6	4	14	8	4	15	11	25	3	15	12	7	
6.0	3	4	7		9	5	7	18	6	8	12	11	
6.5	3	9	7		4		7	7	12	4	15		
7.0	3	9	7		9	5	4		6		3	4	
7.5	3	4	7	8		10		4	9	8	6	11	
8.0		2			4			4	3		3		
8.5			3	4	4	10		7	3			7	
9.0		2			4		4	4	3		3	4	1
9.5			7		4			4	12		3		
10.0								4	3				
10.5					9			4	3				
11.0									6			4	
11.5					9			7					
12.0					9			4					
12.5					9			4		4			
13.0					4						6	4	
13.5			3		4								
14.0								4					
14.5								4	3		3		
15.0								7					
19.0						5							

duration of each sample, t_s (s) and gap, t_g (s)

t_s	197	128	71	86	31	45	675	278	14	38	56	63	377
t_g	299	284	305	266	284	181	58	36	282	285	253	263	

d125 Canopy Site

stain diameter	sample number												
	1	2	3	4	5	6	7	9	10	11	12	13	14
0.25	117	158	275	148	223	257	128	184	181	187	112	95	92
0.5	199	221	140	153	191	146	123	249	207	144	122	190	69
1.0	107	81	65	133	129	94	89	139	131	130	88	76	44
1.5	110	49	117	148	51	98	66	75	68	84	103	70	26
2.0	68	35	70	54	23	64	39	55	51	82	40	47	5
2.5	36	35	75	89	8	56	24	55	42	21	24	41	6
3.0	39	28	60	89	27	30	16	40	34	4	12	13	4
3.5	14	21	28	84	8	39	10	55	38	25	18	28	1
4.0	7	14	19	34	31	21	13	10	13	11	12	9	
4.5	11	18	14	25	31	21		15	30	7	15	6	
5.0	4	14	19	5	12	4		20	21	11	3	3	
5.5		4	9	5	4	9	3	20			12	6	
6.0		7	19	10	4	4	5	25	4		6	9	
6.5		4	9	5	8	4		20	8	18	21	9	
7.0		4	5				5	5	4	11		9	
7.5			5	5			3						
8.0		4				4		5			3	9	
8.5					8						3		
9.0		7	5		4					7			
9.5								10	4	4	3		
10.0			5							4			
10.5					8					4	3		
11.5					8			5	4				
12.0						4		5			3		
13.0					4								
15.5									4				
16.0								5					
16.5													1
19.0										4		3	
21.0												3	
23.0													1
25.0													1
27.0											3		
46.0												3	

duration of each sample, t_s (s) and gap, t_g (s)

t_s	314	168	75	86	15	38	756	172	36	34	43	75	516
t_g	169	236	299	299	321	142	88	172	179	317	241	54	

throughfall sampling started 51 s after rainfall sampling

d178 Open Site

stain diameter	sample number											
	1	2	3	4	5	6	7	8	9	10	11	12
0.25	17	15	32	59	108	129	419	362	86	41	37	26
0.5	44	51	28	86	124	98	223	368	83	55	53	65
1.0	30	45	19	37	44	51	43	172	74	52	44	50
1.5	49	51	8	29	15	10	64	119	25	63	33	30
2.0	62	56	2	26	6	10	26	18	11	63	31	27
2.5	43	55	1	20	6	10	4	36	20	71	13	12
3.0	32	18	1	31		10	4	12	16	41	22	3
3.5	19	13	2	15	15	22	9	18	16	41	22	2
4.0	6	3	1	18		4	4	6	9	16	20	
4.5	8	3	2	11	6	16	9	30	4	38	33	
5.0	9	5		15	8	18	4	6	7	25	13	
5.5	2	3	1	13	2	10	9	6		8	11	
6.0		2		9	4	2	4		2	5	9	
6.5		5		9	4	2			4	16	15	1
7.0			1	9	6	2	4				2	
7.5		3		15	2		4	6	2		4	
8.0				4	4			6		3	2	
8.5			1	7	10	4	9			3		
9.0		2		11	4				2		4	
9.5				7								
10.0				2	4	2	4					
10.5							4	12		3		
11.0			1									
11.5			1		4							
12.0				7	4	2				3		
12.5								6				
13.0					2		4					
13.5							4					
14.0					2	2						
16.0			1			2						
16.5			1									
17.0					2							
17.5								6				
23.5					2							

duration of each sample, t_s (s) and gap, t_g (s)

t_s	926	431	405	128	67	39	68	7	39	282	17	475
t_g	25	612	3033	132	223	296	302	290	481	120	446	

d178 Canopy Site a

stain diameter	sample number									
	1	2	3	4	5	6	7	8	9	10
0.25	14	45	72	242	175	87	182	132	80	26
0.5	45	68	85	162	104	67	243	229	130	35
1.0	54	59	56	73	58	116	68	118	51	22
1.5	70	41	41	41	47	67	42	79	65	22
2.0	51	20	29	45	36	49	30	54	109	9
2.5	24	17	27	6	36	41	46	47	43	4
3.0	9	14	19		11	12	42	11	51	
3.5	9	9	23	3	27	20	27	14	25	
4.0	7	6	6	6	3	6	8	7	14	
4.5		6	10	6	22	26	15	4	36	1
5.0	1	8	4	3	8	3	8	7	18	
5.5		3	4	3	5	3	8	7	22	
6.0			6	6	5	3	11	4	14	
6.5			4		5	12	4	4	18	
7.0		3	2	3	3	6	8		11	
7.5		2				3	4		14	
8.0			8	3		12	8		7	
8.5		2	2			6			7	
9.0			4				4			
9.5			2			3				1
10.0			2			12			4	
10.5				3		9			4	1
11.0			2		3					
11.5						3				
12.0				10						
12.5				3						
13.0			2			3				
13.5				3						
14.0				6						
14.5		2					4			
16.0						3				
17.0				3						
18.0				3						
19.0						3				
20.5			2			3				
22.0						3				
22.5						3				

duration of each sample, t_s (s) and gap, t_g (s)

t_s	946	1058	110	24	105	15	10	242	73	510
t_g	20	3395	201	231	263	310	290	580	487	

throughfall sampling started 78 s after rainfall sampling

d178 Canopy Site d

stain diameter	sample number								
	1	2	3	4	5	6	7	8	9
0.25	53	60	145	303	172	504	213	147	148
0.5	81	66	172	202	153	309	210	83	139
1.0	101	40	128	105	67	208	132	83	181
1.5	68	19	55	57	64	108	54	62	195
2.0	60	8	22	20	38	54	58	56	102
2.5	53	1	22	8	45	54	53	24	88
3.0	38	3	15	4	10	20	8	39	23
3.5	25	1	12	4	13	20	8	11	28
4.0	10	1		4	16		4	11	
4.5	5	2	12	8	13	7	16	8	5
5.0			9	16	10		8		
5.5	5	4	3	4	6	7	8	5	5
6.0	5	1	3		6				5
6.5		1	6	12	13			5	5
7.0			3	4		7	4		
7.5			3	12	3	7	12	3	
8.0		1		12	3	7	4		
8.5			3	4			4		
9.0			3	8	3				
9.5			3	4			4		
10.0		1		4			4		
11.0		1	3						
12.0				4	3				
12.5				4					
13.0						7			
16.5				4		7			
19.0							4		
25.0						7			
25.5						7			
28.0						7			
40.5									5
49.5								3	

duration of each sample, t_s (s) and gap, t_g (s)

t_s	557	615	97	23	78	13	12	247	284
t_g	367	3322	263	212	290	304	262	694	

throughfall sampling started 667 s after rainfall sampling

d211 Open Site

stain diameter	sample number						
	1	2	3	4	5	6	7
0.25	141	62	123	553	85	88	23
0.5	124	160	123	279	74	133	48
1.0	51	98	105	143	52	48	32
1.5	39	102	42	51	39	75	17
2.0	51	111	39		41	15	8
2.5	51	80	39	11	23	13	4
3.0	31	27	33	6	16	8	3
3.5	34	67	30	17	25	3	1
4.0	25	27	9	6	19	10	1
4.5	11	49	15	6	16	13	
5.0	3	18			8	13	2
5.5		13	12	17	2	13	
6.0		13	3	6	4	18	
6.5		22	6	6	4	10	1
7.0	3	9	3			3	1
7.5			3	6	2	5	
8.0		9					
8.5		9				18	
9.0		9				3	
9.5			6	6		3	
10.0			3	6	2		
10.5				6			
11.0		4				5	
11.5						5	
12.5			3				
13.0						3	
13.5				6			
15.5			3				
16.0				6			
16.5				6			
24.5						3	

duration of each sample, t_s (s) and gap, t_g (s)

t_s	76	96	16	6	14	112	419
t_g	52	82	84	88	123	51	

d211 Canopy Site

stain diameter	sample number					
	1	2	3	4	5	6
0.25	87	190	111	400	107	47
0.5	87	255	139	810	124	67
1.0	76	149	183	337	154	26
1.5	91	160	131	295	94	37
2.0	91	77	52	63	53	11
2.5	120	95	20	53	53	2
3.0	73	48	20		23	1
3.5	40	83	8	32	20	2
4.0	11	42	4	21	10	1
4.5	22	30	16		10	
5.0	11	6	4		7	
5.5	4	24	16		3	
6.0		12	4	11		1
6.5	4		8	42		
7.0	4	6	8			
7.5	4		8	21		
8.0		6	12			
8.5	4	6	4		3	
9.5			8	11		
10.5			8		3	
11.0			4			
11.5			12		3	
12.0			4	11		
14.5			4			
15.0			4			
15.5			4			
28.0						1

duration of each sample, t_s (s) and gap, t_g (s)

t_s	107	62	14	13	53	433
t_g	50	94	85	82	104	

throughfall sampling started 42 s after rainfall sampling

d237 Open Site

stain diameter	sample number								
	1	2	3	4	5	6	7	8	9
0.25	5	21	24	4	16	113	574	1116	858
0.5	11	18	12	4	32	301	387	3925	1539
1.0	189	1	27	141	67	94	100	1501	1450
1.5	286	4	104	315	191	371	125	962	1214
2.0	227	32	116	186	129	283	50	77	651
2.5	162	54	83	76	25	75	12	115	89
3.0	119	38	89	27		19			89
3.5	49	13	48	4					30
4.0		25	48	4					
4.5	27	29	33						
5.0	5	24	9						
5.5		19	3						
6.0		10							
6.5		3							
7.5		1							

duration of each sample, t_s (s) and gap, t_g (s)

t_s	266	19	28	29	54	340	457	2143	3522
t_g	50	91	85	138	130	23	1691	3964	

d237 Canopy Site

stain diameter	sample number							
	1	2	3	4	5	6	7	8
0.25	33	92	41	194	597	1848	1440	624
0.5	62	113	57	124	61	1994	1227	559
1.0	71	58	38	89	30	584	245	326
1.5	102	92	133	132	49	243	180	186
2.0	60	110	106	159		97	33	121
2.5	64	64	45	19	4	24	16	280
3.0	21	46	14	16	4		33	
3.5	31	15	7	23		24	16	
4.0	48	6	5	4			16	9
4.5	12	3	5				16	
5.0	5	9		8		24		
5.5	7	3		4	4	24		
6.0	2		2					
6.5							16	
7.0					4			
7.5				4	4		16	
9.0					4			
15.0								9
25.0							16	

duration of each sample, t_s (s) and gap, t_g (s)

t_s	298	101	129	521	462	1590	2106	3385
t_g	18	14	23	130	91	27	496	

throughfall sampling started 76 s after rainfall sampling

APPENDIX 1b Tropical rain forest site: frequency of occurrence of stain diameters (mm) on sample sheets

j10b Open Site

stain diameter	sample number																	
	1	2	3	4	5	6	7	8	9	10	11	12	13	14	15	16	17	18
0.25	17	5	13	70	13	31	34	25	9	22	4	27	40	34	53	42	8	7
0.5		21	13	25	17	15	20	10	16	21	28	43	72	34	117	35	10	45
1.0	90	46	21	14	46	36	26	23	10	36	57	78	78	36	99	66	47	89
1.5	38	62	28	11	22	17	10	20	4	57	105	71	54	75	112	16	75	30
2.0	66	80	8	11	24	22	22	16	12	33	87	41	48	84	89	3	34	1
2.5	61	30	1	20	21	26	32	20	7	16	42	39	14	73	36	11	32	
3.0	27	5	16	18	16	26	18	23	9	14	28	37	34	30	3	5	50	
3.5	23	3	15	16	8	17	16	26	9	16	8	18	28	43			18	
4.0	7	5	43	5	5	10	14	46	2	16	12	20	16	27			8	
4.5	3	31	35	16	17	26	18	25	9	13	8	20	10	14		3	5	
5.0		31	16	20	13	21	18	30	6	22	6	4	4	5		7	5	
5.5		5	6	18	9	19	32	13	9	16	2	8	2			7	10	
6.0		3	8	11	16	24	28	8	24	5	2					2	3	
6.5			9	16	19	10	46	16	21	6	6	2				7	3	
7.0			4	11	5	12	10	16	12	6						8	3	
7.5			3	9	9	3	12	8	9	8						8	10	
8.0			1	12	6	7	12		4	2						1	2	
8.5			1	9	6	2	8		3		2					3		
9.0			3	5	5		2	2	5	2						1		
9.5			4	2	6	3	8		1	2								
10.0			4	4	8	9	4			2								
10.5				2						2						1		
11.0				4	5		2		1									
11.5				9	6		2										2	
12.0				4			2											
12.5				5		2												
13.0				4						2								
13.5			1		2	3	2											
14.0				2	3													
14.5				2	3		2											
15.0								2										
15.5				2	5													
16.0						2												
20.0				2														
20.5					2													
22.5				2														

duration of each sample, t_s (s) and gap, t_g (s)

t_s	10	11	4	5	6	8	10	12	5	15	10	25	45	45	90	90	60	150
t_g	89	105	125	115	129	127	290	288	295	765	290	275	255	255	210	210	450	

j10b Single Canopy Site

stain diameter	sample number										
	1	2	3	4	5	6	7	8	9	10	11
0.25	404	52	296	242	176	97	79	34	35	94	22
0.5	229	89	194	98	133	74	44	31	36	51	5
1.0	176	64	122	80	79	41	28	21	24	44	6
1.5	85	37	42	44	65	28	18	19	7	13	6
2.0	21	54	19	18	26	10	10	9	4	3	2
2.5	43	37	11	15	31	6	9	3	4	2	1
3.0	21	17	11	6	3	7	7	3	2	4	2
3.5	5	15	4	27	14	4	2	2	3	2	
4.0	16	6	15	15	3	4	4		1		
4.5	11	6	11	6	9	3	2	2			
5.0		10	4	6	6	4	1		4	1	
5.5	5	2		9		1		1	2		
6.0	5	4	4				1				
6.5	2		11	6		1	1		1		
7.0		2		3							1
7.5	5										
8.5	5										
9.5		2									
10.0		2			3			1			
10.5	5					1					
11.0				3		1					
12.0					3					1	
12.5		2									
13.0				3							
13.5				3							
15.5					3						
16.0			4								
16.5					3						
18.5					3						
19.0						3					
20.5		2									
21.5	5										
23.0						1					
24.0				3							
25.0							1				
26.0		2			3						
26.5			4	3							
27.0		2				1					
27.5				3							
31.5		4									
32.0	5				3						
34.0		2									
35.0			4								
36.5					3						
43.0			4								

duration of each sample, t_s (s) and gap, t_g (s)

t_s	15	30	30	50	40	80	78	105	145	136	270
t_g	105	150	240	250	260	220	222	195	645	574	

throughfall sampling started 1184 s after rainfall sampling

j10b Multiple Canopy Site

stain diameter	sample number								
	9	10	11	12	13	14	15	16	17
0.25	18	68	219	45	23	90	28	34	20
0.5	35	88	162	74	36	69	21	30	13
1.0	29	60	122	67	40	47	21	23	9
1.5	28	46	105	43	25	59	34	34	16
2.0	24	26	57	49	10	33	23	28	8
2.5	22	5	61	25	6	20	15	18	6
3.0	10	11	32	20	10	18	14	9	3
3.5	9	12	12	4	4	8	5	3	3
4.0	9	4	8	2	3	12	1	1	3
4.5	5	9	4	4	4	4	1	1	
5.0			4	9		6	1	3	1
5.5	1	4	4	2	1	2	1	1	1
6.0	4	4				4		1	
6.5	1			4	1	2		1	
7.0		2		2				2	1
7.5		2	4			4	1	1	1
8.0	1		4			4			
8.5					2				1
9.0				4				1	
9.5						2			1
10.0			4						
10.5				2					
11.0				2					
11.5				2				1	
12.0		2			1	2			
12.5							1		
13.0		2							
13.5			4						
15.0						2			
15.5							1		
17.5				2	1				
18.0	1								
19.0	1					4			
19.5					1				
20.5		2							
22.0		2							
24.0		2							
25.0								1	
26.0					1				
29.0				2					
30.5					1				
32.5					1				
35.5			4						
36.0							1		
46.0		2							
47.0		2							
51.0									1
59.0						2			
68.0					1				
80.0	1								

duration of each sample, t_s (s) and gap, t_g (s)

t_s	35	57	118	105	285	650	310	720	1160
t_g	300	300	300	240	300	330	180	60	

sample 9 started 1484 s after the start of rainfall sampling

j11 Open Site

stain diameter	sample number												
	1	2	3	4	5	6	7	8	9	10	11	12	13
0.25	57	37	15	13	19	1016	322	91	226	228	5	10	15
0.5	91	89	28	13	42	650	138	79	139	136	3	16	18
1.0	63	152	15	14	12	203	73	34	139	21	12	13	1
1.5	34	192	10	17	13	30	59	20	129	33	13	19	8
2.0	8	163	7	6	14	10	17	12	69	12	18	23	5
2.5	4	63	10	4	8	20	10	12	83	12	27	20	
3.0	30	7	1	5	11	10	24	12	18		23	20	
3.5	44	22	6	7	11	10	7	5	9	6	17	12	9
4.0	32	4	5	2	4		7	2	23	3	30	16	9
4.5	17		4	3	18			4	46	1	9	22	12
5.0			6	8	4	10	3	4	92		3	11	4
5.5		7	3	5	7	10	3	7	92	6	1	5	9
6.0			1	4	2		3	12		15		7	6
6.5		4	6	6	2	10	3	7		21	1	4	8
7.0			5	4	6		3	7		12		8	1
7.5			4	8	3	10	3	12		12		8	2
8.0				3	3			5	5	18		4	
8.5			4	5	10			2		15			
9.0			3	3	2			9			1		
9.5			3	2	2		3	4	5	3		1	
10.0				5	3		3	4	5		1		
10.5			4	2	2						3		
11.0			3	2	1								
11.5				4	4	20		2		3	2		
12.0			1	2	2					6	3		
12.5			3	4	1				9	6	2		
13.0			1	2					9	3	1		
13.5								2					
14.0					1								
14.5			1	1		10		2			1		
15.0			2	1	1					3			
15.5					3				5		1		
16.0			1					2	9				
16.5				2						3			
17.0			1		1								
17.5									9				
18.0			1	1	2								
18.5										3			
19.0				1	1								
19.5								2	5	3			
20.0								2					
21.5					1	10							
22.0								2					
22.5			1										
23.5					1								
24.5									5				
29.5							3						
32.0							3						
36.0			1										

duration of each sample, t_s (s) and gap, t_g (s)

t_s	42	30	1	3	2	4	4	3	4	5	9	10	39
t_g	268	203	119	177	78	257	30	269	440	831	401	650	

j11 Single Canopy Site

stain diameter	sample number														
	1	2	3	4	5	6	7	8	9	10	11	12	13	14	15
0.25	48	49	205	192	247	224	135	129	86	30	27	55	104	43	23
0.5	67	99	136	185	213	221	96	106	57	31	28	44	68	27	43
1.0	106	105	62	130	99	98	87	64	37	14	5	24	41	22	14
1.5	220	58	81	40	74	54	99	46	65	7	6	14	35	15	
2.0	204	49	66	58	26	47	57	35	21	22	6	6	24	15	2
2.5	102	31	29	36	4	11	30	23	14	2	6	3	5	10	1
3.0	27	11	18	18	11	18	24	30	24	2	3	6	9	6	4
3.5	8	16	18	18	4	4	9	7	6	5	2	2	5	2	1
4.0	8	2	22	14	7	11	12	5	3	1	2		2	1	
4.5		9	22	4	4	4	18	5	2	2	2		2		1
5.0		2	4	11	11		3	2		2		1			
5.5		4	7		11	7	3		2	2		2		1	
6.0			11			4							2		
6.5		4			4										
7.0		4	4					2		2					
7.5		2	4	4	4					1	2		2		
8.0			7		4	4									
8.5							3							1	
9.0					4	4		2							
9.5							3						2		
10.0													2		
10.5				4											
11.0			7												
11.5				4											
12.0										1					
14.0															1
14.5									2						
15.5							3								
17.5				4											
18.5			4												
20.5						4									
21.5							3								
22.5										1					
23.0								2			1				
23.5				4	4			2							
24.0															
24.5						4									
26.0			4			4				1					
27.0										1					
29.0						4									
30.0										1					
30.5													2		
31.0													2		
32.5					4		6								
33.0			4												
35.0							3								
36.0					4										
37.0			4				3								
39.0			4												
40.0			7												
41.5							3								1
44.0			4												

duration of sample t_s (s) and duration of gap t_g (s)

t_s	249	68	2	4	15	4	8	29	50	92	170	157	210	300	600
t_g	48	245	195	185	156	411	1100	692	490	268	280	300	240	300	

throughfall sampling started 129 s after rainfall sampling

j11 Multiple Canopy Site

stain diameter	sample number																		
	1	2	3	4	5	6	7	8	9	10	11	12	13	14	15	16	17	18	19
0.25	289	112	96	183	332	337	185	250	80	152	218	211	156	219	135	109	136	159	92
0.5	213	151	281	107	399	129	58	306	86	63	135	137	77	121	124	111	231	141	87
1.0	110	148	230	76	163	72	39	99	94	55	66	86	79	73	72	69	126	91	72
1.5	42	112	63	37	73	48	29	44	70	32	93	53	55	90	55	47	87	59	62
2.0	27	46	21	51	28	17	10	12	26	34	66	33	26	59	47	47	35	47	36
2.5	30	26	34	22	11	10	19	16	8	32	42	24	11	38	39	16	28	29	17
3.0	11	7	13	20	34	20	4	8	2	4	21	12	2	45	22	9	17	15	26
3.5	11	7	34	11	22	3	17	4	10	11	7	9	2	10	14	13	3	15	9
4.0		13	4	8			10	4	4	8	3	9	4	3		2	7	3	6
4.5	8	10	8	8	11	10	4	12	4	2	3		2	7	11	2			11
5.0	8		4		6	7		4		4	10	3	2		6				
5.5	4		13		6	3		4	2	6	35		2	3			3		
6.0			4					4	2	2	7	3	2	3	6				
6.5				8	11	3		4		2	10		4	3		4		6	2
7.0	4	3		3	6								2		6				
7.5				3			2			2									
8.0			8	3			2	4	2		3			3			3	3	2
8.5	4		4	3	6								2	3	3		3	3	
9.0												3							
9.5				3				4	2				2		3				
10.0		4	8					4							3			9	
10.5							2					3				2			
11.0		7								2									
12.0																2			
12.5												3							
13.0				3												2			
13.5														3				3	
14.0																			2
14.5					6							3				2			
15.5																2			
16.0		3								2									
16.5									2								3		
17.0								4										3	
17.5															3				
18.0		3					2							3					
18.5		3															3		
19.5															3				
20.0																	3		
22.0				3															
23.0						3				2									
24.0															3				
24.5					6														
26.0																2			
26.5					6					2									
27.0										2									
28.0																			2
29.0				3															
29.5						3													
31.5				6		3													
32.0								4											
34.0				3					2										
35.5			4						2										
39.0						3													
40.0							2												
45.0													2						
45.5											3								
46.0													2						
48.0		3																	
52.0																2			
54.0										2									
55.5												3							
56.5						3													
57.5							2												
58.5														3					
60.0													2						
63.0																	3		
64.5								4										3	
84.0						3													
84.5			4																
85.5			4																

duration of each sample, t_s (s) and gap, t_g (s)

t_s	575	2	4	4	10	5	17	11	34	59	26	20	45	116	237	262	300	615	860
t_g	120	120	120	120	300	300	300	300	300	300	223	300	300	300	300	250	300	300	

throughfall sampling started 30 s before rainfall sampling

j12 Open Site

stain diameter (mm)	sample number										
	1	2	3	4	5	6	7	8	9	10	11
0.25	35	47	277	265	50	24	12	53	21	11	9
0.5	42	11	72	28	16	7	33	73	2	4	8
1.0	29	7	38	6	14	10	37	28	1	4	8
1.5	13	6	23	2	9	16	76	4	1	9	18
2.0	5		15	6	9	17	82	6	2	11	12
2.5			5	2	1	26	27	8	2	12	25
3.0	1		3	2	2	23	12	8	4	12	22
3.5	2	1	3	4	2	22	4	1	4	10	17
4.0						18	1		2	5	10
4.5			3	2	3	12	3		6	14	11
5.0			3	4	11	10			3	10	13
5.5				4	8	2			2	7	1
6.0	1			2	4	1			5	4	4
6.5		1	3	4	5				4	3	
7.0				4	1				2		2
7.5			3	2	9					2	1
8.0		1		12	9				4	1	
8.5				8	9				4		
9.0			3	6	6				2		
9.5			5	8	1				1		
10.0				4					2		1
10.5				6	1				4		
11.0				4							
11.5		1		4							
12.0				6					1		
12.5			3	2					2		
13.0	1	1			1						
13.5		2		4							
14.0		1	3						1		
14.5		1									
15.0		2							1		
15.5	1										
16.0	2		5								
17.0			3								
17.5			3								
18.0	1	1	3								
18.5	1	1									
19.0	1	1									
19.5	1		3								
20.0	1	1	3								
21.0			5								
22.0			5								
22.5			5								
24.0			3								
25.0	1	3									
27.0			3								
27.5	1										
28.0			3								
32.0			3								
33.0			5								
39.0			3								
42.0			3								

duration of each sample, t_s (s) and gap, t_g (s)

t_s	160	10	5	6	9	15	32	120	42	62	230
t_g	58	70	90	94	171	105	208	320	118	178	

j12 Single Canopy Site

stain diameter	sample number							
	1	2	3	4	5	6	7	8
0.25	153	336	288	365	131	42	73	43
0.5	182	236	204	134	110	34	61	29
1.0	60	189	116	52	61	23	29	15
1.5	73	115	167	56	45	18	20	21
2.0	21	21	37	41	25	15	6	4
2.5	3	26	33	33	27	2	14	6
3.0	10	16	9	22	16	3	6	1
3.5	3		19	15	7	3	6	1
4.0	3	16	14	74	7		2	
4.5	8	21	5	15		3	1	
5.0			5		2	1	5	
5.5	3	10			10		2	1
6.0		5			5			
6.5		10				2		
7.0		5	5			1		
7.5		5	5				1	1
8.0	3						1	
8.5								1
9.5			14			1	1	
10.0		5						
10.5						1	1	
11.0							1	
12.5			5					
13.0		5						
14.0						1	1	
14.5		5						
16.0				4				
16.5		5						
17.5		5						
18.5								1
19.5					2			
21.0							1	
23.0			5				1	
23.5						1		
25.5					2		1	
26.0							1	
26.5		5						
27.5					2	1		
30.5						1		
32.5		5						

duration of each sample, t_s (s) and gap, t_g (s)

t_s	225	5	10	25	30	180	120	420
t_g	90	115	110	125	300	300	300	

throughfall sampling started at the same time as rainfall sampling

j12 Multiple Canopy Site

stain diameter	sample number							
	1	2	3	4	5	6	7	8
0.25	458	436	212	257	107	140	104	53
0.5	201	226	79	171	52	100	140	27
1.0	56	132	61	105	45	47	56	13
1.5	40	99	46	97	29	51	51	17
2.0	12	72	41	47	23	23	23	7
2.5	4	39	18	27	27	28	51	8
3.0		11	15	16	16	9	23	5
3.5		17		12	16	7	5	4
4.0		11	10	4	5	9	5	1
4.5		11	3	4	11	12	10	2
5.0		17	3		18	2	5	
5.5	12	17		4	4	2	10	1
6.0		6			2	2		1
6.5	4		3	8	2	7	5	
7.0						2		
7.5	4			4		2	3	
8.0			3				3	
8.5							3	
9.0				4				
9.5				4	2	5		1
10.0				4	2		3	
11.0				4				
11.5					2			
12.0							3	1
13.5		6				2		
15.0			3					
17.0					2			
17.5						2		
18.0			3					1
19.5							3	
20.0						2		1
20.5					2			
22.0				4				
22.5			3		2			
23.0						2		
23.5						2		
24.5			3					
25.0					2			
26.0			3			2		
26.5		6						
27.5	4							
28.0						2		
28.5	4							
29.5	4		3					
30.0							3	
32.0			3					
40.5								3
42.0					2			
44.0					2			
44.5				4				

duration of each sample, t_s (s) and gap, t_g (s)

t_s	60	22	17	36	79	308	828	660
t_g	120	121	120	120	300	300	300	

throughfall sampling started 210 s after rainfall sampling

j13 Open Site

stain diameter	sample number													
	1	2	3	4	5	6	7	8	9	10	11	12	13	14
0.25	7	6	42	32	22	6	13	25	62	91	126	111	31	16
0.5	3	18	23	20	12	12	20	45	6	38	22	86	7	6
1.0	4	19	4	9	7	17	24	20	4	18	1	11		4
1.5	6	33	1	3		55	64	45	8	9	3	23	24	3
2.0	20	44	1	2	1	99	60	52	14	5	9	21	21	5
2.5	15	26		1	18	49	23	48	40	4	4	9	35	6
3.0	14	30	1		17	26	19	14	26	8	9	4	34	1
3.5	15	24			16	18	16	17	17	13	7		15	
4.0	8	13			4	15	5	10	17	11	9	13	14	
4.5		7		4	5	8	5	4	9	11	13	15	16	2
5.0		1	8	7	3		1		15	5	6	11	5	4
5.5		2	17	12	4		1	1	10	14	13	19	5	6
6.0			13	7					10	1	9	9	6	4
6.5			9	11					6	4	26	6	1	4
7.0			7	3					4	4	9	4	7	1
7.5			6	4						5	6	11	7	
8.0			4	7					4	5	3	4	1	
8.5			2	1	1				1	3	6	8	2	
9.0			1	4					1	1	4	6		
9.5				2					1	3	3	9		
10.0											1	6		
10.5										1	1	4	1	
11.0												2		
11.5				1							1			
12.0				1										
12.5												2		
13.5	1													

duration of each sample, t_s (s) and gap, t_g (s)

t_s	162	16	49	60	160	25	23	50	37	25	29	37	68	144
t_g	88	224	81	610	1280	95	97	140	173	125	210	243	352	

j13 Single Canopy Site

stain diameter	sample number										
	1	2	3	4	5	6	7	8	9	10	11
0.25	28	38	104	24	19	169	272	143	276	140	51
0.5	36	78	105	18	27	109	296	120	146	100	41
1.0	15	58	37	6	17	67	99	49	103	65	22
1.5	13	75	8	1	28	42	55	36	76	36	18
2.0	25	27	4	1	27	25	28	24	27	29	10
2.5	21	4	3	2	11	13	12	19	7	18	6
3.0	39			2	12	4	4	15	10	11	6
3.5	19	3	3	2	7	2	12	4	3	13	6
4.0	9		1	2	1	2		4	7	2	5
4.5	3		1		5		12	6	3	4	2
5.0	2		3	1	2	4				2	5
5.5				1		2				4	
6.0			4		1					2	
6.5			1			2					1
7.0					1					2	
7.5								2		2	
8.0										4	
8.5											2
10.0						2			3	2	1
11.0										2	
11.5										2	
14.0										2	
16.5								2			
19.0								2			
22.0									3		

duration of each sample, t_s (s) and gap, t_g (s)

t_s	210	420	180	300	60	180	120	60	90	120	300
t_g	100	3540	480	1170	150	120	120	120	150	180	

throughfall sampling started at the same time as rainfall sampling

j13 Multiple Canopy Site

stain diameter	sample number 1	2	3	4
0.25	21	65	252	203
0.5	23	61	347	121
1.0	19	38	132	68
1.5	13	16	132	34
2.0	7	4	79	31
2.5	2	3	26	17
3.0	5	2	32	5
3.5	2		5	2
4.0	1		11	
4.5		1	11	
5.0				2
6.0			5	
7.0		1	5	
7.5			11	
8.0			5	

duration of each sample, t_s (s) and gap, t_g (s)				
t_s	1070	2235	420	2070
t_g	2900	510	120	

throughfall sampling started
165 s after rainfall sampling

j15 Open Site

stain diameter	sample number																	
	1	2	3	4	5	6	7	8	9	10	11	12	13	14	15	16	17	18
0.25	31	13	72	51	7	10	6	9	66	70	46	3	31	21	31	7	16	1
0.5	21	11	56	9	7	1	4	3	50	20	15	18	50	3	18	5	7	5
1.0	11	4	24	6	5	10	1		21	6	9	35	60	6	29	14	5	8
1.5	7	10	4	5	1	23			21	12	19	41	65	13	16	11	4	14
2.0	7	10		7	3	13			15	7	10	12	14	10	7	9	4	11
2.5	8	7		3	12	11	1	3	19	5	14	33	1	8	13	7	3	5
3.0	3	1		6	7	5	1	6	62	4	21	36		8	13	11	6	5
3.5	9	10		4	2	11	3	4	46	7	18	30		9	9	5	6	8
4.0	4	8		5	1	10	5	6	46	11	11	15		13	7	3	9	5
4.5	7	35		9		10	14	7	19	11	21	2		11	9	3	9	2
5.0	3	24		9		6	5	5	6	16	9	1		15	8	5	6	1
5.5	4	41		10	1	9	5	4	4	22	7			13	8	4	9	
6.0	1	25		3	3	5	1	4		11	3			7	4	2	9	
6.5		21		3	4	5	2	3	2	10	2			7	1	5	5	
7.0		13		2	3	1				11	3			6	1	2	7	
7.5	1	8						2	2	9	2			1	2	3	3	
8.0		6			1		1	1	2	4				1	10	4	2	
8.5		10			1			1		6	1			1		2	2	
9.0		4								2				1		2	1	
9.5		8					2				1				1			
10.0	3	6						1		1	1				1			
10.5	1	3			2		1								2			
11.0	1								4						1	1	1	
11.5	5				1		1								1			
12.0	3				1												1	
12.5	1				1		2											
13.0	2	1			1		1									1		
13.5	2				1													
14.0	3	1			2													
14.5	3				4													
15.0	2				1													
15.5	1				1													
16.0					1													
16.5	1																	
17.0																		
17.5	1																	
18.0	1				1													
19.0	2																	
19.5					1													
20.0	1																	
20.5	1																	
22.0	1																	
22.5	1																	
24.5	1																	
28.5					1													

duration of each sample, t_s (s) and gap, t_g (s)

t_s	6	7	180	150	140	90	165	150	140	15	7	20	240	40	30	40	40	240
t_g	104	143	1290	120	100	195	300	270	160	285	293	460	1080	320	330	380	440	

j15 Single Canopy Site

stain diameter	sample number																		
	1	2	3	4	5	6	7	8	9	10	11	12	13	14	15	16	17	18	19
0.25	490	200	225	47	26	262	195	149	204	117	104	37	47	129	134	180	145	43	67
0.5	271	135	109	27	20	127	111	166	116	72	83	44	47	131	77	102	78	29	32
1.0	153	79	66	26	11	61	59	99	47	37	41	26	20	60	42	64	22	9	11
1.5	100	56	38	13	12	52	52	39	30	27	28	23	18	60	25	38	44	7	5
2.0	41	20	23	10	4	8	14	33	22	25	25	18	6	26	8	13	25	7	3
2.5	18	14	5	3	3	14	9	6	12	13	25	2	5	17	5	9	16	5	4
3.0	18	25	20	4	2	14	5	14	15	13	11	2	5	24	7	7	5	2	
3.5	24	6		2		6	2		7	8	2	5	2		3	4	5	3	2
4.0	6	3		3	1			11	12	2		1	7	10	3	2	4	1	
4.5	6	3	3			3			5	2	5	1		7	5		2	1	
5.0		3	3	1				3	2		5	1	2		3	2		1	1
5.5	18	3			1	3		3		2	2	1			5	4	2		
6.0	6	3	3	2					2			2	1				2		
6.5					1			3	5					2	2		2		
7.0	6		3	1					2	2				2		2	2		
7.5								3		2								1	
8.0			3				2		2	2	4				2	2	2	1	
8.5														2			2		
9.0					1					2	2					2			
9.5								3						2	2				
10.0											2								
10.5								6											
11.0	6																		
11.5		3						3											
12.0												2			2				
12.5																	2		
13.0								3								2			
13.5											4								
14.0			3																
14.5								3								2			
15.0														2					
15.5								3		2						2			
16.0																	2		
17.0					1														
18.0									2										
18.5			3																
19.5								3											
20.5												1							
21.0												1							
21.5						3		3				1							
22.5										2									
23.5	6		3								2								
24.0	6																		
24.5		3									2				2				
25.0											2					2			
25.5	6	3																1	1
26.0							2												
26.5												1			3				
27.0														2	2				
27.5																			1
28.0									2		2				2		2		
28.5				1						2									
29.0										2	4				2				
30.0											2								
31.5		3					2												
32.0																2			
32.5																		1	
33.0																	2		
34.5		3																	
36.5										2									
39.5										2									
47.5									2										

duration of each sample, t_s (s) and gap, t_g (s)

t_s	1	16	95	300	632	171	60	40	20	12	25	105	420	50	60	60	105	300	515
t_g	117	107	143	197	639	378	465	290	280	288	335	495	720	310	360	360	555	403	

throughfall sampling started 32 s after rainfall sampling

j15 Multiple Canopy Site

stain diameter	sample number																										
	1	2	3	4	5	6	7	8	9	10	11	12	13	14	15	16	17	18	19	20	21	22	23	24	25	26	27
0.25	272	203	43	41	30	23	29	108	173	465	26	66	24	28	5	15	179	63	12	42	67	13	33	14	20	13	44
0.5	192	73	54	30	21	28	30	14	127	209	20	59	25	20	15	17	84	33	11	38	25	11	14	17	17	11	54
1.0	56	71	19	14	15	14	11	2	68	79	12	13	5	6	7	10	26	11	10	44	15	6	14	3	10	9	22
1.5	64	37	16	11	3	22	7	12	32	65	12	5	11	5	7	5	13	18	8	30	9	3	11	5	10	6	12
2.0	64	15	6	5	9	10	7	4	20	19	14	4	8	6	2	2	49	4	13	16	9	7	4	4	4	1	7
2.5	48	12	5	6	3	8	2	4	22	37	4	1	1	1	1	2	8	5	7	7		3	3		6	1	4
3.0	12	10	3	7		4	1		5	5	4	2	3	2	2	2	2	1	2	2	1	2	1	2	3		3
3.5	20	12	1	1	1	4	4		2	9	2	2	2	2			2	4	1	2	4	1		1	3		1
4.0	16	2	2			2			2	9	1	1	2		1		2				1			1	1		2
4.5	8	5	2		1	1			5	5		3	1			2		2		1	1			1	2		2
5.0				1		1	1	1			1	1				1			1								
5.5	12	5		1		1	2					1	1						2	2			1		2		1
6.0	4		1		1																						
6.5		2						1			2		1					1		1					1		
7.0				1	1					9	1							1									
7.5	4								2		1	1		1				1		2							
8.0		2		1	1			1				1			2						1						1
8.5									2																		1
9.0			1																						1		
9.5									2																		1
10.0	4								2		1															1	
10.5		2																	1								
11.0		5																									1
11.5										5										1					1		
12.0		5																			1						
13.0														1													
13.5																				1							
14.0																					1	1				1	
14.5							1														1	1					
15.0							1					1		1							1						
16.0		5						1											1								
16.5																			1								
17.0			1																		2	2					
17.5	8											1									1					1	
18.0	4	5										1				1											
18.5				1								1									1	1				1	1
19.0			1	1	2						1		2					2	1		1						1
19.5								1	1			1							1	1	1					1	
20.0		5						1	1	2								2		1	1		1		1		
20.5			1	1	1			1	1			1						2	2		1		2				
21.0							2		1				1						1		1	1	1		1		
21.5	4						2		1					2	1				1						1		
22.0								1				2				4							1		1		
22.5							1	1	1		9	1				2		1									
23.0						1			1													1	1	2			1
23.5					2	1				5		1		1				2						1			
24.0					1				1	7										1			1				1
24.5		2	1				1		2							1				1							
25.0				1			1									2						2					
25.5										2	5																
26.0	4		1											1		1				1							1
26.5	4																										
27.0							1				2				1					1							
27.5		2		1					2			1		1													
28.0			1	2				2																			
28.5					1				1						1			2		1							
29.0			1	1				1						1						1							
29.5											1																
30.0		2									2		1	1					1								
30.5															1				2								
31.0						1					1				1												1
31.5		2			2																			2			
32.0											1		1												1		
33.0												1															
33.5																				1							
34.5																										1	
36.0		2					1				2											1					
37.0				1																							
38.0			1								1				2	1											
39.0		2	1																								
41.0																						1					
44.5		2																									
45.5									2																		
48.5																			1								
53.0													1														

duration of each sample, t_s (s) and gap, t_g (s)

t_s	18	6	11	30	43	165	175	495	752	40	9	13	45	43	54	96	189	26	40	41	39	105	120	135	205	312	318
t_g	120	120	120	120	300	300	300	300	300	320	336	300	300	300	300	300	300	378	300	300	319	300	420	360	300	300	

throughfall sampling started 28 s before rainfall sampling

j16b Open Site

stain diameter	sample number								
	1	2	3	4	5	6	7	8	9
0.25	54	44	33	28	8	15	11	5	21
0.5	11	30	21	24	13	20	29	15	58
1.0	2	6	8	19	13	28	17	22	53
1.5	18	10	14	30	22	45	23	33	65
2.0	9	13	9	30	28	31	37	23	30
2.5	15	8	9	19	26	23	26	30	26
3.0	5	5	3	18	25	29	25	16	21
3.5	11	9	6	16	25	18	26	27	9
4.0	9	7	4	20	18	20	21	10	12
4.5	11	4	4	12	10	10	12	13	3
5.0	9	13	3	12	2	6	10	1	2
5.5	14	3	4	15	1	5	5	4	3
6.0	2	1	2	7	6	4	1		
6.5	5	4	5	7			2	1	
7.0	1	5	3	4	1				
7.5	3	2	3	3	1				
8.0	1	4	5						
8.5			3	4					
9.0		2	3	1					
9.5	1	2	2		1				
10.0	1	1	2						
11.0		1	1						
11.5		1	1	1					
12.0		3	1						
12.5			2						
13.0			1						
14.0		1	2						
16.5		1							

duration of each sample, t_s (s) and gap, t_g (s)

t_s	33	31	26	51	38	43	57	59	177
t_g	507	265	268	339	376	318	397	348	

j16b Single Canopy Site

stain diameter	sample number								
	1	2	3	4	5	6	7	8	9
0.25	152	167	137	113	120	117	103	56	14
0.5	131	101	93	76	79	94	72	42	13
1.0	136	101	48	30	42	79	17	20	20
1.5	58	41	48	41	24	49	49	17	11
2.0	18	10	13	10	15	15	25	13	9
2.5	8	5	10	20	5	17	16	9	3
3.0	3	10	10	10		19	14	2	3
3.5		2	4	2	8	6	8	3	1
4.0	3	10	8	8	8	2	3	1	
4.5	5		4	5	5	4	5	1	
5.0		2	2	2	5	4			
5.5		2	2	3	2	11	2		
6.0	5						2	4	
6.5		5				2		1	
7.0				3					
7.5		2		3	2	2			
8.0		2	2						
8.5		2							
9.5						2			
10.0					2				
11.0				2	2				
11.5			2						
12.0		2			2				
12.5					2				
15.0	3								
16.0		2							
17.5							2		
19.5								1	
20.5				2					
21.0						2			
22.5		2							
24.5		2		2					
25.0		2		2					
25.5								1	
27.0				2					
27.5	3	2							
30.0		2		2					
33.5					3				
37.0		2							

duration of each sample, t_s (s) and gap, t_g (s)

t_s	105	46	115	95	123	80	196	424	319
t_g	410	266	269	289	300	283	284	538	

throughfall sampling started 131 s after rainfall sampling

j16b Multiple Canopy Site

stain diameter	sample number						
	1	2	3	4	5	6	7
0.25	311	201	209	110	19	16	26
0.5	154	103	128	52	37	25	6
1.0	87	29	65	21	15	15	2
1.5	63	60	38	21	6	10	1
2.0	28	29	13	20	6	5	1
2.5	3	17	13	1	1	2	
3.0	14	17	3	8	1	1	
3.5	10			7	2		
4.0	3	2	8	1		1	
4.5	3				1	1	1
5.0		2					
5.5	3	5	5	4	1		
6.0	3						
6.5		2		1			
7.5	3						
8.0			3	1			
9.5	3	2					
10.5		2		1			
17.0					2		
17.5			3	1			
18.5			3	1			
20.0						2	
20.5				3			
21.0		2	3			1	
21.5			3			1	1
22.0	3		3	1	1	1	
22.5			3	1			1
23.0			3			1	
24.0						1	1
25.0						1	
25.5					1		
26.0					1		
27.0		2					
28.5						1	
29.0				1	2		
29.5				3	1		
30.0				1	1		
31.0					2		
34.0					2		
36.0					1		
38.0			3				
39.0					1		
43.5	3						
55.5						1	
56.0					1		
61.5		2					

duration of each sample, t_s (s) and gap, t_g (s)

t_s	950	473	517	450	330	805	600
t_g	120	120	120	125	300	300	

throughfall sampling started 126 s before rainfall sampling

j20 Open Site

stain diameter	sample number												
	1	2	3	4	5	6	7	8	9	10	11	12	13
0.25	30	163	319	125	289	29	30	26	18	5	14	8	5
0.5	40	39	227	81	103	22	18	16	9	14	10	27	
1.0	40	26	69	25	14	8	8	4	31	12	13	39	
1.5	19	7	37	17	11	14	3	17	24	26	7	51	2
2.0	13	6	32	13	6	17	18	14	26	23	9	40	7
2.5	8	9	28	6	6	11	9	18	32	14	12	18	1
3.0	6	2	9	6	9	12	14	29	35	18	24	8	7
3.5	2	17	18	2	6	7	14	26	28	10	25	3	8
4.0	1	7	5	12	3	5	20	12	18	17	12		2
4.5	2	13	9	10	2	4	10	13	10	4	10		3
5.0	1	15	9	15	6	11	9	22	15	3	7		11
5.5	1	7	28	10	17	11	7	5	5	6	4		3
6.0		9	5	2		10	4	4	3	2			2
6.5	1	7	14	8	14	11	7	2			1		3
7.0	1	7	9	8	17	3	7	1	1				
7.5	2	6	5	2	6	12	8	1		1			3
8.0		2	14	6	3		7						2
8.5		2		4	14	14	2						
9.0		6	9	10	6	3	2						
9.5		4	5	2	3	4			1				1
10.0		7	9	2	9	3							
10.5	1	2	5	8	6	1							
11.0		2	5	4	3								
11.5	2			2	3	1							
12.0	1			2	6								
12.5		2	5		3								
13.0	5						1						
13.5					3								
14.0	1												
14.5	1	2		2	3								
15.0	2			2									
15.5	1			2									
16.0	1												
16.5	1												
17.5	1												
19.5					3								
25.5	1												

duration of each sample, t_s (s) and gap, t_g (s)

t_s	69	2	4	4	4	11	6	12	30	75	80	160	180
t_g	123	122	123	157	267	289	294	168	410	145	600	2630	

j20 Single Canopy Site

stain diameter	sample number											
	1	2	3	4	5	6	7	8	9	10	11	12
0.25	275	134	286	122	168	196	146	105	117	75	58	15
0.5	365	144	210	97	174	125	151	63	71	60	36	13
1.0	161	45	51	33	40	104	59	43	64	30	20	13
1.5	81	52	72	43	60	70	37	42	25	33	18	6
2.0	38	22	33	47	60	43	15	25	22	20	9	3
2.5	5	12	11	10	17	15	5	14	15	11	4	
3.0	5	7	11	83	11	9	20	14	3	1	3	1
3.5		2	7	17	9	12	15	11	5	4		1
4.0	9	5	11	4	9	6	2	13		4	1	
4.5	5	7	4	4	3	3	7	4	2	1	2	
5.0		7		2	3	15		2	2	1	1	
5.5		10	4	2			5	7	3		1	
6.0		2		2	3			2				
6.5		2	4		2		5	5		1		
7.0		2		2					2		1	
7.5		5	4									
8.0		2					2	2				
8.5		2			3	3	2					
9.0	5											
9.5		2	4	4							1	
10.0						3	2					
10.5											2	
11.0					3							
11.5			4	2		3	5					
12.0		2										
12.5				2	3		2					
13.5				2								
14.0			4							1		
15.0		2							2			
15.5		2										
17.5		2										
18.5		2						2				
19.0				2			2					
19.5		2										
20.5			4									
23.0						3			2			
23.5								4	2			
24.0										1		
24.5			4									
27.0										1	1	
27.5				2								
29.0				2								
31.5							5					
33.5										1		
34.0					3							
34.5									2			
37.0							2					
39.5								2				
49.0							2					

duration of each sample, t_s (s) and gap, t_g (s)

t_s	17	3	6	4	58	5	20	40	120	360	540	1200
t_g	115	105	145	162	242	295	280	260	300	420	600	

throughfall sampling started 128 s after rainfall sampling

j20 Multiple Canopy Site

stain diameter	sample number													
	1	2	3	4	5	6	7	8	9	10	11	12	13	14
0.25	146	698	49	128	45	56	150	413	174	124	95	81	125	35
0.5	340	370	75	125	38	50	109	254	160	83	57	73	86	47
1.0	168	98	41	89	17	28	66	133	60	88	36	35	53	23
1.5	155	105	25	36	13	16	27	42	26	36	27	19	39	15
2.0	53	21	20	38	9	7	23	95	48	17	23	9	23	3
2.5	9	7	4	15	2	2	2	16	26	17	15	7	12	3
3.0	4	42	6	8	7	2	16	27	17	13	15	4	6	2
3.5		21	2	10	3	3	5	16	14	4	11		4	
4.0	4	14	1	10		1	7		3	4	2	1	6	
4.5				5	1		7	5	3	2	5		8	
5.0	4		1		1	3		11			3		4	2
5.5				3		1	2	5	6	2	2		2	
6.0				3		1					5			1
6.5		7			1	1	2	11	3		2	1		
7.0		7		3					3				2	
7.5								11		2	2			1
8.0									3	2	3	1	2	
8.5		7		8	1			5			2		2	
9.0				3						2		2	4	
9.5			1						3	2				
10.0					1				3					
11.0												1	2	
11.5													2	
12.0				5							3			
12.5					1						3			
13.5						1								
14.0											2			
14.5											2			
15.0				3										
15.5			1	3										
16.0						1	2	5		2	2			
16.5											2			
17.5										2		2		
18.0				3				5		4				
18.5										2	2	2		
19.0						2	2				2		2	1
19.5				3					3	2				
20.0			1	3	1	2	2					1	6	
20.5							2							
21.0						3	1		6	2				
21.5										2		2		3
22.0					1				3		2			1
22.5						1	2		3					
23.0							2	5		4				1
23.5														1
24.0			1									1		2
24.5							2							
25.0			2			1								
25.5														1
26.0							2							
26.5							2			2				
27.0				5										
27.5					1									
28.0				3	2									
28.5			1			1				2	2			
29.0						1								
31.0			1											
32.0						1						2		
33.0									3					
34.0							2							
35.0										2	2			
37.0							2							
38.0				3										
39.0						1			3					
39.5					1									
46.0					1									
47.0			1										2	
47.5												1		
51.0					1									
53.0			1											
57.0					1									
63.5			1											

duration of each sample, t_s (s) and gap, t_g (s)

t_s	165	6	5	14	7	16	22	60	117	173	348	382	1177	825
t_g	120	120	120	120	120	300	300	300	300	300	300	348	360	

throughfall sampling started 10 s before rainfall sampling

APPENDIX 2 Tropical rain forest sites: Depth of rain and throughfall (mm) recorded in all rain gauges

Open Site - rainfall depth (mm)

gauge number	storm number					
	j7	j10b	j10c	j11	j12	j13
1	1.55	3.6	0.9	13.3	1.43	0.05
2	1.55	3.7	1.0	12.3	1.43	0.07
3	1.55	3.7	1.9	12.1	1.43	0.15
4	1.46	3.8	0.9	13.1	1.36	0.17
mean	1.5	3.7	1.2	12.7	1.41	0.11

	j14b	j15	j16a	j16b	j20	j22
1	1.78	2.79	--	0.34	2.86	14.3
2	1.78	2.83	8.92	0.37	2.93	13.79
3	1.85	2.83	8.75	0.37	2.99	12.45
4	1.78	2.86	8.75	0.37	2.93	13.29
mean	1.80	2.83	8.86	0.36	2.93	13.46

Single Canopy Site - throughfall depth (mm)

gauge no	storm number											
	j7	j10b	j10c	j11	j12	j13	j14b	j15	j16a	j16b	j20	j22
1	0.9	3.33	0.93	12.8	0.96	trace	1.98	2.05	8.41	0.03	1.95	14.47
2	0.5	2.09	0.50	11.8	0.98	trace	1.08	1.78	7.40	trace	2.62	10.8
3	0.9	3.36	1.11	10.9	0.89	0.00	1.48	2.30	7.90	0.17	1.78	11.9
4	0.8	3.01	0.77	3.2	0.62	trace	1.23	1.95	0.81	trace	1.75	11.4
5	0.9	2.91	0.84	10.1	1.24	trace	1.72	2.22	7.90	0.13	2.44	11.8
6	0.8	3.31	0.94	11.8	0.94	trace	1.45	1.88	6.90	0.24	2.44	14.5
7	0.7	3.20	0.91	11.9	0.84	0.02	1.98	2.07	8.58	0.07	2.61	0.50
8	1.1	3.82	1.11	13.0	1.16	trace	1.55	2.36	7.57	0.10	2.52	11.44
9	1.0	3.63	1.03	11.6	0.94	trace	1.75	2.56	8.07	0.24	2.78	11.44
10	0.8	3.43	0.87	10.3	0.98	trace	1.75	2.05	8.07	0.22	2.57	13.96
11	1.2	3.47	0.84	19.0	0.91	trace	1.78	2.83	8.24	0.17	2.39	15.31
12	0.8	3.23	1.14	9.6	0.94	trace	1.08	2.29	6.06	0.10	2.42	11.10
13	1.0	3.63	0.94	13.5	0.82	0.00	1.45	2.05	6.73	0.17	2.74	13.29
14	1.1	3.30	1.04	11.4	1.26	trace	1.65	2.42	6.74	trace	2.79	13.63
15	1.4	2.51	1.14	13.6	0.77	trace	1.95	2.86	8.58	0.24	1.92	14.47
16	0.7	3.28	0.61	10.3	1.24	0.00	1.18	1.88	6.22	trace	2.47	10.43
17	1.3	2.88	0.67	13.0	0.82	0.02	1.46	2.15	6.73	0.07	2.71	12.95
18	1.3	2.49	0.81	11.4	1.21	0.03	0.24	2.52	7.40	0.30	2.42	11.44
19	0.6	1.43	0.77	12.6	0.52	0.00	1.45	2.36	12.78	trace	1.95	13.63
20	0.8	3.30	0.30	8.6	0.77	0.00	1.55	1.48	7.23	0.02	1.95	5.72
21	0.8	3.03	0.81	10.9	1.01	trace	1.65	1.95	7.23	0.20	2.42	11.94
22	0.8	2.59	0.91	11.3	1.10	0.02	1.92	2.29	9.08	0.27	2.17	13.12
23	0.9	2.62	0.94	9.8	1.03	0.10	1.58	2.79	6.90	0.17	2.71	11.94
24	0.8	4.05	0.84	10.3	0.98	0.07	1.46	1.85	8.07	0.10	2.86	13.63
25	1.2	3.80	1.11	15.5	1.28	0.02	1.60	2.56	10.09	0.20	2.42	13.46
mean	0.9	3.11	0.87	11.53	0.97	0.01	1.56	2.22	7.63	0.12	2.39	11.93
s.d.	0.3	0.57	0.20	2.68	0.19	0.02	0.26	0.34	1.92	0.09	0.33	3.00

Multiple Canopy Site - throughfall depth (mm)

gauge no.	storm number										
	j7	j10b	j10c	j11	j12	j13	j14b	j15	j16a	j16b	j20	j22
1	no	2.74	0.91	8.4	0.44	trace	0.94	1.75	5.38	trace	2.09	no
2	data	2.10	0.81	7.4	0.47	trace	0.42	0.67	2.86	0.03	2.20	data
3		0.45	0.13	3.4	0.07	trace	0.10	0.61	2.22	0.03	0.45	
4		1.85	0.57	7.9	0.17	trace	0.44	1.28	4.54	0.07	0.45	
5		1.24	0.20	1.5	0.00	trace	0.20	0.64	0.13	trace	0.77	
6		1.55	0.64	8.2	0.37	trace	1.01	1.28	6.06	0.03	1.90	
7		0.27	0.03	5.0	0.13	trace	0.20	0.24	2.25	0.03	0.87	
8		0.64	0.02	2.5	0.00	trace	0.08	0.30	0.81	trace	0.27	
9		0.54	0.03	2.7	trace	0.00	0.13	0.50	1.48	0.07	0.25	
10		7.40	1.16	21.5	0.12	trace	0.77	3.53	22.88	0.03	1.85	
11		0.40	1.13	1.2	0.00	0.00	0.00	trace	1.78	trace	0.07	
12		1.24	0.02	6.1	0.32	trace	0.32	0.54	1.85	trace	0.45	
13		2.04	0.27	4.2	0.40	trace	0.27	0.54	3.36	0.03	0.50	
14		2.78	0.79	18.5	trace	0.00	trace	2.49	9.76	0.03	0.72	
15		1.65	0.19	10.8	0.24	trace	3.8	1.31	4.71	0.07	1.09	
16		trace	0.00	0.14	0.00	0.00	0.00	0.02	1.10	0.03	0.10	
17		4.72	1.51	1.29	0.55	0.00	0.83	0.76	3.13	trace	1.22	
18		0.65	0.09	0.33	0.07	trace	0.40	0.45	2.96	0.03	0.83	
19		1.93	0.46	0.53	trace	0.00	0.45	1.67	3.51	trace	0.90	
20		0.00	0.00	0.15	0.00	0.00	0.00	trace	0.07	trace	0.00	
21		0.76	0.83	0.53	0.28	0.00	0.05	0.55	5.51	trace	0.88	
22		2.00	0.62	1.05	0.24	trace	0.48	0.83	4.10	trace	1.14	
23		2.20	0.45	0.86	0.24	trace	0.52	1.72	2.89	0.21	0.48	
24		2.29	0.10	0.59	trace	0.00	0.45	2.44	6.03	trace	0.52	
25		1.31	0.24	1.03	0.10	0.00	0.52	0.74	4.82	0.03	1.02	
mean		1.67	0.45	4.63	0.17		0.50	0.99	4.17	0.03	0.84	
s.d.		1.55	0.42	5.49	0.17		0.73	0.85	4.38	0.04	0.61	

APPENDIX 3 Tropical rain forest sites: weight of splash (g) recorded in each splash trap

Open Site

trap no.	storm number								
	j7a	j10b	j11	j12	j13	j14b	j15	j16b	j20
1	0.0562	0.0732	1.3336	0.1823	0.0161	0.0338	0.1338	0.0404	0.1886
2	0.0359	0.0395	2.3173	0.1198	0.0221	0.0268	0.0897	0.0314	0.1539
3	0.0316	0.0335	2.3697	0.1480	0.0079	0.0551	0.0765	0.0147	0.2090
4	0.0587	0.0936	1.7560	0.1233	0.0039	0.0222	0.0780	0.0166	0.1543
5	0.0551	0.0579	2.5863	0.1515	0.0108	0.0150	0.0735	0.0166	0.1320
mean	0.0475	0.0595	2.0726	0.1450	0.0122	0.0306	0.0903	0.0239	0.1606

Single Canopy Site - splash weight (g)

trap no.	storm number								
	j7a	j10b	j11	j12	j13	j14b	j15	j16b	j20
1	0.0150	0.4124	5.3925	0.4618	0.0689	0.3523	1.0092	0.1140	1.1214
2	0.0141	missing	3.5910	0.0286	0.0023	0.0886	0.3053	0.0123	0.5737
3	0.0238	0.3029	7.7787	0.2345	0.0101	0.4440	0.4511	0.0327	0.5272
4	0.0456	0.5563	4.9200	0.1246	0.0046	0.1526	0.3745	0.0775	0.7239
5	0.0345	0.2937	6.4556	0.3977	0.0220	0.3006	1.1974	0.0743	0.5889
6	0.0420	0.3715	6.1329	0.0785	0.0238	0.2360	0.5953	0.0755	0.3783
7	0.0444	0.4514	5.3023	0.0769	0.0289	0.2981	0.4854	0.0558	0.5881
8	0.0328	0.3745	4.1309	0.1039	0.0057	0.1106	0.2314	0.0156	0.3142
9	0.0538	0.3847	2.8679	0.0439	0.0117	0.1462	0.2971	0.0410	0.3976
10	0.0120	0.1709	3.1950	0.1032	0.0062	0.0553	0.1862	0.0065	0.3552
11	0.0147	0.4260	2.3045	0.0649	0.0032	0.0773	0.1826	0.0192	0.2622
12	0.0563	0.3310	6.5521	0.1488	0.0118	0.1379	0.3148	0.0104	0.3579
13	0.0565	0.7008	5.5058	0.1392	0.0165	0.2438	0.3512	0.0602	0.4262
14	0.0694	0.4575	7.5623	0.2823	0.0150	0.3192	0.7779	0.0617	0.7578
15	0.0298	0.3662	3.5689	0.1437	0.0088	0.2036	0.2616	0.0483	0.3097
16	0.0534	0.4681	6.3336	0.0425	0.0070	0.1250	0.4210	0.0777	0.1994
17	0.0279	0.3412	4.1470	0.0900	0.0355	0.1292	0.3315	0.0220	0.4110
18	0.0571	0.6153	3.8625	0.1183	0.0129	0.1686	0.4083	0.0458	0.4857
19	0.0277	0.3097	4.0676	0.1134	0.0112	0.2020	0.2660	0.0328	0.3405
20	0.0576	0.2609	4.5843	0.0911	0.0540	0.2330	0.4696	0.0245	0.2167
21	0.0268	0.2260	3.0020	0.1857	0.0154	0.0606	0.0986	0.0066	0.3736
22	0.0313	0.2981	4.3160	0.1335	0.0024	0.2606	0.4343	0.0117	0.2483
23	0.0217	0.3176	4.7710	0.0623	0.0048	0.0872	0.2787	0.0169	0.8240
24	0.0793	0.8623	3.9070	0.0665	0.0088	0.3817	0.8007	0.0799	0.4838
25	0.0397	0.2035	3.1737	0.0801	0.0185	0.1305	0.1961	0.0085	0.5115
mean	0.0386	0.3959	4.6970	0.1366	0.0163	0.1978	0.4290	0.0412	0.4711
s.d.	0.018	0.159	1.470	0.106	0.016	0.106	0.265	0.030	0.213

Multiple Canopy Site - splash weight (g)

trap no.	storm number							
	j7a	j10b	j11	j12	j13	j14b	j15	j16b	j20
1	no	0.0371	0.5256	0.2477	0.0101	0.0107	0.0164	0.0033	0.0522
2	data	0.1896	1.6299	0.1562	0.0078	0.6683	0.2268	0.0177	0.0361
3		0.0591	0.2824	0.0268	0.0049	0.0254	0.0242	0.0070	0.0352
4		0.0689	1.0674	0.0928	0.0028	0.0416	0.1257	0.0060	0.0305
5		0.2066	2.4905	0.0609	0.0105	0.0090	0.1426	0.0032	0.0342
6		0.1381	2.6959	0.0865	0.0018	0.0521	0.1052	0.0069	0.1092
7		0.2929	2.7546	0.1799	0.0012	0.1960	0.2417	0.0754	0.0636
8		0.0207	0.1881	0.0534	0.0010	0.0106	0.0084	0.0090	0.0112
9		0.0788	1.0394	0.1006	0.0088	0.0228	0.0184	0.0023	0.0269
10		0.0336	0.9490	0.0709	0.0018	0.0133	0.0407	0.0028	0.0106
11		0.0777	0.7445	0.1377	0.0220	missing	0.0236	0.0026	0.0494
12		0.1878	0.4801	0.1172	0.0048	0.4776	0.1380	0.0060	0.5959
13		0.0442	0.3583	0.0621	0.0020	0.0442	0.0224	0.0050	0.0413
14		0.1868	0.6665	0.4334	0.0005	0.0898	0.1874	0.0040	0.0688
15		0.3572	2.2442	0.0580	0.0058	0.0224	0.1639	0.0027	0.0326
16		0.1557	3.1047	0.0456	0.0240	0.0597	0.0674	0.0017	0.0820
17		0.0316	0.4562	0.1606	0.0011	0.0291	0.0162	0.0040	0.0256
18		0.1172	2.0592	0.0881	0.0039	0.2752	0.1252	0.0086	0.1814
19		0.1078	3.4266	0.0991	0.0022	0.0421	0.0865	0.0054	0.0254
20		0.5858	0.1180	0.0467	0.0013	0.0054	0.0082	0.0164	0.0060
21		0.0991	2.5680	0.1510	0.0009	0.0365	0.0397	0.0046	0.1052
22		0.0481	0.2364	0.0430	0.0056	0.0077	0.0121	0.0052	0.0330
23		0.1282	1.3923	0.0652	0.0047	0.0756	0.0417	0.0049	0.2339
24		0.2082	3.3501	0.1071	0.0191	0.0642	0.1306	0.0249	0.0756
25		0.0100	0.4060	0.0290	0.0055	0.0029	0.0028	0.0111	0.0042
mean		0.1348	1.4094	0.1088	0.0062	0.0913	0.0806	0.0096	0.0788
s.d.		0.124	1.110	0.086	0.007	0.162	0.073	0.015	0.120